

Kazan Federal University

Zavoiskii Physical-Technical Institute, FRC Kazan Scientific Center
of RAS

International Conference "Magnetic Resonance - Current State and
Future Perspectives" and satellite XXI International Youth
Scientific School "Actual problems of magnetic resonance and its
application"

devoted to the 75-th anniversary of the discovery of Electron Paramagnetic
Resonance by E.K. Zavoiskii

Book of
ABSTRACTS

September 23-27, 2019 Kazan, Russia

The International Conference “Magnetic Resonance - Current State and Future Perspectives” and satellite XXI International Youth Scientific School “Actual problems of magnetic resonance and its application” are devoted to the 75-th anniversary of the discovery of Electron Paramagnetic Resonance by E.K. Zavoiskii in Kazan, Russia, on January 21, 1944.



E.K. Zavoiskii (1907 – 1976)

SUPPORTED BY

The Government and the President of the Republic of Tatarstan



Tatarstan Academy of Sciences



Federal Research Center “Kazan Scientific Center of the Russian Academy of Sciences”



Russian Foundation for Basic Research



Bruker Corporation



Organizing Committee

D.A. Tayurskii (Vice-Rector of Kazan Federal University) – Chairman of the Organizing Committee

A.A. Kalachev –(Head of Kazan Physical-Technical Institute, FIC Kazan SC of RAS) – Chairman of the Organizing Committee

M.S. Tagirov (Head of the Quantum Electronics and Radio spectroscopy Department, Kazan Federal University) – Vice Chairman of the Organizing Committee of Conference and Rector of satellite XXI School

A.V. Dooglav (Kazan Federal University – Scientific Secretary)

A.V. Aganov (Kazan Federal University)

E.M. Alakshin (Kazan Federal University)

V.K. Voronkova (Kazan Physical-Technical Institute)

M.R. Gafurov (Kazan Federal University)

R.M. Eremina (Kazan Physical-Technical Institute)

V.A. Latypov (Kazan Physical-Technical Institute)

R.F. Mamin (Kazan Physical-Technical Institute)

L.V. Mosina (Kazan Physical-Technical Institute)

Yu.N. Proshin (Kazan Federal University)

L.I. Savostina (Kazan Federal University)

L.R. Tagirov (Kazan Federal University, Kazan Physical-Technical Institute)

V.F. Tarasov (Kazan Physical-Technical Institute)

International Advisory Board

Henri Alloul (Paris, France)

Valentin Ananikov (Moscow, Russia)

Vadim Atsarkin (Moscow, Russia)

Elena Bagryanskaya (Novosibirsk, Russia)

Pavel Baranov (St. Petersburg, Russia)

Bernhard Blümich (Aachen, Germany)

Michael Bowman (Tuscaloosa, USA)

Yurii Bun'kov (Grenoble, France)

Annette Bussmann-Holder (Stuttgart, Germany)

Vladimir Dmitriev (Moscow, Russia)

Vladimir Dyakonov (Würzburg, Germany)

Michael Farle (Duisburg, Germany)

Christian Griesinger (Göttingen, Germany)

Jürgen Hennig (Freiburg, Germany)

Vladislav Kataev (Dresden, Germany)

Hugo Keller (Zürich, Switzerland)

Alexander Kokorin (Moscow, Russia)

Igor Koptyug (Novosibirsk, Russia)

Wolfgang Lubitz (Mülheim, Germany)

Klaus Möbius (Berlin, Germany)

Alexander Shengelaya (Tbilisi, Georgia)

Hans Wolfgang Spiess (Mainz, Germany)

Haruhiko Suzuki (Kanazawa, Japan)

Sergey Vasilyev (Turku, Finland)

Joachim Wosnitza (Dresden, Germany)
Kurt Wüthrich (Zürich, Switzerland)

Program Committee

S.I. Nikitin (Head of the Institute of Physics) – Co-Chairman of the Program committee

K.M. Salikhov (Scientific Director of Kazan Physical-Technical Institute) –Co-Chairman of the Program Committee

A.V. Aganov (Kazan Federal University)

V.A. Atsarkin (IREE, Moscow)

M.R. Gafurov (Kazan Federal University)

I.A. Garifullin (Kazan Physical-Technical Institute)

M.V. Eremin (Kazan Federal University)

R.B. Zaripov (Kazan Physical-Technical Institute)

V.V. Klochkov (Kazan Federal University)

Sh.K. Latypov (Kazan Institute of Organic and Physical Chemistry)

B.Z. Malkin (Kazan Federal University)

B.I. Kochelayev (Kazan Federal University)

S.B. Orlinskiy (Kazan Federal University)

R.Z. Sagdeyev (Siberian Branch, Russian Academy of Sciences)

V.D. Skirda (Kazan Federal University),

A.A. Sukhanov (Kazan Physical-Technical Institute)

L.R. Tagirov (Kazan Federal University, Kazan Physical-Technical Institute)

G.B. Teitel'baum (Kazan Physical-Technical Institute)

Yu.I. Talanov (Kazan Physical-Technical Institute)

Local Committee of Conference and School

E.M. Alakshin (Kazan Federal University, Chairman of the Local Committee)

I.P. Volodina (Kazan Federal University, Secretary)

R.M. Eremina (Kazan Physical-Technical Institute)

V.A. Latypov (Kazan Physical-Technical Institute)

G.V. Mamin (Kazan Federal University)

I.G. Motygullin (Kazan Federal University)

E.I. Kondratyeva (Kazan Federal University)

Yu.Yu. Kochneva (Tatarstan Academy of Sciences)

V.V. Kuzmin (Kazan Federal University)

A.V. Bogaychuk (Kazan Federal University)

I.V. Romanova (Kazan Federal University)

T.R. Safin (Kazan Federal University)

S.A. Volodin (Tatarstan Academy of Sciences)

**MAGNETIC RESONANCE:
CURRENT STATE AND FUTURE PERSPECTIVES (EPR-75)**

TOPICS:

- Theory of Magnetic Resonance
- New Methods and Techniques
- Spin Technologies and Devices
- Low-Dimensional, Nanosized, Strongly Correlated Electronic Systems
- Structure and Dynamics of Chemical Systems
- Spectroscopy and Imaging of Biological Systems
- Other Applications of Magnetic Resonance and Related Phenomena

CONFERENCE PROGRAM

22 September, Sunday	
14.00-21.00	Registration Institute of Physics, Hall, 1 st floor
23 September, Monday	
08.00-09.00	Registration Institute of Physics, Hall, 1 st floor
09.00-09.30	Opening Ceremony Main building, Imperial Hall
09.30-12.30	Morning Session Main building, Imperial Hall
09.30-10.00	Smirnov A.I. (Russia, Moscow) - <i>Order by Dynamic or Static Disorder in a Triangular Antiferromagnet RbFe(MoO₄)₂</i>
10.00-10.30	Kabanov V.V. (Slovenia, Ljubljana) - <i>Symmetry Enforced Dirac Points in Antiferromagnetic Semiconductors</i>
10.30-11.00	Atsarkin V.A. (Russia, Moscow) - <i>Spin Current Induced by Magnetic Resonance in Ferromagnet-normal Metal Bilayers</i>
11.00-11.30	Demishev S.V. (Russia, Moscow) - <i>Three and a Half Puzzles in EPR Physics of Strongly Correlated Materials</i>
11.30-12.00	Okubo S. (Japan, Kobe) - <i>High-Field and High-Frequency ESR Studies of Comprising Tetrahedral Clusters Arranged in the Cubic Lattice</i>
12.00-12.30	Eremina R. (Russia, Kazan) - <i>Anisotropic Exchange Interaction in Low-Dimensional Systems</i>
12.30-14.30	Lunch
14.30-16.10	Afternoon Session I – 1 Spectroscopy and Imaging of Biological Systems Institute of Physics, Lecture Hall 110
14.30-15.00	Drescher M. (Germany, Konstanz) - <i>In-Cell EPR Spectroscopy</i>
15.00-15.30	Krumkacheva O.A. (Russia, Novosibirsk) - <i>Triplet Fullerenes as Prospective Spin Labels for Nanoscale Distance Measurements by Pulsed Dipolar EPR</i>
15.30-16.00	Ptushenko V.V. (Russia, Moscow) - <i>Photosynthetic Electron Transfer Reactions in Microalga <i>Lobosphaera</i> incise</i>
14.30-15.00	14.30-15.00 Dvinskikh S.V. (Sweden, Stockholm) - <i>Multinuclear Dipolar NMR Spectroscopy in Liquid Crystals</i>
15.00-15.30	15.00-15.30 Zapevalov V.E. (Russia, Nizhny Novgorod) - <i>Modern Gyrotrons and Their Applications</i>
15.30-15.50	15.30-15.50 Gizatullin B. (Germany, Ilmenau) - <i>Fast Field Cycling NMR Relaxometry Enhanced by DNP for Study Complex Systems</i>

		15.50-16.10	Volkov V.Y. (Russia, Kazan) - <i>Low-Field NMR Full FID Method for the Study of Heterogeneous Objects</i>	Institute of Physics, Hall, 2 nd floor
16.10-16.30	Coffee-break			
16.30-19.50	Afternoon Session I-1 Structure and Dynamics of Chemical Systems	Institute of Physics, Lecture Hall 110	16.30-19.50	Afternoon Session I-2 Other Applications of Magnetic Resonance and Related Phenomena
16.30-17.00	Möbius K. (Germany, Berlin) - <i>Mechanisms for Life without Water - High-Field EPR Studies of Protein/Matrix Interactions</i>	16.30-17.00	Likhtenshtein G.I. (Israel, Beersheva; Russia, Chernogolovka) - <i>Dual Fluorescence-Nitroxide Supermolecules as High Sensitive Redox Probes and Models for Electron Transfer: 34 Years History and Recent Developments</i>	
17.00-17.30	Zaripov R.B. (Russia, Kazan) - <i>ENDOR and DFT Studies of the Cu(II)-bis(Oxamate) Complex</i>	17.00-17.30	Goovaerts E. (Belgium, Antwerp) - <i>Combining Electron ParamagneticResonance Methods to Investigate Materials for Organic Photovoltaics</i>	
17.30-18.00	Eaton S. (USA, Denver) - <i>Intramolecular Effects on Electron Spin Relaxation</i>	17.30-18.00	Sukhanov A.A. (Russia, Kazan) - <i>TR EPR Study of Photoinduced States of Metalloporphyrin. From Monomer to Oligomers</i>	
18.00-18.20	Coffee-break			Institute of Physics, Hall, 2 nd floor
18.20-18.50	Witwicki M. (Poland, Wroclaw) - <i>Application of Experimental and Computational EPR Spectroscopy to Radical Systems</i>	18.20-18.50	Bussmann-Holder A. (Germany, Stuttgart) - <i>Hidden Magnetism in Almost Multiferroic EUTiO₃</i>	
18.50-19.20	Kokorin A.I. (Russia, Moscow) - <i>EPR Spectroscopy of Metal-Oxide Photocatalysts</i>	18.50-19.20	Keller H. (Switzerland, Zurich) - <i>Probing Fundamental Properties of Condensed Matter Systems with Positive Muons</i>	
19.20-19.50	Huber M. (The Netherlands, Leiden) - <i>EPR Approaches to Amyloid Protein Aggregation</i>	19.20-19.50	Martyanov O. (Russia, Novosibirsk) - <i>In situ ESR at Elevated Temperatures and Pressure for Catalysis and Related Phenomena</i>	
20.00-22.00	WELCOME PARTY			Institute of Physics, Dining Hall

24 September, Tuesday

Morning Session I <i>Spectroscopy and Imaging of Biological Systems</i>		Institute of Physics, Lecture Hall 110
09.00-11.00		
09.00-09.30	Kaptein R. (The Netherlands, Culemborg) - <i>NMR Studies of Protein-DNA interaction: Target location and Allosteric Mechanism of Induction</i>	
09.30-10.00	Fielding A. (United Kingdom, Liverpool) - <i>A Bifunctional Spin Label for Ligand Recognition on Surfaces</i>	
10.00-10.30	Dikanov S.A. (USA, Urbana, Illinois) - <i>Influence of Hyperfine Coupling Strain on Two-Dimensional ESEEM Spectra from $I=1/2$ Nuclei</i>	
10.30-11.00	Andersen M. (Denmark, Copenhagen) - <i>EPR and Beer - a Good Combination!</i>	
11.10-11.30	Coffee-break	Institute of Physics, Hall, 2 nd floor
11.30-13.00	Morning Session II - 1 Low-Dimensional, Nanosized, Strongly Correlated Electronic Systems	Institute of Physics, Lecture Hall 110
11.30-12.00	Zvyagin S. (Germany, Dresden) - <i>Pressure-Tuning the Quantum Spin Hamiltonian of the Triangular Lattice Antiferromagnet Cs_2CuCl_4: High-Field ESR Studies</i>	11.30-12.00 Morning Session II - 2 Structure and Dynamics of Chemical Systems
12.00-12.30	Kremer R.K. (Germany, Stuttgart) - <i>Search for the Spin-Nematic Phase in the $J_1 - J_2$ Frustrated Quantum Antiferromagnet $LiCuVO_4$</i>	Gescheidt G. (Austria, Graz) - <i>Applications of EPR and Light-Induced Reactions in Biomimetic Systems and Catalysis</i>
12.30-13.00	Tagirov L.R. (Russia, Kazan) - <i>Ferromagnetic Resonance - a Powerful Tool To Characterize Magnetic Heterostructures</i>	Lapina O.B. (Russia, Novosibirsk) - <i>Catalysts Structure Identification Using DFT-Confirmed NMR Signatures</i>
13.00-14.30	Lunch	
14.30-16.10	Afternoon Session I - 1 Low-Dimensional, Nanosized, Strongly Correlated Electronic Systems	Institute of Physics, Lecture Hall 110
14.30-14.50	Baibekov E.I. (Russia, Kazan) - <i>Experimental Realization of Qubit and Qutrit Quantum Manipulations using EPR of Rare Earth Ions in Single Crystals</i>	14.30-15.00 Afternoon Session I - 2 Other Applications of Magnetic Resonance and Related Phenomena
14.50-15.10	Soldatov T.A. (Russia, Moscow) - <i>Spinon Resonance in Spin-Chain Antiferromagnets with Uniform Dzyaloshinsky-Moriya Interaction</i>	Tarasov V.F. (Russia, Kazan) - <i>EPR Study of Monoisotopic ^{53}Cr Impurity Ions in Forsterite Single Crystal</i>
15.10-15.40	Semeno A. (Russia, Moscow) - <i>ESR Evidence of Spin Glass Behavior in the Absence of the Intrinsic Randomness in GdB_6</i>	15.00-15.20 Shanmugam M. (United Kingdom, Manchester) - <i>Direct Evidence for "Substrate-Induced" Inter-Copper Electron-Transfer in Copper-Containing Nitrite Reductases (AxNIR and RpNIR-Core); Probed by EPR/Cryolytic Reduction/Annealing Studies</i>
		15.20-15.40 Murzakaev V.M. (Russia, Bugulma) - <i>Results Gained from Application of Dielectric and High-Resolution Nuclear-Magnetic Resonance Complex for Assessment of Fluid Type in a Borehole and in Core</i>

15.40-16.10	Ziatdinov A.M. (Russia, Vladivostok) - <i>Electronic Structure near the Fermi Level in Nanostructured Phase of Thermally Reduced Graphene Oxide: ESR, CESR and Magnetic Susceptibility Studies</i>	15.40-16.00	Ulanov V.A. (Russia, Kazan) - <i>EPR of the $Pb_{1-x}Gd_xS$ Narrow Gap Semiconductor Crystals: Observation of Strong Dependence of the EPR Line Profiles on Gadolinium Concentration</i>
16.10-16.30	Coffee-break		
16.30-19.10	Afternoon Session II – 1 <i>Low-Dimensional, Nanosized, Strongly Correlated Electronic Systems</i>	Institute of Physics, Lecture Hall 110	
16.30-16.50	Preisinger M. (Germany, Augsburg) - <i>Effects of Magnetocrystalline Anisotropy on the Triangular to Square Lattice Transformation of Skyrmions</i>	16.30-17.00	Afternoon Session II – 2 <i>New Methods and Techniques</i>
16.50-17.10	Szigeti B.G. (Germany, Augsburg) - <i>New Findings in the Magnetic Phase Diagram of GaV_2Se_8</i>	17.00-17.30	Zapasski V.S. (Russia, St.-Petersburg) – <i>Spin Noise Spectroscopy as an Alternative to Zavoisky’s Technique</i>
17.10-17.30	Skorokhodov E. (Russia, Nizhny Novgorod) - <i>Magnetic Resonance Force Spectroscopy of Co/Pt Multilayer Films with Perpendicular Anisotropy</i>	17.30-18.00	Buntkowsky G. (Germany, Darmstadt) - <i>Hyperpolarisation of Enzyme-Inhibitors with Parahydrogen</i>
17.30-17.50	Khusnuriyalova A.F. (Russia, Kazan) - <i>The Observation by Magnetic Resonance of the Electrochemically Generated Superparamagnetic Cobalt Nanoparticles</i>	18.00-18.30	Matysik J. (Germany, Leipzig) - <i>Photo-CIDNP in Solids</i>
17.50-18.10	Yakushkin S.S. (Russia, Novosibirsk) - <i>Fe_3O_4/DMSO Ferrofluid Synthesis, ESR in situ Study</i>	18.30-19.00	Konstantinova E.A. (Russia, Moscow) - <i>EPR Spectroscopy of Semiconductor Nanomaterials: New Approaches</i>
18.10-18.30	Romanova I. (Russia, Kazan) - <i>Magnetic Resonance in a Dipolar Ferromagnet $LiHoF_4$</i>	19.00-19.30	Bunkov Yu.M. (Russia, Moscow) - <i>Spin Superfluidity at Room Temperature</i>
18.30-18.50	Sarkar R. (Germany, Dresden) - <i>NMR Studies on the Single Crystalline Na_2IrO_3: A Model System to Realize Kitaev Interaction</i>		Samoson A. (Estonia, Tallinn) - <i>H–MAS</i>
18.50-19.10	Young Ben-Li (Taiwan, Hsinchu City) - <i>Electronic Structures in In-doped Topological Insulator ($Pb_{0.5}Sn_{0.5}I_{1-x}In_xTe$) Probed by NMR Spectroscopy</i>		

25 September, Wednesday	
09.00-13.20	Special session: 30 years of the International EPR(ESR) Society (IES) Institute of Physics, Lecture Hall 110
09.00-09.30	Prisner T.F. (Germany, Frankfurt) – <i>Shaping up EPR: Phase/Amplitude Modulated Pulses for Dipolar Spectroscopy</i>
09.30-10.00	Han Songji (U.S.A, California) – <i>Dynamic Manipulation of Electron Spin Dynamics to boost Dynamic Nuclear Polarization</i>
10.00-10.30	Hirata H. (Japan, Sapporo) – <i>Recent Progress in 3D Extracellular pH Mapping of Tumors Using EPR</i>
10.30-11.00	Griesinger C. (Germany, Göttingen) – <i>NMR Spectroscopy in Chemistry and Biology with Applications in Immunology and Neuroprotection</i>
11.00-11.20	Coffee-break Institute of Physics, Hall, 2 nd floor
11.20-11.50	Ohta H. (Japan, Kobe) – <i>Multi-Extreme THz ESR -Recent Applications and the Future</i>
11.50-12.20	Blank A. (Israel, Haifa) – <i>Diamond-Based Quantum Amplifier</i>
12.20-12.50	Van Doorslaer S. (Belgium, Antwerp) – <i>Unravelling the Role of Key Amino-Acids in B-Class Dye-Decolorizing Peroxidases Using EPR Spectroscopy</i>
12.50-13.20	Eichhoff U. (Germany, Gaggenu) – <i>Milestones in the 62 Years Bruker EPR History</i>
13.30-15.00	Lunch
15.00-17.50	Afternoon Session I – 1 Spectroscopy and Imaging of Biological Systems Institute of Physics, Lecture Hall 110
15.00-15.30	Bagryanskaya E.G. (Russia, Novosibirsk) - <i>DNA and RNA Complexes with Human Proteins: Structural Insights Revealed by Pulsed Dipolar EPR with Orthogonal Spin Labeling</i>
15.30-16.00	Zhao Jianzhang (China , Dalian) - <i>Time-Resolved EPR Study of the Intersystem Crossing of Visible Light-Harvesting Electron Donor/Acceptor Dyads</i>
16.00-16.20	Coffee-break Institute of Physics, Hall, 2 nd floor
16.20-16.50	Dzuba S. (Russia, Novosibirsk) - <i>Lipid-Mediated Clustering in Biological Membranes by Spin-Label EPR</i>
16.50-17.20	Khramtsov V.V. (USA, Morgantown) - <i>In Vivo Molecular EPR-Based Spectroscopy and Imaging of Cancer</i>
15.00-15.30	15.00-15.30 Volkov V.I. (Russia , Chernogolovka) - <i>Ionic and Molecular Transport in Synthetic and Biological Membranes Studied by NMR</i>
15.30-16.00	15.30-16.00 Veizin H. (France, Lille) - <i>Operando EPR for Monitoring Living Batteries</i>
16.20-16.50	16.20-16.50 Usachev K. (Russia, Kazan) <i>Structural and Dynamical Studies of the Elongation Factor P from Staphylococcus aureus by NMR and EPR Spectroscopy</i>
16.50-17.10	16.50-17.10 Khodov I.A. (Russia, Ivanovo) - <i>High-Pressure NMR Characterization of Conformation Preferences of Small-Molecules Dissolved in Supercritical Carbon Dioxide</i>

17.20-17.50	Anisimov N.V. (Russia, Moscow) - <i>Whole Body Sodium MRI at 0.5 Tesla</i>	17.10-17.30	Yakhvarov D.G. (Russia, Kazan) - <i>Application of in situ EPR Spectroelectrochemistry for Generation, Observation and Activation of High Reactive Mono-, Bi- and Polynuclear Complexes</i>
		17.30-17.50	Ostroumova G.M. (Russia, Moscow) - <i>Reactive Molecular-Dynamics Study of Onion-like Carbon Nanoparticle Formation</i>
18.00-20.30	POSTER SESSION		Institute of Physics, Hall, 2 nd floor

26 September, Thursday			
09.00-11.00	Morning Session I New Methods and Techniques		Institute of Physics, Lecture Hall 110
09.00-09.30	Fittipaldi M. (Italy, Florence) - <i>Electric Field Modulation of Magnetic Exchange in Molecular Helices</i>		
09.30-10.00	Smith G.M. (UK, St.Andrews) - <i>High Concentration Sensitivity, High Bandwidth and Low Deadtime Pulsed EPR</i>		
10.00-10.30	Eaton G. (USA, Denver) - <i>Multi-Frequency Rapid Scan EPR</i>		
10.30-11.00	Ranjan V. (France, Paris) - <i>High Sensitivity Quantum-limited Electron Spin Resonance</i>		
11.00-11.20	Coffee-break		
11.20-12.30	Morning Session II Spin Technologies and Devices		Institute of Physics, Lecture Hall 110
11.20-11.50	Goldner Ph. (France, Paris) - <i>Optically Detected Spin Resonance in Rare Earth Doped Crystals for Quantum Technologies</i>		
11.50-12.10	Kamashov A. A. (Russia, Kazan) - <i>Superconducting Spin-Valve Effect in a Heterostructures Containing the Heusler Alloy as Ferromagnetic Layers</i>		
12.10-12.30	Sudakov I.V. (Belgium, Antwerp) - <i>Photon Upconversion via Triplet Exciton Fusion in the Super-yellow PPV:PdTPBP Host-Sensitizer System</i>		
12.30-14.00	Lunch		
14.00-17.00	Zavoisky Award		City Hall
19.00	BANQUET		

27 September, Friday	
09.00-11.30	Morning Session I <i>Theory of Magnetic Resonance</i>
09.00-09.30	Salikhov K.M. (Russia, Kazan) - <i>Spin Exchange in Solutions of Paramagnetic Particles. Paradigm Shift</i>
09.30-10.00	Bowman M. (USA, Tuscaloosa) - <i>Electron Spin Relaxation and Motion in Solids: Spin, Spatial, Spectral</i>
10.00-10.30	Geru I.I. (Moldova, Chisinau) - <i>The Time Reversal Symmetry and a Virtual Time Reversal Method in EPR Spectroscopy</i>
10.30-11.00	Dzheparov F.S. (Russia, Moscow) - <i>Theory of Spin Pumping in Fe/NM</i>
11.00-11.30	Feldman E. (Russia, Chernogolovka) - <i>Multiple Quantum NMR Dynamics and Relaxation in One-Dimensional Systems</i>
11.30-11.50	Coffee-break
11.50-13.50	Morning Session II <i>Low-Dimensional, Nanosized, Strongly Correlated Electronic Systems</i>
11.50-12.20	Kochelaev B.I. (Russia, Kazan) - <i>EPR in Superconductors and Kondo-Lattices with heavy Fermions</i>
12.20-12.50	Eremin M.V. (Russia, Kazan) - <i>Toward the Theory of the Spins and Orbital Moments Coupling with Electric Field</i>
12.50-13.10	Augustyniak-Jabłokow M.A. (Poland, Poznań) - <i>Slow Paramagnetic Relaxation in Graphene Oxide and Partially Reduced Graphene Oxide</i>
13.10-13.30	Yusupov R.V. (Russia, Kazan) - <i>Probing Magnetic Inhomogeneity of Pd_{1-x}Fe_x Thin Films with Ultrafast Optical and Magneto-optical Spectroscopy</i>
13.30-13.50	Yermakov A. (Russia, Yekaterinburg) - <i>Formation of Antiferromagnetic Fe-Fe Dimers in Fe Doped TiO₂ Nanoparticles investigated by EPR and Magnetic Methods</i>
14.00-15.00	Lunch
15.00-15.30	Closing
15.30-19.00	Excursion Tour

POSTERS

1. Theory of Magnetic Resonance

1-1. **Bakirov M.M.** (Russia, Kazan) *Spin-Lattice Relaxation Times of Nitroxide Radicals in Solution Under the Influence of Spin-Exchange and Dipole-Dipole*

Interactions

1-2. **Gumarov A.I.** (Russia, Kazan) *FMR Studies of Thin Epitaxial Pd_{0.92}Fe_{0.08}/Pd_{0.9}Fe_{0.04} and Pd_{0.92}Fe_{0.08}/Ag/Pd_{0.96}Fe_{0.04} Heterostructures*

1-3. **Kandrashkin Yu.E.** (Russia, Kazan) *Hyperfine Interaction Promoted Intersystem Crossing*

1-4. **Khairuzhdinov I.r** (Russia, Kazan) *Determination T₁ and T₂ Relaxation Times from CPMG Phase Cycle Pulse Sequences*

1-5. **Zobov V.E.** (Russia, Krasnoyarsk) *Multiple-Quantum NMR Spectroscopy and Quantum Information Delocalization in Solids in the Presence of Magnetic*

Fields Inhomogeneities

1-6. **Zyuzin A.M.** (Russia, Saransk) *Intensity of EPR Absorption Lines in Semiconducting Substances*

2. New Methods and Techniques

2-1. **Al-Muntasaser A.A.** (Russia, Kazan) *SARA Analysis and NMR Relaxation as Prediction Techniques to Estimate the SARA Composition of Heavy and Light*

Oils – Correlations and Deviations

2-2. **Geru I.I.** (Moldova, Chisinau) *Deceleration of Proton Spin-Lattice Relaxation in Water under Ultrasonic Radiation*

2-3. **Khasanova N.M.** (Russia, Kazan) *Quantitative Characterization of the Kerogen Domanic by Low-Field NMR and EPR methods*

2-4. **Konstantinova E.A.** (Russia, Moscow) *Defect Properties of Titania Obtained by Laser Sintering*

2-5. **Konstantinova E.A.** (Russia, Moscow) *EPR Study of Titania Microspheres with Different Chemical Composition*

2-6. **Volkov M.** (Russia, Kazan) *Determination of Insulating Oil Moisture Content by NMR Spectroscopy*

2-7. **Zgadzai O.** (Israel, Haifa) *Selective Addressing and Readout of Optically Detected Electron Spins*

3. Spin Technologies and Devices

3–1. **Stankevich K.L.** (Russia, Moscow) *Spin Pumping Theory of Ferromagnetic – Normal Metal Structures (in the Case of $La_{2/3}Sr_{1/3}MnO_3$ /NM Bilayers)*

3–2. **Zobov V.E.** (Russia, Krasnoyarsk) *Associative Memory on Qutrits by means of Quantum Annealing*

4. Low-Dimensional, Nanosized, Strongly Correlated Electronic Systems

4–1. **Gafurov D.** (Russia, Kazan) *Study of Nonmagnetic Impurities in the Frustrated $S=1/2$ Spin Chains: NMR and Magnetization Study*

4–2. **Gafurov D.** (Russia, Kazan) *Effect of Lithium Deficiency on the Ion Mobility in Frustrated $Li_{1-x}CuSbO_4$ Compound Studied by NMR*

4–3. **Gafurov D.** (Russia, Kazan) *Temperature Evolution of Magnetic Properties of Sodium Iridates $Na(3/2)M(1/2)IrO_3$ ($M = Ni, Cu, Zn$) Probed by NMR and μ SR*

4–4. **Gaifullin R.R.** (Russia, Kazan) *Comparative Study of S/F/S/F and S/F/N/F Superconducting Spin-Valves*

4–5. **Gilmanov M.I.** (Russia, Moscow) *Electron Paramagnetic Resonance Study of $Ho_xLu_{1-x}B_{12}$ Solid Solutions*

4–6. **Goryunov Yu.V.** (Russia, Kazan) *Effect of Landau Levels on the SHFS of the EPR Spectra of Fe^{3+} Precipitates in the 3D Dirac Semimetal Cd_3As_2*

4–7. **Ivanova T.** (Russia, Kazan) *Weak Ferromagnetism in Antiferromagnetic Chains $[Fe(salen)](2-Me-Him)]_n$*

4–8. **Mohammed W.M.** (Russia, Kazan) *Synthesis and Ferromagnetic Resonance Studies of Epitaxial $VN/Pd_{0.96}Fe_{0.04}$ Heterostructure Grown on Single-Crystalline MgO Substrate*

4–9. **Nosov I.Yu.** (Russia, Kazan) *Mössbauer Effect Studies of Eu doped $BiFeO_3$*

4–10. **Semakin A.S.** (Russia, Kazan) *NMR Study of Charge Density Waves in NbS_3 Compound*

4–11. **Sarkar R.** (Germany, Dresden) - *Local Anisotropy and Spin Dynamics in a New Kagome Compound $Fe_4Si_2Sn_7O_{16}$*

4–12. **Vorobeva V.** (Russia, Kazan) *EPR Study of Azomethine Iron(III) Complexes*

- 4-13. **Voronkova V.K.** (Russia, Kazan) *Heteronuclear Clusters Containing Dysprosium Ions: SMM Properties and EPR Possibility*
- 4-14. **Yatsyk I.V.** (Russia, Kazan) *Magnetic Properties of Lanthanum Strontium Ferromanganites Doped with Zinc*
- 4-15. **Zinnatullin A.L.** (Russia, Kazan) *Mössbauer Effect and Magnetic Studies of Fe Implanted ZnO Film*

5. Structure and Dynamics of Chemical Systems

- 5-1. **Andronenko S.I.** (Russia, Kazan) *An EPR Study of the V^{4+} and Cu^{2+} Ions in Single Crystals of β - $Mg_2V_2O_7$ and α - $Zn_2V_2O_7$: Non-Coincident 2 and \tilde{A}^2 Tensors*
- 5-2. **Belov K.V.** (Russia, Ivanovo) *An Investigation of the Conformational Properties of Meferamic Acid in DMSO by Two-Dimensional NMR*
- 5-3. **Borisenko S.N.** (Russia, Rostov-on-Don) *NMR Study of Synthesis of the Phenanthridone Alkaloids from Herbal's Aporphine Alkaloids by Subcritical*

Water

- 5-4. **Dudysheva N.** (Russia, Novosibirsk) *Spin Probe Nanostructure Formation in Glassy Media Studied by EPR*
- 5-5. **Efimov S.V.** (Russia, Kazan) *Phosphorylotropic Rearrangement in Crown Ester Observed by 1H , ^{13}C , and ^{31}P NMR*
- 5-6. **Gafarova A.R.** (Russia, Kazan) *EPR Study of γ -Irradiated Magnesium and Zinc Gluconates*
- 5-7. **Gafarova A.R.** (Russia, Kazan) *Study of Radiation Induced Radicals in Sodium Gluconate*
- 5-8. **Kokorin A.I.** (Russia, Moscow) *EPR Study of Structural Peculiarities of Metal Oxides Intercalated by Benzoazoles*
- 5-9. **Konov K.** (Russia, Kazan) *CW EPR and ESEEM Study of the Verdazyl Radicals*
- 5-10. **Ostrovskaya I.K.** (Russia, Kazan) *On the Theory of Dynamic Heterogeneity of Segments of Linear Macromolecules Generated by the End Segments: the Frequency Nature of This Effect and Possibility of its Experimental Detection Using the Free Induction Decay of Deuterium Nuclei*
- 5-11. **Savinkov A.V.** (Russia, Kazan) *Molecular Mobility and State of n-Hexane Adsorbed in Pillared Montmorillonite Studied by 2D 1H NMR Relaxometry*
- 5-12. **Schäfter D.** (Germany, Stuttgart) *Novel Potential Multi-Qubit Systems with Very Rigid Bridging Ligands*
- 5-13. **Selivanov S.I.** (Russia, St.-Petersburg) *Scalar Relaxation Effects of the First and Second Kinds in NOESY Spectra of Small Organic Molecules in Liquid*

5–14. **Selivanov S.I.** (Russia, St.-Petersburg) *Conformational Analysis of Flexible Molecules in Liquid at Fast Exchange Condition and Population Ratio Determination on Base eNOE Data*

5–15. **Shurtakova D.V.** (Russia, Kazan) *Investigation of Octacalcium Phosphate by EPR Methods*

5–16. **Smorygina A.S.** (Russia, Novosibirsk) *Antimicrobial Peptide Chalciporin A in the Model Membrane*

5–17. **Sobornova V.V.** (Russia, Ivanovo) *Experimental Observation of Hidden Conformations of Strychnine by NMR Spectroscopy*

6. Spectroscopy and Imaging of Biological Systems

6–1. **Anisimov N.V.** (Russia, Moscow) *Fast Macromolecular Proton Fraction Mapping at 0.5 Tesla*

6–2. **Ovcherenko S.S.** (Russia, Novosibirsk) *Structural and Aggregational Features of Intrinsically Disordered Peptide RL2 – Human Milk κ -Casein Fragment with Antitumor and Cell Penetrating Properties*

6–3. **Sannikova N.E.** (Russia, Novosibirsk) *Influence of the Tylopeptin B Antimicrobial Peptide on Structure of Model Biological Membranes by Spin-Label EPR*

6–4. **Spitsyna A.** (Russia, Novosibirsk) *Novel Spin Label Based on OX063 Trityl Applied to Study Human Serum Albumin*

7. Other Applications of Magnetic Resonance and Related Phenomena

7–1. **Bayazitov A.A.** (Russia, Kazan) *Development of “Knee” and “Hand” Receiving and Transmitting Systems for a Specialized MRI with a 0.4 Tesla Field*

7–2. **Chen Jiafu** (China, Hefei) *Selenium-Nitrogen Free Radical (\bullet Nse) and Its EPR Studies*

7–3. **Falin M.L.** (Russia, Kazan) *The Trigonal Yb^{3+} Center in Lithium Calcium Hexafluoroaluminate*

7–4. **Frolova E.N.** (Russia, Kazan) *Spin Properties of the Fe(III) Complexes with Tetradentate Schiff Bases and Photosensitive 4-Styrylpyridine Ligands*

7–5. **Gafurov M.R.** (Russia, Kazan) *EPR of Single Nd^{3+} Ions in $CsCdBr_3$ Monocrystals*

7–6. **Ivanov D.** (Russia, Kazan) *The Study of Kerogen by NMR*

- 7-7. Karataş Ö. (Turkey, Kocaeli) *FMR Analysis of Magnetic Anisotropies in Co-Implanted TiO₂ Rutile*
- 7-8. Kondratyeva E.I. (Russia, Kazan) ³He in Contact with Nanostructures
- 7-9. L'vov S. (Russia, Kazan) *Hyperfine Coupling Constants in Me-Er (Me = Cu, Ag, Au) Binary Dilute Alloys*
- 7-10. Ovchinnikov I.V. (Russia, Kazan) *EPR of Spin-Crossover Compounds [Fe(bzacen)(tvp)]·BPh₄·nCH₃OH*
- 7-11. Timofeev I. (Russia, Novosibirsk) *Multi-Frequency EPR/ENDOR, DNP and AWG Pulse MW Spectroscopy of g-Engineered Triyl-Aryl-Nitroxide Biradicals*
- 7-12. Ulanov V.A. (Russia, Kazan) *EPR of the BaF_{2-x}:Ni crystals: Peculiarities of an Analysis of SHFS of the EPR Spectra of Ni³⁺ Centers when H_{ZFS} >> H_{gz} >> H_{SHFI}*
- 7-13. Yantsen N.V. (Russia, Saransk) *EPR Parameters Temperature Dependences of Carbon-Containing Composites*

XXI INTERNATIONAL YOUTH SCIENTIFIC SCHOOL "ACTUAL PROBLEMS OF MAGNETIC RESONANCE AND ITS APPLICATION" PROGRAM

24 September, Tuesday		
11.40-13.00	Morning Session	Institute of Physics, Hall, 2 nd floor
11.40-12.20	Vasil'ev S.G. (Russia, Chernogolovka) - <i>Application of multiple-quantum (MQ) NMR to study the structure and dynamics of dipolar coupled ½ spin networks in amorphous and crystalline solids</i>	
12.20-12.40	Bochkin G.A. (Russia, Chernogolovka) - <i>Investigation of the free induction decay in fluorine spin chains in fluorapatite in multi-pulse NMR experiment</i>	
12.40-13.00	Germov A.Yu. (Russia, Yekaterinburg) - <i>¹⁴N NMR and magnetic susceptibility of UN in the paramagnetic state</i>	
13.00-14.30	Lunch	
14.30-16.00	Afternoon Session	Institute of Physics, Hall, 2 nd floor
14.30-14.50	Savchenko S.P. (Russia, Yekaterinburg) - <i>Amplification of nuclear magnetostatic oscillations in ferromagnets</i>	
14.50-15.10	Mershev I.G. (Russia, Kaliningrad) - <i>Adiabatic excitation for NMR spectroscopy in magnetic materials</i>	
15.10-15.30	Saad M. (Russia, Kazan) - <i>Emergent Ferromagnetism and Flux Trapping in Dispersed Pyrolytic Graphite Flakes by Mild Vacuum Annealing</i>	
15.30-15.50	Khaliqzadeh A.Sh. (Azerbaijan, Baku) - <i>Features of photoelectric of GaS monocrystal with doped rare earth elements (Yb, Sm)</i>	
15.50-16.10	Parfishina A.S. (Russia, Kazan) - <i>The study of ¹⁶⁹Tm in a single crystal LiYF₄:Tm³⁺ (2%) by pulsed NMR method</i>	
16.10-16.30	Coffee-break	Institute of Physics, Hall, 2 nd floor
16.30-16.50	Yanilkin I.V. (Russia, Kazan) - <i>Ferromagnetic Resonance in Exchange Coupled Ultrathin Epitaxial CoO_x/Co/Ag/Fe/MgO Heterostructures</i>	
16.50-17.10	Skoryunov R.V. (Russia, Yekaterinburg) - <i>Nuclear magnetic resonance study of a carbon-substituted closo-hydroborate NaCB₁₁H₁₂ in nanoporous silica SBA-15</i>	
17.10-17.30	Khankishiyeva R.F. (Azerbaijan, Baku) - <i>EPR investigation of the irradiation crosslinking process of nitrile-butadiene rubber with added various types of nano-metal oxides</i>	
17.30-17.50	Razina E.A. (Russia, Kazan) - <i>High frequency EPR of rare-earth metal ions in LiYF₄</i>	
17.50-18.10	Timoshnikov V.A. (Russia, Novosibirsk) - <i>Investigation of Deferiprone Influence on Generation Oxygen Species in Redox Reactions with Iron and Copper Ions using EPR Spectroscopy with Spin Traps</i>	
18.10-18.30	Prokopyev D.A. (Russia, Yekaterinburg) - <i>NMR study of carbon encapsulated Ni@C nanoparticles</i>	
18.30-18.50	Kobchikova P.P. (Russia, Kazan) - <i>Studying cyclosporin D – micelle complex by high-resolution NMR: Obtaining information on the spatial structure</i>	
18.50-19.10	Ivanova A.V. (Russia, Kazan) - <i>Investigation of the interconversion process of pillar[5]arene using NMR spectroscopy and DFT method</i>	

25 September, Wednesday		
15.00-17.50	Afternoon Session	Institute of Physics, Hall, 2 nd floor
15.00-15.20	Skvortsova P. (Russia, Kazan) - <i>NMR in the study of pillar[5]aren-DNA complexes</i>	
15.20-15.40	Kovalenko E.A. (Russia, Novosibirsk) - <i>Cucurbit[7]uril behavior in PBS buffer solution and RPMI-1640 cell growth medium</i>	
15.40-16.00	Selyutina O. (Russia, Novosibirsk) - <i>The influence of chelators on lipid oxidation</i>	
16.00-16.20	Coffee-break	Institute of Physics, Hall, 2 nd floor
16.20-16.40	Kuzmikov M.S. (Russia, Ivanovo) - <i>Confirmation preferences of carbamazepine molecules in chloroform and supercritical CO₂ by NMR spectroscopy</i>	
16.40-17.00	Shurshalova G.S. (Russia, Kazan) - <i>Lovastatin and Their Interaction with Model Membranes by NMR Data</i>	
17.00-17.20	Kononova P.A. (Russia, Novosibirsk) - <i>Glycyrrhizin-induced changes in the dynamics of single-component and multi-component phospholipid bilayers</i>	
17.20-17.50	Kusova A.M. (Russia, Kazan) - <i>Protein-protein interactions according to protein translational diffusion</i>	

Spin-Lattice Relaxation Times of a Nitroxide Radicals in Solution Under the Influence of Spin-Exchange and Dipole-Dipole Interactions

M.M. Bakirov¹, B.L. Bales², I.T. Khairuzhdinov¹, K.M. Salikhov^{1,3}, R.N. Schwartz⁴

¹Zavoisky Physical-Technical Institute, Kazan, Russian Federation

²Western Institute of Nanoelectronics, University of California, Los Angeles, USA

³Institute of Physics, Kazan Federal University, Kazan, Russian Federation

⁴Electrical and Computer Engineering Department, University of California, Los Angeles, USA

e-mail: pinas1@yandex.ru

For solutions of nitroxide radicals, the shape of EPR spectra was obtained theoretically for arbitrary values of the microwave field induction, taking into account the contributions of the Heisenberg exchange and dipole-dipole interactions to the paramagnetic relaxation of electron spins. A detailed analysis of the effect of saturation in strong microwave fields is carried out. By comparing the experimental data with the results of numerical calculations of several characteristic parameters of the EPR spectrum, the value of the spin exchange rate and the spin-lattice relaxation time of the TEMPOL radical studied experimentally in this work are found. For the illustration, Fig. 1 demonstrates the saturation effect of integral intensity for the low field “nitrogen” hyperfine component of the ¹⁵N nitroxide free radicals EPR spectrum at different rate of the spin exchange at 315 K. In these simulations the fitting parameter were the rate of spin exchange and the rate of the spin-lattice relaxation.

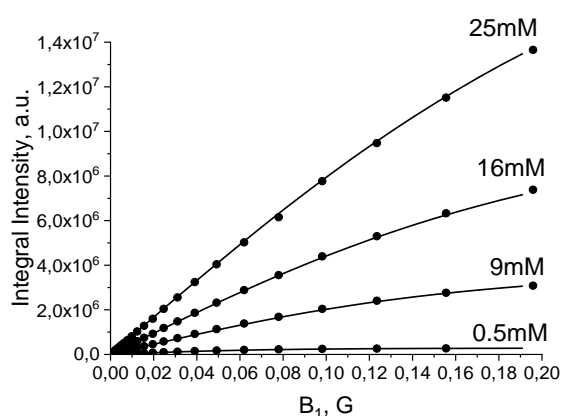


Fig.1. Dependences of integral intensity for low-field EPR line of Tempol¹⁵ND for different concentrations at 315 K. (closed circle-Tempol¹⁵ND experimental data, lines - are model saturation curves)

The spin exchange rate constant which was determined by analyzing spectra under saturation conditions are consistent with a value determined earlier using EPR spectra in linear response regime [1]. The value of the spin-lattice relaxation time obtained in the present work coincides well with the result obtained by the inversion-recovery method.

It is shown that the using of saturation curves for different characteristic parameters leads to almost the same values of the spin exchange rate and of the spin-lattice relaxation time.

[1] B.L. Bales, M.M. Bakirov, R.T. Galeev, I.A. Kirilyuk and K.M. Salikhov, Appl. Magn. Reson. **48**, 1399 (2017).

Electron Spin Relaxation and Motion in Solids: Spin, Spatial, Spectral

M.K. Bowman

Department of Chemistry and Biochemistry, University of Alabama, Tuscaloosa, AL, USA
Novosibirsk Institute of Organic Chemistry, Novosibirsk, Russian Federation

e-mail: mkbowman@ua.edu

Magnetic resonance is a very dynamic phenomenon. Even when the spin system is at equilibrium, there is constant motion and relaxation. All too quickly anything we may do to the spin system is lost and forgotten. This limits what we are able to do with spins, whether it is measuring nanoscale distances with DEER/PELDOR spectroscopy, transferring dynamic nuclear polarization from near an electron spin to bulk nuclei, or making complex calculations with spin qubits. One major limitation is imposed in solids by the interaction of an unpaired electron spin with its nearby nuclear spin and the mutual interactions of the nuclear spins.

Important but simple situations will be discussed. One is the phase memory relaxation of electron spins that limits resolution and sensitivity in echo-based measurements such as DEER/PELDOR, HYSCORE, and Pulse ENDOR. The dynamics of the nuclear spins often drives phase memory relaxation and also appears as spectral diffusion of the electron spins.

However, the electron spin also affects the nuclear spin dynamics. One aspect of this is the so-called nuclear spin diffusion barrier that prevents efficient conduction of nuclear spin hyperpolarization generated at a free radical to the bulk nuclei. This barrier is evident in the magnetic resonance spectrum of the nearby nuclei, which are readily observed via ESEEM, HYSCORE and ENDOR spectroscopies.

Fortunately, there are ways to change and perhaps control the spin system to obtain better resolution, longer distance measurements, slower relaxation, or a breach of the spin diffusion barrier. These include approaches such as echo refocusing, dynamic decoupling, isotopic editing, and changing spin multiplicity. Some examples will be shown.

Theory of Spin Pumping in Fe/NM

F.S. Dzheparov¹, K.L. Stankevich²

¹National Research Center “Kurchatov Institute”, ITEP, Moscow, Russian Federation

²Institute of Radio Engineering and Electronics, Russian Academy of Sciences, Moscow, Russian Federation

e-mail: dzheparov@itep.ru, kl.stankevich@physics.msu.ru

Ferromagnetic resonance in ferromagnet (Fe)/normal metal (NM) bilayers gives rise to so-called spin pumping effect, when precessing ferromagnetic electrons under the condition of the magnetic resonance inject spin polarization into the adjacent NM. This injected polarization produces pure spin current in NM layer [1]. Originally, the effect was described by the formalism based on mesoscopic theory, and reasonable agreement of the theory with experiments was declared, despite the typical samples are not mesoscopical. Another description, based on linear-response theory was developed in Refs. [2,3]. Different approach, is based on Landau-Lifshits-Gilbert equation in [4] and Bloch-Bloembergen equations in [5].

In the present work we develop this formalism to include an important case of metallic ferromagnets into the description of the spin pumping and to reveal the connection of the spin-current with the ferromagnet magnetization. Importance of the last dependence was indicated in Ref. [6]. We describe two possible regimes of the spin pumping. In the first one we consider the case when the speed of establishing of complete spatially uniform quasi-equilibrium in the ferromagnet is fast. In the second case the rate of establishment of quasi-equilibrium between localized and delocalized electrons in the ferromagnet is fast, but spatially homogeneous equilibrium is not established. We formulate initial equations and obtain their solutions; the detailed analysis of the results is fulfilled.

The work was partially supported by the RFBR Grants No. 17-02-00145 and No. 18-37-00170.

- [1] Y. Tserkovnyak, A. Brataas, G.E.W. Bauer and B.I. Halperin, *Rev. Mod. Phys.* **77**, 1375 (2005).
- [2] E. Šimánek, B. Heinrich, *Phys. Rev. B* **67**, 144418 (2003).
- [3] E. Šimánek, *Phys. Rev. B* **68**, 224403 (2003).
- [4] Y. Kajiwara, K. Harii, S. Takahashi et al., *Nature*, **464**, 262 (2010).
- [5] S.M. Rezende, R.L. Rodríguez-Suárez, A. Azevedo, *Phys. Rev. B* **88**, 014404, (2013).
- [6] V.A. Atsarkin, I.V. Borisenko, V.V. Demidov, T.A. Shaikhulov, *J. Phys. D: Appl. Phys.* **51**, 245002 (2018).

Multiple Quantum NMR Dynamics and Relaxation in One-Dimensional Systems

Eduard Feldman

Institute of Problems of Chemical Physics of RAS, Pr. Semenov, 1, Chernogolovka, Moscow Region, 142432, Russia

e-mail: efeldman@icp.ac.ru

Multiple quantum (MQ) NMR dynamics is the foundation of MQ NMR spectroscopy [1], which is widely used to study nuclear spin distributions in solids. At the same time, MQ NMR allows us to investigate decoherence of many-qubit coherent spin clusters since MQ NMR not only creates many-qubit coherent states but also permits the investigation of their relaxation under the action of a correlated spin reservoir [2]. One-dimensional spin systems open new possibilities for the investigation of decoherence, both theoretical and experimental, with MQ NMR methods. The point is that a consistent quantum mechanical theory of MQ NMR dynamics exists only for one-dimensional systems [3]. According to the developed theory [3], only MQ NMR coherences of the zeroth and plus/minus second orders arise in a one-dimensional spin chain initially prepared in the thermodynamic equilibrium state in the approximation of the nearest neighbor interactions.

The relaxation of the MQ NMR coherences can be studied [2, 4] on the evolution period of the MQ NMR experiment [1]. This period begins immediately after the preparation period [1] and the density matrix at the end of that period can be used as the initial state in the relaxation process. The relaxation of the MQ NMR coherences is caused by the secular (with respect to the external magnetic field) dipole-dipole interactions (DDI). We obtained [5,6] the time-dependencies of the intensities of MQ NMR coherences of the zeroth and second orders on the lengths of the evolution period and the preparation period using the ZZ model, which neglects the flip-flop part of the DDI. The obtained theoretical results are in a good agreement with the experimental data which were obtained on the linear chain of ^{19}F nuclei in a single crystal of calcium fluorapatite [5, 6]. We also calculated the second moments of the line shapes of MQ NMR coherences of the zeroth and second orders [7]. This allowed us to obtain semi-phenomenological formulae, describing the decay of MQ NMR coherences.

We showed that the second moment of the line shape of the MQ NMR coherence of the zeroth order does not depend on the flip-flop part of the DDI. The theoretical predictions agree with the obtained experimental data. It is shown that the relaxation of the MQ NMR coherence of the second order can be considered as a model of decoherence in many-qubit coherent clusters [8]. The dependence of the decoherence rate on the number of spins was also obtained. Dynamics and relaxation of MQ NMR coherences are investigated experimentally and theoretically at different orientations relative to the direction of the external magnetic field [9]. Universal curves for dynamics and relaxation were obtained, which describe the experimental data for different orientations of the investigated sample. Those curves prove the dipolar nature of the observed relaxation process [9].

- [1] J.Baum, M.Munowitz, A.N.Garroway, A.Pines, *J.Chem.Phys.* **83**, 5, 2015-2025 (1985).
- [2] G. Kaur, A. Ajoy, P. Cappellaro, *New J. Phys.* **15**, 9, 093035 (2013).
- [3] E.B.Fel'dman, *Applied Magnetic Resonance* **45**, 8, 797-806 (2014).
- [4] S.I.Doronin, E.B.Fel'dman, I.I.Maximov, *J. Magn. Reson.* **171**, 37-42 (2004).
- [5] G.A.Bochkin, E.B.Fel'dman, S.G.Vasil'ev, *Z.Phys.Chem.* **231**, 3, 513-525 (2017).
- [6] G.A.Bochkin, E.B.Fel'dman, S.G.Vasil'ev, V.I.Volkov, *Chem. Phys.Lett.* **680**, 56-60 (2017).
- [7] G.A.Bochkin, S.G.Vasil'ev, I.D.Lazarev, E.B.Fel'dman, *JETP*, **127**, 3, 532-538 (2018).
- [8] G.A.Bochkin, E.B.Fel'dman, S.G.Vasil'ev, V.I.Volkov, *Appl.Magn.Reson.* **49**, 1, 25-34 (2018).
- [9] G.A.Bochkin, E.B.Fel'dman, I.D.Lazarev, A.A.Samoilenko, S.G.Vasil'ev, *J.Magn.Reson.* **301**, 10-18 (2019).

The Time Reversal Symmetry and a Virtual Time Reversal Method in EPR Spectroscopy

I.I. Geru

Institute of Chemistry, Chisinau, Republic of Moldova

e-mail: iongeru11@gmail.com

The Kramers degeneration of energy levels in systems having an odd number of electrons, well-known in EPR spectroscopy, is due to the time-reversal symmetry [1]. Earlier we showed that six more “incomplete” time-reversal operators exist along with the Wigner time-reversal operator \mathbf{T} . Under the action of these operators, a change of the sign occurs not for all three spin projections operators, but only for one or only two of them [2].

In a specific physical situation, the Hamiltonian of the system is only invariant with respect to one of the seven time-reversal operators. Therefore, the interactions that violate the T -symmetry, are also violating the Kramers theorem. It is shown that the Kramers theorem is violated in five of the six cases of T -symmetry breaking. In the sixth case, the lowering of T -symmetry is not sufficient for violating the Kramers theorem.

It is proposed a virtual time reversal (VTR) method that could be used to find out the EPR spectrum registered when the time flows in the opposite direction. The essence of the method consists in registering the EPR spectrum both at $dt > 0$ (natural time flow) and $dt < 0$ (virtual time reversal).

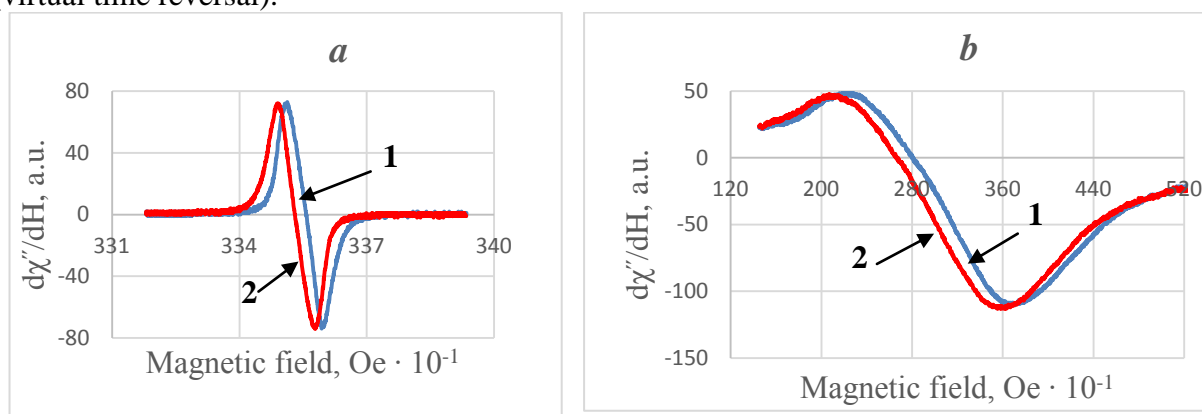


Fig. 1. EPR spectra of DPPH (*a*) and carbon nanotubes (*b*) registered by increasing of H (1) and by VTR method (rotation of the plane, containing the EPR spectrum, registered at decreasing of H , on 180° around the axis lying in that plane and passing through the point of resonance field orthogonally to \mathbf{H} with a virtual transformation $t \rightarrow -t$) (2).

Fig. 1 shows that the symmetric EPR line of DPPH (*a*) and the asymmetric one of carbon nanotubes (*b*) have the same shape as the EPR lines registered at a virtually reversed time flow. The non-coincidence of resonance fields (1 and 2) is caused by non-uniformity of the magnetic field scan at $dH/dt > 0$ and $dH/dt < 0$.

The coincidence of EPR line shapes both at the forward time flow and at its virtual reversal shows the presence of a time reversal symmetry. If such a coincidence is not present in some systems, it does mean that the Wigner’s time-reversal symmetry is violated.

The VTR method can be used in the study of not only the EPR spectra, but also the NMR, ENDOR, and others spectra.

[1] E.P. Wigner, Nachr. Acad. Wiss, Goettingen. Math. Phys. **31**, K1., 546 (1932).

[2] Ion I. Geru, Time-Reversal Symmetry – Seven Time-Reversal Operators for Spin Containing Systems, Springer Tracts in Modern Physics **281** (Springer Nature Switzerland AG, 2018), 362 pp.; <http://doi.org/10.1007/978-3-030-01210-6>.

FMR Studies of Thin Epitaxial Pd_{0.92}Fe_{0.08}/Pd_{0.96}Fe_{0.04} and Pd_{0.92}Fe_{0.08}/Ag/Pd_{0.96}Fe_{0.04} Heterostructures

A.I. Gumarov¹, I.V. Yanilkin¹, A.A. Rodionov¹, A.G. Kiiamov¹, A.M. Rogov¹,
R.V. Yusupov¹, L.R. Tagirov^{1,2}

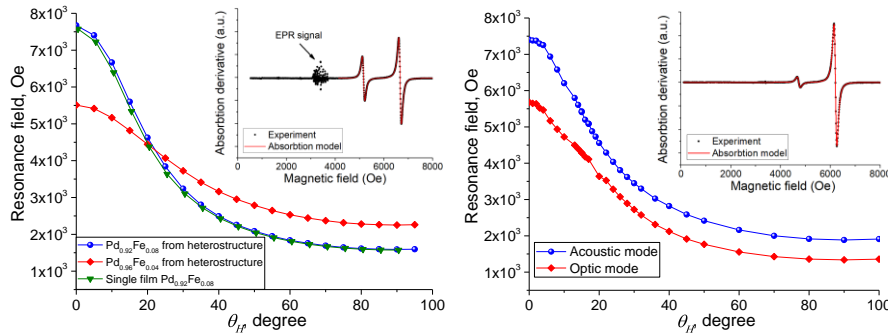
¹Institute of Physics, Kazan Federal University, Kazan, Russia

²Zavoisky Physical-Technical Institute, FRC Kazan Scientific Center of RAS, Kazan, Russia

e-mail: amir@gumarov.ru

The interest to dilute Pd_{1-x}Fe_x ($x = 0.01-0.10$) alloy is motivated by potential applications in superconducting spintronics [1]. In our previous works, we reported on successful synthesis of high-quality epitaxial Pd_{1-x}Fe_x films with $x = 0.01 - 0.8$ and a thickness of 20 nm [2,3]. Similar procedure is suitable for growing of ultrathin-layer epitaxial palladium-iron heterostructures. We expect exchange coupling for perfectly adherent epitaxial magnetic films, and almost no or a weak coupling in an epitaxial heterostructure where the magnetic layers are uncoupled by a 20-nm spacer of silver.

The Pd_{0.92}Fe_{0.08}/Pd_{0.96}Fe_{0.04} and Pd_{0.92}Fe_{0.08}/Ag/Pd_{0.96}Fe_{0.04} heterostructures with 20-nm thickness of every layer were synthesized by molecular-beam epitaxy technique (MBE system by SPECS) under the ultra-high, 3×10^{-10} mbar, vacuum conditions onto the (001)-oriented epi-polished MgO substrates. The epitaxial growth mode of the films was verified by LEED and XRD techniques. Magnetic properties were studied with VSM magnetometry (QD PPMS-9) and ferromagnetic resonance (FMR) – with X-band Bruker ESP300 spectrometer.



FMR spectra were recorded in the in-plane and out-of-plane experiment configurations [4]. The Pd_{0.92}Fe_{0.08}/Ag/Pd_{0.96}Fe_{0.04} sample played a role of reference sample, in which the magnetic layers are separated by the silver spacer layer and thus, magnetically uncoupled. Then, two quasi-independent resonances were observed with the stronger ferromagnetic Pd_{0.92}Fe_{0.08} layer having higher resonance field at $\theta_H = 0^\circ$ (along the film normal) and lower resonance field at $\theta_H = 90^\circ$ (in-plane alignment) compared with the weaker ferromagnetic Pd_{0.96}Fe_{0.04} layer (Fig. 1, left. Insets – FMR spectra for $\theta_H = 10^\circ$). The crossing of the resonances at about 20° was observed according to the expectations. In contrast, the FMR spectrum of the bi-layer Pd_{0.92}Fe_{0.08}/Pd_{0.96}Fe_{0.04} heterostructure shows no crossing at any angle between 0° and 90° (Fig. 1, right). Our analysis shows appearance of collective modes in the system and provides the film parameters and the coupling strength between them.

This work was supported by the RSF project No. 18-12-00459. Synthesis and analysis of the films were carried out at the PCR Federal Center of Shared Facilities of KFU.

- [1] V.V. Ryazanov, V.V. Bol'ginov, D.S. Sobanin *et al.*, Phys. Procedia **36**, 35 (2012).
- [2] A. Esmaeili, I.V. Yanilkin, A.I. Gumarov *et al.*, Thin Solid Films **669**, 338 (2019).
- [3] A. Esmaeili, I.V. Yanilkin, A.I. Gumarov *et al.*, J. Alloys Comp. (2019) (submitted).
- [4] M. Farle, Rep. Progr. Phys. **61**, 755 (1998).

Hyperfine Interaction Promoted Intersystem Crossing

Yu.E. Kandrashkin

Zavoisky Physical-Technical Institute, FRS KSC of RAS, Kazan, Russian Federation

e-mail: yuk@kfti.knc.ru

We present a revised mechanism of the intersystem crossing (ISC) in planar aromatic hydrocarbons which includes an additional pathway due to hyperfine interaction (HFI) promoted singlet-triplet transitions [1]. The influence of the HFI leads to a formation of extra components to the initial non-equilibrium state of the spin subsystem. Several properties of the initial state are predicted, including electron-nuclear ordering and coherence between the nuclear sublevels, as well as the correlation between nuclear spins. The analytical results are compared with the experimental data obtained on photoexcited pentacene in p-terphenyl [2]. In the case of the photoexcited pentacene, the initial spin density matrix developed by the HFI promoted ISC includes two main contributions:

$$\rho_{HFI} \approx -\frac{1}{2} S_z \sum_n a_{n,x} a_{n,y} I_{n,z} \quad (1)$$

$$\rho_{MIX} \approx S_z \sum_n (\lambda_x a_{n,y} I_{n,y} - \lambda_y a_{n,x} I_{n,x}) \quad (2)$$

where S_ζ and $I_{n,\zeta}$ are spin operators of the unpaired electrons and n -th nuclear spin ($\zeta = x, y, z$), λ_ζ and $a_{n,\zeta}$ describe the components of the spin-orbit coupling and the HFI, antisymmetric relative to the interexchange of the unpaired electrons.

The additional contributions to the initial density matrix adequately describe the observed properties in the electron spin echo enveloped modulation and the nuclear hyperpolarization experiments. In total, our analysis provides cogent arguments in favor of involvement of the nuclear spins in the ISC in photoexcited pentacene in p-terphenyl.

This work was partially supported by a Presidium RAS Program No. 5: “Photonic-technologies in probing inhomogeneous media and biological objects”

[1] Yu. E. Kandrashkin *Appl. Magn. Reson.* doi: s00723-019-01131-x (2019).

[2] G. Kothe, T. Yago, J. U. Weidner, G. Link, M. Lukaschek, and T. S. Lin, *J. Phys. Chem. B* **114**, 14755 (2010).

Determination T_1 and T_2 Relaxation Times from CPMG Phase Cycle Pulse Sequences

Iskander Khairuzhdinov, Ruslan Zaripov

Zavoisky Physical -Technical Institute, FRC Kazan Scientific Center of RAS, 420029 Kazan, Russia

e-mail: semak-olic@mail.ru

The Carr-Purcell-Meiboom-Gill (CPMG) pulse sequence is useful to avoid some decoherence pathways into the spin system [1,2]. Long train of echo signals enables efficient measurements of spin-spin relaxation time and the diffusion constant. When the EPR spectrum line width is much less than the microwave field strength, so-called non-selective excitation, the refocusing pulses can be effectively de-phase of magnetization to refocus the magnetic field inhomogeneity at each echo time [3]. In selective excitation case the magnetization will be particularly on longitudinal direction. This leads to a large number of echo signals (Fig 1.). Time decay of echo signals looks like exponential combination of relaxation times T_1 and T_2 in different proportions. Appearance of stimulated and other unwanted echoes can be a drawback in practice because they may interfere with the refocused primary echo. For the N-pulse sequence the number of necessary cycles increases to 2^N and thus for large N values the measuring times become unrealistically long.

In this work we describe way to build CPMG phase cycle sequences.

Analytical expressions for the first four echo signals within the spin density matrix formalism were obtained and analyzed. We performed numerical simulation of CPMG experiment for different relations between inter pulse delays and relaxation times values. Numerical simulations were compared with experimental data.

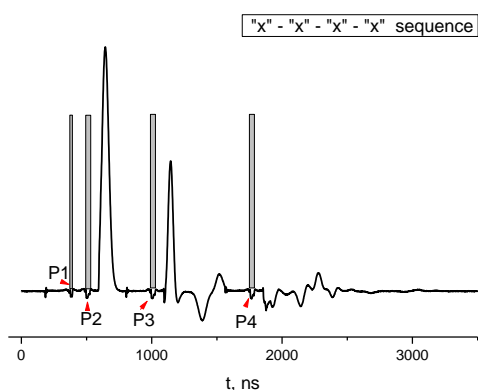


Fig 1. Four pulse echo train sequence.

The reported study was funded by RFBR according to the research project № 18-32-00428.

- [1] H.Y. Carr, E.M. Purcell Phys. Rev. **94**, 630 (1954).
- [2] S. Meiboom, D. Gill Rev. Sci. Instrum. **29**, 688 (1958).
- [3]. Y.-Q. Song Journal of Magnetic Resonance **157**, 82–91 (2002).

Spin Exchange in Solutions of Paramagnetic Particles. *Paradigm Shift*

K.M. Salikhov

Zavoisky physical-technical institute of Russian academy of sciences, Kazan, Russia

e-mail: kevsalikhov@mail.ru

Summary of new vs existing paradigm of spin exchange and its manifestations in EPR spectroscopy is presented.

The new paradigm of spin exchange is fundamentally different from the existing paradigm because:

New paradigm introduces non-equivalent spin exchange, along with an equivalent exchange. New paradigm also recognizes at least three different types of changes in the state of spins, i.e. three types of elementary acts in which the spins of unpaired electrons participate: decoherence of spins, transfer of spin coherence between spins, transfer of spin excitation energy.

The fundamental difference between the new paradigm of spin exchange and the existing paradigm is a multiparticle approach to the description of the motion of all spins in solution. The new paradigm is based on the fact that the transfer of spin coherence during random bimolecular collisions of particles form collective modes of motion of coherence of all spins in solution.

The new paradigm of spin exchange takes into account the transfer of spin coherence induced by the dipole-dipole interaction.

In the new paradigm, the EPR spectrum is the sum of mixed-shape lines corresponding to the collective modes of spin motion. They are the sum of the symmetric Lorentzian absorption line and the asymmetric Lorentzian dispersion line with the frequency and resonance width of the collective mode.

The new paradigm treats the phenomenon of exchange narrowing of EPR spectra in a completely different way. The phenomenon of exchange narrowing occurs because, at a high rate of spin coherence transfer, only one of the collective modes has a large oscillator force, and the other modes have a zero-tending oscillator force, i.e. are the so-called “dark” states.

The new paradigm of spin exchange gives a completely different interpretation of the effect of saturation of EPR spectra of dilute solutions of paramagnetic particles. In fact, due to the transfer of coherence and the transfer of spin excitation between the spins in the microwave field, composite quasiparticles caused by the interaction of photons with the spin system are formed. These quasiparticles can be called spin polaritons.

The protocol for determining the rate of spin exchange processes from EPR spectroscopy data in the new paradigm is quite different from the protocol in the existing paradigm of spin exchange.

This work was supported by the Program of fundamental research of the Presidium of the Russian academy of sciences

- [1] Yu.N. Molin, K.M. Salikhov, K.I. Zamaraev. Spin Exchange. Principles and Applications in Chemistry and Biology. Springer Verlag, Heidelberg Berlin (1980).
- [2] K.M. Salikhov, A.G. Semenov, Yu.D. Tsvetkov. Electron spin echo and its application. Nauka, Siberian branch, Novosibirsk (1976).
- [3] K.M. Salikhov. J. Magn. Res. 63, 271-279 (1985).
- [4] B.L. Bales, M. Peric. J. Phys. Chem. B **101** 8707 (1997).
- [5] K.M. Salikhov. Appl. Magn. Reson. 47, 1207–1228 (2016).
- [6] B.L. Bales, M. M. Bakirov, R. T. Galeev, I. A. Kirilyuk, A. I. Kokorin & K. M. Salikhov. Appl. Magn. Reson. 48, 1375-1397 (2017).
- [7] K.M. Salikhov. Appl. Magn. Reson. 49, 1417–1430 (2018).
- [8] K.M. Salikhov. UFN, 189, issue 10 (2019) DOI 10.3367/UFNe.2018.08.038421.
- [9] B.L. Bales, M. Meyer, S. Smith, M. Peric. J. Phys. Chem. A **112** 2177-2181 (2008).

Multiple-Quantum NMR Spectroscopy and Quantum Information Delocalization in Solids in the Presence of Magnetic Fields Inhomogeneities

A.A. Lundin¹, V.E. Zobov²

¹N.N. Semenov Institute of Chemical Physics, RAS, 117977, Moscow, Russia

²Kirensky Institute of Physics, Federal Research Center KSC SB RAS, Krasnoyarsk, Russia

e-mail: rsa@iph.krasn.ru

The process of the delocalization initially localized quantum information covering all particles of the system is accompanied by redistribution of this information and the appearance of various, generally speaking, not local correlations. In particular, by means of above correlations the quantum register of the computer can be created. This redistribution process of information to various correlations (scrambling) may be accompanied by irreversible violations in the transferring one. These violations can be caused by a variety of reasons. The mentioned disorders refer as loss of coherence (decoherence) as a rule. In particular, decoherence can be caused by imperfection of measuring equipment.

For the study of scrambling, determining its speed, etc., four-particle time correlation functions (TCF) with the English abbreviation OTOC (out-of-time-ordered correlator) are used [1 - 3]. These TCF's, associated with information entropy, contain specific information about the most intimate processes occurring in the system. For example, many-particle entanglement, many-body localization, the development of chaos, and so on. In multiple-quantum spectroscopy, TCF's OTOC's is realized as the second moment of the multiple-quantum NMR spectrum [3].

Usually, the theoretical studies of these TCF's exploit numerical calculations for small spin clusters. However, we have shown analytically that for spin systems with a secular dipole-dipole (DDI) interaction or with the effective two-quantum interaction obtained from one, the second moment of the multiple-quantum spectrum (OTOC) is growing up exponentially with time [4]. The latter means that all the nuclear spins of the sample would be quickly correlated, if there are no processes of decoherence. It has been shown [5] that at the presence of, for example, randomly distributed across the crystal inhomogeneities of magnetic fields exceeding the inter-nuclear DDI, the exponential growth of the TCF is replaced by a power one, i.e., the increase in the number of correlated spins slows down with time, and the excitation is largely localized. This "phase transition", previously discussed for other systems [1], probably associates with the termination of the "entanglement" of the wave functions of spins. Due to the dispersion of local fields, these functions become separable. The effect can be clarified for a pair of 1/2 spins. For DDI, the singlet and triplet combinations will be eigenfunctions, while in the presence of an inhomogeneous field, the products of the functions in the " S_z " representation will become eigenfunctions.

[1] R.-Q. He and Z.-Y. Lu, Phys. Rev. B **95**, 054201 (2017).

[2] K.X. Wei, C. Ramanathan, and P. Cappellaro, Phys. Rev. Lett. **120**, 070501 (2018).

[3] K.X. Wei, P. Peng, O. Shtanko, I. Marvian, S. Lloyd, C. Ramanathan, and P. Cappellaro, arXiv:1812.04776.

[4] V.E. Zobov and A.A. Lundin, J. Exp. Theor. Phys. **103**, 904 (2006).

[5] V.E. Zobov and A.A. Lundin, JETP Letters **105**, 514 (2017).

Intensity of EPR Absorption Lines in Semiconducting Substances

A.M. Zyuzin, A.A. Karpeev, N.V. Yantsen

National Research Mordovia State University, Saransk, Russian Federation

e-mail: zyuzin.am@rambler.ru

The influence of the skin effect and active losses in samples of the semiconducting composite on the EPR absorption line intensity I is investigated. Let the field $h(x)$ of the wave propagating inside the sample decay with the distance x from the surface as $h(x) = h_0 e^{-x/\Delta}$, Δ - skin depth. The field of the signal reflected from the volume element dV located at depth x , and hence the magnitude of its change due to resonance absorption, as a result of the reverse passage to the sample surface will also attenuated as $e^{-x/\Delta}$. This is equivalent to doubling the path on which attenuation occurs.

Since the power density of the microwave field $w \sim \chi'' h^2$, the calculation of the coefficient $\beta(V)$, which takes into account the effect of the skin-effect on the specific intensity $J = I/V$ for samples of cubic shape, was made using the expression:

$$\beta(V) = \frac{24}{a^3} \int_0^{a/2} e^{-\frac{4(a/2-x)}{\Delta}} x^2 dx, \quad (1)$$

where a is the length of the cube edge.

To determine the coefficient $\lambda(V)$, taking into account the effect of active losses in the sample on the intensity, a control sample was used. A number of the control sample hyperfine structure lines spectrum to the left and right of the test sample absorption line were well resolved.

On Fig. 1 shows the experimental and calculated $J/J_0 = \beta(V)\lambda(V)$ dependences of the specific intensity on the sample volume for various values of specific volume resistance. It is seen that the experimental and calculated results agree fairly well with each other.

It is shown that, depending on the conductivity of the investigated

substance, the specific intensity of the absorption line may decrease severalfold with increasing sample volume.

The reported research was funded by Russian Foundation for Basic Research and the government of Mordovia Republic of the Russian Federation, grant № 18-48-130015 r_a.

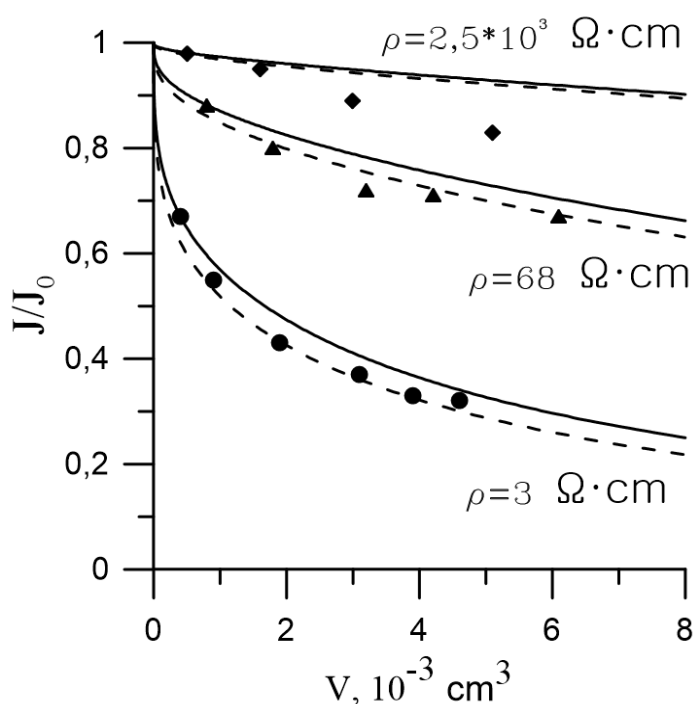


Fig.1. Experimental (points) and calculated dependences of the specific intensity on the sample volume for various values of ρ . The solid line is a sample of a cubic shape, the dashed line is a sample of a spherical shape.

Determination of Insulating Oil Moisture Content by NMR Spectroscopy

M. Volkov, O. Turanova, A. Turanov, L. Gafiyatullin, M. M. Akhmetov

Zavoisky Physical-Technical Institute, FRC Kazan Scientific Center of RAS, Kazan, Russia

e-mail: mihael-volkov@yandex.ru

Insulating oils have wide range of application. They are used in power transformers, turbines of electric power systems, circuit breakers and so on. Some moisture content is always present in them. It increases with the course of time and once the water molecules begin to combine into associates. This phase separation occurs at a water concentration of the order of 10 mg per kg of oil. Such a change is critically important for insulating oils, because it significantly reduces their insulation properties: breakdown voltage, dielectric permeability and so on. As a result, the need of measuring the water content in oil arises periodically.

Now the standard method of measuring the water content in oil is the Karl Fischer titration, however, it has some drawbacks. Therefore new methods of determining the moisture content of oil with a small fraction of water are being developed.

NMR spectroscopy can be used as one of such methods. At the present time NMR is widely used in scientific studies for the identification and determination of amounts of substances in mixtures due to its high sensitivity. Using NMR spectroscopy, three oil samples were studied in this work – fresh mineral GK grade transformer oil, fresh synthetic Midel 7131 oil and benzene containing a defined admixture of water. In a typical ^1H NMR spectrum of transformer oil the signals of aliphatic groups have chemical shifts of 0-3.7 ppm, aromatic group signals have those of 6-7.5 ppm and the weak signal from water has that ≈ 4.8 ppm. The ^1H NMR spectra of the studied GK and Midel transformer oils were recently published [1].

All the described here ^1H NMR spectra were recorded on an Avance III 600 Bruker NMR spectrometer. In the beginning, we obtained a usual ^1H NMR spectrum of transformer oil. Then, we found a water signal in this spectrum and in accordance with its spectral width and chemical shift value we matched the duration and carrier frequency of a selective 180° pulse for it. After that we performed the recording the NMR spectrum with using of spin echo pulse sequence, where the 180° pulse was selective (such a pulse excites effectively only the water signal). It allowed us to increase the receiver gain value in 500 times. In both cases, the coaxial tube insert containing CD_3CN was used for stabilizing the homogeneous static magnetic field via the deuterium channel of the NMR spectrometer.

The numerical values of the integral intensities of the water signals recorded by the pulse sequence with the selective 180° pulse and with the same experimental parameters were determined both for GK and Midel transformer oils and for benzene. Taking into account the fact that under such experimental conditions the $W_{\text{oil}} \cdot m_{\text{oil}} / I_{\text{oil}}$ ratio is constant (where W_{oil} is the moisture content of the oil, m_{oil} is its mass in NMR tube and I_{oil} is the integral intensity of the water signal) and also that the moisture content of benzene is defined, we can calculate the moisture content of the studied GK and Midel transformer oils. In the case of a low concentration of water the accuracy of water content determination based on NMR is higher than that based on KF titration. The proposed method has great potential both for an improvement and for practical applications.

[1] M. Volkov, O. Turanova, A. Turanov, IEEE Trans. Dielectr. Electr. Insul. **25**, 1989 (2018).

SARA Analysis and NMR Relaxation as Prediction Techniques to Estimate the SARA Composition of Heavy and Light Oils – Correlations and Deviations

Ameen A. Al-Muntaser^{1,2}, Mikhail A. Varfolomeev^{1,2}, Vladimir Y. Volkov², Nailia M. Khasanova⁴, Boris V. Sakharov^{2,3}, Muneer A. Suwaid^{1,2}

¹ Department of Petroleum Engineering, Kazan Federal University, Kazan 420008, Russia

² Department of Physical Chemistry, Kazan Federal University, Kazan 420008, Russia

³ State Research Center for Applied Microbiology & Biotechnology, Obolensk 142279 Moscow Region, Russia

⁴ Institute of Geology and Petroleum Technologies, Kazan Federal University, Kazan 420008, Russia

e-mail: aalmuntaser@mail.ru

Eleven samples of crude oil with a wide range of API gravity values (4.6–42.0°), including extra-heavy, heavy, medium and light crude oil, were investigated using the method of low-field nuclear magnetic resonance (LF NMR) and traditional SARA (saturated, aromatic, resins and asphaltenes) fractionation. By means of the traditional SARA analysis (with open column liquid chromatography) oil samples were divided into four classes of chemical groups, namely: saturates, aromatics, resins, and asphaltenes. A preliminary review of the full NMR decays of the transverse magnetization of protons of crude oils in situ makes it easy to determine the type of samples analyzed by the shape and duration of these curves [1]. Mathematical analysis of these curves makes it possible, without destroying samples, to evaluate the content high molecular weight including asphaltenes and resins with short T2 times, and low molecular weight (light) fractions saturates and aromatics including light and heavy aromatics characterized by longer relaxation times T2 and high mobility of molecules. Comparison of the results show high correlation coefficient values between the LF NMR and traditional SARA method data for asphaltenes and resins (R2 about 0.98 and 0.91, respectively) and for the sum of light fractions including saturates and aromatics (R2 ≈ 0.97). At the same time, the correlation coefficient for saturated and aromatic compounds separately gave us weak values (R2 ≤ 0.44 and 0.10, respectively). These low correlations are explained by the fact that in saturates and aromatics there are many molecules with the same molecular weight and, accordingly, with small differences in mobility, that leads to the fusion or coincidence of their NMR relaxation times. These results show that the use of LF NMR relaxation as an alternative method for studying the composition of crude oil allows the determination of asphaltenes, resins and the sum of light fractions without their extraction (in situ), which greatly simplifies and accelerates conventional chromatographic analysis. Component composition determinations can be made for different types of crude oil in a wide range of API density and viscosity values.

[1] 2018. Application of high resolution NMR (1 H and 13 C) and FTIR spectroscopy for characterization of light and heavy crude oils. *J. Pet. Sci. Eng.* 168, 256–262.

[2] Sanchez-Minero, F., Ancheyta, J., Silva-Oliver, G., Flores-Valle, S., 2013. Predicting SARA composition of crude oil by means of NMR. *Fuel* 110, 318–321.

Spin Superfluidity at Room Temperature

Yu.M. Bunkov¹, A.R. Farhutdinov², T.R. Safin², M.S. Tagirov^{2,3},
and P.M. Vetoshko¹

¹Russian Quantum Center, Skolkovo, 143025 Moscow, Russia

²Kazan Federal University, 420008, Kazan, Russia

³Institute of Applied Research of Tatarstan Academy of Sciences, 420111, Kazan, Russia

e-mail: azertli@mail.ru

The conventional magnon Bose-Einstein condensation (BEC of magnons with $k = 0$) has been observed in magnetically ordered materials with repulsive interaction between magnons. In particular it was observed in Yttrium Iron Garnet (YIG) film, magnetized perpendicular to the surface. For YIG film the critical density of non-equilibrium magnons for BEC condensation is $N_{BEC} \sim M - M_z = M(1 - \cos \beta)$, and corresponds to a deflection of precessing magnetization by an angle $\beta \sim 3^\circ$ [1]. Here M is the magnetization and M_z – its projection on the magnetic field. In these conditions the eigen state of magnon BEC is determined by its frequency and does not depend on the exciting RF power [2].

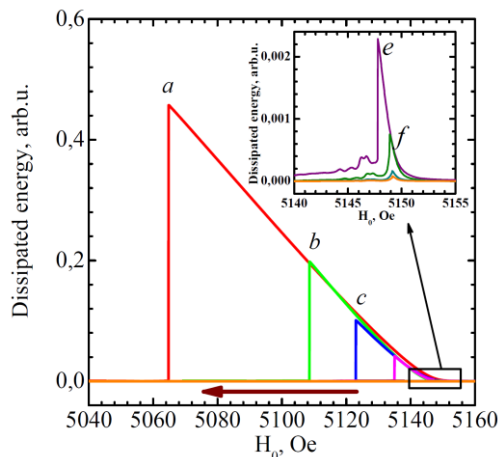


Fig.1. The energy dissipated by a magnon spin system at a magnetic field sweep at different level of exciting RF power. The energy was calculated as a product of absorption signal and the amplitude of magnetic field. The dissipated energy depends on a frequency shift from the resonance and does not depend on the RF power! The enlarged scale is shown in the inset.

The BEC state persists permanently at the conditions, when the losses (evaporation) of quasiparticles are replenished by an excitation of new quasiparticles. This is the first permanent superfluid state, which exists at room temperature. The energy gap of magnon superfluid state can be adjusted by RF pumping frequency. Our discovery opens the way for observation of coherent quantum transport phenomena at room temperature, like magnetic Josephson effect, long distance spin transport, phase slippage, Goldstone modes (analog of second sound in superfluid ^4He) and others. It can be used in many quantum applications of spin superfluidity at room temperature.

[1] Yu.M. Bunkov and V.L. Safonov, *J. Magnetism Magnetic Materials*, **452**, 30–34 (2018).

[2] Yu.M. Bunkov et al., <https://arxiv.org/abs/1810.08051>.

Hyperpolarisation Techniques for the Investigation of Enzyme-Inhibitors and Functional Nanomaterials

Gerd Buntkowsky

Technische Universität Darmstadt, Eduard-Zintl-Institut für Anorganische und Physikalische Chemie, Alarich-Weiss-Straße 8, Darmstadt, 64287, Germany

e-mail: gerd.buntkowsky@chemie.tu-darmstadt.de

Hyperpolarisation techniques such as Dynamic Nuclear Polarization (DNP) or Parahydrogen Induced Polarization (PHIP) are among the most versatile tools for NMR signal enhancement in solid-state respectively solution NMR. In the present talk we first give a short introduction into DNP and PHIP, followed by a number of examples from our recent work. The first set of examples describe results about the dynamic nuclear polarization (DNP) enhanced solid-state nuclear magnetic resonance (NMR) spectroscopy on nanostructured functional materials. First studies on materials based on crystalline nanocellulose (CNC) or microcrystalline cellulose (MCC) and silica nanoparticle, which are used as support material for functionalization or in combination with heterocyclic molecules as ion conducting membranes are reported. Then studies on mixed metal oxides such as V-Mo-W oxides, which are employed as heterogeneous catalyst in bulk-scale production of basic chemicals are shown. The second set of examples shows results from our investigations of a bioactive derivative of the sunflower trypsin inhibitor-1 (SFTI-1), which inhibits matriptase, a colon cancer related enzyme, employing parahydrogen based techniques. The PHIP activity of the inhibitor was achieved by labeling the tetradecapeptide with O-propargyl-L-tyrosine. Employing a carefully optimized automatized PHIP setup. In 1D-PHIP experiments an enhancement of up to ca. 1200 compared to normal NMR was found. This huge enhancement factor permitted the ultrafast single scan detection of 2D-TOCSY spectra of micromole solutions of the PHIP labelled inhibitor. The application of parahydrogen for the detection of low-concentrated intermediates of hydrogenation reactions via the PANEL (PARTIAL NEgative Line experiment) is discussed. Finally some recent results on substituent influences on the SABRE activity of Ir complexes with heterocyclic carbene ligands are discussed.

Multinuclear Dipolar NMR Spectroscopy in Liquid Crystals

S. V. Dvinskikh^{1,2}

¹ Department of Chemistry, KTH Royal Institute of Technology, Stockholm, 10044, Sweden

² Laboratory of Bio-NMR, St. Petersburg State University, St. Petersburg, 199034, Russia

e-mail: sergeid@kth.se

Homo- and hetero-nuclear dipolar spin couplings provide detailed information on dynamic processes and structural properties at the molecular level in anisotropic materials. In liquid crystals, in contrast to isotropic phase, the motion of molecules is not fully isotropic. Thus, the residual dipolar coupling, left after the fast motions, is not averaged to any lower value. ¹³C-¹H dipolar couplings in liquid crystals with natural carbon-13 abundance and ¹⁵N-¹H couplings in ¹⁵N-labelled samples are routinely measured by separated local field spectroscopy in static or magic-angle-spinning samples [1]. Recording ¹³C-¹⁵N and ¹³C-¹³C dipolar NMR spectra in unlabelled materials is challenging because of the combination of two rare isotopes; the fraction of the molecules containing ¹⁵N-¹³C pairs and ¹³C-¹³C pairs is about 0.004% and 0.01%, respectively.

In this report, we describe multinuclear NMR techniques to measure short- and long-range ¹³C-¹⁵N and ¹³C-¹³C dipolar couplings in highly ordered liquid crystalline samples with natural isotopic abundance [2,3,4,5]. Coupling in carbon-13 spin pairs are obtained in double-quantum correlation 2D experiment, where each coupled pair gives a pair of dipole-split doublets [5,6]. We have recently introduced new techniques to selectively record ¹³C and ¹⁵N spectra of naturally occurring ¹³C-¹⁵N spin pairs while suppressing signals of the uncoupled isotopes [3,4,5]. The maximum sensitivity gain was obtained using a ¹³C detection scheme with a ¹⁵N double quantum filter and cross-polarization from protons.

We demonstrate resolved ¹³C-¹³C and ¹³C-¹⁵N dipolar spectra in various mesophases. Coupling constants in the range 10-1000 Hz between spins separated by up to five chemical bonds are measured. Presented experimental methods to characterize dipolar couplings in unlabelled materials provide novel routes to the investigations of molecular structure and dynamics in mesophases. The techniques have been recently applied to investigate local molecular order in novel materials - ionic liquid crystals [3,5,7].

This work was supported by the Swedish Research Council and by the RFBR grant 17-03-00057.

- [1] S. V. Dvinskikh, in *Modern Methods in Solid-State NMR: A practitioners' Guide*, ed. P. Hodgkinson, RSC, Abingdon, 2018.
- [2] L. Jackalin, S. V. Dvinskikh. *Z. Phys. Chem.* **231**, 795 (2017).
- [3] M. Cifelli, V. Domenici, V.I. Chizhik, S.V. Dvinskikh. *Appl. Magn. Reson.* **49**, 553 (2018).
- [4] L. Jackalin, B. B. Kharkov, A. V. Komolkin, S. V. Dvinskikh. *PCCP* **20**, 22187 (2018).
- [5] J. Dai, B. B. Kharkov, S. V. Dvinskikh. *Crystals* **9**, 18 (2018).
- [6] D. Sandström, M.H. Levitt. *JACS* **118**, 6966 (1996).
- [7] J. Dai, B. B. Kharkov, S. V. Dvinskikh. *Crystals*, Submitted (2019).

Multi-frequency Rapid-scan EPR

Sandra S. Eaton, Laura Buchanan, Lukas Woodcock, Joseph McPeak, George A. Rinard,
Richard W. Quine, Yilin Shi, and Gareth R. Eaton

Department of Chemistry and Biochemistry, University of Denver, Denver, CO 80210, USA

e-mail: Gareth.eaton@du.edu

Rapid scan EPR has been implemented at 250 MHz, 700 MHz, 1 GHz, 9-10 GHz [1–4], at 94 GHz [5], and at higher frequencies [6]. At 1 GHz and lower frequencies, the emphasis is on in vivo imaging of species whose relaxation times are too short for effective imaging with pulse techniques. For oximetry with trityl radicals, pulse T_1 measurement is the method of choice. For almost all other in vivo measurements, the desired information is obtained using nitroxide radicals. The scan width needed to measure the full nitroxide spectrum is within the range achievable with rapid scan. Thus, the entire spectrum of interest can be scanned many thousands of times per second. Spectral-spatial imaging, using the full nitroxide spectrum, has been accomplished at 250 MHz (ca. 9 mT) [7]. X-band rapid scan is poised to replace normal field-modulated CW EPR [8]. Bruker is implementing rapid scan, and has announced an accessory to the Bruker X-band spectrometers. All of these applications use sinusoidal or linear magnetic field scans. At higher frequencies, the bandwidth of the resonator can be large enough to permit measurement of organic radicals, such as nitroxides, using microwave frequency scans [5,6].

- [1] Rapid Scan Electron Paramagnetic Resonance, G.R. Eaton and S.S. Eaton, *eMagRes*, **5**, 1529–1542 (2016). DOI 10.1002/9780470034590.emrstm1522.
- [2] Rapid Scan Electron Paramagnetic Resonance, G.R. Eaton and S.S. Eaton, *Handbook of EPR Spectroscopy: Fundamentals and Methods*, D. Goldfarb and S. Stoll, eds., John Wiley & Sons, 503 - 520 (2018).
- [3] Tabletop 700 MHz EPR Imaging Spectrometer, L.A. Buchanan, G.A. Rinard, R.W. Quine, S.S. Eaton, and G.R. Eaton, *Conc. Magn. Reson. B, Magn. Reson. Engin.* **48B** (2018).
- [4] Field-Stepped Direct Detection Electron Paramagnetic Resonance, Z. Yu, T. Liu, H. Elajaili, G.A. Rinard, S.S. Eaton, and G.R. Eaton, *J. Magn. Reson.* **258**, 58 – 64 (2015).
- [5] J.S. Hyde, R.A. Strangeway, T.G. Camenisch, J.J. Ratke, W. Froncisz W-band frequency-swept EPR, *J. Magn. Reson.* **205**, 93–101 (2010).
- [6] O. Laguta, M. Tucek, J. van Slageren, P. Neugebauer Multi-frequency rapid-scan HF-EPR. *Journal of Magnetic Resonance* 296, 138–142 (2018).
- [7] M. Tseitlin, J.R. Biller, H. Elajaili, V. Khramtsov, I. Dhimitruka, G.R. Eaton, and S.S. Eaton, New spectral-spatial imaging algorithm for full EPR spectra of multiline nitroxides and pH sensitive trityl radicals. *J. Magn. Reson.* **245**, 150 – 155 (2014).
- [8] X-Band Rapid-scan EPR of Samples with Long Electron Relaxation Times: A Comparison of Continuous Wave, Pulse, and Rapid-scan EPR, D.G. Mitchell, M. Tseitlin, R.W. Quine, V. Meyer, M. Newton, A. Schnegg, B. George, S.S. Eaton, and G.R. Eaton, *Mol. Phys.* **111**, 2664-2673 (2013).

Milestones in the 62 years Bruker EPR History

Peter Höfer¹, Uwe Eichhoff²

¹Bruker BioSpin GmbH, D 76287 Rheinstetten, Germany, Silberstreifen 4

²Bruker BioSpin GmbH retired; D 76571 Gaggenau, Germany, Max Hildebrandt-Str.40

e-mail: Peter.Hoefler@bruker.com, barbara.uwe@t-online.de

Commercial EPR spectrometers must be universal and offer optimal sensitivity and resolution for all methods and applications. Additionally they should be easily adaptable to other frequency bands. These requirements for cw-EPR have been fulfilled over the years with the development of a signal channel with 24 bit resolution and fast conversion time resulting in a dynamic range of up to 106 db resolving 256.000 points on the y-axis with a minimal conversion time of 320 μ sec. An extremely stable magnetic field controller allows a sweep of 256.000 points. Even an exceptional sweep range with 180.000 points over 14 kG can be realized resulting in 80mG resolution. The sensitivity of the EPR has increased in consecutive steps. In the early 1970 a S/N on the weak pitch of 200:1 was a good value. Improved klystrons led to a twofold increase in our new ESP 300. When good klystrons became almost unavailable, Bruker developed a Gunn diode locked to a cavity, which gave together with a new super high Q cavity (SHQE) an improvement in S/N of more than one order of magnitude. So far all the main requirements for a universal cw-EPR spectrometer for scientific applications have been met successfully. Even with all experience in pulse- and FT-NMR Bruker hesitated a long time to start the development of Pulse EPR. We were convinced, that the only commercially satisfied solution would be a universal high power pulse/FT-EPR spectrometer enabling the use of all known pulse methods and even flexible enough to incorporate new methods unknown at that moment. In 1987 with the ESP380 the first commercial pulse EPR spectrometer was introduced. This was no more an improvement of the previous EPR, this was a revolution in EPR instrumentation. Some necessary microwave-components were not available on the market and had to be developed and produced by the company itself. To cope with the extremely short relaxation times, necessitating high bandwidths, a new line of resonators had to be developed. In 1996 the new universal ELEXSYS spectrometer optimized for cw (E500, E600) and pulse/FT-mode E580, E680) was introduced with a time resolution of 4 nanoseconds. The patternJet II created the pulse sequences and the transient recorder SpecJet II was responsible for the registration of the fast transient signal with a digitization speed of 1 GHz, resulting in a sweep range of 500 MHz. Pulse sequences can be adjusted directly looking at the signal. To overcome the problem of limited bandwidth an arbitrary wave form generator SpinJet-AWG was developed allowing to edit any pulse form with any phase, frequency and modulation. These shaped pulses have a broader bandwidth at a lower power level and significantly increase to possibilities of all Pulse EPR experiments. In contrary to NMR the short EPR-relaxation-times in the nsec range allow a S/N-increase in FT-EPR as compared to cw-EPR only for a very few samples. The merit of Pulse EPR is the access to new information about the spin system but not a gain in sensitivity. During the last year the rapid scan EPR has been developed [1]. An extremely fast, sinusoidal or triangular sweep is applied to the sample in a rapid passage The resonance condition is hit in a time short compared to the relaxation time and in this way saturation is avoided. Compared to standard signal/noise gain of 2 orders of magnitude seems to be possible. In cooperation with the Eaton-group in Denver Bruker has introduced a rapid scan accessory for the ELEXSYS spectrometers. Rapid scan may also give new possibilities for EPR imaging in the much less sensitive S- and L-bands for biomedical research [2].

[1] D.G. Mitchell, R.W. Quine, M. Tseitlin, A.A. Eaton, G.R. Eaton *JMR* **214** (2012) 221-226.

[2] J.R. Biller, M. Tseitlin, R. Quine, G.A. Rinard, H.A. Weismiller et al. *JMR* **242** (2014) 162-168.

Spin-Electric Coupling Revealed by Electric Field Modulated EPR

M. Fittipaldi¹, A. Cini¹, G. Annino², A. Vindigni³, A. Caneschi⁴, B. Kintzel⁵, M. Böhme⁵, W. Plass⁵, and R. Sessoli⁶

¹Department of Physics and Astronomy and INSTM Research Unit, University of Florence, via Sansone 1, I-50019 Sesto Fiorentino, Italy

²Istituto per i Processi Chimico-Fisici, IPCF-CNR, Via G. Moruzzi 1, I-56124 Pisa, Italy

³Laboratorium für Festkörperphysik, ETH Zürich, CH-8093 Zürich, Switzerland

⁴DIEF - Department Industrial Engineering and INSTM Research Unit, University of Florence, Via S. Marta 3, I-50139 Florence, Italy

⁵Institute of Inorganic and Analytical Chemistry, Friedrich Schiller University Jena, Humboldtstr. 8, 07743 Jena, Germany.

⁶Department of Chemistry ‘Ugo Schiff’ and INSTM Research Unit, University of Florence, via della lastruccia 3-13, I-50019 Sesto Fiorentino, Italy

e-mail: maria.fittipaldi@unifi.it

The possibility to operate on magnetic materials through the application of electric rather than magnetic fields - promising faster, more space confined and energy efficient circuits - continues to spur the investigation of magnetoelectric (ME) effects [1]. Symmetry considerations, in particular the lack of an inversion centre, characterize the ME effect. In addition, spin-orbit coupling is generally considered necessary to make a spin system sensitive to a charge distribution. However, a ME effect not relying on spin-orbit coupling is appealing for spin-based quantum technologies. We have very recently reported the detection of a ME effect that we have attributed to an electric field modulation of the magnetic exchange interaction without atomic displacement [2]. The effect is visible in electron paramagnetic resonance (EPR) absorption of molecular helices under electric field modulation (EFM-EPR) and confirmed by specific symmetry properties and spectral simulation.

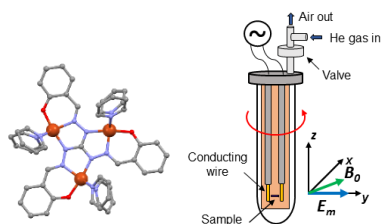


Fig.1. Left: the molecular structure of the spin-frustrated Cu_3 , with a ground state $S=1/2$. Right: schematic view of the modified version of the sample holder used for the EFM-EPR measurements.

After this report, an oscillating electric field ten times stronger was imparted to the sample by an improvement in the experimental setup. This made possible the observation of a ME effect in a single-crystal of a frustrated Cu_3 triangle (Fig. 1). The orientation dependence of the effect was recorded, paving the way to its deep comprehension. Our experiment complements previous time resolved electron spin resonance studies performed on the same Cu_3 molecular cluster in frozen solution, which have shown sizeable effects of electric field pulses [3].

[1] Spaldin, N.A. and Fiebig, M., *Science* **309**, 391-392, (2005).

[2] Fittipaldi, M., Cini, A., Annino, G., Vindigni, A., Caneschi, A., and Sessoli, R., *Nat. Mater.* **18**, 329-334 (2019).

[3] Liu, J., Mrozek, J., Myers, W.K., Timco, G.A., Winpenny, R.E.P., Kintzel, B., Plass, W., and Ardavan, A., *Phys. Rev. Lett.* **122**, 037202 (2019).

Deceleration of Proton Spin-Lattice Relaxation in Water under Ultrasonic Radiation

I.I. Geru

Institute of Chemistry, Republic of Moldova

e-mail: iongeru11@gmail.com

One of the main mechanisms of the nuclear spin-lattice relaxation in liquids is due to the accidental rotational and translational motions of molecules [1]. The nuclear spin-lattice relaxation time can also change as a result of the interaction between the nuclear spins and the acoustical phonons emitted by an external ultrasound source.

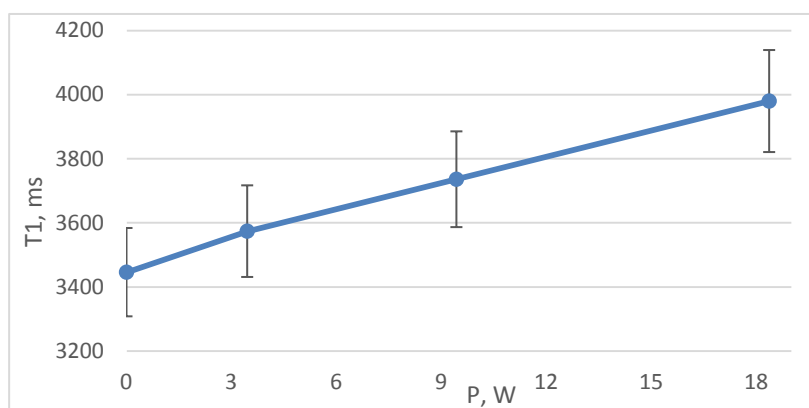


Fig. 1. The dependence of the proton spin-lattice relaxation time T_1 on the ultrasonic radiation power.

Fig. 1 shows an increase in the proton spin-lattice relaxation time T_1 in distilled water under ultrasonic radiation of 22 MHz frequency with increasing the radiation power. Experiments were performed on a Bruker minispec mq20 NMR Analyzer using the Application for determining T_1 based on the inversion recovery pulse sequences and subsequent mono- or biexponential fitting. As it can be seen on the Fig.1, at low power radiation P there is an almost linear dependence of T_1 on the radiation power. Such a behavior of T_1 with increasing of ultrasonic radiation power is also characteristic for the ultrapure and drain-pipe water.

If the correlation time is much less than the Larmor period, then the proton spin-lattice relaxation times, T_1^{rot} and T_1^{trans} due to rotational and, respectively, translational accidental motions of water molecules are

$$T_1^{\text{rot}} = \frac{AT}{\eta(T)}, \quad T_1^{\text{trans}} = \frac{5}{3\pi} \cdot \frac{a^3}{Nb^6} \cdot T_1^{\text{rot}}, \quad A = \frac{1}{2\pi} \cdot \frac{kb^6}{\hbar^2 \gamma^4 a^3}.$$

Here, h , γ , N , $\eta(T)$, k , T , a , and b , are, respectively, the Planck constant, nuclear gyromagnetic ratio, number of ^1H nuclei in the unit volume, temperature dependent water viscosity, Boltzmann constant, absolute temperature, radius of water molecule, and distance between the two hydrogen atoms in the water molecule.

Separate measurements show that water heats up with increasing ultrasound power. The values of $\langle \Delta t \rangle$ averaged over the results of five measurements for each P are $\langle \Delta t \rangle = 0.3, 4.3, 27.7^\circ\text{C}$ for $P = 3.4, 9.4, \text{ and } 18.4 \text{ W}$, respectively. Thus, in the region of low ultrasound heating temperatures, when cavitation effects are still weak, the almost linear increase in T_1 at increasing P (Fig.1) is due to almost linear growth of T_1 at increasing T .

[1] A. Abragam, The principles of nuclear magnetism, Clarendon Press, Oxford, 1961.

Fast Field Cycling NMR Relaxometry enhanced by DNP for Study Complex Systems

B. Gizatullin, C. Mattea, S. Stapf

FG Technische Physik II/Polymerphysik, Technische Universität Ilmenau, D-98684 Ilmenau, Germany

e-mail: Bulat.Gizatullin@tu-ilmenau.de

Fast field cycling (FFC) NMR relaxometry is a method aiming at the determination of T_1 relaxation times of nuclear spins in a wide range of resonance frequencies [1], which provides additional information about rotational and translational molecular motions of complex system such as liquid in porous media, polymers solutions and melts, biological systems etc. However, FFC studies of diluted systems, and extensive studies of multiexponential signal decays, are rather complicated by limitation of relatively low polarization field. Therefore FFC applications mostly restrict to abundant and sensitive nuclei such as ^1H and ^{19}F .

FFC relaxometry enhanced by dynamic nuclear polarization (DNP) [2] is a promising new method for selective hyperpolarization and increasing signal/noise ratio for obtaining more precise FFC data. First studies were devoted to the measurement of the DNP spectrum and enhancement as well as DNP-enhanced dispersion curves of polymer melts [3] in the presence of radicals, effects of fluorination on interaction in simple organic liquid and features of interaction between asphaltenes and low weight molecular part of oil [4, 5].

In this work, a method based on T_2 relaxation time distribution is proposed for a selective measurement of complex systems such as block-copolymer (PS-PB-PS) solutions and porous media. It was shown that SBS block copolymer concentrated solutions provide a well-resolved T_2 distribution (see. Figure 1) which allows to obtain T_2 -resolved DNP spectra and dispersion curves. The maximum DNP enhancement was ~ 28 by solid effect.

As the additional applications for increasing sensitivity of FFC measurements on X-nuclei the ^2H , ^{13}C and ^7Li data in enriched and natural abundance samples of simple liquids with radicals are discussed.

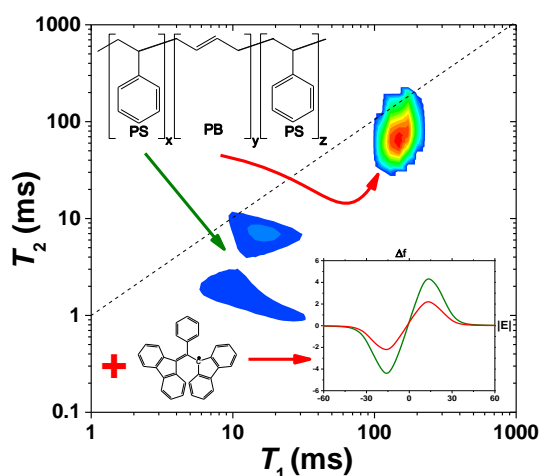


Fig.1. T_1 - T_2 correlation maps of SBS blocks copolymer solution in CDCl_3 . Inset graph shows the T_2 -resolved DNP spectra of corresponding SBS blocks.

- [1] R. Kimmich, E. Ansaldo, *Prog. Nucl. Mag. Res. Sp.*, **44**, 257 (2004).
- [2] O. Neudert, M. Reh, H. W. Spiess, K. Münnemann, *Macromol. Rapid Commun.*, **36**, 885 (2015).
- [3] B. Gizatullin, O. Neudert, C. Mattea, S. Stapf, *Chem. Phys. Chem.*, **18**, 2347 (2017).
- [4] S. Stapf, A. Ordikhani-Seyedlar, N. Ryan, C. Mattea, R. Kausik, D. E. Freed, Y. -Q. Song, M. D. Hürlimann, *Energy Fuel*, **28**, 2395 (2014).
- [5] B. Gizatullin, M. Gafurov, A. Rodionov, G. Mamin, C. Mattea, S. Stapf, S. Orlinskii, *Energy & Fuels*, **32** 11261 (2018).

EPR Approaches to Amyloid Protein Aggregation.

Martina Huber

Department of Physics, Huygens-Kamerlingh Onnes Laboratory, Leiden University,
2300 RA Leiden, The Netherlands

e-mail: huber@physics.leidenuniv.nl

Central to neurodegenerative diseases, such as Alzheimer's and Parkinson's diseases, is the self-aggregation of amyloid proteins that ultimately leads to fibrils, the main constituents of amyloid plaques found in the brains of patients. In the fibrils the proteins adopt a well-ordered, beta-sheet structure, whereas during the aggregation process, disordered states abound. More recent is the discovery that bacteria make use of self-aggregating proteins to generate biofilm and adhesion. The resilience of biofilm is largely due to the extraordinary stiffness and strength of the beta-sheet fibril structures.

Challenges derive first of all from the disordered nature of the aggregating proteins, non-covalent, dynamic interactions between proteins, the heterogeneity of intermediates and the interactions with other partners such as membranes.

We show that many of these challenges can be addressed by EPR. So we demonstrated that the interaction of two helical peptides, designed to form alpha-helical coiled coils can be detected by a combination of continuous wave (cw) and double electron spin-electron spin resonance (DEER). Distances measured between the spin labels attached to the N- or C-termini of the two partners revealed the relative orientation of the pair of peptides in the coiled-coil pair [1]. Similarly, approaches to determine the amyloid fibril structure of alpha-synuclein by DEER were shown [2].

The holy grail of amyloid aggregation is to follow the aggregation in situ, to detect intermediates, and quantify how they develop in time. A continuous wave EPR approach that heavily relies on the higher resolution of high-field/high frequency EPR was applied to reach that goal. We synthesized a set of amyloid peptides with the 2,2,6,6-tetramethyl-N-oxyl-4-amino-4-carboxylic acid (TOAC) spin label. Their sequence was derived from the K11V (KVKVLGDVIEV) amyloid peptide, which self-aggregates to oligomers with a β -sheet configuration [3]. We show that the combination of TOAC and high-field EPR enables us to detect the time development of two types of oligomers, and resolution to single monomer units should be achievable. The approach is illustrated in the Figure.

Thus, in many aspects, EPR alone or in combination with other techniques promises to unravel essential aspects of amyloid aggregation, an inroad to understand the physico-chemical steps of this complex and biologically relevant process.

[1] Kumar, P. *PLOS One* **13**(1): e0191197 (2018).

[2] Hashemi Shabestari, M. *Applied Magnetic Resonance* **46**, 369-388 (2015).

[3] Laganowsky, A. et al., *Science* **335**, 1228–1231 (2012).

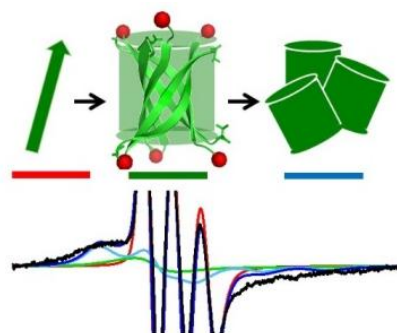


Fig.1. Formation of amyloid oligomers detected in situ. Colors represent the components, which we assign to small oligomers, (green) and larger oligomers.

Quantitative Characterization of the Kerogen Domanic by Low-Field NMR and EPR methods

N.M. Khasanova, B.V. Sakharov, V.P. Morozov, V.Y. Volkov,
M.A. Varfolomeev, D.K. Nurgaliev

Kazan Federal University, Russian Federation

e-mail: nkhasano@yandex.ru

Creating reliable methods for non-invasive study of the shale Domanic rock, as one, the whole of the organic and mineral parts of the substance, and fluids in the pore space are a great need in both experimental and theoretical side. The combined Low-Field NMR proton relaxation technique [1] was implemented to the quantitative determination of the phase state components of the SARA-NMR crude oil [2]. This method for consistent measurement of a free induction signal (FID) and attenuation of the amplitudes of echo signals in a Carr-Purcell-Maybun-Gill pulse sequence was implemented on a Chromatec-Proton 20M NMR analyzer. Another technique was involved the joint use of the EPR method and thermochemical effects on the rock [3] and was implemented at X-band EPR spectrometer (ADANI).

The total amplitudes FID of proton signals and then the proton index (HI) were measured. Reliability of results are consistent with correlation coefficients (R^2) about 0.99 and 0.89 HI-NMR with the OM content based on the results of thermal analysis and, as well as the amount hydrocarbons chloroform extraction respectively.

Table. OM kerogen domanic typing NMR relaxation										DTA OM, %	Extraction HC, %
№ №	Liquid Phases				Solid Phases				index HI, %		
	A _{ol} , %	T _{2l} , mks	A _{olexp} , %	T _{2lexp} , mks	A _{os} , %	T _{2sc} , mks	fam	T _{2sam} , mks			
№1	1,87	1870,6	2,87	142,19	95,26	15,92	0,23	23,33	9,08	7,3	2,94
№2	5,26	1414,3	8,21	312,33	86,53	18,14	0,27	45,68	1,80	2,4	1,34
№3	2,33	1327,2	5,76	249,97	91,91	16,86	0,21	36,28	5,12	5,58	2,08
№4	3,98	1959,8	6,68	450	89,34	17,93	0,24	51,26	2,09	3,42	0,87
№5	3,81	1065,4	5,62	304,44	90,57	17,16	0,22	43,51	3,37	3,39	1,11

The correlation coefficients (R^2) equal 0.57 between content A_{os} solid phase and asphaltens, so as well 0.67 between liquid phase NMR and resins in extraction HC. Thus, we can conclude that the NMR relaxation method in the variant of analysis of FID signals provides a reliable determination of this most important characteristic of the solid organic matter of shale-domanic without destroying the sample.

Mobile hydrocarbons contain an admixture of a vanadyl complex, and these lines are not visible in the EPR spectrum of the rock. The mineral part is represented mainly by syngenetic calcite mixed with manganese and the radical ions SO₂⁻, SO₃⁻, as a result of interaction with hydrocarbons. The correlation coefficients (R^2) equal 0.89 and 0.9 between HI-NMR and the EPR value free radical Corg and R* in extract HC respectively.

[1] E. Trezza, A.M. Haiduc, G.J.W. Goudappel et al. Magn. Reson. Chem., 2006, 44, pp.1023-1030.

[2] V.Y. Volkov, B.V. Sakharov, N.M. Khasanova et al. Georesources, 2018. V. 20. № 4. Part 1. pp. 308-323.

[3] G.R. Bulka, Appl.Magn.Reson. - 1991. - V.2. – P.107-115.

EPR Spectroscopy of Semiconductor Nanomaterials: New Approaches

E.A. Konstantinova^{1,2,3}, A.I. Kororin⁴, V.B. Zaitzev¹

¹Department of Physics, M.V. Lomonosov Moscow State University, Russian Federation

²National Research Center Kurchatov Institute, Moscow, Russian Federation

³Department of Nano-, Bio-, Information Technology and Cognitive Science, Moscow Institute of Physics and Technology, Russian Federation

⁴N. Semenov Institute of Chemical Physics RAS, Moscow, Russian Federation

e-mail: liza35@mail.ru

In recent years, semiconductor nanomaterials are all time in the center of attention of researchers [1-4]. Their structural, electrophysical, and optoelectronic properties are being actively studied. Such an increased interest in these objects is primarily due to their unique properties, which, first of all, include quantum-size and size effects. The latter manifests itself always when we move from bulk material to nanoparticle ensembles, and is expressed in a sharp increase in the specific surface area (several 100 m² per gram of substance). The presence of such a huge specific surface makes nanomaterials a good model object for studying the fundamental laws of adsorption processes, the nature and properties of defects on the surface of nanocrystals and, moreover, opens up the prospect for new practical applications of nanostructured semiconductors [1, 2]. EPR spectroscopy is a generally recognized powerful method for studying semiconductor nanoparticles [2, 4].

We have proposed new, unique EPR-based methods for studying semiconductor nanomaterials: a method for the control of the generation of singlet oxygen and determining its concentration in ensembles of Si nanoparticles, which is based on a change in the relaxation times of spin centers; determination of the band structure of nanooxide semiconductors (energy level position of defect, band gap); detection of charge carrier separation and accumulation in nanoheterostructures. In this work we have studied TiO₂ nanocrystals, TiO₂ based nanoheterostructures (TiO₂/MoO₃, TiO₂/WO₃, TiO₂/V₂O₅, TiO₂/MoO₃/V₂O₅) and TiO₂ based microspheres (TiO₂/MoO₃, TiO₂/WO₃, TiO₂/V₂O₅, TiO₂/MoO₃/V₂O₅) using our new EPR-based methods. Energy diagrams of the investigated oxides with energy level position in the band gap are proposed. We have revealed the effect of separation and accumulation of photoexcited electrons and holes in TiO₂ based nanoheterostructures. These results can be useful for understanding the mechanism of photocatalytic reactions and further practical applications of the TiO₂ based nanomaterials.

The reported study was funded by RFBR according to the research project № 18-29-23051.

- [1] V.G. Dubrovskii, G.E. Cirilin, V.M. Ustinov, *Semiconductors* **43**, 1539 (2009).
- [2] T.V. Sviridova, L.Yu. Sadovskaya, E.A. Konstantinova, N.A. Belyasova, A.I. Kokorin, D.V. Sviridov, *Cat. Lett.* **149**, 1147 (2019).
- [3] R. Anufriev, N. Chauvin, H. Khmissi, K. Naji, G. Patriarche, M. Gendry, C. Bru-Chevallier, *Appl. Phys. Lett.* **104**, 183101 (2014).
- [4] E.A. Konstantinova, A.A. Minnekhanov, A.I. Kokorin, T.V. Sviridova, D.V. Sviridov, *J. Phys. Chem. C*, **122**, 10248 (2018).

Defect Properties of Titania Obtained by Laser Sintering

E.A. Konstantinova^{1,2,3}, A.V. Pavlikov^{1,2}, M.N. Martyshov¹

¹Department of Physics, M.V. Lomonosov Moscow State University, Russian Federation

²National Research Center Kurchatov Institute, Moscow, Russian Federation

³Department of Nano-, Bio-, Information Technology and Cognitive Science, Moscow Institute of Physics and Technology, Russian Federation

e-mail: liza35@mail.ru

In recent years, materials obtained using additive technologies are being actively studied [1,2]. It is important to study a defect properties such structures. One of the effective methods of formation of additive samples is laser sintering [3]. The materials formed in this process have interesting properties and a low cost in comparison with ones, obtained by another way of formation. It is known that titania based materials have unique properties and are characterized by the presence of a large number of point defects that are paramagnetic. Therefore electron paramagnetic resonance (EPR) spectroscopy is powerful technique for their investigation. Therefore, in order to identify these defects and to determine their main parameters both in dark and under illumination, we used this method and the technique developed on the basis of this method to diagnose the radicals formed in the process of various physicochemical effects in the "in situ" mode in the samples obtained with the help of additive technologies.

We have made of the samples using laser sintering (Nd: YAG laser). The titania powder for laser sintering was formed using sol-gel method. Sintering of the titania powder was carried using a 15 W laser radiation power. The scanning speed of the laser beam was 3 cm/s. The EPR spectra were measured with an EPR spectrometer Bruker ELEXSYS-500 (operating frequency 9.5 GHz, sensitivity $5 \cdot 10^{10}$ spin/Gs). Illumination of the samples was carried out directly in the cavity of the spectrometer using a Bruker ER 202 UV mercury lamp (power of 50 W) in a wide spectral range (270-900 nm). To calculate the concentration of paramagnetic centers, we used a standard $\text{CuCl}_2(2\text{H}_2\text{O})$ with a known number of spins.

The initial titania was characterized by the presence of Ti^{3+} /oxygen vacancy centers. However, after the laser sintering process, the EPR signal from these defects disappeared and, instead of it, the signal from the electrons in the conduction band was recorded. The calculated concentrations of Ti^{3+} /oxygen vacancy centers and conduction band electrons are equal ($7.5 \cdot 10^{17} \text{ cm}^{-3}$). Therefore we suppose, that in the additive samples the oxygen vacancies are ionized, due to the movement of electrons to the conduction band, and therefore the vacancies are non-paramagnetic. Illumination of additive titania samples did not lead to a change in the EPR spectrum, which indicates that all oxygen vacancies are ionized (non-paramagnetic). These results can be useful for understanding the mechanism of defect transformation during laser sintering process and further practical applications of the TiO_2 based additive materials.

This work was performed with the financial support of the Ministry of Education and Science of Russia under Agreement No. 14.625.21.0041 of September 26, 2017 (unique identifier RFMEFI62517X0041).

- [1] E.V. Babakova, A.V. Gradoboev, A.A. Saprykin, E.A. Ibragimov, V.I. Yakovlev, A.V. Sobachkin, *Appl. Mech. and Mater.*, **756**, 220 (2015).
- [2] P.A. Kuznetsov, O.V. Vasilyeva, A.I. Telenkov, V.I. Savin, V.V. Bobyr, *News of Mater. Science and Technol.*, **2**, 4 (2015).
- [3] I.V. Shishkovsky, D.M. Gureev, R.V. Ruzhechko, *Techn. Phys. Lett.*, **26**, 262 (2000).

EPR Study of Titania Microspheres with Different Chemical Composition

E.A. Konstantinova^{1,2,3}, G.V. Trusov⁴, V.A. Kulbachinskii¹

¹Department of Physics, M.V. Lomonosov Moscow State University, Russian Federation

²National Research Center Kurchatov Institute, Moscow, Russian Federation

³Department of Nano-, Bio-, Information Technology and Cognitive Science, Moscow Institute of Physics and Technology, Russian Federation

⁴National Research Technological University "MISiS", Moscow, Russian Federation

e-mail: liza35@mail.ru

The most promising area of application titania is photocatalysis — chemical decomposition of organic impurities, including toxic, on the surface of titania [1–3]. Note that the functional characteristics (photoactivity, reactivity, etc.) of titania are determined by its physicochemical properties. In recent years, photocatalytic heterostructures, formed by a large number of oxide-oxide nanoheterojunctions (one of which is nitrogen doped nanocrystalline titanium dioxide due to its high photoactivity) have been actively studied because of their ability to accumulate photoinduced charge carriers [4, 5]. We have studied the photoelectron properties of nanoheterojunctions of various oxides (N-TiO₂/MoO₃, N-TiO₂/WO₃, N-TiO₂/V₂O₅, N-TiO₂/MoO₃/V₂O₅), arranged in the form of microspheres, obtained by the method of aerosol pyrolysis [3]. We have used EPR and UV-Vis spectroscopy for the investigation of TiO₂ based microspheres.

It was established that the main type of radicals in the samples under study are Ti³⁺/oxygen vacancies, N• radicals, Mo⁵⁺ and V⁴⁺ centers. Under illumination, the intensity of the EPR signal from all paramagnetic centers increased. After turning off the light, the complete relaxation of the EPR signal to its original state occurred during approximately the day for the microspheres N-TiO₂/MoO₃, N-TiO₂/WO₃, N-TiO₂/V₂O₅ and for two days for the microspheres N-TiO₂/MoO₃/V₂O₅. This indicates the processes of separation and accumulation of charge carriers in the samples under study. The microspheres consisting of three metal oxides had the best oxidative activity and the most pronounced photocatalytic properties. Note that the photocatalysis takes place during 7-8 hours after turning off the illumination. The obtained results can be useful for development of energy efficient titania based photocatalysts.

The reported study was funded by RFBR according to the research project № 18-29-23051.

- [1] X. Chen, S.S. Mao, *Chem. Rev.* **107**, 2891 (2007).
- [2] O. Oluwafunmilola, M. Maroto-Valer, *J. Photochem. Photobiol. C: Photochem. Rev.*, **24**, 16 (2015).
- [3] A. Tarasov, G.Trusov, A. Minnekhanov, D. Gil, E. Konstantinova, E. Goodilin, Y. Dobrovolsky. *J. Mater. Chem. A*, **2**, 3102 (2014).
- [4] T.V. Sviridova, L.Yu. Sadovskaya, E.M. Shchukina, A.S. Logvinovich, D.G. Shchukin, D.V. Sviridov, *Photochem. Photobiol. A: Chem.*, **327**, 44 (2016).
- [5] E.A. Konstantinova, A.A. Minnekhanov, A.I. Kokorin, T.V. Sviridova, D.V. Sviridov, *J. Phys. Chem. C*, **122**, 10248 (2018).

Photo-CIDNP in Solids

J. Matysik

Institut für Analytische Chemie, Universität Leipzig, 04103 Leipzig, Germany

e-mail: joerg.matysik@uni-leipzig.de

The solid-state photo-CIDNP effect has been discovered by Zysmilich and McDermot in 1994 by ^{15}N solid-state NMR on photosynthetic reaction center (RC) proteins measured under continuous illumination with white light [1]. Understanding the theory [2] allowed to develop on the basis of the effect a fully-fledged analytical method able to study spin-correlated radical pairs [3].

Here we will report on recent progress:

- i) Shuttle MAS NMR experiments: Recently, the field-dependence of the photo-CIDNP effect has been studied in the millitesla range by applying a MAS shuttle system. The effect has indeed been observed in that field range, surprisingly, however, showing a change of the sign: The enhancement curve is turning from enhanced emissive (having its optimum at 5 Tesla) to absorptive (optimum at 1 Tesla). [4]
- ii) Testing several other photosynthetic systems: The occurrence of the solid-state photo-CIDNP effect in diatoms *Phaeodactylum tricorutum* and *Cyclotella meneghiniana* as well as of *Chloracidobacterium thermophilum* has been demonstrated, confirming that all tested photosynthetic systems show the solid-state photo-CIDNP effect. Also in one of these cases, an unexpected change of the sign has been observed. According to chemical shifts, there is apparently no big difference in RCs of plants, algae and diatoms. [5]
- iii) "Spin torch" experiments: Transfer of hyperpolarization from cofactor nuclei of the SCRPs to nuclei in the environment allows for the exploration of the near-by amino acids. Using the heteronuclear spin torch approach, we have recently shown that in bacterial RCs, hyperpolarization can be transferred from selectively labelled cofactors to the proton network of the surrounding protein matrix by inducing $^{13}\text{C} \rightarrow ^1\text{H} \rightarrow ^1\text{H} \rightarrow ^{13}\text{C}$ hyperpolarization transfer. [6]

[1] M.G. Zysmilich, Ann McDermott. J. Am. Chem. Soc. **116**, 8362 (1994).

[2] D. Sosnovsky, N. Lukzen, H.M. Vieth, G. Jeschke, D. Gräsing, P. Bielytskyi, J. Matysik, K. Ivanov, J. Chem. Phys. **150**, 094105 (2019).

[3] B. Bode, S.S. Thamarath, K.B. Sai Sankar Gupta, A. Alia, G. Jeschke, J. Matysik, in: Hyperpolarization methods in NMR spectroscopy (Lars Kuhn, ed.) Springer, pp. 105-121 (2013).

[4] D. Gräsing, P. Bielytskyi, I.F. Céspedes-Camacho, A. Alia, T. Marquardsen, F. Engelke, J. Matysik, Scientific Reports **7**, 12111 (2017).

[5] J.C. Zill, M. Kansy, R. Goss, A. Alia, C. Wilhelm, J. Matysik, Photosynth. Res., online. DOI: 10.1007/s11120-018-0578-9 (2018); J.C. Zill, Z. He, M. Tank, B.H. Ferlez, C.P. Canniffe, Y. Lahav, P. Bellstedt, A. Alia, I. Schapiro J.H. Golbeck, D.A. Bryant, J. Matysik, Photosynthetic Research **137**, 295 (2018); J.C. Zill, M. Kansy, R. Goss, L. Köhler, A. Alia, C. Wilhelm, J. Matysik, Z. Phys. Chem. **231**, 347 (2017).

[6] P. Bielytskyi, D. Gräsing, S. Zahn, A. Alia, J. Matysik, Applied Magnetic Resonance, accepted. <https://doi.org/10.1007/s00723-019-1110-x> (2019); P. Bielytskyi, D. Gräsing, S. Zahn, K.R. Mote, A. Alia, P.K. Madhu, J. Matysik, J. Magn. Reson. **298**, 64 (2019); P. Bielytskyi, D. Gräsing, K.R. Mote, K.B. Sai Sankar Gupta, S. Vega, P.K. Madhu, A. Alia, J. Matysik J. Magn. Reson. **293**, 82 (2018).

Multi-Extreme THz ESR -Recent Applications and the Future-H. Ohta^{1,2}, S. Okubo^{1,2}, E. Ohmichi², T. Sakurai³, H. Takahashi^{1,2}, S. Hara³, Y. Saito³¹Molecular Photoscience Research Center, Kobe University, Japan²Graduate School of Science, Kobe University, Japan³Research Facility Center for Science and Technology, Kobe University, Japan

e-mail: hohta@kobe-u.ac.jp

Recent developments and applications of our multi-extreme THz ESR in Kobe will be presented. Our multi-extreme THz ESR can cover the frequency region between 0.03 and 7 THz [1], the temperature region between 1.8 and 300 K [1], the magnetic field region up to 55 T [1], and the pressure region up to 1.5 GPa [2] simultaneously. Recently we have developed the hybrid-type pressure cell, which consists of the NiCrAl alloy inner cell, the Cu-Be alloy outer cell and the ceramic piston parts, and achieved 2.7 GPa [3]. Using this pressure cell for our high-pressure THz ESR, we have discovered the first-order pressure-induced transition at 1.85 GPa in the Shastry-Sutherland Model Compound $\text{SrCu}_2(\text{BO}_3)_2$ [4]. Moreover, although the magnetic field for THz ESR is limited up to 10 T in Kobe using this hybrid-type pressure cell, we have developed a new system up to 25 T at the high field user facility in IMR, Tohoku University [5]. Some results at IMR will be also shown [6].

Another aspect of multi-extreme THz ESR is the developments of our micro-cantilever ESR up to 1.1 THz [7], and the recent developments of the torque magnetometry [8] and ESR [9] measurements using a commercially available membrane-type surface stress sensor. Recent applications of membrane ESR to the microliter solution sample (myoglobin) will be presented [10].

Finally the future perspectives of our multi-extreme THz ESR will be discussed.

- [1] H. Ohta et al., *J. Low Temp. Phys.* **2013**, 170, 511.
- [2] T. Sakurai et al., *Rev. Sci. Instr.* **2007**, 78, 065107; T. Sakurai, *J. Phys.: Conf. Series*, **2010**, 215, 012184.
- [3] K. Fujimoto et al., *Appl. Mag. Res.* **2013**, 44, 893; T. Sakurai et al., *J. Mag. Res.*, **2015**, 259,108; *J. Mag. Res.*, **2017**, 280, 3 (**Invited review**); H. Ohta et al., *J. Phys. Chem. B* **2015**, 119,13755 (**Invited paper**).
- [4] T. Sakurai et al., *J. Phys. Soc. Jpn.* **2018**, 87, 033701.
- [5] T. Sakurai et al., *J. Mag. Res.* **2018**, 296, 1-4
- [6] S.A. Zvyagin et al., *Nature Communications*, **2019**, 10,1064
- [7] H. Ohta et al., *AIP Conf. Proceedings* **2006**, 850, 1643; E. Ohmichi et al., *Rev. Sci. Instrum.* **2008**, 79, 103903; E. Ohmichi et al., *Rev. Sci. Instrum.* **2009**, 80, 013904; H. Ohta and E. Ohmichi, *Appl. Mag. Res.* **2010**, 37, 881; E. Ohmichi et al., *J. Mag. Res.* **2013**, 227, 9; E. Ohmichi et al., *Rev. Sci. Instrum.* **2016**, 87, 073904; E. Ohmichi et al., *J. Inorganic Biochemistry* **2016**, 162, 160 (**Invited paper**); H. Takahashi, E. Ohmichi, H. Ohta, *Appl. Phys. Lett.* **2015**, 107, 182405.
- [8] H. Takahashi et al., *J. Phys. Soc. Jpn.* **2017**, 86, 063002 (**Editor's Choice**).
- [9] H. Takahashi et al., *Rev. Sci. Instrum.* **2018**, 89, 036108
- [10] T. Okamoto et al., *Appl. Phys. Lett.* **2018**, 113 223702 (**Editors Picks**)

Shaping up EPR: Phase/Amplitude Modulated Pulses for Dipolar Spectroscopy

Thomas F. Prisner

Institute of Physical and Theoretical Chemistry, Center of Biomolecular Magnetic Resonance,
Goethe University Frankfurt, Germany

e-mail: prisner@prisner.de

The advent of fast arbitrary waveform generators in the sub-nanosecond time regime enables new experimental developments in the field of pulsed dipolar EPR spectroscopy. In this talk, new experiments of our research group using such fast phase/amplitude modulated microwave pulses will be described and demonstrated by applications to model compounds and biomolecules. Some of the specific technical and methodical challenges of such shaped pulses in the field of EPR will be discussed and the strengths and new possibilities offered by such pulses will be illustrated [1,2,3].

- [1] Prisner, T.F., (2019), Shaping EPR: Phase and amplitude modulated microwave pulses. *J. Magn. Reson., In press*
- [2] Spindler, P.E., Schops, P., Kallies, W., Glaser, S.J. and Prisner, T.F. (2017), Perspectives of Shaped Pulses for EPR Spectroscopy. *J. Magn. Reson.*, 280, 30-45
- [3] Spindler, P.E., Schops, P., Bowen, A.M., Endeward, B. and Prisner, T.F. (2016), Shaped Pulses in EPR. *eMagRes*, 5, 1477 - 1492

High Sensitivity Quantum-limited Electron Spin Resonance

Vishal Ranjan

Orme des Merisiers, Quantronics, SPEC, CEA Saclay, 91191 Gif sur Yvette, France

e-mail: vishalran@gmail.com

In a conventional ESR spectrometer based on the inductive detection method, the paramagnetic spins precess in an external magnetic field B_0 radiating weak microwave signals into a resonant cavity. These emissions are subsequently amplified and measured. Despite its widespread use, ESR has limited sensitivity, and large amounts of spins are necessary to accumulate sufficient signal. Most conventional ESR spectrometers operate at room temperature and employ three-dimensional cavities. At X-band, they require approximately 10^{13} spins to obtain sufficient signal in a single echo [1]. Enhancing this sensitivity to smaller spin ensembles and eventually the single spin limit is highly desirable.

Exploiting recent progress in circuit-quantum electrodynamics, we have combined high quality factor superconducting micro-resonators and noise-less Josephson Parametric Amplifiers to perform ESR in a new regime, namely Purcell regime. The Purcell regime allows us to explore spin energy relaxation and decoherence in a non-conventional way. Based on these principles, we have achieved an unprecedented measurement sensitivity of better than 10 spins / $\sqrt{\text{Hz}}$ for unit SNR in an inductive-detection ESR. Spin relaxation studies show that T_1 can become pulse amplitude dependent in low mode volume resonators. Moreover, we discuss significances of mechanical strain on spin-linewidth and decoherence mechanisms in our devices.

[1] A. Schweiger and G. Jeschke, Principles of pulse electron paramagnetic resonance (Oxford University Press, 2001).

H-MAS

Ago Samoson

Institute of Health Technologies, TUT, Tallinn, Estonia

e-mail: ago.samoson@ttu.ee

Availability of new materials, powerful design software and engineering experience have facilitated a significant progress in NMR probes, a key to successful experiment. We shall characterize MAS up to 170 kHz by driving pressure and temperature profiles. An approach rate to the “ultimate” ^1H resolution will be compared for various spin densities. H-MAS offers a surprising sensitivity, while reducing the required sample amount by several orders, and is likely to guide a big part of future biomedical NMR applications from solutions to the solid state.

- [1] Agarwal V et al (2014) De novo 3D structure determination from sub- milligram protein samples by solid-state 100 kHz MAS NMR spectroscopy. *Angew Chem Int Ed* 53:12253–12256.
- [2] Sternberg U et al (2018) ^1H line width dependence on MAS speed in solid state NMR—comparison of experiment and simulation. *J Magn Reson* 291:32–39.
- [3] Lin Y-L et al (2018) Preparation of fibril nuclei of beta-amyloid peptides in reverse micelles. *Chem Commun* 54:10459–10462.
- [4] Susanne Penzel, Andres Oss, Mai Liis Org, Ago Samoson, Anja Böckmann, Matthias Ernst, Beat H. Meier, Spinning faster: protein NMR at MAS frequencies up to 126 kHz, *Journal of Biomolecular NMR* 73:19-29, 2019.

High Concentration Sensitivity, High Bandwidth and Low Deadtime Pulsed EPR

R.I. Hunter¹, H. El Mkami¹, D.R. Bolton¹, J.E. Lovett¹, B. Bode², C. Pliotas³, D. Norman⁴,
D. Keeble⁵, R. Wylde⁶, D.A. Robertson¹, P.A.S. Cruickshank¹, G.M. Smith¹

¹ School of Physics and Astronomy, University of St Andrews, UK

² School of Chemistry, University of St Andrews, UK

³ School of Biomedical Sciences, University of Leeds, UK

⁴ School of Life Sciences, University of Dundee, UK

⁵ School of Physics, University of Dundee, UK

⁶ Thomas Keating Ltd, Billingshurst, UK

e-mail: gms@st-andrews.ac.uk

We describe modifications to a high power W-band (94 GHz) pulsed EPR instrument [1] that leads to new levels of performance for pulsed EPR in terms of concentration sensitivity, instantaneous bandwidth and deadtime characteristics. Concentration sensitivity is significantly better than the best commercial high power X-band and Q-band systems. At kW power levels the system has almost 1 GHz instantaneous bandwidth with a near flat frequency response, fully coherent detection and 90 degree pulses of a few nanoseconds duration. Incorporation of a new high performance, fast AWG allows a wide variety of shaped and chirped pulses to be defined that allows this full bandwidth to be exploited. Isolation between excitation pulses and the detection system is sufficiently large that EPR measurements on some systems are possible during a kW pulse, allowing systems with very short relaxation times to be characterised. Reflections in the system are reduced to a level that practical system deadtime is ~ 20ns, limited by low level excitation of high order modes, and work is currently underway to reduce this to a few nano-seconds. Incorporation of a high-bit digital receiver with fast averaging capability gives increased dynamic range. The performance of the instrument is illustrated by examples from nitroxide and Gd PELDOR, ELDOR detected NMR, low deadtime EPR, FT-EPR, ultra-wideband EPR, and zero-deadtime EPR. We discuss the further opportunities that arise.

[1] P.A.S.Cruickshank et al., Review of Scientific Instruments, **80**, pp 103102, (2009).

Dynamic Manipulation of Electron Spin Dynamics to boost Dynamic Nuclear Polarization

Songi Han

University of California Santa Barbara, Santa Barbara, CA 3106-9510, USA

e-mail: songi@chem.ucsb.edu

Dynamic nuclear polarization (DNP) is transforming solid-state (ss) nuclear magnetic resonance (NMR) by providing unprecedented access to low gamma, low natural-abundant NMR active nuclei or surface-active species that were previously impossible to detect. However, the ss-DNP efficiency is significantly decreased at higher B_0 field, higher temperatures, faster MAS, when broad-band paramagnetic species are targeted, or when deviating from a specific solvent mixture optimized for DNP. We discuss mechanisms of DNP obtained by insight into electron spin dynamics and population by pulsed EPR diagnosis under DNP conditions to guide the design of DNP experiments. We demonstrate that moving beyond single frequency continuous wave (CW) irradiation of the electron paramagnetic resonance (EPR) signal – the operating mode of DNP experiments today – to fast and broadband (FAB) saturation using shaped waveform irradiation can enhance the DNP performance under magic angle spinning (MAS), but only if combined with a mixed radical system with distinct spin population, frequency-separated by the nuclear Larmor frequency. We demonstrate that the benefit of FAB DNP will be particularly significant when electron spin lattice relaxation is fast relative to the MAS frequency, i.e. for DNP at elevated temperatures and of paramagnetic species whose EPR line is dominated by conformational distribution and coupling anisotropy that give rise to non-overlapping EPR populations.

Low-Field NMR Full FID Method for the Study of Heterogeneous Objects

V.Y. Volkov¹, B.V. Sakharov¹, N.M. Khasanova², A.A. Al-Muntaser¹,
M.A. Varfolomeev¹, D.K. Nourgaliev²

¹Aleksander Butlerov Institute of Chemistry, Kazan Federal University, Russian Federation

²Institute of Geology and Petroleum Technologies, Kazan Federal University, Kazan, Russian Federation

e-mail: volkovobolensk@mail.ru

Experimental approaches to the study of liquids and solids by NMR methods differ substantially. The solid or rigid component provides a fast decaying NMR signal (FID) that arises after single RF pulse. This FID lasts only a few tens of microseconds. In contrast, FID's of soft or elastic components and liquids extends from microseconds to many seconds and require multi-pulse program such as well-known CPMG pulse sequence. The method of simultaneous measurement the *fast* and *slow* parts of the FID (*Full FID*), based on modified CPMG pulse sequence, was proposed in [V.Y.Volkov, NMRCM 2013, p.119; DOI: 10.13140/2.1.1268.9605]. This method reduces the measurement time and more than one - two orders reduces the number of RF pulses and thereby prevents the "saturation" of the spin system.

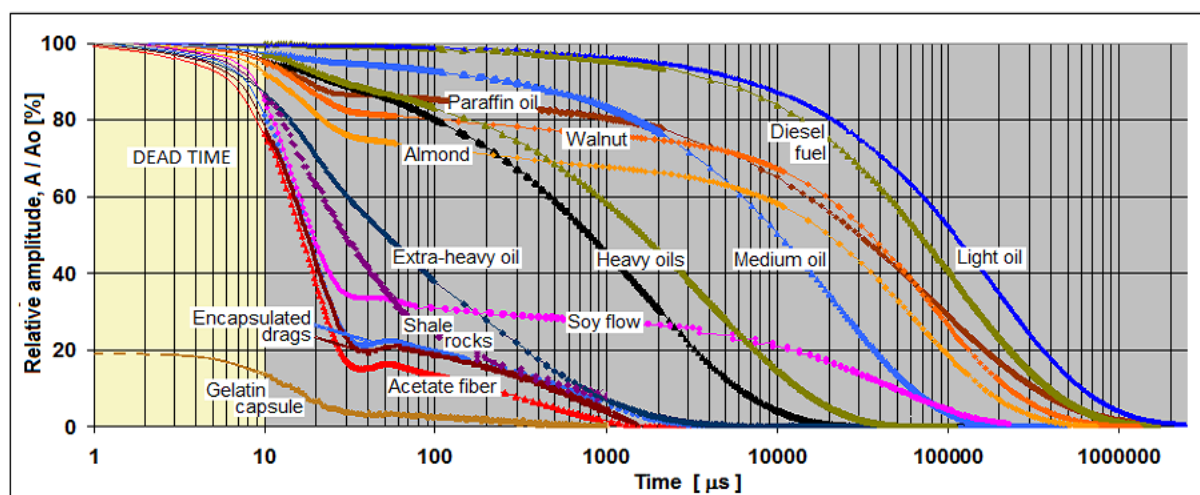


Fig.1. Panoramic pictures of the total NMR relaxation responses of protons (FID + modified CPMG-echo) the some heterogeneous objects. Measured at 20 MHz by NMR analyzer Chromatec Proton-20m, Russia

The main advantage of the proposed method is that it simultaneously registers the signals of all components having relaxation times T_2 of protons in the range from 10^{-5} to 10^{-1} seconds, i.e., the crystalline and rigid (hard) amorphous structures, elastic parts, viscous and liquid phases that are presents in the sample. Over the past years, this method has been successfully used for non-invasive analysis of acetate filters, cereal seeds, sunflower and nuts, multilayer polymeric coatings and insulators, encapsulated medicines and petroleum. The method improves the accuracy of determining the relative amplitudes of components than at the separate measurements FID and CPMG echo signals and then joint processing after finishing measurement session. This technique is more acceptable for on-line control of technological process and production quality in a real working environment and it is suitable for a most type of Low Field NMR relaxometer.

The method is also suitable for the construction of T1-T2 maps, which are widely used at the study of the petrophysical properties of the cores of both traditional oil deposits and shale's. Full FID method provides the record short time of the first point registration after 90° pulse at 10-12 μs for T1-T2 map and the minimum interval between echo signals: $2\tau = 30 \mu\text{s}$.

Spin Noise Spectroscopy as an Alternative to Zavoisky's Technique

V.S. Zapasskii

Spin Optics laboratory, St. Petersburg State University, 198504 St. Petersburg, Russia

e-mail: vzap@rambler.ru

This talk is aimed to attract attention of the EPR spectroscopists to the experimental approach fundamentally different from that of Zavoisky. The classical method of the EPR detection implemented by E.Zavoisky, as well as all modifications of this method, necessarily implied perturbation of the paramagnet at the frequency of spin precession. It is known, however, that magnetic resonance can be observed not only as a feature in the magnetic-susceptibility spectrum of a paramagnet, but also as a feature in the spectrum of its magnetization noise. This noise, in turn, can be detected using the Faraday effect. For the first time, such an approach has been demonstrated experimentally in 1981 [1], and nowadays this technique, commonly referred to as Spin Noise Spectroscopy (SNS) or spectroscopy of spontaneous magnetic resonance, is widely used for studying magnetic resonance and spin dynamics in atomic systems and semiconductors [2-4]. Perhaps the SNS did not acquire sufficient popularity in the community of classical EPR spectroscopists, because it has not been applied so far to dielectric paramagnets. This situation will be soon definitely changed, and the class of objects of the SNS will be essentially widened.

In the talk, we will consider new opportunities that offer the concept of spontaneous magnetic resonance as compared with that of Zavoisky.

- [1] E.B. Aleksandrov and V.S. Zapasskii, "Magnetic resonance in the Faraday rotation noise spectrum," *J. Exp. Theor. Phys.* **54**, 64–67 (1981).
- [2] J.H. Hübner, F. Berski, R. Dahbashi, and M. Oestreich, *Phys. Status Solidi B* **251**, 1824 (2014).
- [3] V.S. Zapasskii, *Advances in Optics and Photonics*, **5**, 131-168, 2013.
- [4] M. Römer, J.H. Hübner, and M. Oestreich, *Rev. Sci. Instrum.* **78**, 103903 (2007).

Modern Gyrotrons and Their Applications

V.E. Zapevalov

Institute of Applied Physics RAS, Nizhny Novgorod, Russian Federation

e-mail: zapev@appl.sci-nnov.ru

Gyrotrons are the most powerful sources of radiation of the millimeter range, capable of operating in long-pulse and continuous modes, which makes it possible to successfully use in experiments on controlled thermonuclear fusion (FC), as well as in the field of material processing technology. The development of new gyrotrons for such applications was previously aimed mainly at increasing the power and efficiency. Recently, biomedical, spectroscopic and informational applications of gyrotrons have been developing rapidly. In accordance with the needs of these areas, significant efforts are directed towards increasing and tuning the working frequency, radiation stability, and control of spectral characteristics. The successes achieved in these areas are also very significant [1-4]. The main areas of application of modern gyrotrons and specific requirements in each area are described. A review of recent achievements, as well as the main problems impeding the further promotion of gyro devices in frequency and power and methods for solving these problems by leading world institutions, is given.

The level of output power of quasi-continuous gyrotrons of the world's leading manufacturers in recent years has reached 1 MW at frequencies up to 170 GHz, and there is a strong tendency to further increase it, at least, to 1.5-2 MW. The efficiency of modern gyrotrons reaches, without recovery of the residual energy of the electron beam, 35–40% in continuous modes and 40–50% in pulsed, and with single-stage recovery, 50% in continuous modes and 70% in pulsed. Multi-frequency versions of megawatt gyrotrons are being successfully developed. A further increase in the power and efficiency of the gyrotron is limited by a number of physical and technical reasons. The overall efficiency of the gyrotron and its limiting power of the gyrotron is determined by the efficiency and the limiting capabilities of its subsystems: the electron-optical system, the resonator, the radiation conversion and output system, the collector (with energy recovery).

Gyrotrons for technological applications, with frequencies from 24 to 300 GHz, have become a reliable tool for creating new ceramic and composite materials. For spectroscopic applications, gyrotrons with frequencies up to 512 GHz with high stability and the possibility of flexible control of output parameters have been developed. As new applications appear the gyrotron complexes are modified in accordance with their needs.

This work was supported by the RSF (grant No. 19-12-00332)

- [1] Gaponov-Grekhov, A.V., and V.L. Granatstein (1994). Applications of High-Power Microwaves, Artech House, Norwood.
- [2] M.A.M. Thumm, “State-of-the-Art of High Power Gyro-Devices and Free Electron Masers”. KIT, Karlsruhe, 2017.
- [3] Thumm, M. High power gyro-devices for plasma heating and other applications. Int. J. Infrared. Millim. Waves, 26, 483–503 (2005).
- [4] G.S. Nusinovich “Introduction to the Physics of Gyrotrons,” The Johns Hopkins University Press, Baltimore-London, 2004.
- [5] M.V. Kartikeyan, E. Borie, M.K.A. Thumm, “Gyrotrons – High Power Microwave and Millimeter Wave Technology,” Springer: Berlin, 2004.

Selective Addressing and Readout of Optically Detected Electron Spins

O. Zgadzai, L. Shtirberg, Y. Artzi, A. Blank

Schulich Faculty of Chemistry, Technion- Israel Institute of Technology, 32000, Haifa, Israel
e-mail: zgoleg@tchnion.ac.il

The experimental capability of spatially-selective addressing, manipulation and readout of a small number of electron spins with high spatial resolution is of fundamental importance because it lies at the basis of many spin-based quantum information devices and sensor technologies. Optically detected magnetic resonance (ODMR) provides ultrasensitive detection of a small number of electron spins for species such as nitrogen-vacancy (NV) centers in diamond, down to the single spin level. This method was recently combined with pulsed magnetic resonance imaging (MRI) technique known as optically detected magnetic resonance imaging (ODMRI) to obtain images of NVs at resolutions ranging from the micron- to the nanoscale [1],[2]. In the present work, we further enhance our imaging resolution to the submicron range and also demonstrate for the first time the high resolution spatially-selective addressing of the electron spins in the sample using powerful and short gradient pulses.

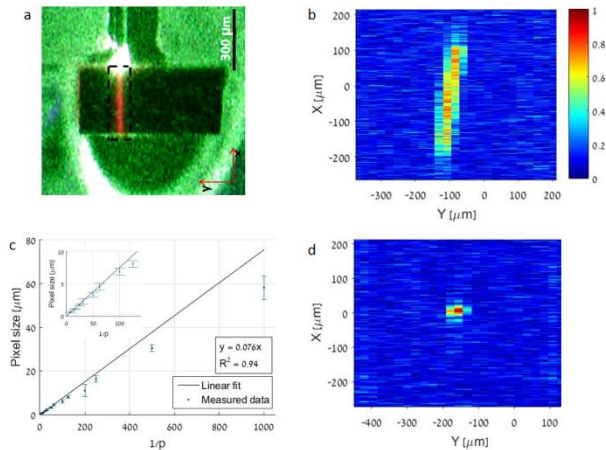


Fig. 1. (Colour on-line) a) Optical microscopic image of the diamond in the resonator during laser illumination, (b) ODMR image of the fluorescence pattern, (c) Experimental plot of resolution (Δx) vs. inverse fraction of gradient power ($1/p$), (d) ODMR image of the fluorescence pattern with the selective pulse applied, showing that only the spins at the center of the sample are addressed and manipulated

The results of our ODMRI experiments without and with selective spin addressing are shown in the Fig. 1. The image, which consists of 1840×60 pixels (in X and Y direction, respectively), was obtained by applying only X and Y phase gradients. The pixel resolution along the X-axis of the image can be obtained by two methods. The first one just makes use of the thickness of the diamond sample ($320 \mu\text{m}$) and the number of pixels in the image along the X-axis (~ 640), to obtain a spatial resolution of $\sim 0.5 \mu\text{m}$. A more accurate method is to acquire a series of images, with increasing maximum gradients (scaled by the parameter $p=0\dots 1$), measure for each image the number of pixels in the fluorescent imaged pattern, and then deduce the relationship between the gradient magnitude and the pixel size. The result of such an analysis is shown in Fig. 1c. The parameter $1/p$ is related to the pixel resolution

in phase-gradient-based magnetic resonance imaging according to the expression:

$$\Delta x = \frac{1}{(\gamma/2\pi) \int_t G dt} = \frac{1}{(\gamma/2\pi) \cdot p \cdot (G_{\max} \cdot \Delta T)} \quad (1)$$

Based on this derivation, we obtain that our pixel resolution is $\sim 470 \text{ nm}$, and the maximum available resolution for $p=1$ is 75 nm . This capability can be further extended to the nanometer scale by employing smaller samples and fibers, with the goal of reaching resolution of $\sim 10 \text{ nm}$, which is required for practical quantum technology applications.

- [1] A. Blank, G. Shapiro, R. Fischer et al., Appl. Phys. Lett. **106** (3), 034102 (2015).
[2] R. L. Walsworth et al, Nat Nanotechnol **10** (10), 859 (2015).

Diamond-Based Quantum Amplifier

A. Blank, A. Sherman

Schulich faculty of chemistry, Technion - Israel Institute of Technology, Haifa, 32000, Israel

e-mail: ab359@technion.ac.il

Unpaired electron spins of nitrogen vacancies in diamond single crystals are known to have many favorable properties of relevance to quantum devices. For example, their electronic spin triplet states have long coherence times and the quantum state of the spins can be read-out optically. Another important property is that upon light illumination the spins are pumped to the $|0\rangle$ state reaching high polarization. Recently, this unique property was exploited to construct a MASER (Microwave Amplifier by Stimulated Emission of Radiation) that takes a green laser input radiation directed to a diamond crystal placed in a high-Q resonator, and produces coherent microwave radiation due to stimulated decay of the spins pumped to the $|0\rangle$ level, down to the $|-1\rangle$ state [1]. While this recent experiment shows how NV MASER can be a microwave source, it is yet to demonstrate more practical aspects of MASER operation, meaning amplification of small microwave signals with minimal noise contribution, possibly even using it as a single microwave photon detector. In the talk, we will discuss the potential of bringing NV MASER technology into these regimes and show our initial work towards demonstrating such MASER as a useful quantum amplifier for a variety of quantum technological applications, such as quantum radar and quantum communication.

[1] J. D. Breeze, et. al. Nature **555**, 493 (2018).

Optically Detected Spin Resonance in Rare Earth Doped Crystals for Quantum Technologies

Sacha Welinski and Philippe Goldner

Chimie ParisTech, PSL University, CNRS, Institut de Recherche de Chimie Paris, 75005 Paris, France

e-mail: philippe.goldner@chimieparistech.psl.eu

Quantum technologies are developed to overcome classical limits in communication and processing but also in new areas like sensing, imaging, and simulations. They will impact all aspects of life by allowing e.g. ultra-secure communications, simulation of complex molecules, or new medical bio-imaging techniques. Many quantum systems are investigated for specific tasks. The next major challenge is to overcome the limits of single systems by associating different quantum systems in hybrid architectures, each selected for its specific properties. Optical interconnection of these systems will also be necessary to further develop functionalities in a global 'quantum internet' [1].

Crystals doped with paramagnetic rare earth ions could play a pivotal role in this scheme by offering a solid-state platform that enables efficient coupling between microwave and optical photons. This has a strong interest in connecting superconducting quantum processors with optical networks to create e.g. distributed quantum processing. In this paper, we will discuss recent advances in the development and spectroscopy of paramagnetic rare earth doped crystals using in particular optically detected electron spin resonance. This technique has recently allowed us to show long spin coherence lifetimes at zero magnetic field and observe spin echoes in an optically excited state in ytterbium and erbium doped Y_2SiO_5 crystals. [2-3]. In this paper, we will discuss these results and the perspectives they open for rare-earth based quantum technologies.

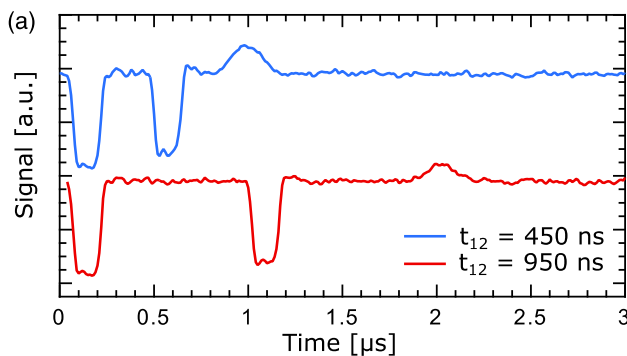


Fig.1. Optically detected spin echoes in the excited state of $\text{Er}^{3+}:\text{Y}_2\text{SiO}_5$.

[1] H.J. Kimble, "The quantum internet," *Nature* 453, 1023–1030 (2008).

[2] S. Welinski, P.J.T. Woodburn, N. Lauk, R.L. Cone, C. Simon, P. Goldner, and C.W. Thiel, *Phys. Rev. Lett.* 122, 247401 (2019).

[3] A. Ortu, A. Tiranov, S. Welinski, F. Fröwis, N. Gisin, A. Ferrier, P. Goldner, and M. Afzelius, *Nat. Mater.* 17, 1–6 (2018).

Superconducting Spin-valve Effect in a Heterostructures Containing the Heusler Alloy as Ferromagnetic Layers

A. A. Kamashev¹, N. N. Garif'yanov¹, A. A. Validov¹, J. Schumann²,
V. Kataev², B. B. chner^{2,3}, Ya. V. Fominov^{4,5,6} and I. A. Garifullin¹

¹Zavoisky Physical-Technical Institute, FRC Kazan Scientific Center of RAS, Kazan, Russia

²Leibniz Institute for Solid State and Materials Research IFW Dresden, Dresden, Germany

³Institute for Solid State Physics, Technical University Dresden, Dresden, Germany

⁴L. D. Landau Institute for Theoretical Physics RAS, Chernogolovka, Russia

⁵Moscow Institute of Physics and Technology, Dolgoprudny, Russia

⁶National Research University Higher School of Economics, Moscow, Russia

e-mail: kamandi@mail.ru

In the present work we investigated magnetic and transport properties of two series of samples MgO/CoO_x(3.5nm)/Py(5nm)/Cu(4nm)/HA(d_{HA}^{RT})Cu(1.5nm)Pb(80nm) (PLAK341) and MgO/Ta(5nm)/HA^{hot}(20nm)/Cu(4nm)/Ni(d_{Ni})Cu(1.5nm)Pb(105nm) (PLAK421) [where $d_{HA}^{RT} = 0.6 - 8$ nm and $d_{Ni} = 0.6 - 2.5$ nm]. The most interesting results for both series of samples are demonstrated on Fig. 1 and Fig. 2.

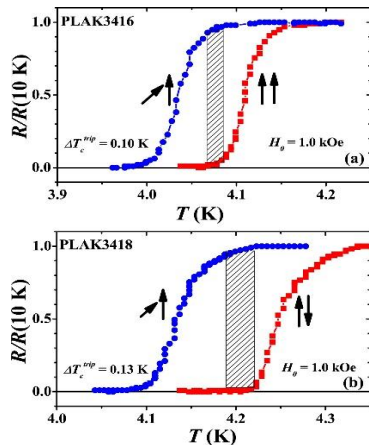


Fig.1. SC transition curves for different configurations of the cooling field used to fix the direction of the magnetization of the Py layer and the applied magnetic field $H_0=1$ kOe that rotates the magnetization of the HA^{RT} layer: (a) sample PLAK 3416 ($d_{HA}^{RT}=4$ nm) (P and PP) and (b) sample PLAK3418 ($d_{HA}^{RT}=0.6$ nm) (for AP and PP) at $H_0=1$ kOe.

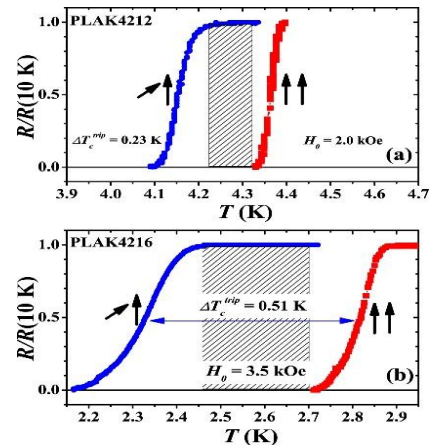


Fig.2. SC transition curves for the P and PP configurations of the magnetization of the Ni layer and the applied magnetic field that rotates the magnetization of the HA^{hot} layer: (a) sample PLAK4212 ($d_{Ni}=0.9$ nm) at $H_0=2$ kOe and (b) sample PLAK4216 ($d_{Ni}=2.5$ nm) at $H_0=3.5$ kOe.

The obtained experimental results show that as a result of the optimal choice of materials for F layers the triplet contribution is probably always predominant in the SSV effect. According to the results of the present work and the data of Ref.[1], the best candidate for the material of the F1 layer in F1/F2/S SSV structure is a half metal. In particular, finding the most appropriate ferromagnet as a half metal with a high degree of spin polarization of the conduction band appears to be a crucial issue. This allows us to increase the area of the full switching ΔT_c^{full} up to 0.3 K which is thirty times larger than that obtained in the first experiment [2].

[1] A. Singh, S. Voltan, K. Lahabi, and J. Aarts, Phys. Rev. X **5**, 021019 (2015).

[2] P.V. Leksin et al., Appl. Phys. Lett. **97**, 102505 (2010).

Spin Pumping Theory of Ferromagnetic – Normal Metal Structures (in the case of $\text{La}_{2/3}\text{Sr}_{1/3}\text{MnO}_3/\text{NM}$ Bilayers)

F.S.Dzheparov¹, K.L.Stankevich²

¹National Research Center “Kurchatov Institute”, ITEP, Moscow, Russian Federation

²Institute of Radio Engineering and Electronics, Russian Academy of Sciences, Moscow, Russian Federation

e-mail: kl.stankevich@physics.msu.ru

The present report is dedicated to a spin current in $\text{La}_{2/3}\text{Sr}_{1/3}\text{MnO}_3/\text{normal metal}$ (NM) bilayers arising due to the effect of spin pumping. Spin pumping was theoretically predicted by A.Brataas et al [1,2] in 2002 and this effect has attracted the growing interest since then [3].

Spin pumping is based on the effect of a ferromagnetic resonance in ferromagnet (Fe)/NM bilayers driven by microwave radiation. Precessing spins of the ferromagnet interact through so-called sd exchange interaction with conduction electrons that propagate due to diffusion motion resulting in the pure spin current in NM. The spin current flows without electric charge transfer that opens new possibilities in spintronics.

$\text{La}_{2/3}\text{Sr}_{1/3}\text{MnO}_3$ is a half metal that gives an opportunity to use it in spintronics for creating fully polarized spin current [4]. Recently, our scientific group [5] experimentally studied spin pumping in $\text{La}_{2/3}\text{Sr}_{1/3}\text{MnO}_3/\text{platinum}$ bilayers.

In this work we present a new theoretical description of the spin pumping effect in $\text{La}_{2/3}\text{Sr}_{1/3}\text{MnO}_3/\text{NM}$ bilayers. Influence of hopping conductivity of the $\text{La}_{2/3}\text{Sr}_{1/3}\text{MnO}_3$ on spin pumping is studied. The interaction between $\text{La}_{2/3}\text{Sr}_{1/3}\text{MnO}_3$ and NM is taken into account by introducing Rado-Weertman boundary conditions [6] at the $\text{La}_{2/3}\text{Sr}_{1/3}\text{MnO}_3/\text{NM}$ interface. We compare our results with spin pumping in insulating Fe/NM bilayers [7].

The work was carried out within the framework of the state task and partially was supported by the Russian Foundation for Basic Research (grants No. 18-37-00170).

- [1] A. Brataas, Y. Tserkovnyak, G.E.W. Bauer, B.I. Halperin, Phys. Rev. B **66**, 060404 (2002).
- [2] Y. Tserkovnyak, A. Brataas, G.E.W. Bauer, Phys. Rev. B **66**, 224403 (2002).
- [3] Y. Xu, D.D. Awschalom, J. Nitta, Handbook of Spintronics, Springer Netherlands (2016).
- [4] X. Li, J. Yang, National Science Review, **Vol. 3**, Issue 3, 365–381 (2016).
- [5] V.A. Atsarkin, I.V. Borisenko, V.V. Demidov, T.A. Shaikhulov, J. Phys. D: Appl. Phys. **51**, 245002 (2018).
- [6] G.T. Rado and J.R. Weertman, J. Phys. Chem. Solids **11**, 315 (1959).
- [7] S.M. Rezende, R.L. Rodríguez-Suárez, A. Azevedo, Phys. Rev. B **88**, 014404, (2013).

Photon Upconversion via Triplet Exciton Fusion in the Super-yellow PPV:PdTPBP Host-sensitizer System

I.V. Sudakov¹, B.Z. Tedlla¹, F. Zhu², M. Cox², B. Koopmans², V.L. Whittle³, J.A. Gareth Williams³, S. Van Doorslaer¹, E. Goovaerts¹

¹Department of Physics, University of Antwerp, Belgium

²Department of Applied Physics, Eindhoven University of Technology, The Netherlands

³Department of Chemistry, University of Durham, United Kingdom

e-mail: ivan.sudakov@uantwerpen.be

The energy conversion in single junction solar cells is limited by the Shockley-Queisser limit linked to the bandgap of the semiconducting material, which defines the energy loss after absorption of higher energy photons, and limits the absorption of photons at the low energy end. Novel device concepts to overcome this limit have been proposed, based on photon conversion processes involving triplet excitons in organic materials. Triplet-triplet fusion, or upconversion via triplet-triplet annihilation (TTA-UC), has already been demonstrated [1,2] to increase the performance of solar cell devices. Understanding of the processes limiting the efficiency of the TTA-UC is important for further optimization of such devices.

In this work, we exploit advanced electron paramagnetic resonance (EPR) techniques as well as optical absorption and fluorescence spectroscopy to investigate the fate of charge excitations in “super-yellow” *poly*-paraphenylene vinylene (SY-PPV) copolymer doped with the triplet sensitizer palladium (*meso*-tetraphenyl-tetrabenzoporphyrin) (PdTPBP). In this system TTA-UC has previously been studied [3], but was found to be quenched as soon as the sensitizer concentration in SY-PPV:PdTPBP films is increased above a few percent. As a function of sensitizer concentration in the films, triplet exciton (TE) and polaron (P) states are monitored by electrically- and optically detected magnetic resonance (EDMR and ODMR) and light-induced EPR, providing indications for TE-P annihilation as quenching mechanism. We demonstrated that selective excitation of the PdTPBP sensitizer leads to the production of TE in the SY-PPV, which was found to be a more efficient pathway compared to the direct ISC in the neat polymer. To shed light on the polaron-related processes, the well-known fullerene acceptor PCBM was introduced as electron trap in binary and ternary blends with the copolymer and the sensitizer. The nature and localization of the TE-P interactions will be discussed on the basis of these results.

[1] C. Li, ACS Photonics, **3**, 784–790 (2016).

[2] Y.Y. Cheng, Chem. Sci., **7**, 559–568 (2016).

[3] V. Jankus, Adv. Funct. Mater., **23**, 384-393 (2013).

Associative Memory on Qutrits by means of Quantum Annealing

V.E. Zobov, I.S. Pichkovskiy

Kirensky Institute of Physics, Federal Research Center KSC SB RAS, Krasnoyarsk, Russia

e-mail: rsa@iph.krasn.ru

At the present stage of development of information technologies, quantum properties of many-body systems open up new possibilities of artificial neural networks [1], including the associative memory [2 - 5]. Quantum superposition of states can be used to store patterns [2 - 5]. As a neuron, a qubit is usually considered - a quantum system with two states. However, in this role a system with three states — qutrit can be used. Among the advantages of qutrits over qubits it expect a faster growth of the Hilbert space, and hence the size of the computational basis with the addition of new elements. This circumstance may be important for increasing the memory capacity. As qutrits, it is suggested to use objects with spin $S = 1$, for example, NV centers in diamond [6]. In this case, there is a large difference in the frequency of transitions between different energy levels, which makes it possible to control the state of the system with the help of transition-selective microwave pulses.

In this work, we consider the associative memory on the qutrits represented by the spins with $S = 1$. As a computational basis, we use a basis $|m_1, m_2, \dots, m_n\rangle$ of the eigenfunctions of the operators S_i^z of the projections of the spins on the Z axis. Each of the projections m_i can take one of three values: 1, 0, -1. To keep in memory p elements represented by p quantum vectors $|\psi_\mu\rangle = |m_1^\mu, m_2^\mu, \dots, m_n^\mu\rangle$, where $\mu = 1, 2, \dots, p$, we chose the projection method of memorization [2, 3], in which the recording is performed through the memory Hamiltonian $H_{mem} = -\sum_{\mu=1}^p |\psi_\mu\rangle\langle\psi_\mu|$. This choice is due to the need to operate with a state with a zero spin projection, the interaction of which with the magnetic field vanishes. The recording and recall of the patterns are carried out by adiabatic variation of the Hamiltonian over time (by quantum annealing) [2 - 5]:

$$H(t) = (1 - t/T)H_0 + (t/T)(1 - t/T)H_{help} + (t/T)(H_{mem} + \Gamma H_{prob}),$$

where $H_0 = -h \sum_{i=1}^n S_i^x$ is the initial Hamiltonian, $H_{prob} = -|\psi_{prob}\rangle\langle\psi_{prob}|$ is a probe Hamiltonian of hint, Γ is a small coefficient. H_{help} is an auxiliary Hamiltonian with off-diagonal projectors which we have proposed to equalize the probabilities of finding the system in different states of superposition. We performed simulations on two and three qutrits and shown an increase in the memory capacity after replacing qubits with qutrits. As a result, we demonstrated the possibility of realizing associative memory on qutrits and pattern recognition by means of quantum annealing.

- [1] V. Dunjko and H. J. Briegel, Reports on Progress in Physics **81**, 074001 (2018).
- [2] R. Neigovzen, J.L. Neves, R. Sollacher, and S.J. Glaser, Phys. Rev. A **79**, 042321 (2009).
- [3] H. Seddiqi and T.S. Humble, Front. Phys. **2**, 79 (2014).
- [4] S. Santra, O. Shehab, and R. Balu, Phys. Rev. A **96**, 062330 (2017).
- [5] C. Dłaska, L.M. Sieberer, and W. Lechner, Phys. Rev. A **99**, 032342 (2019).
- [6] M.F. O’Keeffe, L. Horesh, D.A. Braje, and I.L. Chuang, New J. Phys. **21**, 023015 (2019).

Spin Current Induced by Magnetic Resonance in Ferromagnet-normal Metal Bilayers

V.A. Atsarkin

Kotel'nikov Institute of Radio Engineering and Electronics of RAS, 125009 Moscow, Russia

e-mail: atsarkin@cplire.ru

Spin current is a directed flow of spin angular momentum. The generation and control of spin currents flowing across an interface between media with different magnetic properties have recently attracted considerable interest in both scientific and technical aspects related to spintronics. An effective way to create a “pure” spin current (not related to any charge flow) is the so-called spin pumping (SP) in ferromagnet – normal metal (FM/NM) bilayers. The SP is implemented by excitation of spin precession in the FM layer at ferromagnetic resonance (FMR) and injection of the non-equilibrium spin momentum into the NM film.

Temperature dependence of the pure spin current is of fundamental importance, being directly related to spin-dependent features of the electron transport. The present work is concerned with experimental study of this problem. The experiments have been performed with an epitaxial thin-film bilayers $\text{La}_{2/3}\text{Sr}_{1/3}\text{MnO}_3/\text{Pt}$ deposited on a NdGaO_3 substrate (some early results are published in [1]). The spin current was generated by microwave pumping under conditions of ferromagnetic resonance in the ferromagnetic $\text{La}_{2/3}\text{Sr}_{1/3}\text{MnO}_3$ layer and detected in the Pt layer due to the inverse spin Hall effect. A considerable increase in the spin current magnitude has been observed upon cooling from the Curie point (350 K) down to 100 K. The role of inhomogeneous FMR broadening was established and taken into account. Using the obtained data, the temperature evolution of the mixed spin conductance has been extracted and compared with current theory.

- [1] V.A. Atsarkin, I.V. Borisenko, V.V. Demidov, T.A. Shaikhulov, *J. Phys. D: Appl. Phys.* **51**, 245002 (2018).

Slow Paramagnetic Relaxation in Graphene Oxide and Partially Reduced Graphene Oxide

Maria A. Augustyniak-Jabłokow¹, Krzysztof Tadyszak², Roman Strzelczyk¹, Ryhor Fedaruk³, Raanan Carmieli⁴, Łukasz Majchrzycki⁵

¹ Institute of Molecular Physics, Polish Academy of Sciences, Poznań, Poland

² NanoBioMedical Centre, Adam Mickiewicz University, Poznań, Poland

³ Institute of Physics, University of Szczecin, Szczecin, Poland

⁴ Department of Chemical Research Support, Weizmann Institute of Science, Rehovot, Israel

⁵ Center of Advanced Technology, Adam Mickiewicz University, Poznań, Poland

e-mail: maria.augustyniak@ifmpan.poznan.pl

Graphene oxide (GO) and reduced graphene oxide (rGO) are well-known and widely used forms of the functionalized graphene. Their applications include 2D electronics, optoelectronics, catalysis, energy storage and solar cells. Properties of GO are determined by degree of oxidation and distribution of the functional groups on the surface, while properties of rGO depend on the method and degree of reduction. In both materials the EPR signals were observed. Rapid passage effects under microwave saturation of these signals revealed the presence of slowly relaxing paramagnetic centers in GO [1]. This was confirmed by pulsed EPR techniques [2]. The spin-lattice relaxation time was found to change from $T_1 = 52$ ms at 5 K to 0.153 ms at 240 K. The phase memory time T_m changes non-monotonically with temperature, and reaches its maximum of 2.2 μ s at 5 K (Fig. 1). This dependence was explained by molecular motions of the functional groups and the adsorbed water molecules. The paramagnetic centers can be attributed to the unfunctionalized carbons in the highly functionalized regions of GO.

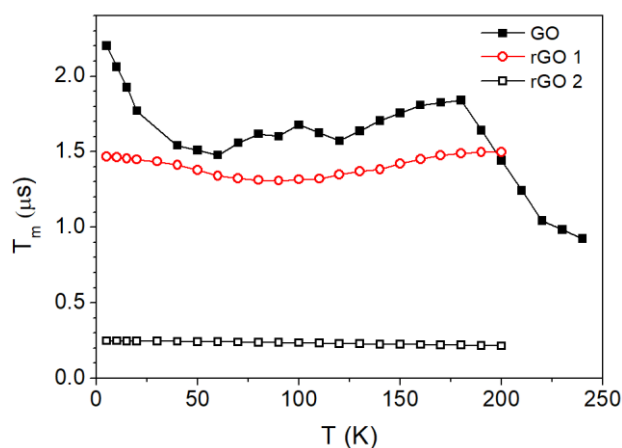


Fig.1. The phase memory time of paramagnetic centers in GO and rGO as a function of temperature.

In rGO, the two-exponential decay of spin echo indicates the presence of two types of paramagnetic centers located in various environment. One of them is characterized by $T_m \sim 1.5$ μ s and in the temperature range of 5 – 200 K it shows a non-monotonical temperature dependence. This center can be associated with small functionalized regions still present in rGO. The second center has much shorter T_m (~ 0.25 μ s) which decreases monotonically with temperature. This center is localized in the strongly defected, nonfunctionalized or weakly functionalized regions of rGO.

The presence of slowly relaxing paramagnetic centers in GO and RGO is unexpected. The observed phase memory times of order of 1 μ s are long enough for realization of qubits.

[1] M.A. Augustyniak-Jabłokow, R. Fedaruk, R. Strzelczyk, Ł. Majchrzycki, Appl. Magn. Reson. **50**, 761 (2019).

[2] M.A. Augustyniak-Jabłokow, K. Tadyszak, R. Strzelczyk, R. Fedaruk, R. Carmieli, Carbon **152**, 98 (2019).

Experimental Realization of Qubit and Qutrit Quantum Manipulations using EPR of Rare Earth Ions in Single Crystals

E.I. Baibekov, G.V. Mamin, M.R. Gafurov, S.B. Orlinskii, B.Z. Malkin, A.A. Rodionov, I.N. Kurkin

Institute of Physics, Kazan Federal University, Kazan, Russian Federation

e-mail: edbaibek@gmail.com

We demonstrate how one can use impurity ions with spin $S > 1/2$ incorporated in anisotropic crystal background in order to implement multiple-level quantum manipulations. In the present study, we use CaWO_4 single crystal containing 0.01 at. % Gd^{3+} . The lowest-energy spectroscopic multiplet of Gd^{3+} ion is $^8S_{7/2}$, representing a good $S = 7/2$ high-spin value. Gd^{3+} ions replace Ca^{2+} at sites with tetragonal (S_4) symmetry. X-band EPR spectrum of Gd^{3+} ion contains various $S_Z \leftrightarrow S_Z'$ transitions, whose frequencies vary with changing the direction of the static magnetic field with respect to the crystal axes [1,2]. One can choose certain field direction, so that two or more transitions are allowed within a rather small energy interval (in our case, $3/2 \leftrightarrow 5/2$ and $5/2 \leftrightarrow 7/2$). These three quantum states $S_Z = 3/2, 5/2, 7/2$ of gadolinium ion form an effective qutrit in our experimental procedure.

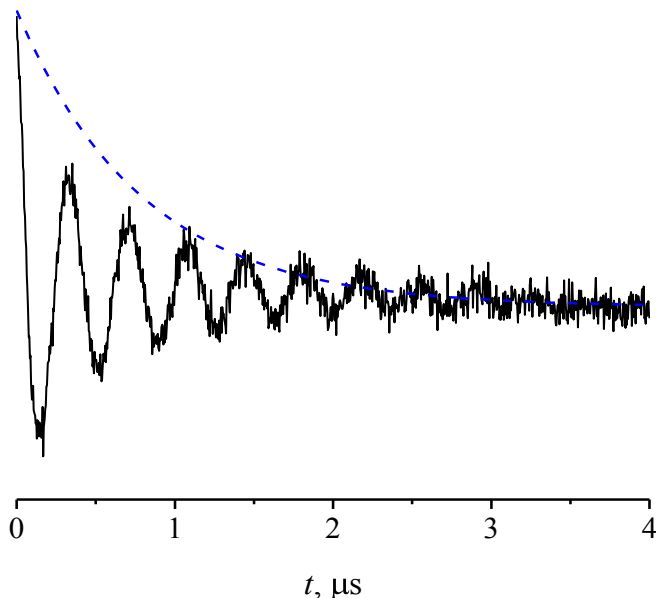


Fig.1. Electron spin echo signal recorded for the transition $3/2 \leftrightarrow 5/2$ of the Gd^{3+} lowest-energy multiplet using double-frequency pulse sequence specified in the text.

In order to demonstrate quantum manipulations involving simultaneously all 3 states, we used pulsed ELDOR (Electron-Electron Double Resonance) techniques. Fig. 1 shows an example of the qutrit manipulation using the following pulse sequence: $\pi/2(\nu_1) - \pi/2(\nu_1) - t(\nu_2) - \pi/2(\nu_1)$. There, $\pi/2$ pulses affected the transition $3/2 \leftrightarrow 5/2$ at the frequency $\nu_1 = 9.74$ GHz, while the third (nutational) pulse of length t was tuned to the transition $5/2 \leftrightarrow 7/2$ at $\nu_2 = 9.49$ GHz. A stimulated spin echo produced on the transition $3/2 \leftrightarrow 5/2$ is disturbed by the third pulse of the frequency ν_2 . The oscillations of the $3/2 \leftrightarrow 5/2$ coherence decay nearly exponentially (a blue dashed line fit) with the characteristic time $0.8 \mu\text{s}$. The decay is predominantly caused by the

inhomogeneous broadening of the transitions; dipolar relaxation contributes to approximately 10% of the observed decay rate.

This work was financially supported by the Russian Science Foundation (Project no. 17-72-20053).

- [1] J.S.M. Harvey, H. Kiefte, Canadian J. Phys. **49**, 995 (1971).
 [2] E.I. Baibekov et al, Phys. Rev. B **95**, 064427 (2017).

Three and a Half Puzzles in EPR Physics of Strongly Correlated Materials

S.V.Demishev

Prokhorov General Physics Institute of Russian Academy of Sciences, Moscow, Russia

e-mail: demis@lt.gpi.ru

In the present talk, we discuss several unsolved problems of EPR physics in various strongly correlated materials, for which experimental data are not completely clarified on a theoretical level. To start, let us consider the integrated intensity $I(T)$ in AF $S=1/2$ quantum spin chains, which demonstrate perfect coincidence with the static magnetic susceptibility $\chi(T) \sim I(T)$ in a wide temperature range [1]. We argue that either in the case of Bonner-Fisher law or in the case of divergent susceptibility specific to a Griffiths phase $\chi(T) \sim 1/T^\alpha$, the temperature dependence of the EPR line width, i.e spin fluctuations, provides the main contribution to observed $I(T)$ dependence even in the limit $T \rightarrow 0$. At the same time, statistical physics requires sharp energy levels for computing $\chi(T)$. Continuing the discussion of the line width problem it is worth to recall the unique relation between line width W and g-factor shift $W/\Delta g = 1.99k_B T/\mu_B$, which was initially derived by us from Oshikawa-Affleck theory for the specific case of AF $S=1/2$ quantum spin chains [2]. Recent experiments show that a similar relation may hold also in 3D metallic systems in completely unexpected way [3].

The second problem is the observation of the magneto-optical mode in $\text{CuGeO}_3:\text{Co}$ with linear oscillation of magnetization [4], which put into question applicability of Landau-Lifshits equation of motion and its universal character. We wish to mark that up to now no explanation of this effect was suggested.

The last puzzle discussed is EPR in strongly correlated magnetic metals. Common sense tells that in the diluted system we should see narrow EPR lines relevant to the limit of an isolated magnetic ion, whereas in the concentrated system lines must be broad and without fine structure. However, experiment demonstrates that narrow lines correspond to the concentrated case and dilution of the system may completely suppress magnetic resonance [5]. The most recent study shows that this anomalous behavior cannot be attributed to Korringa type spin relaxation and may have another different origin requiring theoretical clarification. In addition, special attention should be paid to the cases when oscillating part of magnetization deviates from the total static magnetization, and may even exceed it [6,7].

This work was supported by the Programme of the Russian Academy of Sciences “Electron spin resonance, spin-dependent electronic effects and spin technologies”.

[1] S.V. Demishev, et al., Journal of Superconductivity and Novel Magnetism **20**, 105 (2007).

[2] S.V. Demishev, et al., Europhysics Letters **63**, 446 (2003).

[3] A.V. Semeno, et al., JETP Letters **108**, 237 (2018).

[4] S.V. Demishev, et al., JETP Letters **84**, 249 (2006).

[5] S.V. Demishev, et al., JETP Letters **100**, 28 (2014).

[6] S.V. Demishev, et al., Phys. Rev. B **80**, 245106 (2009).

[7] A.V. Semeno, et al., Scientific Reports, **6**, 39196 (2016).

Toward the Theory of the Spins and Orbital Moments Coupling with Electric Field

M. Eremin

Institute of Physics, Kazan Federal University, Kazan, Russian Federation

e-mail: meremin@kpfu.ru

I revisit the theory of interaction of the spins and orbital moment with electric field focusing on the transition metal compounds without inversion symmetry. As specific examples, I will discuss the terahertz absorption spectrum of Fe^{2+} in tetrahedral environment and optical absorption of Cu^{2+} ions in position with point group symmetry S_4 .

In general case the effective operator describing the coupling of orbital states for a 3d electron with the electric field can be written as follows [1]:

$$H_E = \sum_{p,t} \{E^{(1)}U^k\}_t^{(p)} \sum_j d^{(1k)p}(R_j) (-1)^t C_{-t}^{(p)}(\mathcal{G}_j\varphi_j) \quad (1)$$

The curly brackets denote the Kronecker product of the spherical tensor of the electric field with the unit irreducible tensor operator acting on 3d electron states. The spherical coordinates $R_j\mathcal{G}_j\varphi_j$ denote the positions of lattice ions, the same as in the crystal field theory, $C_{-t}^{(p)}(\mathcal{G}_j\varphi_j) = \sqrt{4\pi/(2p+1)} \cdot Y_{p,-t}(\mathcal{G}_j\varphi_j)$ are components of spherical tensors. The quantities $d^{(1k)p}(R_j)$ are calculated in the local coordinate system with the z-axis along the 3d-ion–ligand direction. They contain two contributions:

$$d^{(1k)p}(R_j) = d_{cf}^{(1k)p}(R_j) + d_{cov}^{(1k)p}(R_j). \quad (2)$$

The first term is associated with an odd crystal field. It is well known in the Judd's theory of electric dipole transitions of rare earth paramagnetic centres [1]. The second term in Eq. (2) is related to the effective electric dipole moment, which arises due to the asymmetry in the overlap of 3d electron states with the shells (2p and 2s) of surrounding ligands and as well to the asymmetry in the amplitudes of probabilities of virtual transitions of electrons from the ligands to the 3d shell. Applying the second quantization technique, I have got

$$d_{cov}^{(1k)p}(R_j) = |e| \frac{\varepsilon + 2}{3} \sum_q (-1)^q \sqrt{(2p+1)} \cdot \begin{pmatrix} 1 & k & p \\ -q & q & 0 \end{pmatrix} \cdot d_q^{(k)}(R_j), \quad (3)$$

$$d_q^{(k)}(R_j) = (2k+1) \sum_{m,m'} (-1)^{l-m} \cdot \begin{pmatrix} l & k & l \\ -m & q & m' \end{pmatrix} \cdot \langle lm | rC_q^{(1)} | lm' \rangle, \quad (4)$$

$$\langle lm | rC_q^{(1)} | lm' \rangle = \lambda_{lm,\rho} \langle \rho | rC_q^{(1)} | \rho' \rangle \lambda_{\rho',lm'} - 2 \langle lm | rC_q^{(1)} | \rho \rangle \lambda_{\rho,lm'}. \quad (5)$$

Here for short, as usual, we denote $\lambda_{lm,\rho} = \gamma_{lm,\rho} + S_{lm,\rho}$. $\gamma_{lm,\rho}$ are the so-called covalency parameters and $S_{lm,\rho}$ are overlap integrals, k are even numbers, 2 and 4, and p are odd numbers, 1,3 and 5.

[1] A.A. Kornienko and M.V. Eremin, Fiz. Tverd. Tela **19** (1), 52 (1977).

Anisotropic Exchange Interaction in Low Dimensional Systems

R. Eremina¹, H.-A. Krug von Nidda²

¹Zavoisky Physical-Technical Institute, FRC Kazan Scientific Center of RAS, Kazan, Russian Federation

²Experimentalphysik V, Center for Electronic Correlations and Magnetism, Institute for Physics, Augsburg University, D-86135 Augsburg, Germany

e-mail: REremina@yandex.ru

Unconventional magnetic ground states and excitations of frustrated quantum-spin chains represent one of the most attractive issues in solid-state physics during the last decades. They appear under a fine balance of competing dominant exchange interactions and are often caused by much weaker interactions or fluctuations. Typically, frustration in quasi-one-dimensional chain magnets is provided by competing interactions, if the nearest-neighbor (NN) exchange is ferromagnetic and the next-nearest neighbor (NNN) exchange is antiferromagnetic. There is a number of magnets which are attractive objects for experimental investigations as realizations of 1D frustrated systems like LiCuVO₄, Rb₂Cu₂Mo₃O₁₂, NaCu₂O₂, LiCu₂O₂, Li₂CuO₂, Li₂ZrCuO₄, and CuCl₂, (see [1] and Refs. therein).

Electron paramagnetic resonance (EPR) is a convenient method to probe anisotropic spin-spin interactions. The EPR linewidth displays the average amplitude of the fluctuating field on the magnetic ion, which can be directly related to the parameters of the anisotropic spin-spin interactions. We present a quantitative analysis of the angular dependence of the paramagnetic resonance linewidth in LiCu₂O₂ and Cs₂CuCl_{4-x}Br_x to determine the anisotropic exchange parameters. For this purpose ESR is the method of choice, because the anisotropy of the line broadening is extremely sensitive to anisotropic interactions, while the isotropic exchange contributions only result in a general isotropic narrowing of the ESR signal. The EPR signal of this system consists of a single exchange-narrowed resonance line. To derive the contribution of the anisotropic symmetric and uniform Dzyaloshinsky-Moriya (DM) interaction to the linewidth in LiCu₂O₂ and Cs₂CuCl_{4-x}Br_x, one starts from the one dimensional Heisenberg Hamiltonian:

$$H_{ij} = J_{ij} \mathbf{S}_i \mathbf{S}_j + \sum_{\alpha=x,y,z} D_{\alpha} \left[\mathbf{S}_i \times \mathbf{S}_j \right]_{\alpha} + \sum_{\alpha,\beta=x,y,z} J_{ij}^{\alpha\beta} S_i^{\alpha} S_j^{\beta} + \sum_{\alpha,\beta=x,y,z} g_{\alpha\beta} \mu_B H_{\alpha} S_{\beta},$$

where J_{ij} and $J_{ij}^{\alpha\beta}$ are the parameters of the isotropic and anisotropic exchange interactions, D_{α} ($\alpha = x, y, z$) are parameters of antisymmetric DM interaction in the coordinate system with the z -axis parallel to the applied magnetic field and the last term is the interaction of spins with an external magnetic field. From the angular dependence of the linewidth in three crystallography planes, using the equations from [2], we obtained the components of the DM vector and anisotropic exchange interaction as well as the effective exchange parameter J . The schematic pathway of the relevant anisotropic spin-spin coupling between two neighboring chains and possible exchange path allowing the existence of the Dzyaloshinskii-Moriya interaction between neighboring Cu²⁺ ions within the chains in LiCu₂O₂ are considered.

[1] Z. Seidov, T.P. Gavrilova, R.M. Eremina, L.E. Svistov, A.A. Bush, A. Loidl, and H.-A. Krug von Nidda. Phys. Rev. B **95**, 224411 (2017).

[2] R.M. Eremina, Magnetic Resonance in Solids. Electronic Journal **16**, 14102 (2014).

Study of Nonmagnetic Impurities in the Frustrated $S=1/2$ Spin Chains: NMR and Magnetization Study

D. Gafurov^{1,3}, M. Iakovleva^{1,2}, I. Scurschii⁴, M.-I. Sturza², H-J. Grafe², V. Kataev²,
B. Buechner² and E. Vavilova¹,

¹Zavoisky Physical-Technical Institute, FRC Kazan Scientific Center of RAS, Kazan, Russia

²Leibniz Institute for Solid State and Materials Research IFW Dresden, Dresden, Germany

³Institute of Physics, Kazan Federal University, Kazan, Russian Federation

⁴Hochfeld-Magnetlabor Dresden (HLD-EMFL), Helmholtz-Zentrum Dresden-Rossendorf, Dresden, Germany

e-mail: londonstyle1998@gmail.com

LiCuSbO_4 is a system where ions Cu^{2+} ($S=1/2$) form well-isolated one-dimensional frustrated antiferromagnetic spin Heisenberg chains along the crystallographic axis a . The absence of a long-range magnetic order up to very low temperatures suggests the realization of the quantum spin liquid ground state. Frustration of the exchange interactions in the spin-chains creates a strong field dependence of the magnetic properties of the material. As it was found in [1], strong indications of a magnetic field-induced spin nematic liquid state is observed in LiCuSbO_4 above a field of $\sim 13\text{T}$. Substitution of a part of copper ions by non-magnetic Zn cuts the chains and creates the paramagnetic centers at the ends of chain segments, which can have a strong effect on magnetic properties of the compound. Here we present the results of the magnetization and NMR study of the series of $\text{LiCu}_{(1-x)}\text{Zn}_x\text{SbO}_4$ samples with $0 < x < 0.3$. Our experiments shows that non-magnetic doping suppress the crossover to spin-liquid phase whereas low-dimensional maximum of the nuclear relaxation at 30-90 kG remains pronounced at $T \sim 50\text{K}$.

The work of E.V., M.I. and D.G. was supported by RFBR through grant No. 18-02-00664.

[1] H-J. Grafe et.al., Scientific Reports **7**, 6720 (2017).

Effect of Lithium Deficiency on the Ion Mobility in Frustrated $\text{Li}_{1-x}\text{CuSbO}_4$ Compound Studied by NMR

D. Gafurov^{1,3}, M. Iakovleva^{1,2}, M.-I. Sturza², B. Buechner² and E. Vavilova¹

¹ Zavoisky Physical-Technical Institute, FRC Kazan Scientific Center of RAS, Kazan, Russia

² Leibniz Institute for Solid State and Materials Research IFW Dresden, Dresden, Germany

³ Institute of Physics, Kazan Federal University, Kazan, Russian Federation

e-mail: londonstyle1998@gmail.com

One of the main factors determining the characteristics of lithium batteries is the cathode material. The electric current in the electrolytes and the cathode materials is caused by the movement of lithium ions. Ion mobility is the main parameter of current ion conductivity. NMR is a power tool for studying the ion mobility. It includes the investigations of NMR line shape, studying of the nuclear spin-lattice relaxation temperature dependence, a magnetic field gradient NMR and some other techniques. Here we present the results of NMR study of frustrated spin-chain compound $\text{Li}_{1-x}\text{CuSbO}_4$ with a different index of Li-deficiency. A series of samples was investigated in temperature range 300K - 460K at a frequency of 12 MHz. The temperature dependence of the ^7Li NMR linewidth shows a gradual change of the activation energy of lithium ion jumps with an increase of the x index.

The work of E.V., M.I. and D.G. was supported by RFBR through grant No. 18-02-00664.

**Temperature Evolution of Magnetic Properties of Sodium Iridates $\text{Na}_{(3/2)}\text{M}_{(1/2)}\text{IrO}_3$
($\text{M} = \text{Ni}, \text{Cu}, \text{Zn}$) probed by NMR and μSR**

D. Gafurov¹, E. Vavilova¹, G. Prando², H-J. Grafe³, V. Kataev³, B. Buechner³

¹Zavoisky Physical-Technical Institute, FRC Kazan Scientific Center of RAS, Kazan, Russia

²Dipartimento di Fisica, Università degli Studi di Pavia, Pavia, Italia

³Leibniz Institute for Solid State and Materials Research IFW Dresden, Dresden, Germany

e-mail: londonstyle1998@gmail.com

One of the actual problems of the physics of strongly correlated and frustrated compounds is the interplay of spin, orbital, charge, and lattice degrees of freedom in complex 5d iridium oxides. Depending on the lattice geometry, it can be a realization of different spin configurations from the Heisenberg to the Kitaev models. The introduction of 3d transition metal ions into the initial matrix creates the basis for the formation of various types of ground state due to the interaction of 5d and 3d magnetic subsystems. This work presents the results of an experimental study of the magnetic properties of honeycomb sodium iridates $\text{Na}_{(3/2)}\text{M}_{(1/2)}\text{IrO}_3$, where the transition metal ions $\text{M} = \text{Ni}, \text{Cu},$ and Zn replace Na in the center of the hexagons. The study of such a system by local spin probe methods (in particular, μSR and NMR) are very informative [1]. Our experiments allow to trace the influence of the 3d element magnetism on the temperature evolution and the ground state of the magnetic system, its dimensionality and ordering.

The work of E.V. and D.G. was supported by RFBR through grant No. 18-02-00664.

[1] M. Iakovleva et.al., Phys. Rev. B **98**, 174401 (2018).

Comparative Study of S/F/S/F and S/F/N/F superconducting Spin-Valves

R.R. Gaifullin^{1*}, V.N. Kushnir^{2,3}, R.G. Deminov¹, L.R. Tagirov^{1,4}, M.Yu. Kupriyanov^{1,5,6},
A.A. Golubov^{6,7}

¹Institute of Physics, Kazan Federal University, Kazan, Russian Federation

²Belarus State University of Informatics and Radioelectronics, Minsk, Belarus

³Theoretical Physics Department, Belarusian State University, Minsk, Belarus

⁴Zavoisky Physical-Technical Institute, FRC Kazan Scientific Center of RAS, Kazan, Russian Federation

⁵Skobeltsyn Institute of Nuclear Physics, Moscow State University, Moscow, Russian Federation

⁶Moscow Institute of Physics and Technology, Dolgoprudny, Russian Federation

⁷Faculty of Science and Technology and MESA+ Institute of Nanotechnology University of Twente, Enschede, The Netherlands

e-mail: gaifullin.rashid@gmail.com

We investigate the critical temperature T_c of Superconductor/Ferromagnet/Ferromagnet type of multilayer structures, which can be switched from the superconducting state to the normal state and vice versa by applying a small external magnetic field in a determined direction. At noncollinear magnetizations of the F layers the long-range triplet superconducting pairing is generated [1]. Previously it was shown that the transition temperature T_c in S/F1/F2 [2] and S/F1/N/F2 [3] structures (N is a normal metal) can be a non-monotonic function of the angle α between magnetizations of the two F layers, against the monotonic $T_c(\alpha)$ behavior obtained for the F1/S/F2 trilayers [4].

Using the matrix method [5] for solving linearized Usadel equations, the critical temperature of S1/F1/S2/F2 structure is obtained. We study the influence of an additional superconducting layer on different spin-valve effect modes of the S/F/F three-layer spin valve – the direct effect ($T_c(\alpha = 0^\circ) < T_c(\alpha = 180^\circ)$), the triplet spin-valve effect ($T_c(\text{noncollinear}) < T_c(\alpha = 180^\circ)$), $T_c(\alpha = 0^\circ)$ and the inverse switching effect ($T_c(\alpha = 0^\circ) > T_c(\alpha = 180^\circ)$) – by variation the layers thicknesses, interfaces transparencies and the exchange splitting energies. We explore possible ways to switch the spin valve effects from one to the other. And we are looking for conditions under which superconductivity in an additional S2 layer is conserved and affects on the superconducting T_c , and conditions under which the superconductivity is suppressed and S2 layer plays a role of a normal metal. We compare S1/F1/S2/F2 structure with S1/F1/N/F2 structure which has the additional normal layer. The possibility of increasing the efficiency of the spin valve modes in the structure with the additional S or N layer is discussed.

This work was supported by the RSF project No. 18-12-00459. V.N.K. thanks the project “Materials science, new materials and technologies” by GPNI of the Republic of Belarus, the Nanotech subprogram (2016–2020).

[1] F.S. Bergeret, A.F. Volkov, K.B. Efetov, Rev. Mod. Phys. **77**, 1321 (2005).

[2] Ya.V. Fominov, A.A. Golubov, T.Yu. Karminskaya, M.Yu. Kupriyanov, R.G. Deminov, L.R. Tagirov, JETP Lett. **91**, 308 (2010).

[3] R.R. Gaifullin, R.G. Deminov, L.R. Tagirov, M.Yu. Kupriyanov, Ya.V. Fominov, A.A. Golubov, to be submitted.

[4] Ya.V. Fominov, A.A. Golubov, M.Yu. Kupriyanov, JETP Lett. **77**, 510 (2003).

[5] V.N. Kushnir, DSc dissertation, Minsk, (2014).

Electron Paramagnetic Resonance Study of $\text{Ho}_x\text{Lu}_{1-x}\text{B}_{12}$ Solid Solutions

M. I. Gilmanov¹, S. V. Demishev^{1,2,3}, A. N. Samarin¹, N. Yu. Shitsevalova⁴,
V. B. Filipov⁴ and N. E. Sluchanko^{1,2}

¹ Prokhorov General Physics Institute of RAS, Moscow 119991, Russia

² Moscow Institute of Physics and Technology, Dolgoprudny 141700 Moscow region, Russia

³ National Research University Higher School of Economics, Moscow 101000, Russia

⁴ Institute for Problems of Materials Science of NASU, Kyiv 03680, Ukraine

e-mail: gilmanov@lt.gpi.ru

Investigation of the systems with strong electron correlations by means of electron paramagnetic resonance (EPR) is complicated because of high frequency quantum fluctuations of magnetic moment. Therefore the examples of observation of the EPR line in this class of compounds are quite rare. However in case of the dodecaborides EPR signal previously was detected in two systems, YbB_{12} [1] and $\text{Zr}_{1-x}\text{Lu}_x\text{B}_{12}$ [2], which are known to undergo the order-disorder cage glass phase transition at $T^* \sim 60\text{K}$ [3].

In current work we report the results of the first observation of EPR in solid solutions $\text{Ho}_{1-x}\text{Lu}_x\text{B}_{12}$ ($x=0.01-1.0$). The measurements were carried out at the frequency $f=60\text{ GHz}$ with use of the original technique described elsewhere [4]. A single broad ($\Delta B \approx 0.4-1\text{ T}$) and isotropic resonance line with g-factor $g \sim 5$ was detected at low temperatures in the paramagnetic phase for concentrations above $x > 0.01$. It was discovered, that at temperatures above T^* line intensity drops drastically, basically making an EPR signal to become non-observable. This finding could be ascribed to the change in the spin-lattice relaxation time connected with lowering of the amplitude of vibrations of Ho^{3+} ions inside B_{24} cavities in the boron cage. Another striking feature of observable spectra, which is universal for all studied antiferromagnetic (AFM) crystals is a broadening of EPR line below $T \sim 3T_N$ due to AFM correlations (short range AFM order). We argue that the observed behavior cannot be described in terms of magnetic response from isolated Ho^{3+} ion response and should be treated as an effect of vibrationally coupled clusters of holmium ions.

This work was supported by RSF grant №17-12-01426.

[1] T.S. Altshuler et al, Phys. Rev. B **68**, 014425 (2003).

[2] N.E. Sluchanko et al, Phys. Rev. B **93**, 085130 (2016).

[3] N.E. Sluchanko et al, JETP **113**, 468 (2011).

[4] A.V. Semeno et al, Phys. Rev. B **79**, 014423 (2009).

Effect of Landau Levels on the SHFS of the EPR Spectra of Fe³⁺ Precipitates in the 3D Dirac Semimetal Cd₃As₂

Yu.V. Goryunov¹, A.N. Nateprov²

¹ Federal Research Center KazSC RAS, Kazan, Russian Federation

² Institute of the Applied Physic, Chisinau, Republic of Moldova

e-mail: gorjunov@kfti.knc.ru

One of the most interesting properties of Dirac materials is the linear spectrum of electronic excitations in the conduction band, from which follows such a feature of carrier scattering by impurities as the suppression of backscattering. In this connection, one open an extensive field of research of the influence of various impurities that fabricate in the material the scattering centers of various nature, both magnetic and non-magnetic, with the formation of a localized magnetic moment or without its localization. It is obvious that the simplest and therefore more understandable for studying the effect of impurities on the Dirac semimetal is the introduction of magnetic ions with zero orbital angular momentum into it.

A number of samples of the known Dirac semimetal α -Cd₃As₂ doped from 1 to 5 at.% Fe were prepared. However, the expected EPR signal, similar to the previously observed intense resonance line from the Eu²⁺ ion, was not found. In the case of a low concentration of iron even at room temperature, it was observed the consisting of 6 groups of resonance lines hyperfine structure (HFS) of the spectrum that characterize for spin 5/2. In each group consisting of at least three lines of super-hyperfine structure (SHFS), the intensity ratio was about the same as 3: 1: 1. This is not entirely clear if it is assumed that the source of the main SHFS is the spin 3/2 of the ⁷⁵As ligand nucleuses. The g-factor calculated from the two central intense lines of the HFS is $g = 2.0036 \pm 0.0005$ and close to the g-factor of the free electron. However, the distance between the resonance lines was different (from 90 to 100 Oe), which is unusual for an ion with zero orbital and nuclear spins. The shift of the resonance lines of the spectrum with an increase in the magnetic field was clearly non-linear in nature, which was also detected by increasing the width of the lines with increasing field.

A possible explanation of the observed effect to which the report is devoted may be the following. The valence state of Fe³⁺ iron in α -Cd₃As₂, apparently, is not peculiar to it. because the valence state of the substituted Cd²⁺ ion is 2+, and its size is larger than even the Fe²⁺ ion. Therefore, this state of Fe³⁺ is most likely stabilized by some features of the lattice (dislocations, growth defects), which delay additional electrons upon themselves. Since the general behavior of all lines of the SHFS is the same, then, without being distracted by the mechanisms of forming the SHFS, let us point out its cause: interaction with conduction electrons located at the Landau level crossing the Fermi level. This interaction contributes to the mechanism of interconfigurational interaction with ligands proposed by A. Abraham, due to which s-states of conduction electrons are mixed into the 3s²3d⁵ states. The density of states at the Fermi level and, together with this, the diamagnetic contribution to the resonant field H from s-electrons are described by the term 1/(H-H_n). The introduction of the H_n field is related to the fact that the density of states at the Fermi level, depending on the position of the Landau levels, oscillates with the magnetic field, such as the conductivity and magnetic susceptibility of α -Cd₃As₂. The obtained results on the deviation of the lines of the SHFS from their normal positions with increasing field are perfectly described by such a term.

Weak Ferromagnetism in Antiferromagnetic Chains $[\text{Fe}(\text{salen})(2\text{-Me-Him})]_n$

T. Ivanova¹, D. Chachkov², O. Turanova¹, I. Ovchinnikov¹

¹Zavoisky Physical-Technical Institute, FRC KSC of RAS, Kazan, Russian Federation

²Kazan Department of Joint Supercomputer Center of Russian Academy of Sciences – Branch of Federal Scientific Center "Scientific Research Institute for System Analysis of the RAS", Kazan, Russian Federation

e-mail: alex@kfti.knc.ru

Polynuclear structures based on salen-containing tetradentate ligands exhibit a wide range of magnetic properties in various temperature ranges. Recently, one-dimensional antiferromagnetic compounds with canted magnetic moments, in which weak ferromagnetism arises due to antisymmetric exchange interactions, are attracted much attention. The specificity of the manifestation of exchange interactions between Fe(III) ions in the compound $[\text{Fe}(\text{salen})(2\text{-Me-Him})]_n$ was studied by the methods of magnetic resonance spectroscopy and of magnetic susceptibility in the temperature range (5-300). K. In the spectra of magnetic resonance, signals from linear (signal **1**) and zigzag (signal **2**) antiferromagnetic chains coexisting in the sample were observed. The shift of signal **2** towards weak magnetic fields is explained by the spontaneous ferromagnetic magnetization arising in a zigzag chain due to the noncollinearity of the magnetic moments forming it. The features of the temperature and field dependence of the magnetization also indicate the existence of weak ferromagnetism in the sample. In the frozen solution of $[\text{Fe}(\text{salen})(2\text{-Me-Him})]_n$ complexes in chloroform, signal **2** is absent. This may be caused by a change in the configuration of the zigzag chain when the solvent molecule included in the complex.

The theoretical calculation of the models of these structures was carried out to study the effect of the solvent on the chain configuration. The hybrid method of density functional theory B3PW91 / 6-31G (d) was used for calculations. Since the considered structures have a multiplicity of 6 (spin 5/2), this method was used in the variant of open electron shells. The calculation of model structures with different multiplicities confirms the experimentally observed spin 5/2. According to the calculation, such structures have the minimum energy. The structures with spin 3/2 and 1/2 have relative energy $\Delta E = 27.4 \text{ kJ/mol}$ and $\Delta E = 27.1 \text{ kJ/mol}$, respectively.

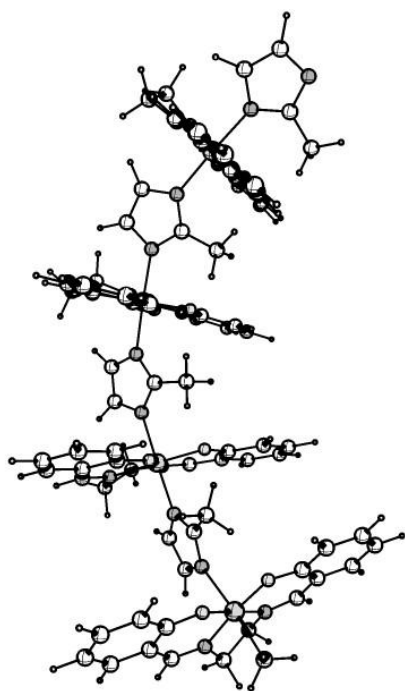


Fig.1 Fragment of structure

A fragment of a chain of four centers was considered (Fig.1). According to the results of quantum chemical modeling, it can be noted that solvent molecules can be actively incorporated into the polymer chains due to the formation of a large number of hydrogen bonds (up to 5 pieces per solvent molecule). When this happens, the free rotation of the Fe (salen) and (2-Me-Him) polymer fragments relative to each other occurs. Optimization of model structures has shown that when the solvent enters the molecule, the configuration of the chain becomes closer to linear and, accordingly, it is possible to talk about a decrease in the noncollinearity of the magnetic moments. This trend agrees with the experimental observations.

Symmetry Enforced Dirac Points in Antiferromagnetic Semiconductors

V.V. Kabanov

Jozef Stefan Institute, Jamova 39, 1000 Ljubljana, Slovenia

e-mail: viktor.kabanov@ijs.si

It is shown that the symmetry enforced Dirac points exist at some time reversal symmetric momenta in antiferromagnetic compound GdB_4 . These Dirac points may be controlled by the external magnetic field or by the deformation of the crystal. Application of the external magnetic field leads to splitting of these points into Weyl points or to opening of a gap depending on the field direction. The application of the symmetry breaking deformation also opens a gap in the spectrum. Suppression of the antiferromagnetic order leads to the formation of the nodal line instead of the Dirac points. This indicates that the symmetry enforced Dirac semimetals may be effectively used in different spintronic devices.

The Observation by Magnetic Resonance of the Electrochemically Generated Superparamagnetic Cobalt Nanoparticles

A.F. Khusnuriyalova^{1,2}, A. Petr³, A.T. Gubaidullin², A.V. Sukhov^{1,2}, V.I. Morozov²,
B. Büchner³, V. Kataev³, O.G. Sinyashin², D.G. Yakhvarov^{1,2}

¹Alexander Butlerov Institute of Chemistry, Kazan Federal University, Kazan, Russian Federation

²Arbuzov Institute of Organic and Physical Chemistry of FRC Kazan Scientific Center of RAS, Kazan, Russian Federation

³Leibniz Institute for Solid State and Material Research, Dresden, Germany

e-mail: aliya15071993@mail.ru

The development of fundamental and applied chemistry is proceeding in several priority areas. The investigation of nanoscale particles of transition metals are of high interest. These derivatives are widely used in various technological processes. This is primarily caused by the specific properties of nanoparticles themselves and the materials modified by them. These systems are subject to the principles of self-organization and allow the formation of nanomaterials that applied in various technologies such as production of microelectronic elements, sensors and optical devices, the synthesis of new materials with desired properties [1]. Cobalt nanosized particles occupy a special place among known metal nanoparticles as they allow to create the catalysts, magnetic recording devices, composites, carriers of biological products [2].

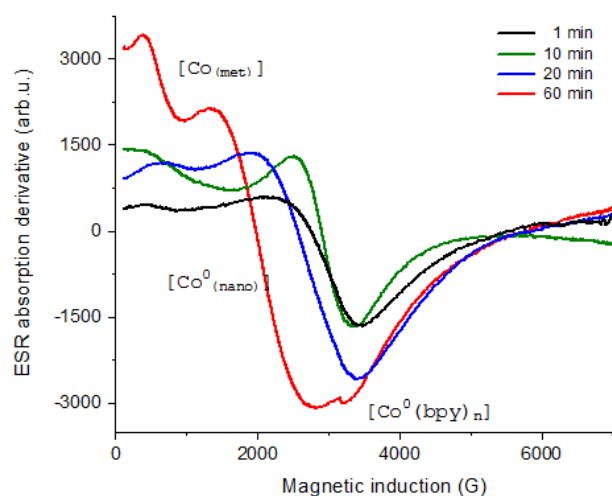


Fig.1. EPR spectra of the electrochemically generated CoNPs.

We have found that electrochemical reduction of coordinatively unsaturated cobalt dibromide 2,2'-bipyridine (bpy) complexes results in the formation of cobalt nanoparticles (CoNPs). The process of the electrochemical generation of CoNPs was monitored by *in situ* EPR-spectroelectrochemistry where the signals of the ferromagnetic resonance (FMR) have been observed for these species (Fig.1).

According to small-angle X-ray scattering (SAXS) analysis the average diameter and the average length of the formed cylindrical CoNP is varied from 9 to 10 nm and 30-32 nm, respectively, and correlates to the g-value and the broadness of the FMR signal observed by *in situ* EPR-spectroelectrochemistry during the electrochemical process [3].

This work is supported by the Russian Science Foundation (project no. 18-13-00442).

[1] J. Zhang, J. Xu, Y. Wang, H. Xue, H. Pang, Chem. Rec. **18**, 91 (2018).

[2] M. Imadadulla, M. Nemakal, L.K. Sannegowda, New J. Chem. **42**, 11364 (2018).

[3] A.F. Khusnuriyalova, A. Petr, A.T. Gubaidullin, A.V. Sukhov, V.I. Morozov, B. Büchner, V. Kataev, O.G. Sinyashin, D.G. Yakhvarov, Electrochim. Acta. **260**, 324 (2018).

EPR in Superconductors and Kondo-Lattices with heavy Fermions

B.I. Kochelaev

Institute of Physics, Kazan Federal University, Kazan, Russian Federation

e-mail: bkochelaev@gmail.com

Electron paramagnetic resonance (EPR) is able to give an important and in some cases unique information on properties of systems with strongly correlated electrons such as superconductors and Kondo-lattices with heavy fermions. In this report some results obtained by the cooperation of the experimental and theoretical investigations will be described.

The first study of the EPR on paramagnetic impurities in superconductors has shown that the well-known Slichter-peak, found by the NMR measurements in superconductors, was absent in some cases in the EPR experiments. It happens due to formation of collective spin excitations by conduction electrons and impurities what has been enhanced by the transition into superconducting state. It was found also that an exchange interaction between impurities via superconducting electrons is sufficiently modified in comparison with RKKY interaction in normal metals.

Discovery of the high-temperature superconductivity in layered doped copper oxides created very intensive investigations of a transformation of parent dielectric antiferromagnetic compounds into metals and further into superconductors by doping. It was found on the basis of the EPR measurements that distortion of the long range antiferromagnetic order happens due to coplanar elliptical domain walls created by linear chains of localized holes in the oxygen electronic shells of the CuO_2 planes. A delocalization of the holes can be realized in a phase separation in metal and dielectric regions which was consistent with the EPR results. It was found that a creation of the mentioned stripes could be supported by interactions of the holes via phonons. This model is consistent with the observed strong planar oxygen isotope effect on a critical temperature T_c of under-doped cuprates and which is reduced till zero at the optimal doping [1,2]. Many experimental and theoretical investigations show an important role of antiferromagnetic fluctuations in the CuO_2 planes for the correlations of superconducting electrons. It was quite natural to study them by the EPR of the Cu^{2+} ions. However all attempts to observe this signal were unsuccessful, although it was easy to observe the EPR of the Cu^{+2} ions in many metals and dielectrics. The years-long problem of this “EPR-silence” was solved using the bottleneck effect between the EPR-probes Mn^{2+} and the Cu^{2+} spin system.

Properties of a normal metal with paramagnetic impurities sufficiently depend on a type of their exchange interactions with conduction electrons. In the antiferromagnetic case the Kondo effect appears to screen the impurity spin by the spin cloud of conduction electrons. According to the common belief, based on the single ion Kondo effect, the EPR signal should not be observable below the Kondo temperature. However a rather narrow EPR signal of Yb^{3+} ions in the YbRh_2Si_2 crystal was found at temperatures well below the thermodynamically determined Kondo temperature (25 K) [3]. A detailed analysis has shown that the EPR signal could be observed due to formation of the collective spin excitations of the Yb^{3+} ions and conduction electrons which was enhanced in the Kondo-lattice.

[1] S. Weyeneth, K.A. Müller, *J. Supercond. Nov.* **24**, 1235 (2011).

[2] B.I. Kochelaev, K.A. Müller, A. Shengelaya, *J. Mod. Phys.* **5**, 473 (2014).

[3] J. Sichelschmidt, V.A. Ivanshin, J. Ferstl, C. Geibel, F. Steglich, *Phys. Rev. Lett.*, **91**, 156401 (2003).

**Search for the Spin-Nematic Phase in the $J_1 - J_2$ Frustrated
Quantum Antiferromagnet LiCuVO_4**

Reinhard K. Kremer

Max Planck Institute for Solid State Research, Stuttgart, Germany

e-mail: rekre@fkf.mpg.de

The search for unconventional states in quantum matter is at the forefront of current research in solid state physics. In this respect, frustrated quantum magnets are topical candidates since they are widely known to be able to realize atypical ground states. In this class of materials $J_1 - J_2$ frustrated quantum spin chains have attracted exceptional attention. For example, such systems have been demonstrated to realize helimagnetic order and spin-current induced type-II multiferroicity. Moreover, they are considered prime candidates to be able to establish spin-nematic phases. In my talk I shall review recent experimental investigations including high-field NMR and ultrasound attenuation experiments into the spin-nematic phase close to magnetic saturation in the $J_1 - J_2$ frustrated quantum antiferromagnet LiCuVO_4 .

Synthesis and Ferromagnetic Resonance Studies of Epitaxial VN/Pd_{0.96}Fe_{0.04} Heterostructure Grown on Single-Crystalline MgO Substrate

W.M. Mohammed¹, R.V. Yusupov¹, I.V. Yanilkin¹, I.R. Vakhitov¹, A.I. Gumarov¹,
A.M. Esmaceli¹, M.N. Aliyev², L.R. Tagirov^{1,3}

¹Institute of Physics, Kazan Federal University, 420008 Kazan, Russia

²Baku State University, 1148 Baku, Azerbaijan

³Zavoisky Physical-Technical Institute of RAS, 420029 Kazan, Russia

e-mail: waelmohammed88@yahoo.com

Superconductor-ferromagnet (S/F) heterostructures find application as an innovative elemental base for a new generation of ultrafast processors (superspintronics) [1,2]. In the present work, we describe the growth of epitaxial S/F heterostructure and investigate its magnetic properties. Magnesium oxide substrate was chosen because of a small lattice mismatch between the MgO ($a_0=0.421$ nm), vanadium nitride VN ($a_0=0.413$ nm) and palladium Pd ($a_0=0.386$ nm), favoring the cube-on-cube epitaxial growth. After annealing of the MgO substrate under UHV conditions, 15 nm thick VN layer was deposited in an UHV magnetron chamber by reactive sputtering of a high-purity vanadium target in argon and nitrogen gas mixture. Then, 20 nm thick film of Pd_{0.96}Fe_{0.04} alloy was grown by co-evaporation of high-purity Pd and Fe onto a MgO/VN structure. The epitaxy between the VN and Pd_{0.96}Fe_{0.04} was achieved by the annealing of the structure at 600°C for 20 min. At each of the technological stages, the low-energy electron diffraction (LEED) pattern had been taken (see Fig. 1, MgO, VN and PdFe alloy from left to right).

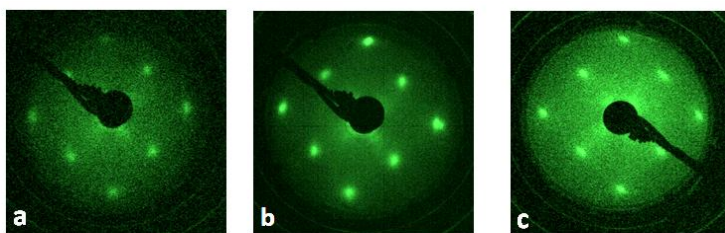


Fig. 1

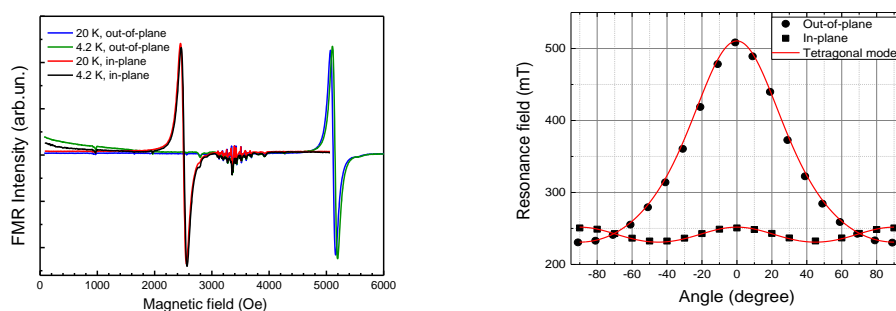


Fig. 2

Magnetic properties of the VN/Pd_{0.96}Fe_{0.04} thin-film heterostructure have been studied with the *dc* VSM magnetometry (Quantum Design PPMS-9) and FMR (Bruker ESP300) spectroscopy techniques (see the FMR spectrum and the resonance field angular dependence in Fig. 2). Magnetic anisotropy constants were determined from the simultaneous fit of the in-plane and out-of-plane angular dependences presented in Fig. 2 (right).

The work is supported by the RSF Project No 18-12-00459.

[1] V.V. Ryazanov, V.V. Bol'ginov, D.S. Sobanin, *et al.*, Phys. Procedia **36**, 35 (2012).

[2] M.A. Manheimer, IEEE Trans. Appl. Supercond. **25**, 1301704 (2015).

Mössbauer Effect Studies of Eu doped BiFeO₃

I.Yu. Nosov, A.L. Zinnatullin, and F.G. Vagizov

Institute of Physics, Kazan Federal University, Kremlyovskaya 18, 420008 Kazan, Russia

e-mail: vanka.nosov@mail.ru

Materials that have two types of ordering, magnetic and ferroelectric, i.e. multiferroics attract a lot of attention due to interesting applications in multifunctional devices. BiFeO₃ is one of the most promising among them. This is due to the fact that this material exhibits a high Curie temperature of ferroelectric ordering of $T_C \approx 1100$ K and the antiferromagnetic G-type ordering with a critical temperature of $T_N \approx 640$ K [1]. Bismuth ferrite has perovskite-type crystal structure and rhombohedral unit cell. There are two cationic positions in the structure called as A (occupied by Bi³⁺) and B (occupied by Fe³⁺) [2].

BiFeO₃ reveals spinoidal magnetic structure. This leads to compensation of bulk magnetization, which creates a barrier to using in full the potential advantages of the material. There are several ways to suppress the spinoidal structure. One of them is substitution of cationic positions by metals [2]. In this work we report results of synthesis and investigation of europium doped bismuth ferrite.

Bi_{1-x}Eu_xFeO₃ (x = 0, 0.05, 0.1, and 0.15) samples were synthesized by standard solid-state reaction (ceramic) route. Bi₂O₃, Fe₂O₃, and Eu₂O₃ powders in stoichiometric ratio (with the purity no less 99.5%) were mixed and thoroughly grinded in agate mortar during 4 hours. Ethanol was used as a protective medium. The resulting mixture was dried at ~ 50 ° C for 5 hours and then placed in a hot zone of a tube furnace preheated to 650 ° C for 10 minutes. After annealing, the samples were moved to the cold zone of the furnace and cooled to ambient temperature. XRD patterns of the samples display presence of secondary phases which are often noted in reports as Bi₂Fe₄O₉ and Bi₂₅FeO₃₉ [3, 4, 5]. The samples were one time leached in diluted nitric acid with aim to remove these impurities. After leaching the samples were washed in deionized water for deactivation of the acid. Finally, brown colored powders were dried again at ~50 °C for 5 hours.

The synthesized samples were studied by X-Ray powder diffraction (XRD), ⁵⁷Fe and ¹⁵¹Eu Mössbauer spectroscopy. The XRD results show the single phase composition of the samples after leaching. The XRD reflexes are shifted to large 2θ values with an increasing of Eu content. It should be associated with smaller values of the Eu³⁺ ionic radius compared with Bi³⁺. The ¹⁵¹Eu Mössbauer spectra consist of a single absorption line with an isomer shift close to the value found for for Eu₂O₃. It indicates that the Eu ions are in the 3+ valence state. With increasing europium concentration, the value of the isomer shift becomes closer to the value for europium oxide. The ⁵⁷Fe Mössbauer spectra consist of two magnetic sextets. The isomer shifts of the components increase with the doping concentration, while the hyperfine magnetic field decreases. The effect of Eu doping on the magnetic and dielectric properties of BiFeO₃ will also be discussed.

This work was supported by the Russian Government Program of Competitive Growth of Kazan Federal University and by RFBR, project number 18-02-00845.

- [1] G. Catalan, *Adv. Mater.* **21**, 2463 (2009).
- [2] D. Kothari, *J. Phys.: Condens. Matter* **22**, 356001 (2010).
- [3] A. Sobolev, *AIP Conference Proceedings* **1622**, 104 (2014).
- [4] H. Han, *Inorg. Chem.* **56**, 11911 (2017).
- [5] M. Mahesh Kumar, *Appl. Phys. Lett.* **76**, 2764 (2000).

High-field and High-frequency ESR studies of Comprising Tetrahedral Clusters Arranged in the Cubic Lattice

S. Okubo^{1,2}, S. Shimoshiro², Y. Saito³, S. Hara³, T. Sakurai³, T. Okamoto², H. Takahashi¹, E. Ohmichi², H. Ohta^{1,2}, R. Okuma⁴, Z. Hiroi⁴

¹Molecular Photoscience Research Center, Kobe University, Japan

²Graduate School of Science, Kobe University, Japan

³Research Facility Center for Science and Technology, Kobe University, Japan

⁴Institute for Solid State Physics, University of Tokyo, Japan

e-mail: sokubo@kobe-u.ac.jp

Geometrically spin frustrations has attracted much attention due to existence of exotic ground state such as the spin liquid states, which are yielded high degeneracies around the ground state by competing nearest neighbor interactions. In actual magnets, realization of high degeneracy in the ground state is inhibited by off symmetric interactions or defects of spin structure resulting from slight distortions of the crystal structure or unanticipated impurities in the crystal. And those induce magnetically ordered states. However, its own high degeneracies often bring multiple transitions to low symmetry, which is driven by weak magnetic anisotropy, due to release entropy. Pharmacosiderite, $\text{Fe}_4(\text{AsO}_4)_3(\text{OH})_4 \cdot 6\text{-}7\text{H}_2\text{O}$, is consistent with spin-5/2 Fe^{3+} tetrahedral clusters arranged in the primitive cubic lattice. It crystallizes in the space group with a lattice constant of $a = 7.98 \text{ \AA}$ [1]. Fe^{3+} ion is located at center of FeO_6 octahedra, which forms regular octahedra. Edge shared four FeO_6 octahedra, which consists of a Fe^{3+} ions tetramer, are located at the corner of the cubic unit cell as shown in figure 1. Some physical properties have been already reported. The magnetic susceptibility has a broad maximum around 13 K, and an upturn below 6 K [2]. The Weiss temperature is estimated to be $\Theta = -155 \text{ K}$ from fitting of inverse plot of the magnetic susceptibility [3]. And also the specific heat shows a peak at 6 K [3]. A long-range antiferromagnetic order occurs at $T_N = 6 \text{ K}$ from these results. Although the system belongs to an antiferromagnetic order below T_N , the Mössbauer effect shows only broadened quadruple splitting spectra at 4 K. The spectrum becomes splitting into six-line below 2.8 K [2, 3]. This behavior indicates that the spins significantly fluctuate in the ordered state, which is suggested that spins still frustrate between tetramers in the cubic lattice. To observe spin dynamics and magnetic anisotropy of the ground state, high-field and high-frequency ESR studies of pharmacosiderite have been carried out in the temperature region from 300 K to 1.8 K. We used powder and tiny single crystal samples for pulsed high-field ESR measurements and membrane force detection ESR measurements [4], respectively. A single absorption line of EPR was observed at $g = 2$. Linewidth becomes broader below 60 K, and resonance shifts was observed below 15 K, which consists with broad maximum of the magnetic susceptibility. Moreover, ESR absorption line splits into two components below 4 K. It suggests that this system has multiple transitions below $T_N = 6 \text{ K}$ from microscopic viewpoint. The spin structure of 1.8 K will be discussed.

[1] M. J. Buerger *et al.*, *Z. Kristallogr. Cryst. Mater.* **125**, 92 (1967).

[2] M. Takano *et al.*, *J. Phys. Soc. Jpn.* **31**, 298 (1971).

[3] R. Okuma *et al.*, *J. Phys. Soc. Jpn.* **87**, 093702 (2018).

[4] H. Takahashi *et al.*, *Rev. Sci. Instr.* **89**, 083905 (2018).

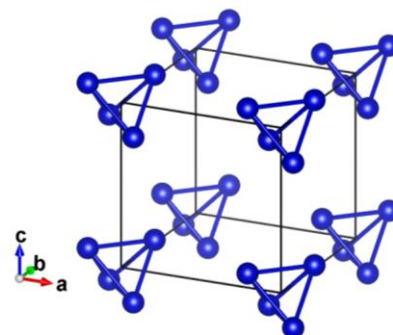


Fig. 1 Nearest neighbor bonding between Fe^{3+} ions in pharmacosiderite.

Effects of Magnetocrystalline Anisotropy on the Triangular to Square Lattice Transformation of Skyrmions

Markus Preißinger¹, Dieter Ehlers¹, Kosuke Karube², Hans-Albrecht Krug von Nidda¹, Bertalan Szigeti³, Yasujiro Taguchi², Vladimir Tsurkan¹ and István Kézsmárki¹

¹ Experimentalphysik V, EKM, Universität Augsburg, 86135 Augsburg, Germany

² RIKEN Centre for Emergent Matter Science (CEMS), Wako 351-0198, Japan

³ Department of Physics, Budapest University of Technology and Economics, 1111 Budapest, Hungary

e-mail: markus.preissinger@physik.uni-augsburg.de

The β -manganese-type alloys $\text{Co}_{10-x}\text{Zn}_{10-x}\text{Mn}_{2x}$ exhibit a helical state below the Curie-temperature T_c [1] (150K $\text{Co}_7\text{Zn}_7\text{Mn}_6$ to ca. 500K $\text{Co}_{10}\text{Zn}_{10}$). Below the phase transition an equilibrium skyrmion lattice state occurs in weak magnetic fields in the range of 400Oe. This state can be quenched down to lower temperatures by rapid field cooling (1K/min). Below a certain temperature the metastable triangular skyrmion lattice transforms into a square lattice [2].

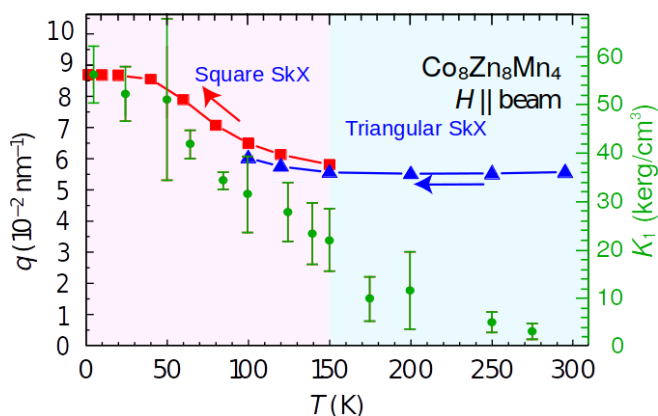


Fig.1. Temperature dependence of the q -vector of the squarelattice face (red), the triangular phase (blue) and the anisotropy constant K_1 (green).

The magnetocrystalline anisotropy in the ferromagnetic phase is determined by ferromagnetic resonance measurements. We discuss the magnetocrystalline anisotropy and its impact on the phase transition between the two types of skyrmion lattices. On cooling the temperature dependent q -vector of the skyrmion lattice turns out to be correlated to the the temperature dependence of the anisotropy constants K_1 and K_2 . On reducing the Mn content the overall anisotropy becomes stronger and the 6th order anisotropy contribution K_2 is enhanced as compared to K_1 .

[1] T. Hori et al., J. Magn. Magn. Mater. 310, 1820–1822 (2007).

[2] K. Karube et al., Nature Materials 15, 1237–1243 (2016).

Magnetic Resonance in a Dipolar Ferromagnet LiHoF₄

I. Romanova¹, B.Z. Malkin¹, O. Morozov¹, M.S. Tagirov¹, E. Sergeicheva², S. Sosin²

¹Kazan Federal University, 420008 Kazan, Russian Federation

²P. Kapitza Institute for Physical Problems, 119334 Moscow, Russian Federation

e-mail: romanova.irina.vladimirovna@gmail.com

We report on the magnetic resonance studies of an Ising-type dipolar ferromagnet LiHoF₄. This system is known to demonstrate the magnetic ordering below $T_c=1.5$ K as well as the quantum critical behavior under magnetic fields applied perpendicular to the easy-axis ($H \perp c$) [1]. Previous high-frequency EPR study [2] uncovered resonance spectra typical of a strongly anisotropic paramagnet, while a low-frequency NMR experiment probed collective electron-nuclear degrees of freedom in magnetic fields close to a quantum phase transition [3]. This work is aimed at investigating the low-lying EPR-mode at $H \perp c$ in the intermediate frequency range in the paramagnetic phase and its transformation below T_c . The measurements were performed on single-crystal samples at temperatures 0.4 – 10 K (using ⁴He and ³He setups) and under magnetic fields up to 10 T.

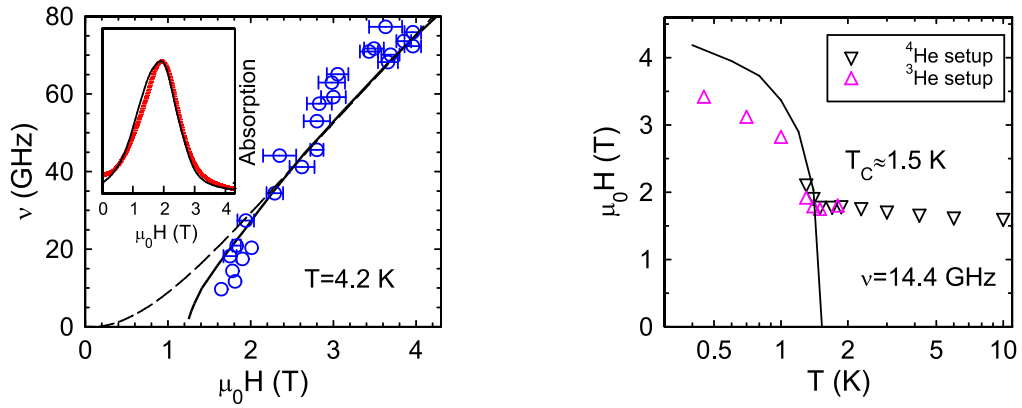


Fig.1. (Left panel) Frequency-field diagram obtained from broad-band measurements at $T=4.2$ K (symbols); solid and dashed lines: results of calculations, this work and from [2], respectively. (Right panel) Temperature evolution of the absorption maximum on undergoing magnetic phase transition.

The results obtained in the paramagnetic phase are represented in Fig. 1 (left panel). The inset shows a typical resonance absorption recorded at $\nu=14.4$ GHz along with the straightforward theoretical modeling (solid line in the inset) which takes into account the hyper-fine interaction in a single Ho³⁺ ion and its dipolar interactions with the four nearest-neighbors. The resulting frequency-field diagram for the absorption spectra measured at $T=4.2$ K in the frequency range 9 – 80 GHz can be adequately reproduced by our theoretical approach (see solid line in the left panel of Fig. 1 and compare it to previous calculations from [2]). On further cooling through the magnetic ordering transition, the resonance absorption line rapidly broadens and shifts to higher fields (see Fig. 1, right panel). This shift appears to be in a fairly good coincidence with the temperature dependence of the critical field of the transitions observed in [1] (shown by solid line). Further theoretical study of this effect is required.

This work was partially supported by RFBR grant №18-42-160012 p_a.

[1] D. Bitko, T.F. Rosenbaum and G. Aeppli, Phys. Rev. Lett. **77**, 940 (1996).

[2] J. Magariño *et al.*, Phys. Rev. B **21**, 18 (1980).

[3] I. Kovacevic *et al.*, Phys. Rev. B **94**, 214433 (2016).

Local Anisotropy and Spin Dynamics in a New Kagome Compound $\text{Fe}_4\text{Si}_2\text{Sn}_7\text{O}_{16}$

S. Dengre¹, R. Sarkar¹, J.-C. Orian², C. Baines², L. Opherden³, M. Uhlarz³,
T. Herrmannsdörfer³, T. Söhnel⁴, C. D. Ling⁵, M. Allison⁵, J. Gardner⁶, and H.-H. Klauss¹

¹Institute of Solid State and Materials Physics, TU Dresden, 01062 Dresden, Germany

²Laboratory for Muon-Spin Spectroscopy, PSI, 5232 Villigen, Switzerland

³Institute of Resource Ecology and Dresden High Magnetic Field Laboratory, Helmholtz-Zentrum Dresden-Rossendorf, D-01328 Dresden, Germany

⁴School of Chemical Sciences, University of Auckland, Auckland 1142, New Zealand

⁵School of Chemistry, University of Sydney, Sydney 2006, Australia

⁶Australian Centre for Neutron Scattering, Australian Nuclear Science and Technology Organization, Menai 2234, Australia

e-mail: rajibsarkarsinp@gmail.com

We present results of $^{(117/119)}\text{Sn}$ nuclear magnetic resonance (NMR), μSR and bulk *ac* - *dc* susceptibility experiments on $\text{Fe}_4\text{Si}_2\text{Sn}_7\text{O}_{16}$, which is a new Fe-based ($S=2$) kagome compound and a classical analogue of Herbertsmithite. NMR studies of grain aligned powder sample clearly reveal the presence of planar anisotropy in $\text{Fe}_4\text{Si}_2\text{Sn}_7\text{O}_{16}$. This allows us to measure the Knight Shift (the local susceptibility) and the spin-lattice relaxation rate (the low energy dynamical susceptibility) in two different directions even for the polycrystalline specimen. Both low energy static and dynamic properties reflect strong temperature dependent anisotropic behavior. The zero field μSR experiments show the presence of correlated dynamic magnetism down to 20 mK. By using susceptibility data, we identify the presence of two relevant energy scales, i.e. a spin glass-like state at around 3 K and a possible spin-liquid state below 500 mK. Taken together, $\text{Fe}_4\text{Si}_2\text{Sn}_7\text{O}_{16}$ presents an interesting kagome system with a coexistence of static and dynamic magnetism, which deserves further theoretical and experimental investigations.

NMR Studies on the Single Crystalline Na₂IrO₃: A Model System to Realize Kitaev Interaction

R. Sarkar¹, Z. Mei², A. Ruiz³, H.-H. Klauss¹, J. G. Analytis³ and N. J. Curro²

¹ Institute of Solid State and Materials Physics, TU-Dresden, 01062 Dresden, Germany

² Department of Physics, University of California, Davis, California 95616, USA

³ Department of Physics, University of California, Berkeley, California 94720, USA

e-mail: rajibsarkarsinp@gmail.com

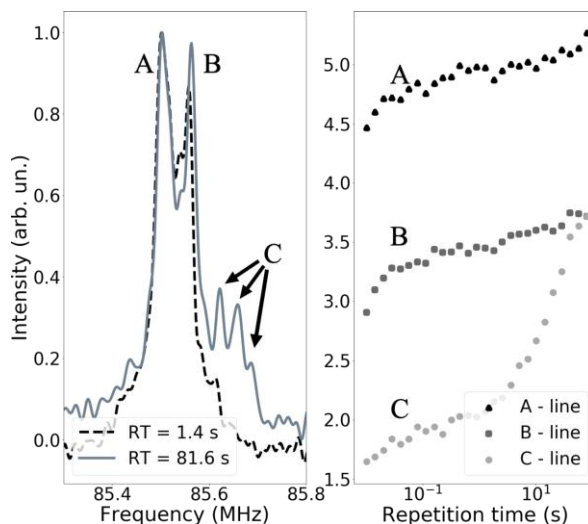
We present results of ²³Na nuclear magnetic resonance (NMR) measurements on single crystalline Na₂IrO₃, a possible candidate to realize Kitaev spin model on the honeycomb lattice. The NMR shifts (²³K(%)), that is the measure of local susceptibility, have been studied in two crystallographic orientations. The NMR shifts reflect strong anisotropic behavior similar to the bulk susceptibility. However, below a temperature T* ~ 50 K, the shift deviates from the bulk susceptibility. This anomalous behavior may be related to the exchange anisotropic bond interaction connected to the magnetic frustration. In contrast to the Knight shift, the spin-lattice relaxation rate ²³(1/T₁) is isotropic in the paramagnetic state and exhibits a strong peak at T_N. Deep in the ordered state, ²³(T₁T)⁻¹ approaches a constant value as a function of temperature, suggesting the presence of significant dynamics and/or the band of excitations associated with the close proximity of quantum spin liquid ground state of Na₂IrO₃.

NMR Study of Charge Density Waves in NbS₃ CompoundA.S. Semakin¹, I.R. Mukhamedshin¹, S. G. Zybtev², V. Ya. Pokrovskii²¹Institute of Physics, Kazan Federal University, Kazan, Russian Federation²Kotel'nikov Institute of Radio Engineering and Electronics, Moscow, Russian Federation

e-mail: al.semakin@gmail.com

Peierls transition, at which electrons condense into charge density waves (CDWs), have been observed in several trichalcogenides like NbSe₃, TaS₃ and NbS₃. They are typical quasi-1D CDW conductors as their crystal structures are formed of metallic chains surrounded by trigonal prismatic cages of chalcogen atoms. Though these compounds are apparently isoelectronic, their properties are rather diverse, even if isomers of the same compound are considered. While the semiconducting phase of NbS₃ (hereafter NbS₃-I) do not show any Peierls transitions, the second phase of NbS₃ (hereafter NbS₃-II) exhibits three CDWs with transition temperatures about 470, 360 and 150 K [1].

Using ⁹³Nb NMR we have studied the oriented samples of NbS₃-I and NbS₃-II phases. We have found that at T=5 K the ⁹³Nb NMR spectra of both phases are almost identical: two lines A and B can be distinguished in the NMR spectra and they correspond to nonequivalent groups of ⁹³Nb nuclei. For nuclei A and B, the quadrupole splitting frequency is $\nu_{QA} = 0.55$ MHz and $\nu_{QB} = 1.8$ MHz, respectively, and the relaxation times of the longitudinal and transverse components of the nuclear magnetization almost coincide. However at much longer repetition time (RT) of the pulse sequence another group C of nuclei starts to be resolved in the spectra, as they have very large values of the spin-lattice relaxation time compared to the A and B lines. Also, the magnetic shift of the C line is larger than of the A and B lines. Both of these facts indicate that line C corresponds to the non-conductive chains of Nb atoms. It is important to note that the line C has an internal structure which was observed at different temperatures, so there are several non-conductive chains in both phases NbS₃-I and NbS₃-II.



(a) ⁹³Nb NMR central line spectra of NbS₃-II sample at T=30 K and H₀||b. (b) The dependence of the intensity of the NMR lines corresponding to the groups of nuclei A, B, and C on the repetition time of the pulse sequence.

This work was funded by the Russian Foundation for Basic Research (project 17-02-01343).

[1] P. Monceau, Adv. Phys. 61, 325 (2012).

ESR Evidence of Spin Glass Behavior in the Absence of the Intrinsic Randomness in GdB₆

A. Semeno¹, M. Anisimov¹, A. Bogach^{1,4}, M. Gilmanov^{1,2}, V.B. Filipov³,
N. Yu. Shitsevalova³ and S. V. Demishev¹

¹Prokhorov General Physics Institute of RAS, Vavilov str. 38, 119991 Moscow, Russia

²Moscow Institute of Physics and Technology, Institutskii per. 9, 141700 Dolgoprudny, Moscow Region, Russia

³Frantsevich Institute for Problems of Materials Science NAS, Krzhyzhanovsky str. 3, 03680 Kiev, Ukraine

⁴National University of Science and Technology "MISIS" Moscow 119049, Russian Federation

e-mail: semeno@lt.gpi.ru

Randomness is believed to be the crucial criterion for the realization of the spin glass state scenario. Here we report the first observation of the spin glass behaviour in the systems with antiferromagnetic interactions GdB₆ and Gd_{0.75}La_{0.25}B₆ which is caused not by the intrinsic randomness of the spin structure but by the random shifts of Gd³⁺ spins from the centrally symmetrical positions in the regular cubic lattice. In Gd_{0.75}La_{0.25}B₆ this mechanism results in the freezing of random spin configurations at $T_f \approx 10.5$ K where the maximum of magnetization is observed. Below T_f the magnetic state depends on the antecedent sample history thus confirming the emergence of spin glass state. The coincidence of the temperature dependencies of ESR linewidth obeying the power law $\Delta H(T) \sim ((T - T_D)/T_D)^{-\alpha}$ with $\alpha = -1.18$ and $\alpha = -1.09$ in the paramagnetic phases of Gd_{0.75}La_{0.25}B₆ and GdB₆ demonstrates the identity of spin glass origin of the short range magnetic correlations, which underlie the line broadening. In the case of Gd_{0.75}La_{0.25}B₆ it leads to the width divergence at $T_D = 9.5$ K while in GdB₆ the coherent AFM phase transition takes place at $T_N = 15.5$ K thus hiding the expected divergence temperature $T_D = 13.2$ K. So the properties of GdB₆ in the AFM phase are defined by the competition of the coherent spin shift with random displacement spin configurations, thus leading at $T < T_D$ to the onset of the complicated low temperature antiferromagnetic phase AFM2 with peculiar hysteretic behavior. The observation of hysteresis of ESR spectrum at $4.2 \text{ K} \leq T < 10 \text{ K}$ allows suggesting the presence of several nonequivalent positions of Gd³⁺ ions in the AFM2 phase.

Magnetic Resonance Force Spectroscopy of Co/Pt Multilayer Films with Perpendicular Anisotropy

E. Skorokhodov, R. Gorev, M. Sapozhnikov, N. Gusev, O. Ermolaeva,
and V. Mironov

Institute for Physics of Microstructures, Nizhny Novgorod, 603950, Russia

e-mail: evgeny@ipmras.ru

Dynamics of spin waves in inhomogeneously magnetized ferromagnets is of great interest from the point of view of applied and fundamental studies [1]. One of the new effective methods for studying spin waves is magnetic resonance force microscopy (MRFM) [2]. The advantage of MRFM is the possibility of studying magnetization oscillations at small spatial scales. This method is particularly effective in the study of spin-wave resonances in the patterned ferromagnetic nanostructures. In addition, using MRFM probes with a large magnetic moment can be created in the sample area where localized spin waves are excited.

Studied film Co/Pt are multi-periodic (5 periods) structure, consisting of alternating layers of Co (0.5 nm) and Pt (1 nm) grown by magnetron sputtering method. The hysteresis loop of the obtained films has a rectangular shape. The coercive field is 200 Oe. After magnetization in the external field, the film remains homogeneously magnetized and demonstrates the labyrinth domain structure in the demagnetized state. NSG-01 cantilever with glued CoSm particle with a diameter of about 10 μm was used as a probe sensor. The uniform magnetic state was achieved by applying a magnetic field greater than 400 Oe perpendicular to the film plane. MRFM spectra in the form of dependence of the probe oscillation amplitude on the microwave pump frequency at different values of the external perpendicular field are shown in fig. 1 (a). The resonance in the form of a dip on the amplitude-frequency characteristic is shifted to the high frequency region and is associated with the main mode of the FMR of the Co/Pt film. As the probe-sample distance decreases, a region with inverted magnetization is formed in the film, which is accompanied by the appearance of an additional resonance on the dependence of the cantilever amplitude on the distance (fig. 1 (b)).

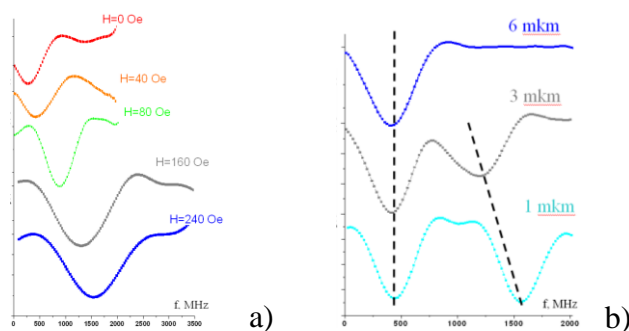


Fig. 1. (a) MRFM spectra of a uniformly magnetized film Co/Pt in an external magnetic field. Probe-sample distance 6 mkm; (b) MRFM spectra of Co/Pt film depending on probe-sample distance. Magnetic field 40 Oe

Also it will be presented a study of the influence of the character of the domain structure of the Co-Pt film on its microwave properties.

This work was supported by Russian Science Foundation (grant # 18-72-10026).

[1] A. Volodin, C. VanHaesendonck, E.V. Skorokhodov, R.V. Gorev, and V.L. Mironov, *Appl. Phys. Lett.* 113, 122407 (2018).

[2] J.A. Sidles, *Phys. Rev. Lett.* 68, 1124 (1992).

Order by Dynamic or Static Disorder in a Triangular Antiferromagnet RbFe(MoO₄)₂A.I.Smirnov¹, T.A. Soldatov¹, T. Kida², A. Takata², M. Hagiwara², O. Petrenko³,
M. E. Zhitomirsky⁴¹ P.L. Kapitza Institute for Physical Problems RAS, 119334 Moscow, Russia² AHMF Center, Osaka University, Osaka 560-0043, Japan³ Warwick University, CV4-7AL Coventry, UK⁴ CEA-INAC, 38054 Grenoble, France

e-mail: smirnov@kapitza.ras.ru

The ground state of the two-dimensional Heisenberg antiferromagnet on a triangular lattice (AFMTL) in a magnetic field is strongly degenerate in a mean-field approximation. The selection of the ground state from the pool of degenerate configurations is performed by the so-called “order-by-disorder” mechanism, implying a contribution of thermal and quantum fluctuations to free energy. This contribution of dynamic fluctuations is lifting degeneracy, see, e.g. [1]. A weak random potential of impurities was shown to compete with order-by-disorder mechanism, by lifting degeneracy via local violation of frustration. Thus, a weak chaotic modulation of exchange network may be a reason of a cardinal change of spin structure of AFMTL [2]. We have tested these theoretical predictions in experiments with $S=5/2$ AFMTL RbFe(MoO₄)₂ [3], doped with potassium up to a concentration of 15% (this doping means substitution of nonmagnetic Rb per nonmagnetic K-ions). The susceptibility of doped samples shows a reduced Néel temperature, but the Néel transition is almost as sharp as in a pure compound. The 1/3-magnetization plateau, being an evidence of a phase, stabilized by dynamic fluctuations, was completely suppressed by doping, in correspondence with [2]. The present multifrequency ESR investigation in a range 25-150 GHz reveals a strong change of the antiferromagnetic resonance spectrum by doping: the descending branch observed in pure samples, disappears completely in doped samples, indicating a change of the ground state. The theoretical analysis of the ESR spectra of the proposed spin configurations is in a correspondence with “Y-type” structure (one sublattice opposite field, two sublattices tilted) for the pure compound, while for the doped samples the spectrum indicates the “anti-Y” structure (one sublattice along field and two - tilted) [4]. The recent ⁸⁷Rb NMR study [5] is also in a correspondence with the above change of the spin structure at 15 % - doping, while at 7.5 %-doping the initial structure is still conserved. These facts directly demonstrate, that spin fluctuations play important role in formation of a spin structure for a pure compound, while a random potential of impurities results in a drastic change of the spin structure.

[1] A.V. Chubukov, D.I. Golosov, *Journal of Physics: Condensed Matter* **3**, 69 (1991).[2] V.S. Maryasin and M.E. Zhitomirsky, *Phys. Rev. Lett.* **111**, 247201 (2013).[3] L.E. Svistov *et al*, *Phys. Rev. B* **67**, 094434 (2003).[4] A.I. Smirnov *et al*, *Phys. Rev. Lett* **119**, 047204 (2017).[5] Yu.A. Sakhratov *et al*, *Phys. Rev. B* **99**, 024419 (2019).

Spinon Resonance in Spin-Chain Antiferromagnets with Uniform Dzyaloshinsky-Moriya Interaction

T.A. Soldatov^{1,2}, A.I. Smirnov¹, K.Yu. Povarov³, M. Hälg³, W.E.A. Lorenz³, A. Zheludev³

¹P.L. Kapitza Institute for Physical Problems of RAS, Moscow, Russian Federation

²Moscow Institute of Physics and Technology, Dolgoprudny, Russian Federation

³Swiss Federal Institute of Technology in Zürich, Zürich, Switzerland

e-mail: tim-sold@yandex.ru

Spin $S = 1/2$ chains with antiferromagnetic exchange interaction demonstrate quantum-disorder ground state with zero value of the ordered component and spin-spin correlations decayed according to a power law with the distance between spins [1]. In antiferromagnetic spin $S = 1/2$ chains elementary excitations are fractionalized - they carry spin $S = 1/2$ and are called as spinons. Such excitations demonstrate properties of fermions. In processes of neutron scattering or absorption of photons they obey the selection rule $\Delta S_z = 0, +/- 1$ and are excited in pairs, forming the so-called two-spinon continuum, studied in detail in neutron scattering experiments (see, for example, [2]).

Using the electron spin resonance (ESR) technique in a wide frequency (0.5 – 350 GHz), magnetic field (0 – 12 T) and temperature (0.45 – 80 K) ranges we investigate the fine structure of spinon continuum in the center of Brillouin zone which appears under the action of uniform Dzyaloshinsky-Moriya interaction. In magnetic field this structure has the form of a so-called spinon doublet and is associated with the difference in the energy of spinons moving in opposite directions [3]. In zero field we observe opening of an energy gap.

In crystals with magnetic ions Cu^{2+} ($S = 1/2$) the very unusual excitation spectrum is observed in the paramagnetic (spin-liquid) phase, which differs greatly from the signal expected in the Heisenberg approximation at the Larmor frequency.

Our work reveals magnetic resonance of the spinon type in three spin-chain compounds with uniform Dzyaloshinsky-Moriya interaction between magnetic ions in antiferromagnetic chains: Cs_2CuCl_4 , $\text{K}_2\text{CuSO}_4\text{Br}_2$, $\text{K}_2\text{CuSO}_4\text{Cl}_2$ [4,5,6]. These crystals differ from each other significantly by parameters J'/J and D/J' , where J is intra-chain exchange, J' is inter-chain exchange and D is Dzyaloshinsky-Moriya characteristic parameter. As a result, we establish empirical criteria which determine the temperature of formation and the magnetic field of destruction of spinon doublet in antiferromagnetic spin $S = 1/2$ chains with uniform Dzyaloshinsky-Moriya interaction.

[1] Bethe H. // Z. Physik. – 1931.

[2] Dender D. C. // Physical Review Letters. – 1997.

[3] Gangadharaiah S., Sun J., Starykh O. A. // Physical Review B. – 2008;
Karimi H., Affleck I. // Physical Review B. – 2011.

[4] Smirnov A. I., Soldatov T. A., Povarov K. Yu., Shapiro A. Ya. // Physical Review B. – 2015.

[5] Smirnov A. I., Soldatov T. A., Povarov K. Yu., Hälg M., Lorenz W. E. A., Zheludev A. // Physical Review B. – 2015.

[6] Soldatov T. A., Smirnov A. I., Povarov K. Yu., Hälg M., Lorenz W. E. A., Zheludev A. // Physical Review B. – 2018.

New Findings in the Magnetic Phase Diagram of GaV_4Se_8

Bertalan György Szigeti¹, Sándor Bordács², Ádám Butykai², Korbinian Geirhos¹, Dieter Ehlers¹, Björn Miksch³, Jonathan Stuart White⁴, Hans-Albrecht Krug von Nidda¹, Peter Lunkenheimer¹, Vladimir Tsurkan¹, Marc Scheffler³, Martino Poggio⁵ and István Kézsmárki¹

¹Experimental Physics V, Center for Electronic Correlations and Magnetism, University of Augsburg, 86135, Augsburg, Germany

²Department of Physics, Budapest University of Technology and Economics, 1111, Budapest, Hungary

³I. Physical Institute, University of Stuttgart, 70569, Stuttgart, Germany

⁴Laboratory for Neutron Scattering and Imaging, Paul Scherrer Institute, 5232, Villigen, Switzerland

⁵Department of Physics, University of Basel, 4056, Basel, Switzerland

e-mail: bertalan.szigeti@physik.uni-augsburg.de

GaV_4Se_8 is a multiferroic member of the lacunar spinel family, which is found to host a robust Néel-type skyrmion lattice (SkL) on the full temperature range below the paramagnetic state down to lowest temperatures of investigation and on a wide field range. The SkL state is observed in its polar rhombohedral phase, formed below its structural transition from the

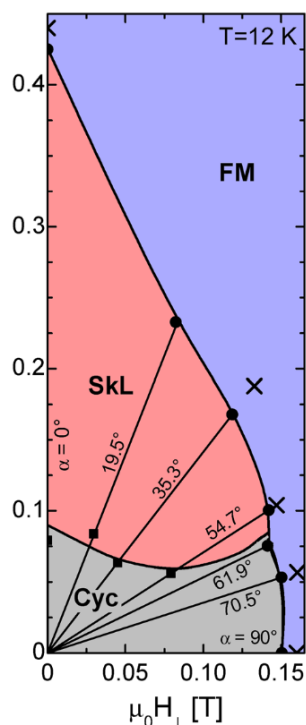


Fig.1. Stability regions of the cycloidal (Cyc), SkL and ferromagnetic (FM) states at 12 K on the H_c - H_\perp plane, where H_c and H_\perp are the field components along and perpendicular to the polar axis of the magnetic domain. [1]

room temperature cubic phase and survives even in oblique field directions [1]. This wide stability range is due to the polar, easy-plane anisotropic nature of GaV_4Se_8 . In oblique magnetic fields we observed an additional modulated phase besides the cycloidal and the SkL states, using small-angle neutron scattering, magnetic torque, magnetization and magnetocurrent measurements also supported by broadband electron spin resonance studies. The formation of this novel modulated phase shows strong connection with the reorientation process of the modulation vectors.

[1] Bordács, S., et al., Sci. Rep. 7.1, 7584 (2017).

Ferromagnetic Resonance – a Powerful Tool to Characterize Magnetic Heterostructures

L.R. Tagirov^{1,2}

¹Zavoisky Physical-Technical Institute, FRC Kazan Scientific Center of RAS, 420029 Kazan, Russia

²Institute of Physics, Kazan Federal University, 420008 Kazan, Russia

e-mail: Itagirov@mail.ru

Operating parameters of spintronic devices are essentially determined by magnetic properties of their functional ferromagnetic components. Being fabricated at nanometer scale of thickness, these components (basically layers or structures patterned from them) are very hardly to be measured. Because of tiny amount of a material (important for X-ray, SQUID, VSM techniques), limited access to sub-surface layers (LEED, MOKE, XPS, SEM) and laboriousness of the probe preparation (TEM), a combination of the above mentioned techniques has to be applied for structural characterization of the magnetic nanostructures. As concerns the magnetic properties, important for spintronic applications magnetic anisotropies can hardly be obtained by MOKE (needs access to free surface of a magnetic layer or, in case of ultrathin magnetic heterostructures, gives integral nonselective signals, non-equally weighted because of limited penetration depth of the light into metallic layers) or by SQUID/VSM techniques (provides integral non-selective response of the net magnetic moment).

In the survey report, we demonstrate that ferromagnetic resonance (FMR) is a highly sensitive, straightforward tool to measure basic magnetic properties as well as fine details of the magnetic anisotropies of ultra-thin-film ferromagnetic nanostructures. The continuous wave resonator and microstrip resonator techniques are considered. It is argued how magnetic properties of several ferromagnetic layers can be acquired in a simultaneous measurement by FMR utilizing selectivity to a kind of ferromagnetic material, sensitivity to its thickness and properties of adjacent layers. Using FMR one can easily determine easy and hard axes for the magnetization alignment of each of the ferromagnetic layers. The modeling of angular dependencies (for in-plane and out-of-plane geometries of measurements) of the FMR field for resonance allows to identify diverse magnetic anisotropies and extract several contributions to them, including that with non-collinear principle axes. Studying temperature evolution of the FMR spectra and material parameters that follow from the modeling, one can formulate most detailed model of the magnetic anisotropy unavailable without utilizing the FMR technique. Being complemented by SQUID/VSM measurements, FMR provides unique characterization tool to get maximum data for the optimization of functional properties of studied magnetic nanostructures.

The valuable contribution of my colleagues, I.A. Garifullin, R.I. Khaibullin and A.A. Bukharaev (KFTI of RAS, Kazan); R.V. Yusupov and I.V. Yanilkin (KFU, Kazan); I. Golovchanskiy (MISIS, Moscow); B. Aktaş, B.Z. Rameev, M. Özdemir, F. Yıldız and S. Kazan (GIT, Gebze); B. Heinrich (SFU, Burnaby) to the original works is gratefully acknowledged. This work was supported by the RSF project No. 18-12-00459.

EPR Study of Azomethine Iron(III) Complexes

V. Vorobeva^{1,2}, M. Gruzdev³, U. Chervonova³¹Zavoisky Physical-Technical Institute, Kazan, Russian Federation²Kazan National Research Technological University, Kazan, Russian Federation³G. A. Krestov Institute of Solution Chemistry of the Russian Academy of Sciences, Ivanovo, Russian Federation

e-mail: vvalerika@gmail.com

Iron compounds are being actively investigated due to their biological importance, such as antibacterial, antifungal, antiviral and anticancer activity. Iron(III) Schiff base complexes can be used as MRI contrast agents, so interest to the study of these compounds is now increasing sharply.

In this work the magnetic properties of novel azomethine complexes of iron(III) based on esters of biphenyl-4-carboxylic acid with Cl^- , NO_3^- and PF_6^- counter ions will be presented. Synthesis and emissive properties were presented earlier [1]. The compounds were examined by FT-IR, NMR spectroscopy, chromatography, elemental analyses, MALDI-ToF-MS method differential scanning calorimetry and thermal gravimetric analysis [1].

The EPR spectra were recorded in a wide range of temperatures from 300 to 4 K. EPR results showed that all compounds contain only high-spin ($S = 5/2$) iron(III) centers. Spectra were simulated by using EasySpin Matlab program.

Compounds with different counter ions display different EPR behavior: for compounds with Cl^- and PF_6^- counter ions - spectra contain two main high-spin ($S = 5/2$) intense signals - with effective g-factors $g_1 \sim 2$ (I-type) and a weaker one, with $g_2 \sim 4.3$ (II-type) (Figure 1 a, b). On cooling down, the broad line (I-type) shows a monotonous increase of the linewidth and shift in the low-field. These specific features are typical for the ferromagnetic resonance line.

While, for compound with NO_3^- counter ion EPR spectra demonstrated an abnormally broadened signal in the low field, which probably indicates a magnetic ordering of ferromagnetic nature (Figure 1 c).

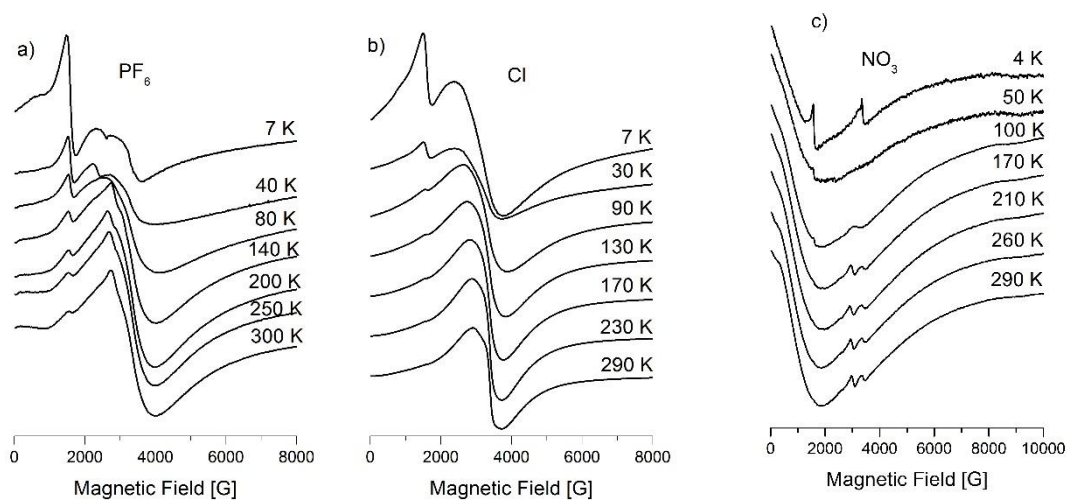


Fig.1 EPR spectra of the compounds with PF_6^- (a), Cl^- (b) and NO_3^- (c) counter ions.

[1] M.S. Gruzdev, J. Mol. Struct. **1176**, 529 (2019).

Heteronuclear Clusters Containing Dysprosium Ions: SMM Properties and EPR Possibility

V.K. Voronkova¹, R.T. Galeev¹, L.V. Mingalieva¹, A.A. Sukhanov¹, Y. Peng², A. K. Powell²

¹Zavoisky Physical-Technical Institute, FRC Kazan Scientific Center of RAS, Kazan, Russian Federation

²Institute of Inorganic Chemistry, Karlsruhe Institute of Technology, Karlsruhe, Germany

e-mail: vio@kfti.knc.ru

Clusters containing rare-earth ions have caused considerable interest in recent decades as promising for creating single molecular magnets (SMM) due to a high magnetic anisotropy of rare-earth ions. The Dy(III) ion may represent an ideal ion for single-molecule magnetism. In the strictly axial ligand field, the main term ${}^6H_{15/2}$ of the dysprosium ion is split into 8 well-isolated doublets, which provides an energy barrier that prevents the inversion of the spin. Impressive progress has been achieved for a molecule with one dysprosium ion; a high-temperature SMM with a blocking temperature $T_B=80K$ has been synthesized [1].

The key issue of studies of clusters containing 3d and dysprosium ions is the problem of the influence of 3d-4f and 4f-4f interactions on the magnetization blocking and quantum tunneling of the magnetization (QTM) effects. Various clusters have been synthesized and investigated, but the questions remain. This problem was studied mainly by the dynamic susceptibility method and the changes in the SMM properties are described using *ab initio* calculations of the parameters of isolated complexes and interactions between different ions.

The EPR method, which makes it possible to control the splitting of the lower states of clusters, is practically not used due to the complexity of observing the EPR spectrum for such clusters. Our work demonstrates the utility of spin resonance to studying 3d-4f and 4f-4f interactions by the example of two series of the tetranuclear clusters, some of which exhibit the SMM behavior. Only the type and position of the substituent R change in the first series of isostructural $[Fe_2Dy_2(OH)_2(teaH)_2(RC_6H_4COO)_6]$ complexes, where R=meta-CN, para-CN, meta-CH₃, para-NO₂ and para-CH₃, but this significantly changes the SMM properties of Fe₂Dy₂ clusters [2]. The M₂Dy₂ clusters with different 3d ions form second series M₂Dy₂ (m³-OH)₂(L)₂(O₂CPh-Me-p)₆ complexes, M=Cr, Fe and Al, the synthesis, characterization and magnetic studies of these tetranuclear clusters were described earlier [3]. EPR studies are carried out on polycrystalline samples in X-, Q- and W-bands. The features of the shape of the spectra of clusters containing dysprosium ions are analyzed, the experimental spectra are described using calculated spectra for tetranuclear clusters. The EPR data are compared with the results of *ab initio* calculations and the dynamic susceptibility data, which characterize the SMM properties of these compounds. It is shown that the EPR study of such clusters adds to and refines *ab initio* data, in particular, indicates a deviation from the Ising model in some clusters, which is not considered in *ab initio* calculations.

V.V.K. thanks the Presidium RAS Program No. 5: "Photonic technologies in probing inhomogeneous media and biological objects" for financial support.

[1] Fu-Sh. Guo, B. M. Day, Yan-C. Chen, et al. *Science*, **362**, 1400 (2018).

[2] V. Vieru, L. Ungur, V. Cemortan, A. Sukhanov et al., *Chem. Eur. J.* **24**, 16652 (2018).

[3] Y. Peng, M.K. Singh, V. Mereacre et al., *Chem. Sci.*, 2019, DOI:10.1039.

Fe₃O₄/DMSO Ferrofluid Synthesis, ESR *in situ* Study

Yakushkin S.S., Kirillov V.L. and Martyanov O.N.

Boreskov Institute of Catalysis, Novosibirsk, Russia

e-mail: stas-yk@catalysis.ru

Ferrofluids are the stable colloids of magnetic nanoparticles that do not aggregate and sediment under gravity or magnetic forces. Ferrofluids are considered as an important types of artificial “smart nanofluids” [1]. Generally the ferrofluid synthesis approaches can be divided into two categories of one-step and two-step processes. While two-step methods became popular due to the variety of the viable nanoparticles synthesis processes at industrial scale [2], one step methods allow one to simplify the synthesis route and get rid of different steps including drying, storage, transportation, and dispersion procedures, each one of which may influence resulting ferrofluid properties. However it means in case of one-stage ferrofluid synthesis it is important to control many parameters at once to get ferrofluids with desired structure, size characteristics and magnetic properties. To find an effective synthetic method it's necessary to study the initial stages of colloid formation.

New facile one step synthesis of few nanometers Fe₃O₄ particles colloid was suggested in the Boreskov Institute of Catalysis based on the modification of co-precipitation method [3,4] proceeding in surfactant like environment. The method allows one to get ferrofluids based on Fe₃O₄ nanoparticles with narrow size distribution that show superparamagnetic behavior at room temperature.

The electron spin resonance (ESR) method *in situ* was applied to investigate the initial stages of the colloid formation. The magnetic structure of few-nanometer sized nanoparticles interrelates strongly with its structure, surface state and magnetic interparticle interactions. Here we report the results of ESR study of Fe₃O₄ ferrofluid. The special attention is paid to the initial stages of magnetic nanoparticles ensemble formation.

The work was supported by RFBR (Project 18-33-00501)

- [1] A. Joseph and S. Mathew, *ChemPlusChem* **79**, 1382 (2014).
- [2] W. Yu and H. Xie, *J. Nanomater.* **2012**, 1 (2012).
- [3] V.L. Kirillov, D. A. Balaev, S.V. Semenov, K.A. Shaikhutdinov, and O.N. Martyanov, *Mater. Chem. Phys.* **145**, 75 (2014).
- [4] V.L. Kirillov, S.S. Yakushkin, D.A. Balaev, A.A. Dubrovskiy, S.V Semenov, Y.V Knyazev, O.A. Bayukov, D.A. Velikanov, D.A. Yatsenko, and O.N. Martyanov, *Mater. Chem. Phys.* **225**, 292 (2019).

Magnetic Properties of Lanthanum Strontium Ferromanganites Doped with Zinc

R.M. Eremina¹, I.V. Yatsyk¹, A.A. Gabidullina², A.L. Zinnatullin², F.G. Vagizov²,
A.G. Badelin³, V.K. Karpasuk³, Z.I. Seidov⁴

¹Zavoisky Physical-Technical Institute, FRC Kazan Scientific Center of RAS, Kazan, Russia

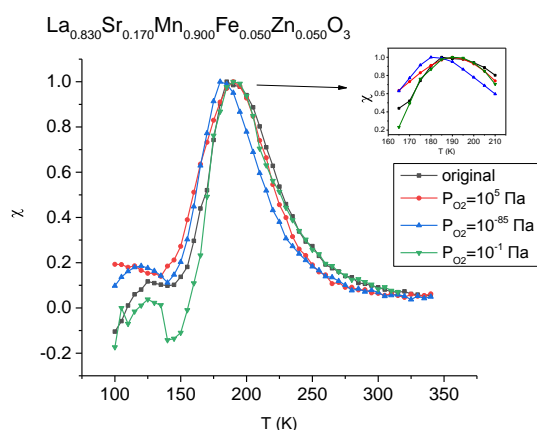
²Kazan (Volga Region) Federal University, Kazan, Russia

³Astrakhan State University, 414056 Astrakhan, Russia

⁴Institute of Physics, Azerbaijan National Academy of Sciences, Baku, Azerbaijan

e-mail: I.Yatzyk@gmail.com

Manganites of the following composition $R_{1-x}A_xMnO_3$ attract much attention, where R is trivalent rare-earth ion, and A - divalent alkaline-earth ion. Such interest was caused by the rich phase diagram caused by competing processes [1]. Hole doped manganites different ordering is observed: orbital and charge [2, 3] and the existence of electronic phase separation [4, 5, 6, 7]. The transition from a paramagnetic insulator to a metal ferromagnet is based on the competition of two interactions: antiferromagnetic superexchange and ferromagnetic double-exchange [8, 9, 10].



The aim of this work is to study by ESR, magnetometry and Mossbauer effect methods magnetic properties of $La_{1-c}Sr_cMn_{1-x-y}Fe_xZn_yO_3$. Based on the obtained experimental data we can suggest the presence of ferromagnetically correlated regions in the investigated samples. ESR measurements of $La_{1-c}Sr_cMn_{1-x-y}Fe_xZn_yO_3$ in X-band (at 9.4 GHz) were carried out on a ER 200 SRC Bruker (EMX/plus) spectrometer in the temperature range from 100 to 340 K.

Support by the RFBR grant 18-52-

06011 is acknowledged.

- [1] M. Imada, A. Fujimori, and Y. Tokura, *Reviews of Modern Physics* 70, 1039 (1998).
- [2] R.M. Kusters, J. Singleton, D.A. Keen, R. McGreevy, W. Hayes, *Reviews of Modern Physics* 155, 362-365 (1989).
- [3] R. von Helmolt, J. Wecker, B. Holzapfel, L. Schultz, and K. Samwer, *Physical Review Letters* 71, 2331 (1993).
- [4] J. Deisenhofer, D. Braak, H.-A. Krug von Nidda et al., *Physical Review Letters* 95, 257202 (2005).
- [5] A.M. Kadomtseva, Yu.F. Popov, G.P. Vorob'ev, K.I. Kamilov, A.A. Mukhin, V.Yu. Ivanov, A.M. Balbashov, *Physics of the Solid State* 48, 2134-2136 (2006).
- [6] V.V. Kabanov, R.F. Mamin and T.S. Shaposhnikova, *Journal of Experimental and Theoretical Physics* 108, 286-291 (2009).
- [7] R.M. Eremina, I.I. Fazlizhanov, I.V. Yatsyk et al, *Physical Review B* 84, 064410 (2011).
- [8] Clarence Zener, *Physical Review* 82, 403 (1951).
- [9] P.W. Anderson and H. Hasegawa, *Physical Review* 100, 675 (1955).
- [10] P.-G. de Gennes, *Physical Review* 118, 141 (1960).

Formation of Antiferromagnetic Fe–Fe Dimers in Fe Doped TiO₂ Nanoparticles investigated by EPR and Magnetic Methods

A. Yermakov^{1,2}, A. Gubkin^{1,2}, M. Uimin^{1,2}, A. Korolev^{1,2}, L. Molochnikov³, E. Rosenfeld¹, A. Minin^{1,2}, A. Volegov^{1,2}, D. Boukhvalov⁴, S. Konev²

¹M. N. Mikheev Institute of Metal Physics, Ural Branch of the Russian Academy of Sciences, Yekaterinburg, Russian Federation

²Institute of Natural Sciences, Ural Federal University, named after the first President of Russia B. N. Yeltsin, Yekaterinburg, Russian Federation

³Ural State Forest Engineering University, Yekaterinburg, Russian Federation

⁴College of Science, Institute of Materials Physics and Chemistry, Nanjing Forestry University, Nanjing 210037, P. R. China

e-mail: yermakov@imp.uran.ru

The study of magnetic states in the diluted magnetic semiconductors (DMS) doped with magnetic 3d-ions is of particular interest because of their possible technological applications. It is well-known that DMS on the base of TiO₂ nanomaterials are promising materials for spintronics, catalyst, and sensor applications. However, the underlying mechanisms which are responsible for the electronic structure and the magnetism in DMS are still a subject of hot debate [1].

In this research, we report the results of the comprehensive experimental and theoretical study of magnetic properties of TiO₂ nanoparticles (20 nm) doped with Fe at various concentrations ranging up to ~ 5 at. %. The electron paramagnetic resonance (EPR) and magnetic measurements data evidence the mixed magnetic state, where paramagnetic Fe³⁺ ions coexist with short-range antiferromagnetic correlations caused by negative exchange interaction between neighboring Fe³⁺ ions. A quantum mechanical model of the Fe-based magnetic cluster represented as a set of dimers with strong (~ 100–300) K at small distances and weak (~ 1 K) exchange interactions at larger one has been proposed (Fig.1).

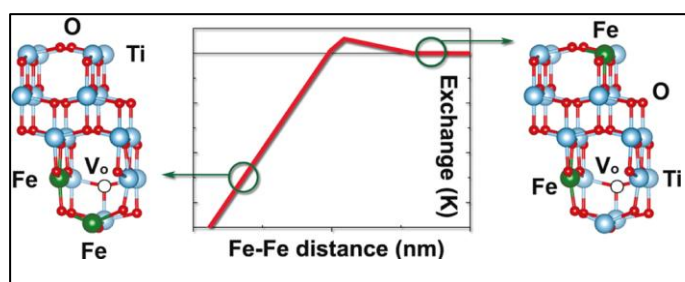


Fig. 1. Value of exchange interactions versus of Fe-Fe distances in TiO₂.

Our model was found to provide a good description of the magnetic properties of TiO₂:Fe nanopowders. The density-functional theory (DFT) calculations revealed Fe³⁺ oxidation state of the iron center in the vicinity of an oxygen vacancy in the crystal structure of anatase. The DFT calculations confirmed that two types of Fe³⁺ spin-pairs with weak and strong exchange interactions can be formed in the vicinity of an oxygen vacancy. The accumulation of magnetic moment carriers and formation of magnetic clusters in TiO₂ nanoparticles with anatase structure were found to be a general tendency for all studied TiO₂:Fe including TiO₂: Co nanopowders. Future studies are necessary to obtain direct experimental evidence for the existence of magnetic clusters in the TiO₂ matrix and to clarify the fundamental origin of the selective accumulation of the magnetic complexes.

[1] J.M.D. Coey, M. Venkatesan, P.J. Stamenov. *Phys.: Condens. Matter* **28**, 485001 (2016).

[2] A.Ye. Yermakov, A.F. Gubkin, A.V. Korolev et al. *J. Phys. Chem. C*, **123**, 1494 (2019).

Electronic Structures in In-doped Topological Insulator $(\text{Pb}_{0.5}\text{Sn}_{0.5})_{1-x}\text{In}_x\text{Te}$ Probed by NMR SpectroscopyBen-Li Young¹, Ping-Chun Tsai¹, Genda Gu²¹Department of Electrophysics, National Chiao Tung University, Hsinchu City 30010, Taiwan²Condensed Matter Physics & Materials Science Department, Brookhaven National Laboratory, Upton, New York 11973, USA

e-mail: blyoung@mail.nctu.edu.tw

SnTe is the first topological crystalline insulator (TCI) to be realized experimentally, and soon after the Pb-doped $(\text{Pb}_{1-x}\text{Sn}_x)\text{Te}$ is also verified as a TCI.[1] Doping indium further induces superconductivity in both systems. $(\text{Pb}_{1-x}\text{Sn}_x)_{1-y}\text{In}_y\text{Te}$ has been considered as a topological superconductor candidate since its topological surface states remain intact for low In content.[2-4] Here we report our NMR experiments on the investigation of the electronic band structures in $(\text{Pb}_{0.5}\text{Sn}_{0.5})_{1-x}\text{In}_x\text{Te}$, for $x = 0, 0.1, 0.2$, and 0.3 .

First, we found that the NMR frequency shifts of ^{117}Sn , and ^{207}Pb are dominated by the spins of free charge carriers, whereas the ^{125}Te frequency shift is determined by the orbital moments of the bound electrons. By analyzing these shifts, we conclude that In substitution for $0 \leq x \leq 0.3$ provides not just hole carriers but also lifts the chemical potential from the valence bands to the conduction bands, in consistent with the results from the electric transport measurements.[5,6]

We also utilize frequency shift to investigate the diamagnetism in $(\text{Pb}_{0.5}\text{Sn}_{0.5})_{1-x}\text{In}_x\text{Te}$. We found that their magnetic susceptibilities are dominated by the orbital diamagnetism which is weakened by In substitution. This infers that the spin-orbit interaction which is essential to the topological phase probably is also modified by In substitution.

The superconductivity in the $x = 0.3$ sample is investigated by the nuclear spin-lattice relaxation rate $(1/T_1)$ as a function of temperature. A Hebel-Slichter coherence peak is observed near the critical temperature, suggesting that the superconducting gap in the bulk is fully opened.

This work was supported by Ministry of Science and Technology, Taiwan (Grants No. MOST 104-2112-M-009-013).

- [1] S-Y. Xu, et al., Nat. Commun. 3, 1192 (2012).
- [2] T. Sato, et al., Phys. Rev. Lett. 110, 206804 (2013).
- [3] A.S. Erickson, et al., Phys. Rev. B 79, 024520 (2009).
- [4] G. Balakrishnan, et al., Phys. Rev. B 87, 140507(R) (2013).
- [5] R.D. Zhong, et al., Phys. Rev. B 90, 020505(R) (2014).
- [6] R.D. Zhong, et al., Crystals 7, 55 (2017).

Probing Magnetic Inhomogeneity of Pd_{1-x}Fe_x Thin Films with Ultrafast Optical and Magneto-optical Spectroscopy

R.V. Yusupov¹, A.V. Petrov¹, S.I. Nikitin¹, I.V. Yanilkin¹, A.I. Gumarov¹,
A.G. Kiiamov¹, L.R. Tagirov^{1,2}

¹Institute of Physics, Kazan Federal University, Kazan, Russia

²Zavoisky Physical-Technical Institute, FRC Kazan Scientific Center of RAS, Kazan, Russia

e-mail: ryusupov.kazan@gmail.com

Josephson superconductor-ferromagnet-superconductor (S/F/S) structures attract an interest of the scientific community due to the possible use in digital logics and memory elements based on cryogenic spintronics [1]. Characterized by high, up to terahertz, working frequency and extremely low, of the order of 10^{-19} W, energy per switch [2], these elements gain significant advantage in comparison with classic high-temperature ones based on semiconductors.

Palladium-rich Pd_{1-x}Fe_x alloys with $x < 0.10$ are considered as promising materials for F-layer in S/F/S structures. One of the critical requirements for the F-layer is magnetic homogeneity. In the case of intrinsically inhomogeneous Pd_{1-x}Fe_x alloy, magnetic properties of which are controlled by the local iron content, this requirement is difficult to satisfy. In particular, film composition and conditions of synthesis should be found that verify its magnetic homogeneity. For this, experimental approaches sensitive to magnetic inhomogeneity are needed. Neutron scattering can hardly be used for several nanometer thick films. Stationary methods like dc magnetometry or magneto-optical Kerr effect as well as ferromagnetic resonance techniques reflect mainly the properties of the ferromagnetic fraction and are not sensitive to nanometer scale inhomogeneities.

Here we report on a study of Pd_{0.94}Fe_{0.06} film with femtosecond optical and magneto-optical spectroscopy methods. Time scales of the photo-induced demagnetization and magnetization recovery are determined; the latter exhibits a critical slowing down on approach of the ferromagnetic ordering temperature $T_C = 190$ K from below. It is shown that the dynamics of the reflectivity after photoexcitation pulse undergoes an evolution from a two-exponential in the paramagnetic phase to a four-component in the range of $80 \text{ K} < T < T_C$ with a tendency towards simplification to a three-component at $T < 50$ K. We argue that such an evolution, along with the manifestation of an additional rising component in the magnetic response at $80 \text{ K} < T < T_C$, indicates the magnetic and electronic inhomogeneity of the film associated with the distribution of local iron concentrations on a nanoscale. Volume fraction of the residual paramagnetic phase at low temperatures is estimated as $\sim 10\%$. The obtained results show that time-resolved laser spectroscopy in the femto- and picosecond range is an effective tool for studying the magnetic inhomogeneity of thin films of Pd_{1-x}Fe_x alloys with low concentration of iron, promising for cryospintronic applications [3].

This work was supported by the RSF project No. 18-12-00459.

[1] V.V. Ryazanov, Phys. Usp. **42**, 825 (1999).

[2] D.S. Holmes, A.L. Ripple, M.A. Manheimer, IEEE Trans. Appl. Supercond. **23**, 1701610 (2013).

[3] A.V. Petrov *et al.*, JETP Lett. **110**, 197 (2019).

Electronic Structure near the Fermi Level in Nanostructured Phase of Thermally Reduced Graphene Oxide: ESR, CESR and Magnetic Susceptibility Studies

A.M. Ziatdinov

Institute of Chemistry, Far Eastern Branch of the Russian Academy of Sciences.
Vladivostok 690022, Russia

e-mail: ziatdinov@ich.dvo.ru

Experimental discovery of novel important quantum properties of electrons of the π -states stabilized on the zigzag edges of honeycomb carbon structures [1,2] prompted researchers to find the means of their transfer to the macroscopic level with the aim of further utilization in the functional materials. One of the promising directions for solving the mentioned problem is the formation of spatially extended networks including the percolation ones of electrically connected nanographenes with zigzag edges in certain structures. The principal results of our works in this field are presented in this report.

In the graphene oxide (GO) and its thermally reduced derivatives (TRGO) the presence of various structures of nanoscale π -conjugated regions of the carbon framework, including their electrically connected percolation clusters, has been proven with the structural methods of investigation [3]. In the nanostructured phases of TRGO the anomalously high density of states of the current carriers near the Fermi level has been revealed with the magnetic methods of investigation (ESR, CESR and magnetic susceptibility measurements). It has been shown that the reason for that may be stabilization of specific π -electronic states on the zigzag regions of break lines of the carbon net. The conclusion has been drawn on the potential suitability of nanostructured derivatives of GO for the formation of percolation structures of nanographenes with zigzag edges in these compounds and solving the problem of transferring peculiar quantum properties of electrons of the edge π -states to the macroscopic level.

The studies have been carried out with financial support from the Ministry of Science and Higher Education of Russia (State Assignment No. 265-2019-0001).

[1] Magda G., Jin X., Hagymasi I. et al., *Nature*, 514, 608 (2014).

[2] Kinikar A., Sai T.P., Bhattacharyya S. et al. *Nature Nanotech.* 12, 564 (2017).

[3] Ziatdinov A.M. *Materials Today: Proceedings.* 5, 26183 (2018).

Mössbauer Effect and Magnetic Studies of Fe Implanted ZnO Film

A.L. Zinnatullin¹, A.I. Gumarov¹, A.G. Kiiamov¹, B.F. Gabbasov¹, R.V. Yusupov¹, and
F.G. Vagizov¹,
V.I. Nuzhdin², V.F. Valeev², and R.I. Khaibullin²

¹Kazan Federal University, Kremlyovskaya 18, 420008 Kazan, Russia

²Zavoisky Physical-Technical Institute, FRC Kazan scientific center of RAS, SibirskyTrakt
10/7, 420029 Kazan, Russia

e-mail: almaz.zinnatullin@gmail.com

Wide-gap semiconductor oxide materials doped with transition 3d metals are in focus of researchers' interest during a few decades. It is due to theoretical explanation of ferromagnetic order in manganese doped diluted magnetic semiconductors and prediction of room temperature ferromagnetism in diluted magnetic oxides [1]. Such magnetic semiconducting/dielectric materials have great prospects in the field of spintronic devices [2]. A lot of researchers reported about ferromagnetic response in these compounds. However, some scientists associate these properties with formation of secondary magnetic phases from introduced impurities and show an absence of magnetic order in diluted systems. Magnetic response due to defects formation was reported also. The contradictory conclusions of many works make actual the relevant research on the synthesis of diluted magnetic oxides and explanation of the nature of room temperature ferromagnetism in these materials.

In this work we report results of synthesis and investigation of iron implanted zinc oxide thin film. ZnO film with thickness of 150 nm was deposited by rf magnetron sputtering technique on Si(001) substrate. Then, the film was implanted with 40 keV Fe⁺ ions to the fluence of $1.25 \cdot 10^{17}$ ion/cm². The implanted ZnO film was annealed at the temperature of 800 K for 30 min in a high vacuum. Crystal structure and phase composition of the sample was studied by X-Ray diffraction technique after the each step of the preparation. Chemical and magnetic states of iron impurity were examined by X-Ray Photoelectron and Mössbauer spectroscopies. Magnetic properties of the sample were studied by vibrating sample magnetometry and ferromagnetic resonance spectroscopy.

It was found that the virgin ZnO thin film keeps the orientation of (001). The implanted iron ions almost uniformly distributed through the film until the depth of 80 nm. The impurities are in 2+ and 3+ valence states and substitute the Zn positions in ZnO host matrix. The part of Fe³⁺ in cationic positions is ferromagnetically ordered. However, the system is metastable. Vacuum annealing leads to destroying the magnetically ordered Fe³⁺ clusters. As a result of the annealing, iron ions move to film surface, and magnetite (Fe₃O₄) nanoparticles are formed. Magnetic response decreases by a factor of 6. It was found that resulting magnetization vector is in the sample plane.

The reported study was funded by the Russian Government Program of Competitive Growth of Kazan Federal University and by RFBR, project № 18-02-00845. A.I. Gumarov acknowledges support by RFBR according to the research project □№ 18-32-01039. The work of A.G. Kiiamov was funded by the subsidy allocated to Kazan Federal University for the state assignment in the sphere of scientific activities (project № 3.9779.2017/8.9). Authors from ZPTI indicate that ion implantation was performed in the frame of state assignment of FRC Kazan Scientific Center of RAS, No AAAA-A18-118041760011-2.

[1] T. Dietl, Science **287**, 1019 (2000).

[2] S. Wolf, Science **294**, 1488 (2001).

**Pressure-Tuning the Quantum Spin Hamiltonian of the Triangular
Lattice Antiferromagnet Cs_2CuCl_4 : High-Field ESR Studies^{*,**}**

Sergei Zvyagin

Dresden High Magnetic Field Laboratory (HLD-EMFL), Helmholtz-Zentrum Dresden-Rossendorf, 01328 Dresden, Germany

e-mail: s.zvyagin@hzdr.de

Spin-1/2 triangular-lattice antiferromagnets are important prototype systems to investigate phenomena of the geometrical frustration in condensed matter. Apart from highly unusual magnetic properties, they possess a rich phase diagram (with ground states, ranging from an unfrustrated square lattice to a quantum spin liquid), yet to be confirmed experimentally. One major obstacle in this area of research is the lack of materials with appropriate (ideally tuned) magnetic parameters. Using Cs_2CuCl_4 as a model system, we demonstrate an alternative approach, where, instead of the chemical composition, the spin Hamiltonian is altered by hydrostatic pressure. The application of high-field high-pressure electron spin resonance and magnetization techniques allowed us to accurately monitor exchange parameters. Our experiments indicate a substantial increase of the exchange coupling ratio from 0.3 to 0.42 at a pressure of 1.8 GPa, revealing a number of emergent field-induced phases.

*In collaboration with: D. Graf, T. Sakurai, S. Kimura, H. Nojiri, J. Wosnitza, H. Ohta, T. Ono, and H. Tanaka.

Published in: S. Zvyagin et al., Nat. Comm. **10, 1064 (2019).

An EPR Study of the V^{4+} and Cu^{2+} Ions in Single Crystals of β - $Mg_2V_2O_7$ and α - $Zn_2V_2O_7$: non-coincident g and \tilde{A}^2 Tensors

S.K. Misra¹, S.I. Andronenko²

¹Physics Department, Concordia University, Montreal, Canada

²Institute of Physics, Kazan Federal University, Kazan, Russian Federation

e-mail: SIAndronenko@kpfu.ru

The angular variations of V^{4+} and Cu^{2+} EPR spectra in β - $Mg_2V_2O_7$ and α - $Zn_2V_2O_7$ were recorded for orientations of the external magnetic field in three mutually perpendicular planes at 120 K and 295 K, as well as in the temperature range from 110 to 295 K at some chosen orientations of the magnetic field. The principal values of the g and \tilde{A}^2 tensors for the V^{4+} and Cu^{2+} ions, as well as the orientation of their principal axes were determined from the angular variations of the EPR line positions in three mutually perpendicular planes, using a rigorous least squares fitting procedure, using the eigenvalues and eigenvectors of the SH matrix, especially adapted to the case of non-coincident principal axes of the g (Zeeman) and \tilde{A}^2 (hyperfine interaction) -tensors for the monoclinic and triclinic space-group symmetries in β - $Mg_2V_2O_7$ and α - $Zn_2V_2O_7$, respectively [1,2], varying the appropriate Euler angles relating the non-coincident principal axes of the g and \tilde{A}^2 -tensors. The principal values of the g - and \tilde{A}^2 -tensors of the Cu^{2+} ion in these crystals are found to have similar values, which implies that the Cu^{2+} ion has the same $|0\rangle$ ground state in the two crystals. The orientations of the principal axes the g and \tilde{A}^2 -tensors of the Cu^{2+} ions are found to be non-coincident with each other. This is because the Cu^{2+} ion in β - $Mg_2V_2O_7$ is 6-fold coordinated, whereas it is 5-fold coordinated in a trigonal bipyramidal configuration in α - $Zn_2V_2O_7$. The principal values of the g - and \tilde{A}^2 -tensors of the Cu^{2+} and V^{4+} ions at 120 K are listed below.

Cu^{2+}	g_z	g_x	g_y	A_z (GHz)	A_x (GHz)	A_y (GHz)
$Mg_2V_2O_7$	2.015±0.001	2.283±0.001	2.358±0.001	0.24±0.01	0.13±0.01	0.0±0.01
$Zn_2V_2O_7$	1.999±0.001	2.283±0.001	2.358±0.001	0.26±0.01	0.17±0.01	0.0±0.01

The principal values of the g and \tilde{A}^2 -tensors of the V^{4+} ions are the same in the two crystals. The orientations of the principal axes the g and \tilde{A}^2 -tensors of the V^{4+} ions are found to be non-coincident, but similar, to each other in α - $Zn_2V_2O_7$ and β - $Mg_2V_2O_7$ crystals [3].

V^{4+}	g_z	g_x	g_y	A_z (GHz)	A_x (GHz)	A_y (GHz)
$Mg_2V_2O_7$	1.932±0.001	1.969±0.001	2.002±0.001	0.49±0.01	0.17±0.01	0.16±0.01
$Zn_2V_2O_7$	1.932±0.001	1.976±0.001	2.011±0.001	0.50±0.01	0.19±0.01	0.18±0.01

The V^{4+} ion is tetrahedrally coordinated in both crystals with the Γ_3 doublet being the ground state, which for the V^{4+} ions in β - $Mg_2V_2O_7$ and α - $Zn_2V_2O_7$ are found to be similar, because the local environments of V^{4+} ions in the corresponding VO_4 configurations are almost identical in the two crystals.

This work was supported by NSERC (SKM) and the Ministry of Education and Science of Russian Federation, project allocated to Kazan Federal University (#3.2166.2017/4.6).

[1] S.K. Misra, J. Magn. Reson. **23**, 403 (1976).

[2] S.K. Misra, Physica B **151**, 433 (1988).

[3] S.K. Misra, S.I. Andronenko, Magn. Reson. Solids **20**, 18101(8p) (2018).

An Investigation of the Conformational Properties of Mefenamic Acid in DMSO by Two-dimensional NMR

I.A. Khodov^{1,2}, S.V. Efimov², K.V. Belov¹, L.A.E. Batista de Carvalho³

¹G.A. Krestov Institute of Solution Chemistry of the Russian Academy of Sciences, Ivanovo, Russian Federation

²Institute of Physics, Kazan Federal University, Kazan, Russian Federation

³University of Coimbra, Rua Larga, Coimbra, Portugal

e-mail: iakh@isc-ras.ru

This abstract presents the main results of research on the conformational preference of the molecule mefenamic acid. This compound is used as a drug and belongs to the group of NSAID (nonsteroidal anti-inflammatory drugs). The main idea of this research is to determine the conformation preference of mefenamic acid dissolved in deuterated DMSO using two-dimensional NMR and quantum chemistry calculation. The obtained information can help one to determine the way of nucleation mechanisms.

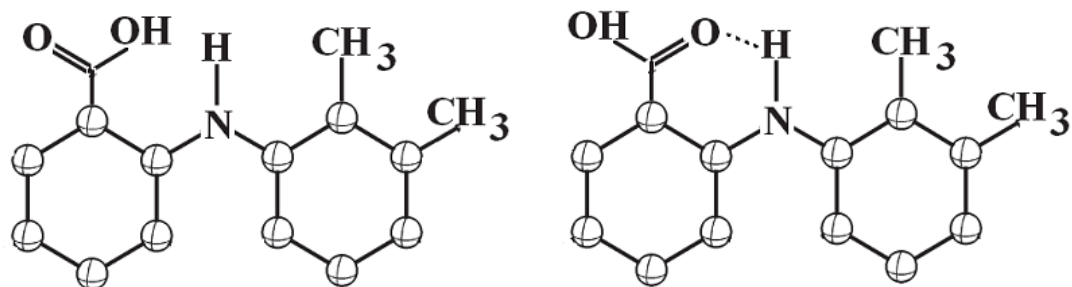


Figure 1. Structure of the mefenamic acid polymorphs molecules MEF II (left) and MEF I (right).

Two crystalline forms, called MEF I and MEF II, having different positions of the carboxyl group, are formed by different conformations of the mefenamic acid molecules (Fig.1)[1].

Recently we have shown that the molecular conformation, existing in the saturated solution, may define the polymorphic type, obtained by evaporation of this solution [2,3].

In this work we present the conformation equilibrium of mefenamic acid in solution and discuss it in the frame of polymorphic phenomena.

Acknowledgements. The study was carried out with financial support of Russian Foundation for Basic Research (project 18-29-06008 MK), Ministry of Science and Higher Education and of the Russian Federation (projects 01201260481 and 01200950825), and under grant of Council on grants of the President of the Russian Federation (projects project nos. 18-29-06008, 18-03-00255 and 17-03-00459). Prof. V.V. Klochkov (from Kazan Federal University) and Prof. M.G. Kiselev (from ISC RAS) are appreciated for the helpful discussions of the NMR spectroscopy results.

[1] E.H. Lee, S.R. Byrn, and R. Pinal, *J. Pharm. Sci.* **101**, 4529 (2012).

[2] I.A. Khodov, S.V. Efimov, M.Y. Nikiforov, V.V. Klochkov, and N. Georgi, *J. Pharm. Sci.*, 103 (2014).

[3] I.A. Khodov, S.V. Efimov, M.G. Kiselev, L.A.E. Batista De Carvalho, and V.V. Klochkov, *J. Mol. Struct.*, 1113 (2016).

NMR Study of Synthesis of the Phenanthridone Alkaloids from Herbal's Aporphine Alkaloids by Subcritical Water

S.N. Borisenko, E.V. Maksimenko, S.S. Khizrieva, G.S. Borodkin, N.I. Borisenko

Southern Federal University, Stachky Av. 194/2, Rostov-on-Don, 344090, Russia

e-mail: boni@ipoc.rsu.ru

In the present paper, the NMR technique is used to study the synthesis of phenanthrene alkaloids from herbal's aporphine [1] alkaloids in subcritical water [3,4]. Phenanthrene derivatives obtained semi-synthetically from the plant's alkaloids have the higher value of antioxidant activity and may exhibit new therapeutic applications other than the original aporphine substances.

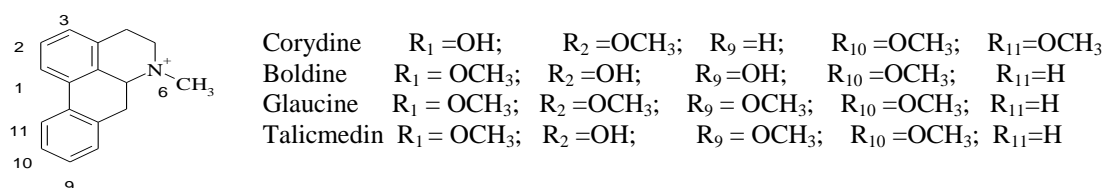


Fig.1 Typical structure of the aporphine herbal's alkaloids

The synthesis of the seco-glaucine was selected as a model study. The glaucine is an alkaloid contained in various kinds of plants, such as *Glaucium flavum*, *Glaucium oxylobum*, *Croton lechleri* и *Corydalis yanhusuo*. The technique of synthesis of the phenanthrene seco-glaucine from glaucine using medium of subcritical water (Fig. 2) is studied in the temperature range 100 °C to 250 °C.

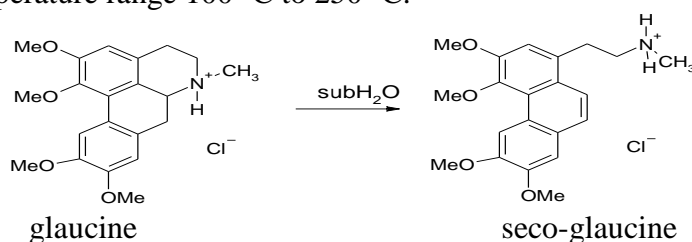


Fig.2.

It is shown that the maximum yield of the target phenanthrene's alkaloid (seco-glaucine) is achieved at a temperature of 250 °C in water medium without catalytic additives. The studied technique for synthesis of the phenanthrene's alkaloids makes possible to develop environmentally friendly technologies for the production of new kinds of drugs based on the herbal's aporphine's alkaloids which are widely distributed in the plant kingdom.

This research was supported by the internal grant of the Southern Federal University (Project No **ВнГр-07/2017-04**) and was performed using instruments from the Center for Collective Use 'Molecular Spectroscopy' of Southern Federal University.

- [1] P. O'Brien, C. Carrasco-Pozo, H. Speisky, *Chem Biol Interact* **159**(1), 1 (2006).
 [2] A.A. Galkin, V.V. Lunin, *Russian Chem Rev*, **74**, 21 (2005).
 [3] A.V. Lekar, O.V. Filonova, S.N. Borisenko, *et al.*, *Russian J Phys Chem B*, **7**, 829 (2013).

Spin Probe Nanostructure Formation in Glassy Media Studied by EPR

Natalia Dudysheva, Elena Golysheva, and Sergei Dzuba

Physics Department, Novosibirsk State University, 630090, Russia, and
Voevodsky Institute of Chemical Kinetics and Combustion, Russian Academy of Sciences,
Novosibirsk, 630090 Russia

e-mail: nata.dudysheva@gmail.com

In cell membranes, proteins, cholesterol and other biomolecules can form nanostructures – clusters or aggregates. These structures are involved in different cell processes, for example, cell adhesion, receiving and sending signals. Despite the intensive investigations, the mechanism of the nanostructure formation has not been clarified yet.

In order to elucidate this issue, in this work glassy *ortho*-terphenyl (OTP) was chosen as a nonpolar disordered medium which simulates internal part of the biological membranes. Nitroxide free radicals (1R and 2R) were used as a model for guest molecules (Fig. 1). Pulsed EPR was employed to study their spatial distribution. The magnetic dipolar interaction of electron spins contributes to the two-pulse electron spin echo (ESE) decay by the mechanism of so-called “instantaneous diffusion”, which allows obtaining information on the spin probe spatial distribution.

Two types of spatial distribution were found in these studies. In the case of 1R, the excluded volume around the probe was detected at low probe concentrations (< 2 mM) which is replaced by clustering at larger concentrations. In the case of 2R, the clustering of probes was found for all their concentrations.

It was proposed that these two types of spatial distribution are determined by a relative value of energy of the interaction between host molecules and between the host and guest molecules. To support this suggestion, study of 1R in polar water-glycerol glass was performed, in which host-host interaction is expected to prevail. The obtained results have shown that the probe spatial distribution is indeed random in this case.

The parameters of the probe spatial distribution in *ortho*-terphenyl were obtained by simulation of the spin-spin dipolar interaction contribution to the ESE decay.

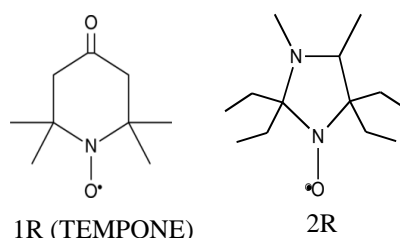


Fig. 1. Chemical structures of nitroxide free radicals (spin probes)

Intramolecular Effects on Electron Spin Relaxation

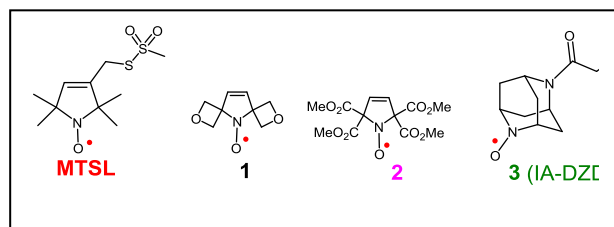
Sandra S. Eaton and Gareth R. Eaton

Department of Chemistry and Biochemistry, University of Denver, Denver, CO 80210, USA

e-mail: Sandra.eaton@du.edu

Long spin echo decay times are important for applications of radicals as spin labels for double electron electron spin resonance (DEER) and for design of molecular qubits.

The longest distances that can be obtained by DEER are limited by the spin echo dephasing time T_m , which determines the length of the time window during which the dipolar evolution curve can be monitored. For MTSL and most other common nitroxides, there are gem-dimethyl groups on the two carbons adjacent to the nitroxide N-O moiety. Rotation of these methyl groups at rates that are comparable to the inequivalences in hyperfine couplings to the methyl protons is a very effective dephasing mechanism that shortens T_m at



temperatures between about 80 and 273 K. To perform DEER at temperatures above 80 K and eventually at ambient temperatures we are working with the group of Prof. Andrzej Rajca at the University of Nebraska on the Values of T_m (μs) in 9:1 trehalose:sucrose design and characterization of spin labels without methyl groups on the alpha carbons, including radicals 1, 2, and 3.^{1, 2} The absence of the gem-dimethyl groups dramatically lengthens T_m at temperatures above 80 K. To restrict motion, radicals were immobilized in glassy trehalose or in trehalose:sucrose mixtures, which increases T_m at temperatures up to ambient. Values of

	80 K	150 K	293 K
MTSL	2.4 ^a	0.33 ^a	
1	4.4	3.6	0.70
2	3.9	3.6	0.42
3	2.9	2.3	0.38

T_m for these radicals are shown in the Table .

We are working with the group of Prof. Joseph Zadrozny at Colorado State University to determine factors that impact the spin echo dephasing of vanadium(IV) complexes.³ We have examined the impact of methyl groups in the trialkylammonium cations of $[\text{R}_3\text{NH}]\text{V}(\text{C}_6\text{H}_4\text{O}_3)_2$ in o-terphenyl, which decreases dramatically as the length of the alkyl chain is increased from ethyl to octyl.

- [1] S. Huang, J.T. Paletta, H. Elajaili, K. Huber, M. Pink, S. Rajca, G.R. Eaton, S.S. Eaton, and A. Rajca, *J. Org. Chem.* 82 (2017) 1538 - 1544.
 [2] S.S. Eaton, A. Rajca, Z. Yang, and G.R. Eaton, *Free Radical Res.* 52 (2018) 319 - 326.
 [3] C.-Y. Lin, T. Ngendahimana, G.R. Eaton, S.S. Eaton, and J.M. Zadrozny, *Chemical Science* 10 (2019) 548 - 555.

Phosphorylotropic Rearrangement in Crown Ester Observed by ^1H , ^{13}C , and ^{31}P NMR

S.V. Efimov¹, F.Kh. Karataeva², V.V. Klochkov¹

¹Institute of Physics, Kazan Federal University, Kazan, Russian Federation

²Alexander Butlerov Institute of Chemistry, Kazan Federal University, Kazan, Russian Federation

e-mail: Sergej.Efimov@kpfu.ru

Different intramolecular processes are met in the behavior of *N,N'*-(bis)diizopropoxy-phosphorylamidocarbonyl)-1,10-diaza-18-crown-6-ester (DA-18-C-6) dissolved in CDCl_3 , CD_2Cl_2 , and CD_3CN [1]. These are hindered rotation around the C–N bond leading to *trans*- and *cis*-rotamers, triad prototropy in C–N–P, and macrocycle ring inversion. Phosphorylotropic rearrangement in another compound, *N,N'*-(bis)diizopropoxy-thiophosphorylamidocarbonyl)-1,10-diaza-18-crown-6-ester dissolved in DMSO was studied earlier by ^1H , ^{13}C , and ^{31}P NMR [2]. Phosphorylotropic form (see figure 1) was also observed in analogous crown esters in amide substituents $(\text{O}i\text{Pr})_2\text{P}(\text{X})\text{NHC}(\text{Y})-$, which arises due to the migration of the thiophosphoryl group to the heteroatom (O or S) at the carbon atom. The advantage of using DMSO as the solvent is the possibility to study the system at high temperatures (up to 373 K) and shifting the chemical equilibrium between different molecular forms due to the polar character of the medium (permittivity $\epsilon = 49$).

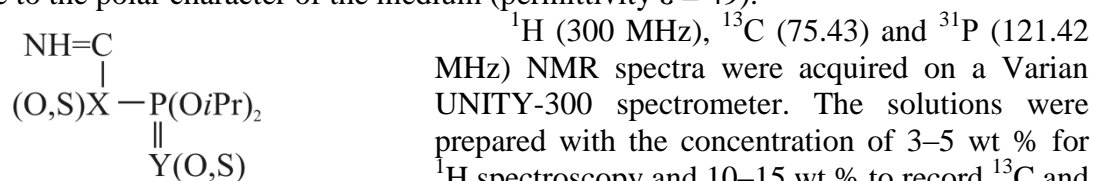


Fig. 1. Phosphorylotropic form appearing upon heating of the crown ester in DMSO.

^1H (300 MHz), ^{13}C (75.43) and ^{31}P (121.42 MHz) NMR spectra were acquired on a Varian UNITY-300 spectrometer. The solutions were prepared with the concentration of 3–5 wt % for ^1H spectroscopy and 10–15 wt % to record ^{13}C and ^{31}P spectra. The chemical shift referencing was made using an internal standard.

It was found that new signals appear and increase their intensity upon heating. While the initial content of the phosphorylotropic form, according to corresponding ^1H NMR signal at 4.5 ppm, is 11%, its fraction increases to 71% in the temperature range of 298–373 K, and is still growing to 85% at further cooling down back to 298 K. Similar irreversible transformations are observed also in the methyl resonance region at 1.3 ppm and also in ^{13}C and ^{31}P spectra. Namely, amide and phosphorylotropic forms show the carbon NMR signals at 71.4 and 69.9 ppm, respectively; corresponding phosphorus lines appear at 0.77 and 10.73 ppm, respectively.

The following conclusion can be made based on the analysis of the spectral data: the DA-18-C-6 molecule experiences a transition from the amide form into the phosphorylotropic form with the yield of 85% in the temperature range of 293–373–293 K.

The work was supported by the Russian Science Foundation (project no. 18-73-10088).

[1] F.Kh. Karataeva et al, Russ. J. Gen. Chem. **68**, 743 (1998).

[2] F.Kh. Karataeva, Russ. J. Gen. Chem. **69**, 1139 (1999).

EPR Study of γ -Irradiated Magnesium and Zinc Gluconates

A.R. Gafarova, G.G. Gumarov, M.M. Bakirov, V.Yu. Petukhov

Zavoisky Physical-Technical Institute, FRC Kazan Scientific Center of RAS

e-mail: albina-gafarova@mail.ru

It is known that the bioavailability and effectiveness of the treatment of certain drugs, in particular the salts of gluconic acid, depends on their stereochemical structure [1, 2]. Previously, it was shown that it is possible to determine the conformational structure of gluconic acid salts using EPR spectroscopy in the X- and Q- bands [3]. Due to the fact that no absorption signal was observed in the EPR spectrum of the original calcium gluconate, to obtain information about the sample, it was proposed to introduce artificial defects into it, that is, to create paramagnetic centers using ionizing radiation. The obtained EPR spectra have a pronounced hyperfine structure and can be decomposed into 4 components [3]. It was established that the components correspond to different positions of the paramagnetic centers in the carbon chain, that made it possible to establish the conformation of the molecule. The work presents the results of applying this method of studying the conformational structure for the magnesium and zinc salts of gluconic acid.

Samples of pure laboratory magnesium gluconate and zinc gluconate from Sigma Aldrich were used as starting materials. The samples were preliminarily irradiated by photons using the Rocus gamma-therapeutic device with Co^{60} - source (energy of 1.25 MeV). EPR spectra were obtained with Bruker EMX Plus spectrometer in the X- band at a frequency of 9.3 GHz. The EPR spectra were analyzed using MatLab Easy Spin.

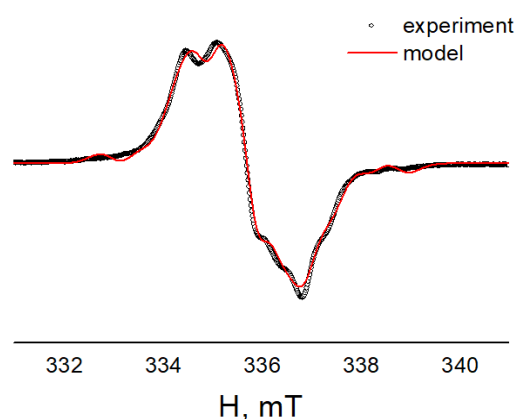


Fig.1. EPR spectrum and the result of modeling gamma-irradiated magnesium gluconate.

It has been established that, when gamma-irradiation of magnesium and zinc gluconates, paramagnetic centers appear that are stable at room temperature. The EPR spectra can be described by four components: a doublet of triplets, a triplet, a doublet of doublets, a doublet. The parameters of the components of the obtained spectra turned out to be close to the values obtained when describing the EPR spectra of irradiated calcium gluconate [3]. At the same time, the proximity of the obtained hyperfine coupling constants for the gluconic acid salts studied (Ca, Mg, Zn) indicates the proximity of torsion angles in the H – C – C – H chain, that is, the similarity of the conformational structure of these compounds. The main difference in the results of the decomposition of the experimental spectra lies in the relative intensities of the components. It is assumed that this may be due to the difference in deviations of the torsion angles from pure gauche- and trans- configurations.

[1] Konygin G.N. *et al.*, Patent of Russia № 2373185 (2009).

[2] Konygin G.N. *et al.*, Materials of conf. "Actual issues of Pediatric Surgery", 56 (2003).

[3] Gafarova A.R. *et al.*, Modern development of magnetic resonance 129 (2018).

Study of Radiation Induced Radicals in Sodium Gluconate

A.R. Gafarova, G.G. Gumarov, M.M. Bakirov, V.Yu. Petukhov

Zavoisky Physical-Technical Institute, FRC Kazan Scientific Center of RAS

e-mail: albina-gafarova@mail.ru

Previously [1], solutions of sodium gluconate in water were studied in a wide range of concentration. The ^1H NMR spectra allowed revealing the fact of constancy of the conformation of sodium gluconate in aqueous solutions in the studied concentration range, the presence of hydrogen bonds between sodium gluconate and water and the formation of associates. Fitting of the theoretical spectra to the experimental ones allowed us quite accurately to find the dihedral angles for the sodium gluconate molecule and on their basis to plot a 3D structure of the molecule in an aqueous solution. However, the determination of conformations using ^1H NMR spectroscopy is limited to the study of liquid solutions. Previously, it was shown that it is possible to determine the conformational structure of initial gluconic acid salts using EPR spectroscopy [2]. It was established that the components correspond to different positions of the paramagnetic centers in the carbon chain that made it possible to establish the conformation of the molecule. The work presents the results of applying this method of studying the conformational structure for the sodium gluconate.

Samples of pure laboratory sodium gluconate from Acros Organics were used as starting materials. The samples were irradiated by photons with Co^{60} - source (energy of 1.25 MeV). EPR spectra were obtained with Bruker EMX Plus spectrometer in the X- band at a frequency of 9.3 GHz. The EPR spectra were analyzed using MatLab Easy Spin.

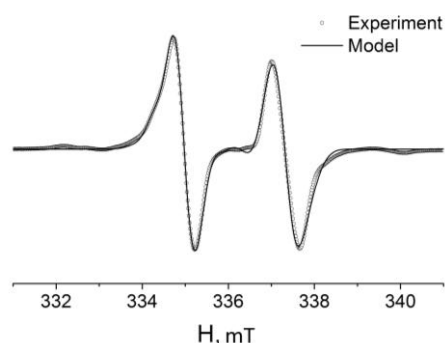


Fig.1. EPR spectrum and the result of modeling gamma-irradiated sodium gluconate.

The EPR spectrum of sodium gluconate (powdered, in the solid state) irradiated with gamma quantum can be decomposed into two components: a doublet with a hyperfine interaction constant of 67 MHz and a doublet with constants of 72.5 and 17.7 MHz (Fig. 1).

It is known [3] that when polyols are irradiated with high-energy quant, the observed paramagnetic centers (π -radicals on carbon atoms) are formed due to the detachment of a proton bounded to carbon. In this case, a single doublet may correspond to a single positive content of gluconic acid salts - the second carbon atom C2. In

accordance with the ratio of McConnell, torsion angles between the axis of the π -radical and the direction of the C – H bond on the adjacent carbon atom can be estimated: doublet - 36° , doublet of doublets 32° and 66° . Such angles indicate a strong deviation from the ideal gauche-configuration of a part of the chain H-C2-C3-H. As a result, it means the maximum torsion stress in a given section of the chain. It is assumed that the formation of a dangling bond on C2 leads to a partial stress relief. As a result, a large concentration of radicals on C2 is observed - about 80%, as follows from the EPR data. For some irradiated gluconates (calcium, magnesium and zinc), a more uniform distribution of paramagnetic centers along the carbon chain is observed, which corresponds to a smaller deviation of the torsion angles from the ideal trans- and gauche- configurations.

[1] Akhmetov M.M. *et al.*, Journal of Molecular Structure 1193, 373 (2019).

[2] Gafarova A.R. *et al.*, Modern development of magnetic resonance 129 (2018).

[3] Kochetkov N.K., Kudrjashov L.I. *et al.*, Radiation Chemistry of Carbohydrates 256 (1979).

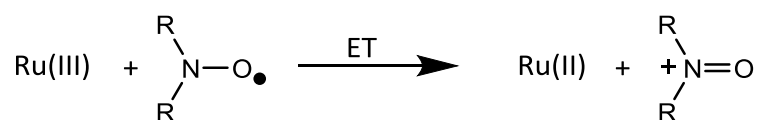
Applications of EPR and Light-Induced Reactions in Biomimetic Systems and Catalysis

Georg Gescheidt, Lev Weiner, Antonio Barbon, Max Schmallegger

Institute of Physical and Theoretical Chemistry, Graz University of Technology,
Stremayrgasse 9, 8010 Graz, Austria

e-mail: g.gescheidt-demner@tugraz.at

This presentation will show our recent attempts to quantify the ability of phospholipids to mediate electron-transfer. Our approach is based on the oxidation of nitroxides by Ru(III) (Scheme). We trigger the formation of Ru(III) by the photo-oxidation of Ru(II) using peroxydisulphate, a technique developed by Weiner and colleagues [1].



Scheme. Oxidation of stable nitroxyl radicals by Ru³⁺

I will show how this technique can be applied to follow electron transfer across phospholipid membranes, which contain selectively nitroxide-substituted stearic acids.

Moreover, I will describe how EPR can be utilized to monitor the formation of Cu nanoparticles in aqueous and alcoholic solutions (Figure) using photo-induced procedures.

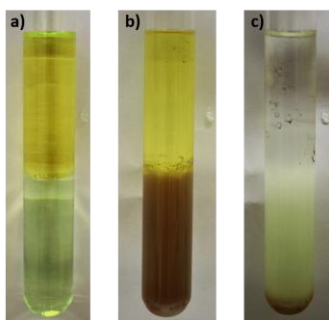


Figure. 2-phase system consisting of cyclohexane/methanol containing **1**, CuSO₄ and styrene. a) Parent mixture; b) Cu nanoparticles after 120 s of irradiation of the bottom methanol solution c) After subsequent irradiation (120 s) of the upper cyclohexane phase. The milky precipitate is polystyrene.

- [1] T. Eliash, A. Barbon, M. Brustolon, M. Sheves, I. Bilkis, L. Weiner, *Angew. Chemie - Int. Ed.* **2013**, 52, 8689–8692.

High-pressure NMR Characterization of Conformation Preferences of Small-Molecules Dissolved in Supercritical Carbon Dioxide

I.A. Khodov^{1,2}, S.V. Efimov², M.G. Kiselev¹

¹ Institute of Solution Chemistry of the RAS, Ivanovo, Russian Federation

² Institute of Physics, Kazan Federal University, Kazan, Russian Federation

e-mail: ilya.khodov@gmail.com

The application of this approach to the study of conformational preferences in a fluid seems very promising in relation to obtaining information on the processes occurring at the molecular level. One of the key tasks for obtaining this kind of information is adapting NMR methods for high temperatures and pressures.

High-pressure NMR spectroscopy has been utilized to study the conformation behavior of small molecules dissolved in supercritical CO₂. The 2D NOESY spectrum was analyzed to determine the conformation preference. A change in the conformation distribution is postulated to describe the nucleation mechanism of different polymorphic forms. At the CO₂ supercritical parameters of state, there is an apparent coincidence conformation preference of the small molecules in fluid volume and in solid phase. This fact is confirmed by the results of computer simulation.

The study was carried out with financial support from the Russian Foundation for Basic Research (project 18-29-06008 MK), Ministry of Science and Higher Education of the Russian Federation (projects 01201260481 and 01200950825), and the grant of Council on grants of the President of the Russian Federation (project MK-1409.2019.3).

[1] I.A. Khodov, S.V. Efimov, V.V. Klochkov, L.A.E. Batista De Carvalho, M.G. Kiselev, J. Mol. Struct., **1106**, 373 (2016).

[2] S.V. Efimov, I.A. Khodov, E.L. Ratkova, M.G. Kiselev, S. Berger, V.V. Klochkov, J. Mol. Struct., **1104**, 63 (2016).

EPR Spectroscopy of Metal-Oxide Photocatalysts

A.I. Kokorin¹, E.A. Konstantinova²¹N. Semenov Institute of Chemical Physics RAS, Moscow, Russian Federation²Department of Physics, M.V. Lomonosov Moscow State University, Russian Federation

e-mail: alex-kokorin@yandex.ru

Photocatalysis is currently assumed as one of the most perspective pathways for ‘green’ chemistry, environmental control and self-cleaning. For better understanding mechanisms of photocatalytic processes, scientists all over the world are usually used model reactions in which different organic dyes are mineralized or partially oxidized in aqueous solutions. Photocatalytic activity is studied mainly using bare TiO₂ or its metal-doped systems [1, 2].

In this work we have studied photooxidation of Rhodamine B and Rhodamine 6G on vanadium modified Hombikat UV 100 TiO₂ and mixed TiO₂/V₂O₅ oxides in a wide range of vanadium content. Structure and properties of V⁴⁺ and VO²⁺ paramagnetic centers (PCs) formed on TiO₂ surface or in the bulk were studied by X-band EPR.

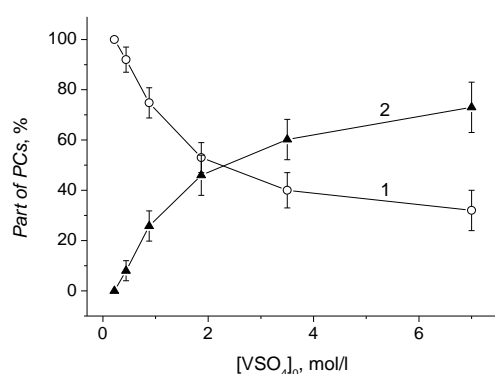


Fig.1. Parts of the isolated (1) and aggregated (2) VO²⁺ PCs formed on V-TiO₂ Hombikat UV 100 surface as a function of added VOSO₄ amount.

Two types of PCs, aggregated and isolated ones, were revealed and described quantitatively both in surface V-modified TiO₂ samples and in TiO₂/V₂O₅ mixtures. EPR results were compared with photocatalytic data and it was concluded that the most probable catalytically active centers are the isolated VO²⁺ centers on the V-doped TiO₂ surface [3]. Fig.1 shows changes of the content of isolated and aggregated VO²⁺ PCs formed on V-TiO₂ Hombikat UV 100 surface as a function of VOSO₄ salt added to the aqueous suspension of bare TiO₂ for its modification.

Similar mixed-oxide photocatalytic systems such as TiO₂/MoO₃, TiO₂/WO₃ and TiO₂/MoO₃:V₂O₅, continued being active in the dark during up to 10 h after switching off the lamp irradiation [4]. It should be noted that all these systems are nanostructured wide band gap oxide semiconductors containing different PCs in the structure characterized by their energy levels inside the band gap of the certain metal oxide [5]. Photophysical properties of such compounds will be discussed in the paper of Prof. E.A. Konstantinova.

This work is supported by Russian Foundation for Basic Research (Grant No. 18-53-00020-Bel-a).

- [1] X. Chen; S.S. Mao, Chem. Rev. **107**, 2891 (2007).
- [2] H. Zhang, G. Chen, D.W. Bahnemann, J. Mater. Chem. **19**, 5089 (2009).
- [3] A.I. Kokorin, V.I. Pergushov, A.I. Kulak, Catal. Lett. (2019) (in press).
- [4] T.V. Sviridova, L.Yu. Sadvovskaya, E.A. Konstantinova, N.A. Belyasova, A.I. Kokorin, D.V. Sviridov, Catalysis Letters **149**, 1147 (2019).
- [5] E.A. Konstantinova, A.A. Minnekhanov, A.I. Kokorin, T.V. Sviridova, D.V. Sviridov, J. Phys. Chem. C, **122**, 10248 (2018).

EPR Study of Structural Peculiarities of Metal Oxides Intercalated by Benzoazoles

A.I. Kokorin¹, E.A. Konstantinova², Ye.N. Degtyarev¹, M.V. Sivak¹,
T.V. Sviridova³, D.V. Sviridov³

¹N. Semenov Institute of Chemical Physics RAS, Moscow, Russian Federation

²Department of Physics, M.V. Lomonosov Moscow State University, Russian Federation

²Department of Chemistry, Belarus State University, Minsk, Belarus Republic

e-mail: alex-kokorin@yandex.ru

The layered transition-metal oxides (MoO_3 [1, 2], WO_3 [3], V_2O_5 [4]) possesses the interlamellar volume large enough to enable insertion of ions or small organic molecules, this results in formation of organic-oxide hybrid materials. Chemical intercalation leads to the structural transformations [5]. Such intercalated materials exhibit unusual catalytic properties and are successfully used in photoswitching systems and can play a role of nanocontainers.

In this work using X-band EPR we demonstrate that the intercalation of bebzotriazole (BTA) into MoO_3 and V_2O_5 changes structural features of such oxide systems which reveal properties of the container depot systems for anti-corrosion applications.

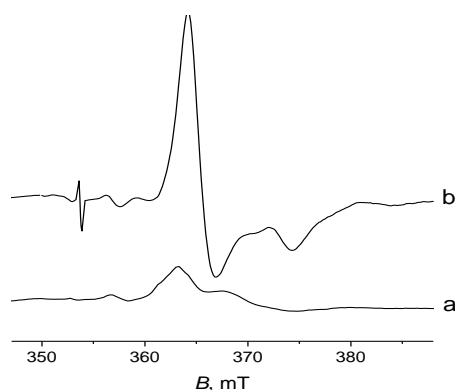


Fig.1. Experimental EPR spectra of bare MoO_3 (a) and MoO_3/BTA (b) at 77 K.

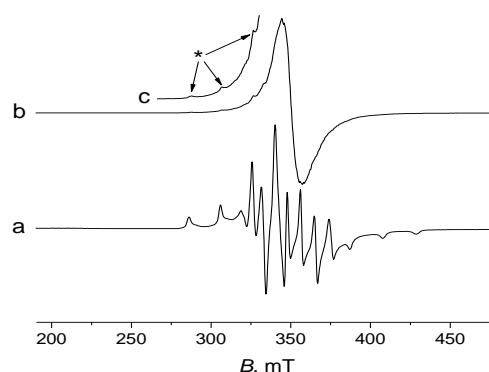


Fig.2. EPR spectra of V_2O_5 (a) and $\text{V}_2\text{O}_5/\text{BTA}$ (b) at 77 K. Spectra are normalized by the amplitude. c is fivefold enlarged part of b, arrows show the lines of the spectrum a.

Figs. 1 and 2 show typical EPR spectra of bare and modified by BTA MoO_3 and V_2O_5 nanosized oxides containing 20 mass% BTA. Noticeable changes in EPR spectra are evidently observed resulting in *ca.* fivefold increasing the content of paramagnetic centers and in changes of the phase structure in the case of $\text{V}_2\text{O}_5/\text{BTA}$ (Fig. 2).

This work is supported by Russian Foundation for Basic Research (Grant No. 18-53-00020-Bel-a).

- [1] M. Atsharpur, A.Mahjoub, M.M. Amini, J. Inorg. Organomet. Polym. Mater. **19**, 298 (2009).
- [2] T. Rostamzadeh, K. Riché, S.S. Akbarian-Tefaghi, et al., Flat. Chem. **5**, 9(2017).
- [3] D. Hunyadi, E. Majzik, J. Matyasi, et. Al., RSC Adv. **7**, 46726 (2017).
- [4] J.-P. Jolivet, M. Henry, J. Livage, *Metal Oxide Chemistry and Synthesis: From Solution to Solid State* (Wiley, Chichester, 2000).
- [5] W. Li, F. Xia, J. Qu, et al., Nano Res. **7**, 903 (2014).

CW EPR and ESEEM Study of the Verdazyl Radicals

K. Konov

Zavoisky Physical-Technical Institute, Kazan, Russian Federation

e-mail: kostyakov@gmail.com

Verdazyl radicals are established family of stable free radicals. Their photoactive conjugates have wide perspective in application as spin probes. CW spectra at room temperature of verdazyl solution contain 9 lines due to interaction of the electron spin with (as supposed) 2 different sets of 2 equivalent ^{14}N nuclei of the tetrazinyl ring. It seems HFI tensor should be anisotropic, at least close to an axial symmetry. But at room temperature the spectra are averaged by fast molecular motion. CW and ESE-detected spectra recorded at liquid nitrogen temperature show notable anisotropy of HF and g-tensor parameters.

In this work verdazyl radicals were studied in a matrix of oriented liquid crystal which confine studied molecules so that an asymmetry of magnetic properties could be revealed.

Two and three pulse ESEEM spectra were recorded showing considerable line shift due to anisotropic ^{14}N HF interaction.

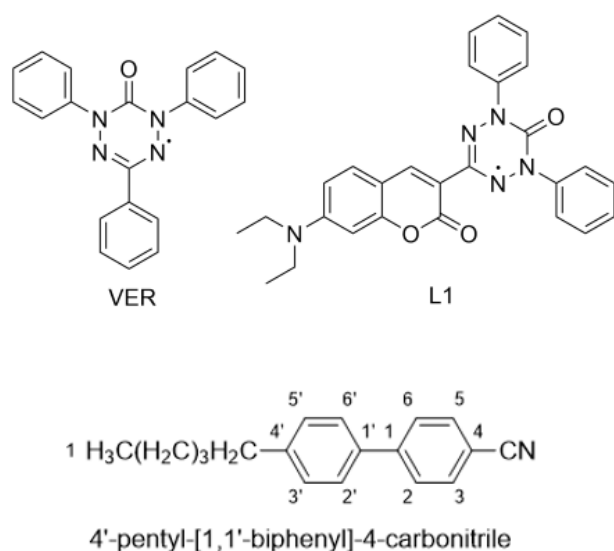


Fig.1. The structures of the studied verdazyl radicals and the structure of the nematic liquid crystal

Catalysts Structure Identification Using DFT-Confirmed NMR Signatures

O.B. Lapina^{1,2}, A.A. Shubin^{1,2}, E. Papulovskiy¹¹Borekov Institute of Catalysis, pr. Lavrentieva, 5, 630090, Novosibirsk, Russian Federation²Novosibirsk State University, Pirogova street, 1, 630090, Novosibirsk, Russian Federation

e-mail: olga@catalysis.ru

Currently, much attention is paid to improving the sensitivity of the NMR method. However, even with a very good sensitivity of the method, the interpretation of the spectra remains a priority. This problem is especially relevant for quadrupole nuclei. The successes achieved in recent decades in the NMR of quadrupole nuclei made it possible to develop NMR crystallography, a method for solving the problems of materials science and catalysis. NMR Crystallography combines state-of-the-art multinuclear Solid-State NMR with DFT computations. This method became a powerful tool for structure determination in biochemistry and in material science. As for catalysts, NMR crystallography has great potential since it could be served not only for characterization of the structure of surface sites, but also for characterization of their catalytic activity. NMR Crystallography is multistage investigation: the first step suggests verification NMR crystallography approach to the systems under study on the example of individual compounds. After that, it is possible to start the next step which consists of identifying NMR parameters of real catalysts by SSNMR experiments.

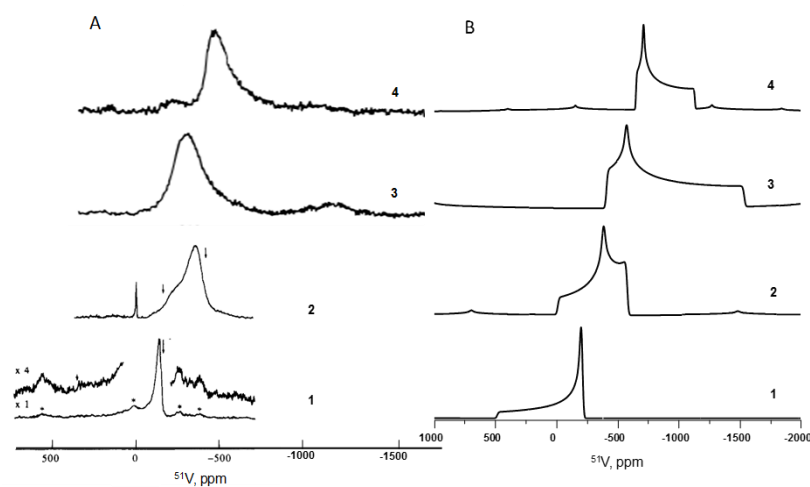


Fig.1. A – experimental static ^{51}V NMR spectra of: 1 – VOCl_3 at 77K, 2 – $\text{VOCl}_3/\text{SiO}_2$, 3 - $\text{VOCl}_3/\text{SiO}_2 + \text{H}_2\text{O}$, 4 – sample 3 after dehydration
B – theoretical static ^{51}V NMR spectra of the following vanadia sites: 1 – solid VOCl_3 , 2 – $\text{VOCl}_2(\text{OSi})$, 3 – $\text{VO}(\text{OSi})_3(\text{H}_2\text{O})$, 4 - $\text{VO}(\text{OSi})_3$.

In this presentation, we offer a lightweight version of the NMR crystallography approach, using as a test not the full set of all NMR parameters, but the NMR signatures of sites. This approach, consisting in the maximum similarity of experimental and theoretical spectra, will be demonstrated using vanadium and niobium catalysts as an example. Fig. 1 shows the experimental and theoretical ^{51}V NMR spectra obtained during the

preparation of vanadium catalysts on silica gel. It can be seen that at each stage there is good agreement between the spectra, although the individual NMR parameters do not prove to be so informative. For example, the use of high magnetic fields in NMR studies is increasingly leading to the characterization of systems based only on the isotropic shift value. However, theoretical calculations can not yet guarantee reliable information about the structure of the center based on the knowledge of only one parameter.

Acknowledgements. Authors thank funding provided via RFBR projects № 17-03-00531 and № 17-53-150018.

**Mechanisms for Life without Water -
High-field EPR studies of protein/matrix interactions**

Möbius K.

Department of Physics, Free University Berlin, Berlin, Germany

e-mail: moebius@physik.fu-berlin.de

All vital activities are dependent on protein polymers when embedded in aqueous environments (the "matrix"). Thus, generally water is an indispensable ingredient of Life. However, certain micro-organisms, plants and animals (no vertebrates) exist which can survive long periods of complete dehydration (*anhydrobiosis*) under high temperatures. In the anhydrobiotic state, their intracellular matrix often contains large amounts of the non-reducing disaccharide sugars, such as trehalose or sucrose. Trehalose is known to be most effective in protecting biostructures from drying to cell death. Until now, the molecular mechanism of this anhydrobiotic biostability in disaccharide matrices is largely unknown. Several hypotheses are discussed in the literature predicting selective changes in the first solvation shell of the protein-water-trehalose system upon dehydration with subsequent changes in the H-bond network. Thus, deciphering how proteins function on the molecular level of protein-matrix interactions is a key to understand life with and without water to survive prolonged periods of drought in the Global Warming Scenario of the looming climate change.

We report on recent results from fast-laser and high-field EPR spectroscopies on light-induced cofactor ion radicals of photosynthetic reaction centers (RCs) in sucrose and trehalose matrices as well as nitroxide spin-probes at different protein concentrations and hydration levels, partly using isotope labeled water (D_2O and $H_2^{17}O$), probing the protein-matrix interactions at various time scales [1, 2]. Our results suggest that the observed biostability originates in the high rigidity of the dry disaccharide glass matrix coating the RC protein surface already at room temperature. The functional impact will be briefly discussed.

This is collaborative work with A. Savitsky, A. Nalepa, W. Lubitz (MPI for Chemical Energy Conversion, Mülheim (Ruhr); M. Malferrari, F. Francia, G. Venturoli (University of Bologna); A. Semenov (Moscow State University).

[1] M. Malferrari, A. Savitsky, W. Lubitz, K. Möbius, G. Venturoli, *J. Phys. Chem. Lett.* **2016**, 7, 2544-2548.

[2] A. Nalepa, M. Malferrari, W. Lubitz, G. Venturoli, K. Möbius, A. Savitsky, *Phys. Chem. Chem. Phys.* **2017**, 19, 28388-28400.

Reactive Molecular-Dynamics Study of Onion-like Carbon Nanoparticle Formation

G.M. Ostroumova^{1,2}, N.D. Orekhov^{1,2}, V.V. Stegailov^{1,2,3}

¹Joint Institute for High Temperatures of the Russian Academy of Sciences, Moscow, Russian Federation

²Moscow Institute of Physics and Technology, Moscow Region, Dolgoprudny, Russian Federation

³National Research University Higher School of Economics, Moscow, Russia

e-mail: g.gulnaz@phystech.edu

Formation of carbon nanoparticles is an important type of complex non-equilibrium processes that require precise atomistic theoretical understanding. MD studies are able to describe separately the mechanisms of formation of nuclei and the mechanisms of their growth. In this work, we consider the process of ultrafast cooling of pure carbon gas from 6000 to 2500 K that results in nucleation of an onion-like fullerene. Modelling of the nucleation process in carbon gas requires an accurate model for atomic interactions that can capture bond formation and dissociation processes as well as different variants of hybridization (sp, sp², sp³). Reactive Force Field (ReaxFF) [1] is among the most widely used reactive models.

All MD calculations are performed using LAMMPS program package

³). In this work we perform fast cooling of carbon gas where temperature changes as the linear function of modelling time from T=6000 K to 2500 K. Temperature is controlled by the Nose-Hoover thermostat. The length of the MD trajectory is 2.5 ns, which gives the cooling rate 1.4 K/ps.

We study the consecutive stages of fullerene-like nanoparticle formation and identify the corresponding temperature ranges.

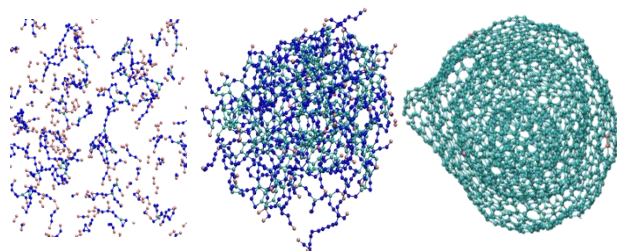


Fig.1. The stages of the fullerene formation

Our results show that the system goes through the stage of a predominantly sp-hybridized low-density polymer gel and then through the stage of a dense sp²-hybridized liquid particle before it transforms into a fullerene-like state during the third stage.

Analysis of hybridization and graphitization reveals the underlying microscopic mechanisms connected with rearrangements of dihedral angles and density changes.

The results of this work have been published recently [3].

[1] Van Duin A. C. T. et al., J. Phys. Chem. (a) **105**, 9396 (2001).

[2] S. Plimpton, J. Comp. Phys., **117**, 1-19 (1995).

[3] G. Ostroumova, Diam. Rel. Mater., **94**, 14-20 (2019).

**On the Theory of Dynamic Heterogeneity of Segments of Linear Macromolecules
Generated by the End Segments: the Frequency Nature of This Effect and Possibility of Its
Experimental Detection Using the Free Induction Decay of Deuterium Nuclei**

I.K. Ostrovskaya, N.F. Fatkullin

Kazan (Volga region) Federal University, Institute of Physics, Kazan, Russia

e-mail: nail.fatkullin@kpfu.ru

It is shown that in melts of linear macromolecules the effect of dynamic heterogeneity produced by the presence of end segments is not vanishing in the limit as $N \rightarrow \infty$, where N is number of Kuhn segments in the macromolecule. The effect is of the frequency nature, i.e. the classification of the segments into the “middle segments” and, the more mobile, “end segments,” largely depends on the time of observations. As the latter increases, the symmetric growth of the “end” section of the polymer chain occurs from both ends of the macromolecule covering the entire macromolecule at times of about the terminal relaxation time. This effect gives rise to nontrivial experimentally observable consequences, e.g. the free induction decay of deuterium nuclei in monodisperse polymer melts of macromolecules must have an extended interval with power law of decay, $g(t) \propto t^{-\beta}$, where $\beta = 1$ for reptation model and $\beta = (\alpha - 2)^{-1}$ for isotropic renormalized Rouse models, where $\alpha > 2$ is the exponent of molecular mass dependence of the terminal relaxation time of macromolecules. When $\alpha \leq 2$, the influence of dynamic heterogeneity effects on the shape of the free induction decay is weaker, although is still experimentally observable if the measurements are sufficiently accurate.

Molecular Mobility and State of n-Hexane Adsorbed in Pillared Montmorillonite Studied by 2D ^1H NMR Relaxometry

A.V. Savinkov¹, A.A. Shinkarev², V.E. Gorelysheva², A.S. Egorova¹

¹Institute of Physics, Kazan Federal University, Kazan, Russian Federation

²Institute of Petroleum, Chemistry and Nanotechnologies, Kazan National Research Technological University, Kazan, Russian Federation

e-mail: andrey.savinkov@gmail.com

The texture characteristics of the catalyst significantly affect the heterogeneous catalytic reactions. Among the catalytic processes that depend on the structure of the porous space, one can distinguish the conversion of hydrocarbons (cracking, isomerization), alkylation, acylation, and others. Investigation of the interaction mechanisms of reagent molecules with the pore surface of the catalyst is an important issue in explaining the catalytic properties of the catalysts.

Layered aluminosilicates belonging to the clay minerals are not catalysts in nature, but the incorporation of cations of the type $[\text{Me}_{13}\text{O}_4(\text{OH})_{24}(\text{H}_2\text{O})_{12}]^{7+}$ (Me = Al, Fe, Zr ...) into the interlayer space of crystalline structure by means of the pillaring process significantly improves their catalytic properties. As a result of the pillaring process, the distance between the silicate layers is stabilized at values of $\sim 0.5\text{--}2$ nm and leads to the appearance of two-dimensional micropore system in the pillared montmorillonite.

The NMR method allows to determine the molecular mobility of a liquid in layered silicates [1], coupling of adsorbed molecules with the crystal lattice of smectites [2] and to determine in details the state and behavior of fluids in clay minerals of various origin [3]. In the present work, the molecular mobility of n-hexane adsorbed in a porous medium of the Al-pillared montmorillonite and the features of the interaction of n-hexane molecules with the surface of the crystalline matrix in pores were studied by two-dimensional NMR relaxometry. In the present work interaction of n-hexane molecules with the surface of the crystalline matrix as well as the molecular mobility of n-hexane adsorbed in a porous medium of the Al-pillared montmorillonite were studied by two-dimensional NMR relaxometry.

It was found that n-hexane is not adsorbed in micropores of pillared montmorillonite at a distance between silicate layers (in the interlayer space) of ~ 0.50 nm, however, n-hexane is adsorbed in micropores if the interlayer distance ~ 0.95 nm. The n-hexane molecules in micropores (interlayer space) are predominantly adsorbed on the basal planes of the crystalline structure. Such n-hexane molecules are characterized by small values of the spin-spin and spin-lattice relaxation times of ^1H nuclei due to significant restrictions on molecular motion. When the weight content of n-hexane in the Al-pillared montmorillonite powder sample exceeds $\sim 10\text{--}11\%$, the filling of macropores in the interparticle space begins. Driven mechanism of ^1H nuclear relaxation of adsorbed n-hexane in porous medium of pillared montmorillonite was defined as relaxation due to paramagnetic impurities.

[1] H.Y. Carr, E.M. Purcell, Phys. Rev. B **94**, 630 (1954).

[2] А.А. Вашман, В.С. Пронин, *Ядерная магнитная релаксация и ее применение в химической физике*. М.: Наука (1979) 234 с.

[3] В.Н. Эрих, *Химия нефти и газа*. Л.: «Химия» (1979), 284 с.

Novel potential Multi-Qubit Systems with Very Rigid Bridging Ligands

Dennis Schäfer¹, Joris van Slageren¹

¹Institute of Physical Chemistry, University of Stuttgart, Pfaffenwaldring 55, D-70569 Stuttgart, Germany

e-mail: dennis.schaefer@ipc.uni-stuttgart.de

As the current semiconductor technology approaches its limits, scientists around the world are looking for solutions to use quantum phenomena for computing purposes. Although theoretically established, a practical application of quantum computing is still very complicated. 2-Qubit-based quantum gates needed to complete the ensemble of universal gates [1] are rare, thus encouraging the hunt for such systems.

To use a multi-qubit quantum gate, the dipolar coupling has to be bigger than a typical operation time (approx. 10 ns). As this directly correlates to the distance between the qubits, long bridging ligands are needed. These should be very rigid, ensuring a spatial and electronic separation of the qubits.

Inspired by the work on photo switches from Belser et al. [2] in the 90's, which incorporate requirements stated above, as well as the recent insights on the potential of nuclear spin-free 1,3-dithiole-2-thione-4,5-dithiolate (dmit) coordination environments [3], this project focused on the synthesis and characterization of EPR active coordination compounds with ligands like **bafcb** and **dmit**₂Ad.

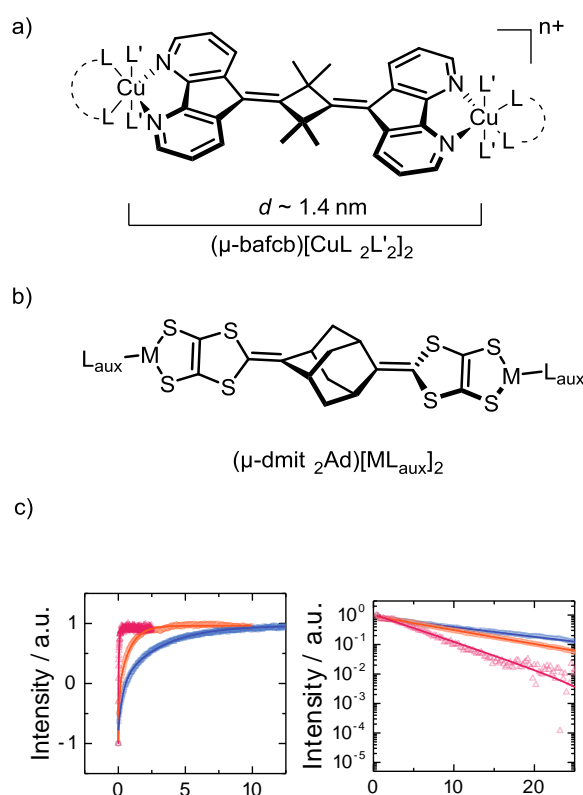


Figure 1. *a*) Cu(II) dimer with **bafcb** as a bridging ligand, *b*) **dmit**₂Ad ligand featuring the well-established **dmit** coordination site, work in progress. *c*) Temperature dependency of T_1 and T_m of *a*) with $L = \text{Cl}$, $L' = \text{Py-d}_5$, $n = 0$ (@ 7K: $T_m = 13.00(5) \mu\text{s}$).

- [1] a) D. P. DiVincenzo, Fortschr. Phys., 2000, 48, 771–783, b) A. Barenco, H. Weinfurter, et al., Phys. Rev. A, 1995, 52, 3457–3467.
 [2] a) P. Belser, V. Balzani, et al., Coord. Chem. Rev., 1999, 190–192, 155–169; b) S. Bernhard, P. Belser, Synthesis (Stuttg.), 1996, 1996(2), 192–194; c) V. Balzani, L. Flamigni, et al., J. Phys. Chem., 1996, 100, 16786–16788.
 [3] a) M. Atzori, E. Morra, et al., J. Am. Chem. Soc., 2016, 138 (35), 11234–11244; b) C.-J. Yu, M. J. Graham, et al., J. Am. Chem. Soc., 2016, 138 (44), 14678–14685.

Scalar Relaxation Effects of the First and Second Kinds in NOESY Spectra of Small Organic Molecules in Liquid

Stanislav I. Selivanov, Siqi Wang, Alexander S. Filatov, Alexander V. Stepanov

Institute of Chemistry, State University of Saint-Petersburg, University prospect 26, 198504, Saint-Petersburg, Russia

e-mail: nmr.group.spbu@gmail.com

Nuclear Overhauser effect (NOE) is very important for structural and conformational analysis of organic molecules in liquid. Experiments on NOE base are one of the main applications of nuclear magnetic resonance (NMR) spectroscopy to elucidation of both the solution state conformation of chemical compounds and internal mobility of their fragments. Intensive usage of NOE is founded on cross-relaxation rate σ_{ij} dependence on internuclear distance r_{ij} and effective correlation time τ_c^{eff} : $\sigma_{ij} \sim \tau_c^{eff}(r_{ij})^{-6}$. Many problems of collections and analysis of NOE data for estimating their information about spatial molecular geometry and conformational flexibility both for macromolecules in spin-diffusion limit ($\omega_0\tau_c > 1$) and small rapidly tumbling molecules in extreme narrowing limit ($\omega_0\tau_c < 1$) were widely discussed [1, 2] during last decades. In case of fast (in NMR time scale) conformational exchange between two or more spatial structures time-dependent conformational fluctuations may lead to dependence of the observed scalar coupling constants J_{H-H} on time. The latter may lead to the appearance of additional inherent contribution of scalar relaxation mechanism of the first kind into cross-relaxation rates between two protons for which NOE values are defined [4]. Separating the contributions of dipole-dipole and scalar relaxation mechanisms into effective cross-relaxation rate σ^{eff} is difficult. Only a few examples of dominant scalar input σ^{sc} over dipole-dipole one σ^{dd} are known [1, 3, 4]. In practice the more common case is scalar relaxation of the second kind which is often observed between vicinal protons in spin-system NH-CH due to quadrupolar relaxation of ^{14}N atom [5].

In this report scalar relaxation effects of the first and second kinds in 2D NOESY and 1D NOE-difference spectra are shown on the examples of two-position fast (in NMR time scale) conformational exchange investigation in some steroid estrogens and in adducts of ninhydrin-derived azomethine ylide with cyclopropenes. The possibilities of quantitative separation of scalar and dipole-dipole inputs to cross-relaxation rate σ^{eff} are discussed.

NMR investigations were performed in the Resource Centers “Magnetic Resonance Research Centre” of the Saint-Petersburg State University. Siqi Wang thanks the China Scholarship Council for its support. The study was carried out under the financial support of the Russian Foundation for Basic Research (grant no. 18-33-00464).

- [1] D. Neuhaus, M.P. Williamson, “*The Nuclear Overhauser Effect in Structural and Conformational Analysis*” (2nd ed.), Wiley-VCH, New York, 2000. 619 P.
- [2] B. Vögeli, *Prog. Nucl. Magn. Reson. Spectrosc.*, 2014, **78**, 1–46.
- [3] S.I. Selivanov, A.G. Shavva, *Russ. J. Bioorg. Chem.*, 2002, **28**(3), 194–208.
- [4] I. Kuprov, D.M. Hodgson, J. Kloesges, C.I. Pearson, B. Odell, T.D.W. Claridge, *Angew. Chem. Int. Ed.*, 2015, **54**(12), 3697–3701.
- [5] N.R. Skrynnikov, S.F. Lienin, R. Brusweiler, R.R. Ernst, *J. Chem. Phys.*, 1998, **108**(18), 7662–7669.

Conformational Analysis of Flexible Molecules in Liquid at Fast Exchange Condition and Population Ratio Determination on Base eNOE Data

Stanislav I. Selivanov, Nikita M. Chernov, Igor P. Yakovlev

Institute of Chemistry, State University of Saint-Petersburg, University prospect 26, 198504, Saint-Petersburg, Russia

e-mail: nmr.group.spbu@gmail.com

The problems of collection and processing of nuclear Overhauser effect (NOE) data and their correct analysis being overcome, the possibility of accurate quantitative determination of interproton distances by 2D NOESY [1, 2] or 1D NOE [3] experiments has appeared. As a result of the development of such methodology, a new term emerged - the **exact nuclear Overhauser effect (eNOE)**, which is understood as a quantitative distance estimation with relative accuracy within $\pm 5\%$ of the actual value [4, 5]. Simultaneously, in case of flexible molecules the same approach was effectively used. Firstly, to determine accurately the ratio of conformers under conditions of fast (in NMR time scale) of conformational exchange. Secondly, to estimate accurately (within 1%) the fraction of the minor conformer (at the level 1–2 %) in which two protons are situated much closer than in case of the dominant form [6, 7]. This possibility of using NOE experiments is especially important for structural and conformational analysis of organic molecules in liquid when there are no other experimental methods for determining the ratio of conformers using (for example, measurements of averaged by fast exchange chemical shifts or scalar constants).

This report presents the results of eNOE application for the quantitative estimation of the ratio of the two conformers in liquid associated with fast in NMR time scale restricted rotation of side substitutions around simple C-C bond in some selected chromone-containing allylmorpholines [8]. To achieve this goal, the cross-relaxation rates for two pairs of protons were measured with high accuracy using volume integration of the corresponding cross-peaks in the NOESY spectra which were recorded for each compound at several mixing times in the interval 0.1 – 1.4 s. Comparison of the experimental data obtained for selected proton pairs with their corresponding calculated values led to a quantitative evaluation of the proportion of the minor conformer with an error $\pm 2\%$ for its population values of about 20%.

NMR investigations were performed in the Resource Centers “Magnetic Resonance Research Centre” of the Saint-Petersburg State University.

- [1] N.H. Andersen, H.L. Eaton, X. Lai, *Magn. Reson. Chem.* 1989, **27**(6), 515–528.
- [2] S.I. Selivanov, A.G. Shavva, *Russ. J. Bioorg. Chem.*, 2002, **28**(3), 194–208.
- [3] K. Stott, J. Keeler, Q.N. Van, A.J. Shaka, *J. Magn. Reson.*, 1997, **125** (2), 302–324.
- [4] B. Vögeli, *Prog. Nucl. Magn. Reson. Spectrosc.*, 2014, **78**, 1–46.
- [5] C.P. Butts, C.R. Jones, E.C. Towers, J.L. Flynn, L. Appleby, N.J. Barron, *Org. Biomol. Chem.*, 2011, **9** (1), 177–184.
- [6] A. Kolmer, L.J. Edwards, I. Kuprov, C.M. Thiele, *J. Magn. Reson.*, 2015, **261**, 101–109.
- [7] C.R. Jones, M.D. Greenhalgh, J.R. Bame, T.J. Simpson, R.J. Cox, J.W. Marshalla, C.P. Butts, *Chem. Commun.*, 2016, **52**(14), 2920–2923.
- [8] N.M. Chernov, R.V. Shutov, O.I. Barygin, M.Y. Dron, G.L. Starova, N.N. Kuz'mich, I.P. Yakovlev, *Eur. J. Org. Chem.*, 2018, **45**, 6304–6313.

Investigation of Octacalcium Phosphate by EPR Methods

D.V. Shurtakova¹, G.V. Mamin¹, M.R. Gafurov¹, S.B. Orlinskii¹, I. Smirnov², A. Fedotov²,
V. Komlev²

¹Institute of Physics, Kazan Federal University, Kazan, Russian Federation

²A.A. Baikov Institute of Metallurgy and Materials Science, Russian Academy of Sciences

e-mail: darja-shurtakva@mail.ru

Synthetic calcium phosphates are commonly used for medical applications including restoring a function of damaged tissues of the body, healing bone defects, treatment fractures and replacement of bones. Also calcium phosphates are involved in formation of atherosclerotic plaques. In both cases, it is necessary to know the exact composition and structure of materials.

In this work, we investigated nanosized particles of octacalcium phosphate (OCP $\text{Ca}_8\text{H}_2(\text{PO}_4)_6 \cdot 5\text{H}_2\text{O}$) by conventional and pulsed EPR methods in X- and W-bands. The EPR spectra were measured after X-ray and gamma irradiation.

The experimental data were fitted simultaneously for both bands using the EasySpin module of MatLab. The obtained parameters were compared with the parameters for the nanosized hydroxyapatite (HAp $\text{Ca}_{10}(\text{PO}_4)_6(\text{OH})_2$) [1].

The EPR spectra of OCP samples are shown in figure 1. Our fitting model supposes the existing of three centers. We assume that nitrogen complexes introduced the samples during the wet chemical reaction by analogy with hydroxyapatite. We also introduced CO_2^- centers, as in the W-band there is an oblong hill with a g-factor of 1.996. For the best fitting, there is a need to introduce an additional unknown center in the model. The nature of this center requires clarification.

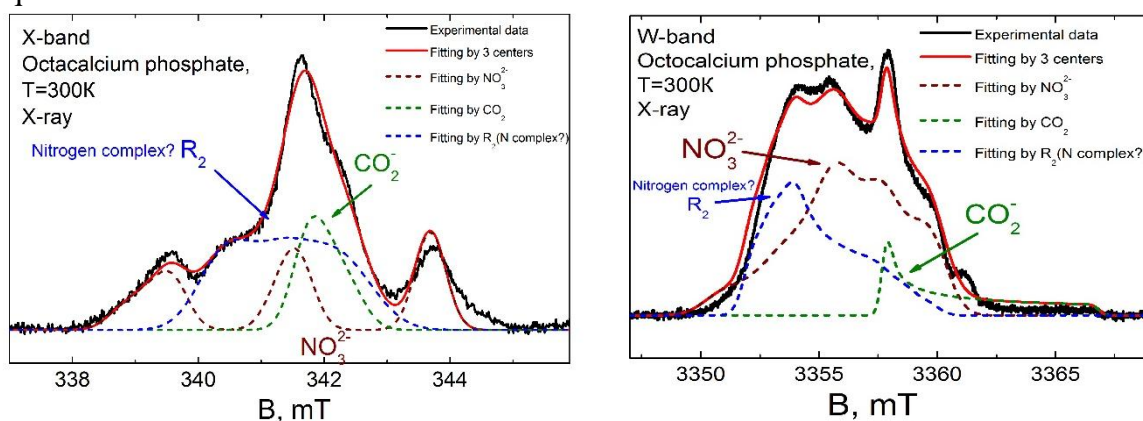


Figure 1 – Fittings of the pulsed EPR spectra of OCP after X-ray in W- and X-bands

The results can be used for the identification of OCP and HAp phases in complex calcium phosphate systems of synthetic and biological origins.

The financial support by RFBR grant 18-29-11086 is acknowledged.

[1] Gafurov, M., et al. Appl Magn Reson 45, 1189 (2014).

Antimicrobial Peptide Chalciporin A in the Model Membrane

Smorygina A.S.,^{1,2} Matveeva A.G.,^{1,2} Syryamina V.N.,^{1,2} Biondi B.,^{3,4} Formaggio F.,^{3,4}
Dzuba S.A.^{1,2}

¹Institute of Chemical Kinetics and Combustion, Novosibirsk, Russia

²Department of Physics, Novosibirsk State University, Novosibirsk, Russia

³Department of Chemical Sciences, University of Padova, Padova, Italy

⁴Institute of Biomolecular Chemistry, Padova Unit, CNR, Padova, Italy

e-mail: anna.smor.mr@gmail.com

After the discovery of antibiotics that saved millions of lives, the rising antimicrobial resistance has become a new problem. The antibiotic resistance results in growing medical costs, longer hospitalizations and increased mortality. An alternative direction of the drug development could be antimicrobial peptides (AMP). These low molecular weight compounds consisting of amino acids are amphiphilic, with hydrophilic and hydrophobic residues. The peptide benefit is in the activity against different pathogens and difficulty in resistance development.

Antimicrobial peptides can destroy the bacterial membrane in various ways. Their interaction with the membrane can be described by the following scheme: binding to the membrane, its perturbation and destruction. Previously, it was believed that antimicrobial peptides act only at high concentrations, forming pores in the membrane. But recently it was found that the antimicrobial activity of peptides is manifested at lower concentrations as well. So, other mechanisms of the peptide are to be proposed. In particular, Alamethicin A (the long peptide) and Trichogin GA IV (the short peptide) were found to redistribute fatty acids in the membrane. This peptide-induced changes in the membrane lateral structure could result to changes in the lipid homeostasis, protein palmitoylation, lateral mobility, that could result to the membrane destabilization and be an alternative way of the peptide antimicrobial activity.

In the framework of the project for the study the influence of AMPs with different length on the lipid membrane properties, the medium-length peptide Chalciporin A was studied here. The Chalciporin A influences on the distribution of stearic acids in the model biological membrane and peptide self-assembling process were investigated by pulse dipolar EPR spectroscopy. The 1-palmitoyl-2-oleoyl-sn-glycero-3-phosphocholine (POPC) lipids were used as constituents of a model membrane, and stearic acid spin-labeled in the 5th carbon position (5-DSA) in these studies modeled fatty acids.

Different distribution of the fatty acids in the membrane was found for peptide-free and peptide-containing model membranes (peptide/lipid=1/200): with Chalciporin A the local fatty acid concentration significantly increases. That indicates on the peptide ability to modify the biological membrane normal functioning via redistribution its components. The lipid component redistribution in the membrane plane could be related with the peptide self-assembling – Chalciporin tends to form local clusters at P/L=1/500.

The work is supported by RSF, grant # №15-15-00021.

Experimental Observation of Hidden Conformations of Strychnine by NMR Spectroscopy

V.V. Sobornova¹, K.V. Belov², S.V. Efimov³, V.V. Klochkov³, I.E. Ereemeev¹, I.A. Khodov^{2,3}

¹ Ivanovo State University of Chemistry and Technology, Ivanovo, Russian Federation

² G.A. Krestov Institute of Solution Chemistry of the RAS, Ivanovo, Russian Federation

³ Institute of Physics, Kazan Federal University, Kazan, Russian Federation

e-mail: iakh@isc-ras.ru

Besides its high toxicity, strychnine possesses a very interesting structure (Figure 1) consisting of several cyclic fragments. Strychnine was first isolated in the beginning of the XIX century. Determination of its chemical structure after the first discovery required more than a century. The molecular structure of this molecule was obtained based on X-ray diffraction, residual dipolar couplings (RDC) and other methods. It seemed that the question of its molecular structure is finally solved; the molecule was regarded as rigid, without any conformational flexibility. However, Schmidt and co-authors [1] showed that the strychnine molecule can have different conformers. They arise due to the flexibility of the ring F. Later this suggestion was proved by Butts et al. [2]. After that another centre of conformational mobility was discovered, attributed to the ring C [3]. Moreover, molecular dynamics simulations allowed suggesting that there is also the third conformer [4].

We were interested in the question of the presence of minor conformers in solutions. In the present work we report on the existence of hidden conformers of the strychnine molecule in a number of solvents, analyse the literature data on molecular simulations, and compare them with an experiment.

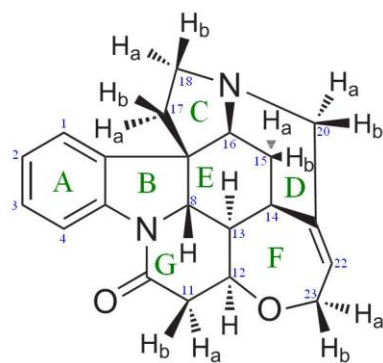


Figure 1. Molecular structure of strychnine

To solve this problem, we applied a complex NMR approach involving one- and two-dimensional methods (¹H, ¹³C, HSQC, NOESY). Nuclear Overhauser effect (NOE) spectroscopy [5, 6] was used to determine the conformer fractions. Thus, information on all hypothetical conformations of the strychnine molecule was obtained; structural peculiarities of the studied object were analysed experimentally, and distribution of the revealed conformations of the molecule in various organic solvents was found. Obtained information and additional calculations will help to shed light on the

mechanisms of formation of hidden strychnine conformers.

- [1] M. Schmidt, F. Reinscheid, H. Sun, H. Abromeit et al., *Eur. J. Org. Chem.*, **6** (2014).
- [2] C. Butts, C. Jones, J. Harvey, *J. Chem. Commun.*, **47** (2011).
- [3] G. Bifulco, R. Riccio, G. Martin, A. Buevich, R. Williamson, *J. Org. Lett.*, **15** (2013).
- [4] G. Tomba, C. Camilloni, M. Vendruscolo, *J. Methods*, **148** (2018).
- [5] I.A. Khodov, S.V. Efimov, M.Y. Nikiforov, V.V. Klochkov, and N. Georgi, *J. Pharm. Sci.*, **103** (2014).
- [6] I.A. Khodov, S.V. Efimov, M.G. Kiselev, L.A.E. Batista De Carvalho, and V.V. Klochkov, *J. Mol. Struct.*, **1113** (2016).

Ionic and Molecular Transport in Synthetic and Biological Membranes Studied by NMR

Vitaly I. Volkov

Institute of Problems of Chemical Physics RAS Acad. N.N.Semenov av., 1142432,
Chernogolovka, Russia

e-mail: vitwolf@mail.ru

The interconnection of cation hydration, water and ionic translational mobility has been investigated in Nafion membrane and based on polyethylene and grafted sulfonated polystyrene MSC membranes [1-3]. The main particularities of sulfonate groups hydration, water molecule and alkaline metal cation translational mobility and ionic conductivity were revealed by high resolution NMR, pulsed field gradient NMR and impedance spectroscopy techniques. It was determined that at low water content counter ion H^+ forms hydroxonium ion $H_3O_2^+$, but with humidity increasing cation $H_9O_4^+$ is also arisen. The hydration numbers are 4, 6 and 3 for Li^+ , Na^+ and Cs^+ correspondingly [2]. Self-diffusion coefficients of water molecules and cation Li^+ , Na^+ , Cs^+ (for the first time in ion-exchangers) were measured directly by pulsed field gradient NMR on 1H , 7Li , ^{23}Na , ^{133}Cs nuclei. The conductivity values are the next row $Li^+ < Na^+ < Cs^+ < H^+$, which is agreed with self-diffusion data [1].

The self-diffusion of water and lipids in water-mouse RBCs suspension were investigated. The intracellular water restriction size ($2.1 \mu m$), erythrocyte water permeability (about $10^{-5} m/s$), intracellular residence time (about 20 ms), water permeability activation energy ($24.1 \pm 1.9 kJ/mol$) were calculated. The lipid self-diffusion coefficients are varied from $3 \cdot 10^{-12} m^2/s$ to $10^{-11} m^2/s$ depending on temperature and diffusion time. The lipid lateral self-diffusion activation energy is about $25 \pm 2.9 kJ/mol$ [4].

Self-diffusion of water-soluble fullerene derivative $C_{60}[S(CH_2)_3SO_3Na]_5H$ was characterized. It was found that a fraction of the fullerene molecules ($\sim 13\%$ of the fullerene derivative added in aqueous RBC suspension) shows a self-diffusion coefficient of $5.5 \pm 0.8 \cdot 10^{-12} m^2/s$, which is close to the coefficient of lateral diffusion of lipids in the erythrocyte membrane ($D_L = 7 \cdot 10^{-12} m^2/s$). This experimental finding evidences the absorption of the fullerene derivative by RBC. Fullerene derivative molecules are also absorbed by RBC ghosts and phosphatidylcholine liposomes as manifested in self-diffusion coefficients of $(7.9 \pm 1.19) \cdot 10^{-12} m^2/s$ and $(7.7 \pm 1.16) \cdot 10^{-12} m^2/s$, respectively. The fullerene self-diffusion shows unrestricted behavior as compared to the restricted lateral self-diffusion of lipids. Therefore, the fullerene derivative molecules are, probably, fixed on the RBC surface. The average residence time of the fullerene derivative molecule on RBC is about $438 \pm 65 ms$ [5].

This work was supported by Russian Foundation for Basic Research (projects No. 18-08-00423 A).

- [1] Vitaly Volkov, Alexander Chernyak, Olga Yarmolenko, Vladimir Tverskoi, Daniil Golubenko, Proc.Int. Conf. Ion transport in organic and inorganic membranes, 356, 20–25 May, Sochi (2019).
- [2] V.I. Volkov, A.A. Marinin, Russian Chemical Reviews 82 (3) 248 - 272 (2013).
- [3] A.V. Chernyak, S.V. Vasil'ev, I.A. Avilova, V.I. Volkov, Appl. Magn. Res. 50, 577 (2019).
- [4] I.A. Avilova, A.V. Smolina, A.I. Kotelnikov, R.A. Kotelnikova, V.I. Volkov, V.V. Loskutov, Appl. Magn. Res. 47, 335 (2016).
- [5] Avilova I.A., Khakina E.A., Kraevaya O.A., Kotelnikov A.I., Kotelnikova R.A., Troshin P.A., Volkov V.I., BBA – Biomembranes. 1860, 1537 (2018).

Application of Experimental and Computational EPR Spectroscopy to Radical Systems

M. Witwicki¹, J. Jeziarska¹, A. Ozarowski²

¹Faculty of Chemistry, University of Wrocław, ul. Joliot-Curie 14, 50-383 Wrocław, Poland

²Magnetic Field Laboratory, Florida State University, 1800 East Paul Dirac Drive, Tallahassee, FL 32310, USA

e-mail: maciej.witwicki@chem.uni.wroc.pl

Electron paramagnetic resonance (EPR) spectroscopy has turned out to be indispensable in studies of radical systems [1]. However, the analysis of experimental EPR spectra is not always straightforward. Modern computational techniques can provide EPR parameters (g tensor, hyperfine coupling constants and zero field splitting) with an accuracy sufficient for a meaningful comparison with their experimental counterparts and thus they can support or verify conclusions derived from experiments, link spectral features to the structural properties or provide additional information that is not experimentally accessible [2]. Herein we present

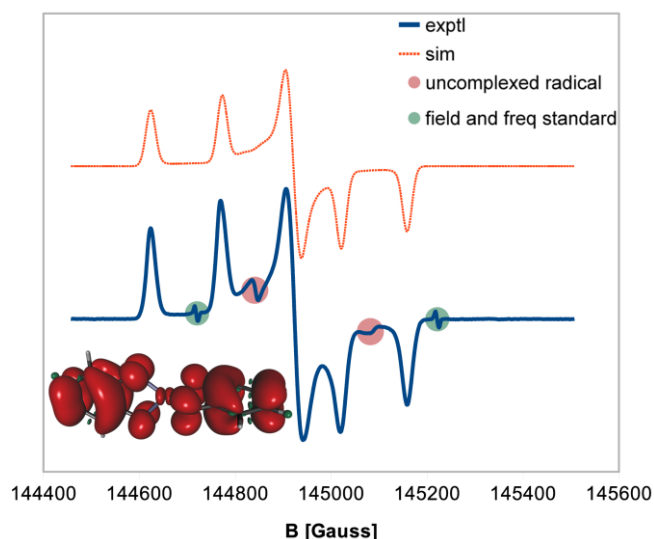


Fig. 1. EPR spectrum of biradical $Zn(sq)_2$ complex recorded at 406 GHz along with spin density for the $S = 1$ state.

a joint experimental and computational investigation of phosphinyl and semiquinone radicals. Effects of substitution, hydrogen bonding and coordination of metal ions on EPR properties are analyzed. In the case of semiquinones it is demonstrated how this approach can be used to solve environmental problems, namely how to identify radicals generated in the soil by its contamination with heavy metal ions. In this work X-, Q-band and high-field/high-frequency EPR (exemplified in Fig. 1) as well as density functional theory (DFT) and *ab initio* methods were employed.

Acknowledgement. This work was financially supported by the National Science Centre (NCN, grant no.

2018/02/X/ST5/01186). The computations were performed using computers of the Wrocław Centre for Networking and Supercomputing (grant no. 47). A part of this work was accomplished at the NHMFL, which is funded by the NSF through the cooperative agreement No. DMR-1157490 and the State of Florida.

[1] Electron Paramagnetic Resonance. Elementary Theory and Practical Applications, J.A. Weil and J.R. Bolton, Wiley-Interscience, Hoboken, (2007).

[2] Calculation of NMR and EPR Parameters, M. Kaupp, M. Bühl, V.G. Malkin, Wiley-VCH, Weinheim, (2004).

Application of *in situ* EPR Spectroelectrochemistry for Generation, Observation and Activation of High Reactive Mono-, Bi- and Polynuclear Complexes

D.G. Yakhvarov^{1,2}, A.F. Khusnuriyalova^{1,2}, A. Petr³, B. Büchner³, V. Kataev³, V.I. Morozov¹, Z.N. Gafurov¹, G. Giambastiani⁴, L. Lukoni⁴, O.G. Sinyashin¹

¹Arbuzov Institute of Organic and Physical Chemistry of FRC Kazan Scientific Center of RAS, Kazan, Russian Federation

²Alexander Butlerov Institute of Chemistry, Kazan Federal University, Kazan, Russian Federation

³Leibniz Institute for Solid State and Material Research, Dresden, Germany

⁴Institute of Chemistry of Organometallic Compounds, Florence, Italy

e-mail: yakhvar@iopc.ru

The creation and design of new molecules and materials bearing unique electrochemical, magnetic and catalytic properties are one of key research priorities of modern synthetic chemistry. The combination of electrochemical techniques and coordination chemistry can be considered as a new powerful tool in preparation and investigation of new types of mono-, bi- and polynuclear complexes, metal-organic frameworks (MOFs) and nanosized material bearing practically useful electrochemical, magnetic and catalytic properties. Transition metal complexes containing two or more interconnected metal coordination centers are of high practical interest for different areas of applied chemistry, molecular biology and pharmacology [1]. In the same time, the investigation of the structure and electronic properties of organonickel sigma-bonded complexes, which are characterized as high reactive intermediates of various catalytic and electrocatalytic reactions, is very important from the view point of the creation of new types of the efficient and ecologically friendly “green” catalytic systems for various applications [2].

Herein, we present our results obtained by using of the electrochemical technique, such as *in situ* EPR spectroelectrochemistry for generation, activation and investigation of the properties of various types of organonickel complexes bearing Ni-C sigma-bond [3] and formed by unsymmetrical pincer-type ligands [4], magnetically active binuclear nickel [5] and cobalt [6] complexes. Recent application of the electrochemical methods involves generation and *in situ* observation of superparamagnetic cobalt, nickel and iron nanoparticles [7].

Financial support from the Russian Science Foundation (project no. 18-13-00442) is gratefully acknowledged.

- [1] M. O’Keeffe, O.M. Yaghi, Chem. Rev. **112**, 675 (2012).
[2] D.G. Yakhvarov, A.F. Khusnuriyalova, O.G. Sinyashin, Organometallics **33**, 4574 (2014).
[3] D.G. Yakhvarov, A. Petr, V. Kataev, B. Büchner, S. Gómez-Ruiz, E. Hey-Hawkins, S.V. Kvashennikova, Yu.S. Ganushevich, V.I. Morozov, O.G. Sinyashin, J. Organomet. Chem. **750**, 59 (2014).
[4] L. Luconi, C. Garino, P.C. Vioglio, R. Gobetto, M.R. Chierotti, D. Yakhvarov, Z.N. Gafurov, V. Morozov, I. Sakhapov, A. Rossin, G. Giambastiani, ACS Omega **4**, 1118 (2019).
[5] D. Yakhvarov, E. Trofimova, O. Sinyashin, O. Kataeva, P. Lönnecke, E. Hey-Hawkins, A. Petr, Yu. Krupskaya, V. Kataev, R. Klingeler, B. Büchner, Inorg. Chem. **50**, 4553 (2011).
[6] D.G. Yakhvarov, E.A. Trofimova, A.B. Dobrynin, T.P. Gerasimova, S.A. Katsyuba, O.G. Sinyashin, Mendeleev Commun. **25**, 27 (2015).
[7] A.F. Khusnuriyalova, A. Petr, A.T. Gubaidullin, A.V. Sukhov, V.I. Morozov, B. Büchner, V. Kataev, O.G. Sinyashin, D.G. Yakhvarov, Electrochim. Acta. **260**, 324 (2018).

ENDOR and DFT Studies of the Cu(II)-bis(oxamato) Complex

R.B. Zaripov¹, S. Avdoshenko², I.T. Khairuzhdinov¹, K.M. Salikhov¹, V.K. Voronkova¹,
S. Weheabby³, T. Ruffer³, A. Popov², B. Büchner^{2,4}, V. Kataev⁴

¹ Zavoisky Physical–Technical Institute, FRC Kazan Scientific Center of RAS, Kazan, Russia

² Leibniz Institute for Solid State and Materials Research IFW Dresden, Dresden, Germany

³ Technische Universität Chemnitz, Fakultät für Naturwissenschaften, Institut für Chemie, Chemnitz, Germany

⁴ Institut für Festkörperphysik, Technische Universität Dresden, Dresden, Germany

e-mail: zaripov.ruslan@gmail.com

Advanced pulse ESR techniques are useful tools to determine hyperfine (HF) and quadrupole (Q) tensors of the paramagnetic transition metal complexes. The knowledge of these tensors is essential for the estimation of the spin density distribution around the paramagnetic center and for the assessment of magnetic exchange pathways in polynuclear molecular networks [1]. In this work, we report the effect of structural “host-guest” interaction which we observed by studying Cu(II)-(bis)oxamate molecules of [nBu4N]2[Cu(opba)] (opba = o-phenylene-bis(oxamato)) hosted by the diamagnetic single crystal [nBu4N]2[Ni(opba)] matrix with advanced pulse ESR methods at X - band frequencies [2,3].

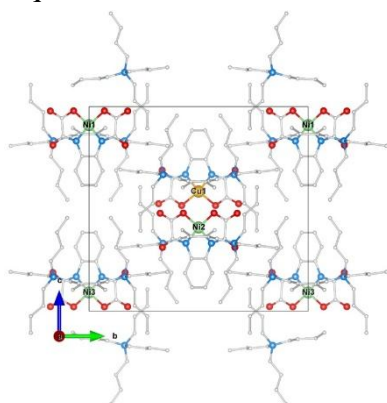


Fig.1 a/b/c projection of VASP optimized Cu1 in Ni-polymorphs matrix

Though this effect cannot be seen in the ESR spectra due to an insufficient resolution of the transferred HF coupling, it should be seriously considered for a correct interpretation of high resolution ENDOR spectra and consequently for an accurate determination of the HF and Q tensors.

The authors acknowledge support from Presidium RAS Program No. 5: Photonic technologies in probing inhomogeneous media and biological objects.

[1] A. Aliabadi et al., *J. Phys. Chem. B* **119**, 13762 (2015).

[2] M.A. Abdulmalic et al., *Dalton Trans.* **44**, 8062 (2015).

[3] B. Bräuer et al., *Inorg. Chem.* **47**, 6633 (2008).

EPR and Beer - a Good Combination!

Mogens L. Andersen

Department of Food Science, University of Copenhagen, Rolighedsvej 26, DK-1958
Frederiksberg C, Denmark.

e-mail: mola@food.ku.dk

Beer is sensitive to oxygen and different beer ageing phenomena such as haze formation, flavor changes, and light sensitivity involves oxidatively generated radicals as central intermediates. Electron paramagnetic resonance spectroscopy (EPR) has made it possible to unravel the mechanistic interconnections between these deteriorating mechanisms based depends on delicate interactions between compounds with prooxidant and antioxidant properties. EPR-based methods have been found useful for not only evaluating the effects of oxidation on the final beer but also during different stages of the processes during malt production and in the brew house. As an example, recent EPR studies have shown that peptides have a major effect on the extraction of copper, a suggested prooxidative metal, during the initial stages of brewing.

Whole Body Sodium MRI at 0.5 Tesla

N.V. Anisimov, E.G. Sadykhov, O.S. Pavlova, D.V. Fomina, A.A. Tarasova, Yu.A. Pirogov

Lomonosov Moscow State University, Moscow, Russian Federation

e-mail: anisimovnv@mail.ru

Experiments on sodium (^{23}Na) MRI, including the construction of MRI of the whole human body (WB) from head to toe, are described. The studies were performed on a clinical 0.5T scanner Bruker Tomikon S50 which was designed primarily for recording ^1H signals (21.1 MHz). ^{23}Na MRI provides diagnostic information, since sodium is actively involved in cellular processes [1]. It is believed that progress in ^{23}Na MRI is possible only with the use of strong magnetic fields – from 3T and above. However, for open-type magnets and compact magnetic systems under development, it is still difficult to achieve fields greater than 1T [2]. Therefore, it is of interest to identify possibilities of ^{23}Na MRI for weak fields – less than 1T.

The gyromagnetic ratio for ^{23}Na is 3.8 times less than for a proton, and the sodium content in living tissues is about $2 \cdot 10^3$ times less than that of hydrogen. This imposes high demands on the sensitivity of the ^{23}Na MRI equipment. To increase the signal-to-noise ratio (SNR), the sampling rate (BW) defining the receiver bandwidth was set as small as possible $\sim 10^3$ Hz [3]. This, in turn, determined the use of a large echo time (TE) in the scanning pulse sequence. The research strategy assumed a minimal modification of the scanner. Therefore, only simple transceiver probehead was made — 20-cm square-shaped frame coil (4 turns) tuned to the Larmor frequency of ^{23}Na (5.6 MHz). Scanning was performed using the gradient echo method with TR/TE=44.7/12 ms, FA=46° (5 ms rectangular pulse), BW=2.87 kHz, echo position was 0.25. In-plane resolution was 6.6×6.6 mm², data matrix was $N \times N$, where $N=80$. There was no slice selection. To increase the SNR about 4 times, for data of the K space, exponential apodization was applied: $K_A(i,j)=K(i,j) \cdot \exp(-(|i-i_0|-|j-j_0|)/kN)$, where $i,j=1 \div N$ – coordinates of the K-space, i_0, j_0 – echo position. For our case, $i_0=20$, $j_0=40$, $k=0.1$. Custom written software was used. As a result, images were obtained, in which human organs are represented with the SNR up to 30. The sensitivity zone of the coil is about 20 cm. Therefore, to assemble the WB ^{23}Na MRI, 9 separate body segments in prone and supine positions were scanned. The scan time of one body segment was 30 min. Fig. 1 shows the sum of the WB ^{23}Na MR images (40×170 cm²) obtained in prone and supine positions for a healthy volunteer – a 28-year-old male.

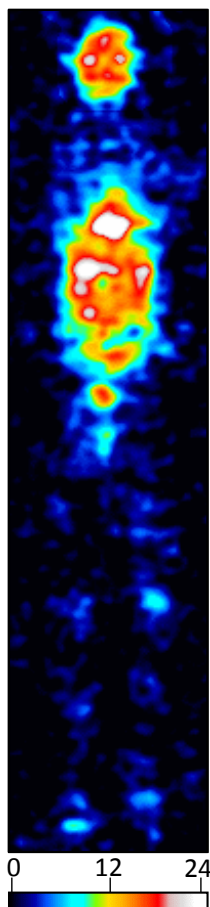


Fig.1. The sum of the WB ^{23}Na MR images obtained in prone and supine positions.

The distribution of contrast for different organs and tissues, in general, corresponds to that obtained at 3T [4]. There are significant reserves to increase sensitivity and reduce scan time – the replacement of the frame coil by the volume coil. Then it is possible to increase the informativeness of the study by performing a slice selective scan, as well as applying pulse sequences with a short TE.

- [1] G. Madelin, et al., Prog. Nucl. Mag. Res. Sp. **79**, 14, (2014).
- [2] C.Z. Cooley, et al., IEEE Trans. Mag. **54**(1),5100112, (2018).
- [3] N.V. Anisimov, et al., Appl. Mag. Res. (2019) (in printing).
- [4] F. Wetterling, et al., Phys. Med. Biol. **57**(14), 4555, (2012).

Fast Macromolecular Proton Fraction Mapping at 0.5 Tesla

N.V. Anisimov¹, O.S. Pavlova¹, V.L. Yarnykh²

¹Lomonosov Moscow State University, Moscow, Russian Federation

²University of Washington, Seattle, USA

e-mail: anisimovnv@mail.ru

The effect of the magnetization transfer (MT) caused by cross-relaxation between the protons of water and macromolecules is widely used in MRI to modify tissue contrast. Of interest are maps of macromolecular proton fraction (MPF), especially for detecting brain pathologies. To calculate the MPF map, one needs to build maps: T_1 and proton density (PD) and analyze the MT-weighted images (MT-WI). To obtain the last ones, MT saturation pulse (RF pulse with a large detuning $\Delta - 10^2 \div 10^4$ Hz) is entered at the beginning of the scanning pulse sequence. While the conventional analysis of MT-WI requires at least three samples [1], the single-point method [2] provides accurate MPF maps from one sample, if the amplitude of the MT-pulse and Δ are set optimal. In this case, to build MPF map, it is sufficient to perform only three scans: two of them are needed to build a T_1 and PD maps, and one more - to obtain MT-WI.

So far, fast MPF mapping has been implemented only at high magnetic fields (≥ 1.5 T). We present the first implementation of this method in low-field MRI. A 0.5T clinical scanner Bruker Tomikon S50 was used for this. It is equipped with a 2 kW transmitter LPPA 2120 and a 16.86 mT/m gradient system (0.5 ms rise time). The 3D spoiled gradient echo method was used with TR/TE=30/5 ms and voxel size of $1 \times 1 \times 1.3$ mm³. The total study time was 22 min. To construct T_1 and PD maps, variable flip angle (VFA) method was used, for which the FA was set to 30° and 5° (1 ms pulse). To obtain an MT-WI we set FA=10°. Spoiling gradient area was 14 mT·ms/m. 8 ms MT-pulse had a Gaussian shape. Its parameters ($\Delta=1.5$ kHz, FA=600°) were in accordance with the recommendations of studies [2,3]. T_1 , PD and MPF maps were calculated using custom-written software. Fig. 1 shows the results of study for a 22-years old female. It was found that MPF values for different brain structures are close to those obtained in stronger fields. In particular, it concerns the average values for the white and gray matter of the brain -14.2 and 7.5, respectively.

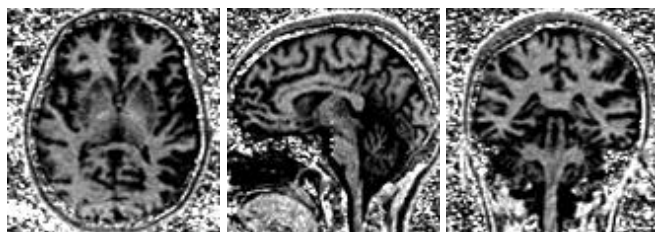


Fig. 1. MPF map of the human brain in orthogonal projections.

In additional proof-of-concept experiment we obtained MPF maps of the rat brain with a similar technique – Fig. 2. For this purpose, a 3 cm (3 turns) ring receive coil was made. The scans were performed with the above parameters with resolution $0.25 \times 0.25 \times 1$ mm³. Eight signal averages were applied with the total study time of about 1.5 hour. According to preliminary data, the values of MPF in white and gray matter structures were close to those reported for ultra-high field measurements [3].

In summary, this study proves the independence of MPF on magnetic field strength, since quantitative MPF estimates obtained using a low-field scanner (0.5T) are close to those reported for high-field machines (from 3T to 11.7T). The possibility of fast MPF mapping for low field allows us to hope that the method will also be applicable to open-type magnets and compact portable magnetic systems.



Fig. 2. MPF map of the rat brain.

- [1] V.L. Yarnykh, *Magn. Reson. Med.* **47**, 929 (2002).
- [2] V.L. Yarnykh, *Magn. Reson. Med.* **68**, 166 (2012).
- [3] A.V. Naumova, et al. *Neuroimage* **147**, 985 (2017).

DNA and RNA Complexes with Human Proteins : Structural Insights revealed by Pulsed Dipolar EPR with Orthogonal Spin Labeling

Elena G. Bagryanskaya^{1,2}, Olesya A. Krumkacheva,^{1,2,3} Georgiy Shevelev,^{2,4} Alexander Lomzov,^{2,4} Nadezhda Dyrkheeva,⁴ Andrey A. Kuzhelev,^{1,2,3} Victor M. Tormyshev,^{1,2} Yuliya Polienko,^{1,2} Matvey Fedin,^{2,3} Dmitrii Pyshnyi,^{2,4} Olga Lavrik^{2,4}, Alexey Chubarov^{2,4}, Tatiana, Godovikova^{2,4}

¹N. N. Vorozhtsov Novosibirsk Institute of Organic Chemistry SB RAS, Pr. Lavrentieva 9, Novosibirsk 630090, Russia;

²Novosibirsk State University, Pirogova Str. 2, Novosibirsk 630090, Russia;

³International Tomography Center SB RAS, Institutskaya Str. 3a, Novosibirsk 630090, Russia;

⁴Institute of Chemical Biology and Fundamental Medicine SB RAS, Pr. Lavrentieva 8, Novosibirsk 630090, Russia

e-mail: egbagryanskaya@nioch.nsc.ru

Pulsed dipolar (PD) EPR techniques are based on the measurement of a magnetic dipole–dipole interaction between two spin labels by means of microwave pulses. Various approaches of PD EPR are actively used, in particular pulsed electron double resonance (PELDOR or DEER) and double quantum coherence (DQC). Trityl radicals or TAMs have appeared recently as an alternative source of spin labels for measuring long distances in biological systems [1]. In this presentation we overview our recent results on PD EPR study of DNA and RNA complexes with human proteins and discuss the advantages of spin labels based on TAM radicals using several examples [2-4].

We applied pulse dipolar electron paramagnetic resonance (EPR) spectroscopy in combination with molecular dynamics (MD) simulations to investigate in-depth the conformational changes in DNA containing an apurinic/aprimidinic sites (abasic or AP sites) and in a complex of this DNA with AP endonuclease 1 (APE1) [2]. The use of different (orthogonal) spin labels in the enzyme and in the DNA substrate has a crucial advantage allowing for detailed investigation of local damage and conformational changes in AP-DNA alone and in its complex with APE1 [2]. New spin labels based on the very hydrophilic OX063 with very-low toxicity and little tendency for aggregation was tested on human serum albumin (HSA) as one of the most abundant protein in blood plasma. [3] Development of C₆₀-based label for dipolar EPR spectroscopy using model covalent pairs of C₆₀ with trityl (C₆₀-TAM) radicals having long phase relaxation time up to room temperature [4].

Acknowledgments. This work was supported by the Ministry of Science and Education of the Russian Federation (grant No. 14.W03.31.0034) and Russian Science Foundation for Basic Research (grant No.18-04-00393).

[1] O. Krumkacheva, E. Bagryanskaya, Trityl radicals as spin labels, From the book: Electron Paramagnetic Resonance: Volume 25, 2016, 25, 35-60.

[2] O.A. Krumkacheva, et al. NAR, 2019, accepted.

[3] V.M. Tormyshev, et al. Chem. Eur. Jour. 2019, submitted.

[4] O.A. Krumkacheva, et al. Angewante Chemie, 2019, submitted.

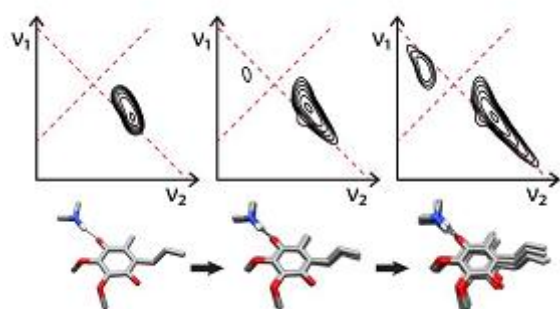
Influence of Hyperfine Coupling Strain on Two-Dimensional ESEEM Spectra from $I=1/2$ Nuclei

Sergei A. Dikanov

University of Illinois, Urbana, 61801, U.S.A.

e-mail: dikanov@illinois.edu

Hydrogen bonding between semiquinone (SQ) intermediates and sidechain or backbone nitrogens in protein quinone processing sites (Q-sites) is a common motif. Substantial progress has been achieved in the characterization of Q-sites in the SQ state using two-dimensional (2D) ESEEM, particularly its most popular 4-pulse version called HYSCORE. Uniform or selective ^{15}N (nuclear spin $I = 1/2$) protein labeling has been widely used in these



experiments. Previous studies on SQs from multiple protein environments have reported specific features in the ^{15}N HYSCORE spectra not reproducible by a theory based on fixed hyperfine (hfi) parameters, and the source of these lineshape distortions remained unknown. In this work, using the ^{15}N spectra of the SQ in the Q-sites of wild-type and mutant D75H cytochrome bo_3 ubiquinol oxidase from *E. coli*, we have explained the observed additional features as originating from a -strain of the isotropic hfi

coupling. In 2D spectra the a -strain manifests as well-resolved lineshape distortions of the basic cross-ridges and accompanying lines of low intensity in the opposite quadrant that allow its direct analysis (see figure). We have shown that their appearance is regulated by the relative values of the strain width Δa and parameter $\delta = |2a+T| - 4v_{15\text{N}}$. a -strain provides a direct measure of the structural dynamics and heterogeneity of the O...H...N bond in the SQ systems. The experimental spectra provide direct quantitative information about the strain of the hfi coupling reflecting geometric fluctuations in the corresponding structures. Potentially one can expect the a -strain effects from any $I = 1/2$ spin; typical of them are ^1H , ^{13}C , ^{15}N , ^{19}F , ^{29}Si and ^{31}P . Considering the properties of powder type X-band 2D spectra, the strain effects are most probable to be observed for ^{13}C , ^{29}Si and ^{31}P in addition to ^{15}N , because it requires nuclei with moderate isotropic couplings of 5-10 MHz to satisfy the condition $|2a+T| \sim 4v_1$. However, by employing the multifrequency approach one can expand the range of hfi couplings suitable for observation of the a -strain effects to lower and/or higher values.

In-cell EPR Spectroscopy

Malte Drescher

Department of Chemistry and Konstanz Research School Chemical Biology,
University of Konstanz, Konstanz, Germany

e-mail: malte.drescher@uni-konstanz.de

One of the most exciting and most challenging tasks in Chemical Biology is the development and application of methods enabling to unravel protein structure and dynamics in the native environment, i.e. within the cell. In general, in cell EPR spectroscopy in combination with site-directed spin labelling has emerged as a valuable tool in this context because it is virtually background free and provides important structural information, e.g. distance restraints.

Many in-cell EPR experiments and some of the examples presented here [1], too, rely on the delivery of spin-labeled protein to the cell, e.g. by microinjection or permeabilization of the membrane via osmotic shock or electroporation.

On the other hand, several bio-orthogonal labelling strategies are suited for in vivo labelling. These strategies are based on the incorporation of genetically encoded non-canonical amino acids: We identified the non-canonical amino acid pENF as suitable choice for bio-orthogonal spin labeling via click chemistry [2]. As an alternative, we developed and synthesized a nitroxide-based spin label that can be ligated to proteins by an inverse-electron-demand Diels-Alder (DA_{inv}) cycloaddition to genetically encoded noncanonical amino acids. The nitroxide moiety is shielded by a photoremovable protecting group with an attached tetraethylene glycol unit to achieve water solubility of this PaNDA (Photoactivatable Nitroxide for DA_{inv} reaction) label [3].

However, by now, even in cases with confirmed in vivo labeling, purification and concentration of spin-labeled protein was required prior to distance determination. Here, we report for the first time on the combination of in vivo bio-orthogonal spin labeling by click chemistry and direct in cell DEER distance determination without any purification step. The combination of bio-orthogonal labeling with in-cell DEER measurements does not require additional delivery steps of spin-labeled protein to the cells. We expressed eGFP in E.coli and use copper-catalyzed azide-alkyne cycloaddition (CuAAC) for the site-directed spin labeling of the protein in vivo, followed by in-cell EPR distance determination. Intracellular distance measurements of in vivo spin-labeled eGFP are in agreement with in vitro measurements and with calculations based on the rotamer library of the spin label [4].

[1] J. Cattani et al., *Phys. Chem. Chem. Phys.* **19**, 18147 (2017).

[2] P. Widder et al., *ACS Chem. Biol.* **14**, 839 (2019).

[3] A. Kugele et al., *ChemBioChem*, DOI: 10.1002/cbic.201900318 (2019).

[4] P. Widder et al, *ChemRxiv*, DOI:10.26434/chemrxiv.9746222.v1 (2019).

Lipid-Mediated Clustering in Biological Membranes by Spin-Label EPR

Sergei Dzuba

Institute of Chemical Kinetics and Combustion, Russian Academy of Sciences, 630090
Novosibirsk, Russia, and
Department of Physics, Novosibirsk State University, 630090, Novosibirsk, Russia

e-mail: dzuba@kinetics.nsc.ru

Developing methods for quantifying membrane heterogeneities is a challenging task because of their transient nature and small size. Recently, evidences were obtained that transient membrane heterogeneities can be frozen at cryogenic temperatures. This allows application of solid-state pulsed EPR techniques, such as electron spin echo (ESE), pulsed double electron-electron resonance (PELDOR or DEER), ESE envelope modulation (ESEEM). These techniques are sensitive to the nanoscale distance range between spin-labeled molecules.

We studied model membranes – lipid bilayers, which were prepared from different kinds of lipids, including their saturated and unsaturated types, and cholesterol (Chol). The spin-labeled substances were 5(16)-doxyl-stearic-acid (DSA), which mimics behavior of fatty acids, 3 β -doxyl-5 α -cholestane (d-chlstn, the spin-labeled Chol analog), spin-labeled lipids and spin-labeled peptides (synthesized by Prof. Formaggio and coworkers); these peptides are known for their antimicrobial action.

The found local concentration of DSA and d-chlstn molecules was remarkably higher than the mean concentration in the bilayer, evidencing the formation of lipid-mediated clusters of these molecules. Spin-labeled stearic acids were found to form two-dimensional molecular clusters while d-chlstn molecules are clustered into stacked one-dimensional structures. Clustering of d-chlstn was found to be different for the bilayers comprised from saturated or unsaturated phospholipids: in the former case, the data were explained by encapsulation of d-chlstn molecules in lipid shells so preventing them to approach each other closer than some distance, R_{min} , which was found to vary between ~ 2.5 nm and 5 nm.

Antimicrobial action of peptides in bacterial membranes is commonly related to their self-assembling which results in pore formation. PELDOR technique highlighted the onset of oligomerization of spin-labeled peptides. ESEEM technique for D₂O-hydrated bilayers shows that oligomerization is accompanied by peptide re-orientation towards a *trans*-membrane disposition. For the spin-labeled stearic acids embedded, the study of concentration dependence of ESE decays and of ESEEM in presence of a deuterated peptide analog indicates that the stearic acids molecules are attracted by peptide molecules, forming nanoclusters. Such capturing action on the fatty acids may represent an additional mechanism of the peptide antibiotic activity.

A Bifunctional Spin Label for Ligand Recognition on Surfaces

A.J. Fielding¹, M.A. Hollas², S.J. Webb³, S.L. Flitsch³

¹ Pharmacy and Biomolecular Science, Liverpool John Moores University, James Parsons Building, Byrom Street, Liverpool, L3 3AF, UK

² Department of Chemistry, Photon Science Institute, University of Manchester, Oxford Road, Manchester, M13 9PL, UK

³ Department of Chemistry, Manchester Institute of Biotechnology, University of Manchester, 131 Princess Street, Manchester, M1 7DN, UK

e-mail: a.j.fielding@ljmu.ac.uk

In situ monitoring of biomolecular recognition, especially at surfaces, still presents a significant technical challenge. Electron paramagnetic resonance (EPR) of biomolecules spin-labelled with nitroxides can offer uniquely sensitive and selective insights into these processes, but new spin-labelling strategies are needed. We report the synthesis and study of a bromoacrylaldehyde spin-label (BASL), which features two attachment points with orthogonal reactivity (Figure 1). We have created the first examples of mannose and biotin ligands coupled to aqueous carboxy-functionalized gold nanoparticles through a spin-label. EPR spectra were obtained for the spin-labelled ligands both free in solution and attached to nanoparticles. The labels were recognised by the mannose-binding lectin, Con A, and the biotin-binding protein avidin-peroxidase. Binding gave quantifiable changes in the EPR spectra from which binding profiles could be obtained that reflect the strength of binding in each case. [1] Further application as a protein spin label will be discussed.

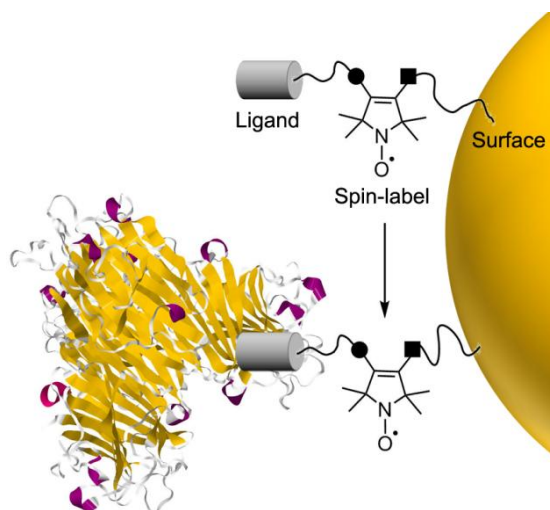


Figure 1. The concept of using a bifunctional spin-label for studying surface-ligand binding to proteins.

[1] M.A. Hollas, S.J. Webb, S.L. Flitsch, A.J. Fielding, *Angew. Chem. Int. Ed* **2017**, 56, 9449-9453.

Probing the Solution Structure of the *E. coli* Multidrug Transporter MdfA using DEER Distance Measurements with Nitroxide and Gd(III) Spin Labels

Eliane H. Yardeni^{1#}, Thorsten Bahrenberg^{2#}, Richard A. Stein³, Smriti Mishra³, Elia Zomot¹, Bim Graham⁴, Kellie L. Tuck⁵, Thomas Huber⁶, Eitan Bibi¹, Hassane S. Mchaourab³, Daniella Goldfarb²

¹Department of Biomolecular Sciences, Weizmann Institute of Science Rehovot 76100, Israel

²Department of Chemical and Biological Physics, Weizmann Institute of Science, Rehovot 76100, Israel

³Department of Molecular Physiology and Biophysics, Vanderbilt University, Nashville, TN, USA

⁴Monash Institute of Pharmaceutical Sciences, Monash University, Parkville VIC 3052, Australia

⁵School of Chemistry, Monash University, Wellington Road, Clayton, Victoria, Australia

⁶Research School of Chemistry, The Australian National University, Canberra, ACT 2601, Australia

e-mail: Daniella.goldfarb@weizmann.ac.il

Methodological and technological advances in EPR spectroscopy have enabled novel insight into the structural and dynamic aspects of spin-labeled integral membrane proteins. In addition to an extensive toolkit of EPR methods, multiple spin labels have been developed and utilized, among them Gd(III)-chelates which offer high sensitivity at high magnetic fields. Here, we applied a dual labeling approach in conjunction with Q-band (nitroxide) and W-band (Gd(III)) double electron-electron resonance (DEER) measurements to characterize the solution structure of the detergent-solubilized multidrug transporter MdfA from *E. coli*. Our results identify highly flexible regions of MdfA, which may play an important role in its functional dynamics. Comparison of distance distributions on the periplasm with those calculated using inward- and outward-facing crystal structures of MdfA show that, in detergent micelles, the protein adopts a predominantly outward-facing conformation, although more closed than the crystal structure. Parallel DEER measurements with the two types of labels led to similar distance distributions, demonstrating the feasibility of using W-band spectroscopy with a Gd(III) probe.

In a second step, we demonstrate the successful reconstitution of Gd(III)-labeled MdfA into Nanodiscs on a couple of double mutants. After successful reconstitution, the main distance between the spin labels diminishes for mutants labeled on the periplasm, but not on the cytoplasm. We assume that the conformation of MdfA might be dependent on its environment; however, a different relative orientation of the spin labels might as well be a possible explanation for this observation. Additionally, binding of a substrate induces a large conformational change in one mutant.

NMR Spectroscopy in Chemistry and Biology with Applications in Immunology and Neuroprotection

L. Wong¹, J. Maier¹, Daniel Sieme¹, J. C. Fuentes¹, N. Nath^{1,2}, P. Vemulapalli¹, N. Karschin¹, H. Sun^{1,3}, J. Kühn⁴, S. Pirkuliyeva⁴, A. Batth⁴, M. Engelke⁴, S. Ryzanov^{1,5}, L. Antonschmidt^{1,5}, A. Martinez Hernandez⁶, A. Fischer⁷, G. Eichele⁶, D. Becker¹, S. Becker¹, A. Leonov^{1,5}, M. Reggelin⁸, J. Wienands⁴, A. Giese⁹, and C. Griesinger^{1,5}

¹Dept. for NMR-based Struct. Biology, Max-Planck Institute for Biophysical Chemistry

²present address: Gauhati University, Guwahati, India

³present address: FMP, Berlin, Germany

⁴Institute of Cellular and Molecular Immunology, Georg August University of Göttingen, Göttingen

⁵DFG-Center for the Molecular Physiology of the Brain, Göttingen

⁶Genes and Behavior Dept., Max-Planck Institute for Biophysical Chemistry, Göttingen;

⁷European Neuroscience Institute Göttingen

⁸Institute of Organic Chemistry, Technical university of Darmstadt, Darmstadt, Germany

⁹Center for Neuropathology and prion research, LMU, Munich, Germany

e-mail: cigr@nmr.mpibpc.mpg.de

NMR spectroscopy is versatile for the investigation of structure and dynamics of molecules important in chemistry and biology. After an introduction into the technique, examples of the determination of the configuration of organic molecules will be shown with quantities down to a few 10s of mikrograms [1].

Fast kinetics of protein dynamics will be discussed on examples of folded on unfolded proteins [2].

Further, the role of partially disordered proteins in droplet formation is investigated. The adaptor protein SLP65 which interacts with CIN85 [3]. The two proteins are essential for B cell activation. The protein is found to be mainly unstructured and its various segments entertain different functions or interact with membranes, SH3 domains and forming coiled coils. The two proteins alone but also with vesicles perform phase separation at physiological conditions which is essential for function.

Interaction studies between diphenylpyrazole (DPP) compounds and α -Synuclein in membranes will be shown which indicate binding between these compounds and the backbone of α -Synuclein. These interactions are of interest since DPP compounds lead to disease modifying therapies for Parkinson's, Alzheimer's, Creutzfeldt Jacob disease and Type II diabetes mellitus [4] as well as some cancers [5].

[1] Hallwass, F. et al. *Angew. Chem., Int. Ed.* **2011**, *50*, 9487; N. Nath, et al. *J. Am. Chem. Soc.* **2016**, *138*, 548; Liu, Y. et al. *Nat. Prot.* 2018, <https://doi.org/10.1038/s41596-018-0091-9>

[2] C. Smith et al. *Proc. Natl. Acad. Sci. USA.* *113*, 3296-74 (2016); C. Smith et al. *Angew. Chem. Int. Ed.* *54*, 207-10 (2015).

[3] M. Engelke et al. *Science signaling*: *7* (339) ra79 (2014); J. Kühn et al. *Science signaling*: *9* (434) ra66 (2016).

[4] J. Wagner et al. *Acta Neuropath.* *125*, 795-813 (2013); J. Wagner et al. *Act. Neuropath.* *130*, 619-631 (2015); A. Hernandez et al. *EMBO Mol. Med.* *10*, 32-47 (2018); Heras Garvin et al. *Mov. Disord.* 2019; Wegrzynowicz et al. *Act. Neuropath* (2019) <https://doi.org/10.1007/s00401-019-02023-x>.

[5] E. Turriani, et al. *Proc. Natl. Acad. Sci. USA* *114*, E4971-E4977 (2017).

Recent Progress in 3D Extracellular pH Mapping of Tumors Using EPR

Hiroshi Hirata

Division of Bioengineering and Bioinformatics, Graduate School of Information Science and Technology, Hokkaido University, North 14, West 9, Kita-ku, Sapporo, 060-0814, Japan

e-mail: hhirata@ist.hokudai.ac.jp

In this talk, an overview of the recent progress in three-dimensional (3D) extracellular pH mapping of murine tumors using EPR is presented [1]. Acidification in the extracellular space is one of the hallmarks of solid tumors as well as the low-oxygen status (hypoxia). Using spectral-spatial EPR imaging and a pH-sensitive nitroxyl radical (dR-SG) [2,3], a method of 3D pH mapping was established. With a home-built 750-MHz CW-EPR spectrometer/imager, known pH solution samples were visualized to verify the 3D pH mapping method. Also, a progress in acidification of solid murine tumors (squamous cell carcinoma, SCC VII) was monitored *in vivo* five and eight days after SCC VII cell implantation to mouse hind legs. A shift in the extracellular pH of tumor-bearing legs was observed as well as an increase of the acidic tumor volume during the tumor growth. Moreover, the distribution of extracellular pH was visualized for different tumor xenograft mouse models of human-derived pancreatic ductal adenocarcinoma cells (MIA PaCa-2, SU.86.86, and Hs766t) [4]. *In vitro* and *in vivo* pH mapping demonstrated that the acidification in murine tumors could be quantitatively visualized with the reasonable accuracy of pH using EPR and the dR-SG probe.

The author expresses his gratitude to Dr. Igor Kirilyuk, Novosibirsk Institute of Organic Chemistry for his probe synthesis, and Prof. Valery Khramtsov, West Virginia University for his insightful discussion of EPR-based pH measurements. This work was supported by JSPS KAKENHI grants JP26249057 and JP19H02146.

- [1] D.A. Komarov et al., *Anal. Chem.* **90**, 13938 (2018).
- [2] A.A. Bobko et al., *Magn. Reson. Med.* **67**, 1827 (2012).
- [3] A. Samouilov et al., *Anal. Chem.* **86**, 1045 (2014).
- [4] J.W. Wojtkowiak et al., *Cancer Metab.* **3**, 2 (2015).

NMR Studies of Protein-DNA Interaction: Target Location and Allosteric Mechanism of Induction

Robert Kaptein

Utrecht University, Utrecht, The Netherlands

email: r.kaptein@uu.nl

How do gene regulatory proteins find their target sequences? We have investigated this process in detail using the *E. coli* lac repressor as a model. First, we have solved the structures of complexes of lac repressor headpiece (the DNA-binding domain) both with lac operator and with non-operator DNA by NMR. As it had been suggested that non-specific binding combined with sliding along the DNA could play an important role in target location, we measured the rate of sliding for the non-specific complex from NMR line-broadening. The surprising result was that the 1D diffusion constant for sliding is orders of magnitude smaller than expected and indeed measured by single molecule fluorescence spectroscopy. Thus, the simple sliding model cannot explain the high target location rate for lac repressor. A more likely mechanism is a combination of 1D sliding and 3D hopping. The implications for the general problem of target location of DNA-binding proteins will be discussed.

Another aspect of gene regulation is the switch between repression and induction. We have studied this process with special focus on the allosteric coupling mechanism.

In Vivo Molecular EPR-Based Spectroscopy and Imaging of Cancer

V.V. Khramtsov¹

¹In Vivo Multifunctional Magnetic Resonance center and Department of Biochemistry,
West Virginia University, Morgantown, USA

e-mail: valery.khramtsov@hsc.wvu.edu

Tumor hypoxia, extracellular acidosis (pH_e), accumulation of reducing equivalents, elevated levels of intracellular glutathione (GSH) and interstitial phosphate (Pi) are recognized hallmarks of cancer in solid tumors [1, 2]. Noninvasive in vivo EPR-based spectroscopy and imaging of $p\text{O}_2$, pH_e , GSH, Pi, and redox provide unique insights into biological processes in the tumor microenvironment (TME), and may serve as a tool for preclinical screening of anticancer drugs and optimizing TME-targeted therapeutic strategies [1, 3]. EPR is uniquely suited for *in vivo* studies having advantages over optical methods such as sufficient depth of penetration into living tissues and over another magnetic resonance modality, NMR/MRI, due to the absence of background endogenous signals. On the other side, it requires application of stable in vivo exogenous spin probes with spectral properties sensitive to the microenvironment parameters. We described the basic principles of designing functional probes based on the nitroxide and trityl radicals involved in reversible exchange processes such as spin exchange with diradical oxygen molecule, proton exchange with protons and Pi, and thiol-disulfide exchange with GSH [4] and developed a kit of the paramagnetic probes for chemical TME profiling [5]. This presentation overviews recent progress in the probe synthesis and application using spectroscopic and imaging EPR-based techniques (such as low-field L-band EPR, Overhauser-enhanced MRI and rapid scan EPR imaging) in various animal models of cancer. These include concurrent longitudinal monitoring of tissue oxygenation, acidosis, and reducing capacity in A549 human lung carcinoma and HCT 116 human colon carcinoma xenografts under therapeutic intervention; concurrent pH_e , $p\text{O}_2$ and Pi measurements in human non-metastatic PC14 vs. highly metastatic PC14HM lung adenocarcinoma xenografts as well as in MMTV-PyMT breast cancer model during tumor progression which emulates human tumor staging. Our data identified interstitial Pi as a new TME marker for tumor progression and aggressiveness contributing to a scientific basis to evoke public awareness of increased phosphate consumption in developed countries owing to high content of the phosphate-based modifiers in processed foods, and the potential health risk. *Supported by NIH grants CA194013, CA192064 and U54GM104942.*

- [1] V.V. Khramtsov and R.J. Gillies. Janus-faced tumor microenvironment and redox, *Antioxid Redox Signal*, 21, 723-29 (2014).
- [2] A.A. Bobko, T.D. Eubank, B. Driesschaert, I. Dhimitruka, J. Evans, R. Mohammad, E.E. Tchekneva, M.M. Dikov, and V.V. Khramtsov, Interstitial inorganic phosphate as a tumor microenvironment marker for tumor progression. *Sci Rep*, 7, 41233 (2017).
- [3] V.V. Khramtsov. In vivo molecular EPR-based spectroscopy and imaging of tumor microenvironment and redox using functional paramagnetic probes. *Antioxid Redox Signal*, 28, 1365-77 (2018).
- [4] V.V. Khramtsov, A.A. Bobko, M. Tseytlin, and B. Driesschaert, Exchange phenomena in the EPR spectra of the nitroxyl and trityl radicals: multifunctional spectroscopy and imaging of local chemical microenvironment, *Analyt. Chem.* 89, 4758–4771 (2017).
- [5] A.A. Bobko, T.D. Eubank, B. Driesschaert, and V.V. Khramtsov, In vivo EPR assessment of pH, $p\text{O}_2$, redox status and concentrations of phosphate and glutathione in tumor microenvironment, *J. Vis. Exp.* (133), e56624 (2018).

Triplet Fullerenes as Prospective Spin Labels for Nanoscale Distance Measurements by Pulsed Dipolar EPR

Olesya A. Krumkacheva,^{1,2,3} Ivan O. Timofeev,^{1,3} Larisa V. Politanskaya,^{2,3} Yuliya F. Polienko,^{2,3} Evgeny V. Tretyakov,^{2,3} Olga Yu. Rogozhnikova,^{2,3} Dmitry V. Trukhin,^{2,3} Victor M. Tormyshev,^{2,3} Alexey S. Chubarov,^{3,4} Elena G. Bagryanskaya,^{2,3} Matvey V. Fedin^{1,3}

¹International Tomography Center SB RAS, Novosibirsk, 630090, Russia

²N.N.Vorozhtsov Institute of Organic Chemistry SB RAS, Novosibirsk, 630090, Russia

³Novosibirsk State University, Novosibirsk, 630090, Russia

⁴Institute of Chemical Biology and Fundamental Medicine SB RAS, Novosibirsk, 630090, Russia

e-mail: olesya@tomo.nsc.ru

Precise nanoscale distance measurements by Pulsed Dipolar Electron Paramagnetic Resonance (PD EPR) play crucial role in structural studies of biomolecules and their complexes. The properties of spin labels used in this approach are of paramount importance, since they determine the sensitivity limits, attainable distances and proximity to biological conditions, including physiological temperatures. Nitroxide radicals are most common spin labels used in structural studies of proteins, nucleic acids and their complexes. The broad use of nitroxides owes to their small size and the abundance of methods for their site-directed introduction in biomolecules. However, the sensitivity of PD EPR on nitroxide labels is often insufficient, and distance measurements with label concentrations less than $\sim 10^{-5}$ M are rarely feasible.

Herewith [1], we propose and validate the use of photoexcited fullerenes as spin labels for PD EPR distance measurements. Hyperpolarization and narrower spectrum of fullerenes compared to other triplets (e.g., porphyrins) boost the sensitivity, and superior relaxation properties allow PD EPR measurements up to a near-room temperature. The capabilities of new approach are demonstrated using fullerene-nitroxide and fullerene-triarylmethyl pairs, as well as supramolecular complex of fullerene with nitroxide-labeled protein. The fullerene-triarylmethyl pair (C₆₀/TAM) exhibits the most suitable properties for pulse dipolar EPR spectroscopy, such as high signal-to-noise ratio and high modulation depth. The use of C₆₀/TAM labeling scheme can lead to a ~ 1000 times faster sampling of PELDOR data at optimum conditions, drastically saving the accumulation time. This allows distance measurements for systems with as low spin concentration as ~ 1 μ M or less, even at X-band. Therefore, photoexcited triplet fullerenes can be considered as new spin labels with the outstanding spectroscopic properties for future structural studies of biomolecules.

This study was financially supported by the Ministry of Science and Education of the Russian Federation (grant 14.W03.31.0034) and by Russian Foundation for Basic Research (no. 18-04-00393).

[1] Krumkacheva, O., Timofeev, I., Politanskaya, L., Polienko, Y., Tretyakov, E., Rogozhnikova, O., Trukhin, D., Tormyshev, V., Chubarov, A., Bagryanskaya, E. and Fedin, M. *Angew. Chem.* (2019), doi:10.1002/ange.201904152.

Structural and Aggregational Features of Intrinsically Disordered Peptide RL2 – Human Milk κ -Casein Fragment with Antitumor and Cell Penetrating Properties

S.S. Ovcherenko^{1,3}, A.V. Shernyukov^{1,3}, O.A. Chinak², E.A. Sviridov¹, V.M. Golyshev², A.S. Fomin², I.A. Pyshnaya², E.V. Kuligina², V.A. Richter² and E.G. Bagryanskaya^{1,3*}

¹N.N. Vorozhtsov Novosibirsk Institute of Organic Chemistry SB RAS, Novosibirsk, Russian Federation

²Institute of Chemical Biology and Fundamental Medicine SB RAS, Novosibirsk, Russian Federation

³Novosibirsk State University, Novosibirsk, Russian Federation

e-mail: ovcherenkoserjy@gmail.com

Intrinsically disordered proteins (IDP) play a pivotal role in dynamic regulatory and assembly processes in the cell. Recently a human κ -casein proteolytic fragment (8.6 kDa) was found to induce apoptosis of human breast adenocarcinoma MCF-7 and MDA-MB-231 cells with no cytotoxic action toward normal cells [1,2]. Then some recombinant analogs of the κ -casein fragment have been designed and their biological activities have been compared. Among these analogs, RL2 has the highest antitumor activity, but the amino acid residues and secondary structure, that are responsible for RL2's activity, remain unclear.

We characterized the therapeutic agent lactaptin (RL2) by a combination of physicochemical methods: NMR, EPR, circular dichroism, dynamic light scattering, atomic force microscopy, and a cytotoxic activity assay [3]. This combination of the methods used allowed us to investigate the structural properties of RL2 that may affect its activity. It was observed that RL2 forms an insignificant amount of aggregates and can form micelles as κ -casein can, but unlike the latter, RL2 is unable to form fibrils. The N-terminal region (aa 1–43), responsible for RL2 multimerization and partially for its activity, includes the only region with an α -helical propensity (aa 30–41). Moreover, Cys8 in this sequence is an essential residue for RL2 activity. NMR analysis of RL2 samples confirmed the presence of S–S homodimers and RL2-BME adducts. Our results may form the foundation for future research into the mechanism of RL2 anticancer activity by NMR spectroscopy.

The obtained data reveal that RL2 aggregation properties, which are important for intravenous injection, may be changed by introduction of a small organic molecule at the cysteine position.

This work is supported by the Ministry of Education and Science of the Russian Federation (state contract no. 14. W03.31.0034)

- [1] V.A. Richter, A.A. Vaskova, O.A. Koval, E.V. Kuligina, *Biol. Med. (Aligarh)* S2: 002 (2015).
- [2] V.V. Nekipelaya, D.V. Semenov, M.O. Potapenko, E.V. Kuligina, Y.Y. Kit, I.V. Romanova, V.A. Richter, *Dokl. Biochem. Biophys.* **419**, 58-61 (2008).
- [3] O.A. Chinak, A.V. Shernyukov, S.S. Ovcherenko, E.A. Sviridov, V.M. Golyshev, A.S. Fomin, I.A. Pyshnaya, E.V. Kuligina, V.A. Richter and E.G. Bagryanskaya, *Molecules*, 2019 in press.

Photosynthetic Electron Transfer Reactions in Microalga *Lobosphaera incisa*V.V. Ptushenko^{1,2}, N.P. Isaev³, L.V. Kulik³, A.E. Solovchenko⁴, B.V. Trubitsin⁵¹A.N. Belozersky Institute of Physico-Chemical Biology, M.V. Lomonosov Moscow State University, Moscow, Russia²N.M. Emanuel Institute of Biochemical Physics of RAS, Moscow, Russia³V.V. Voevodsky Institute of Chemical Kinetics and Combustion of SB RAS, Novosibirsk, Russia⁴Faculty of Biology, M.V. Lomonosov Moscow State University, Moscow, Russia⁵Faculty of Physics, M.V. Lomonosov Moscow State University, Moscow, Russia

e-mail: ptush@belozersky.msu.ru

The microalga *Lobosphaera incisa* was previously found to be tolerant to chilling stress [1]. In this study, we demonstrated the ability of *L. incisa* cultures to grow even at the temperature around 0 °C. This kind of tolerance is indicative of the presence of efficient mechanisms protecting its photosynthetic apparatus (PSA) from photodamage. The measurements of chlorophyll fluorescence (CF) induction showed a high level of nonphotochemical quenching (NPQ) of fluorescence in the microalgal cells grown at low temperatures likely facilitating protection of PSA to photodamage. At the same time, we found that a high NPQ can be induced by cationic penetrating antioxidants like SkQ1 or SkQ3 [2]. This raised a question of the mechanism of SkQ-induced NPQ, and whether it could be used to enhance the tolerance to photodamage of *L. incisa* cells subjected to chilling stress.

To solve the problem, we studied the SkQ effects on the electron transfer reactions in *L. incisa* cells measuring kinetics of the EPRI signal usually attributed to oxidized chlorophyll dimer P₇₀₀ of photosystem II (P₇₀₀⁺). In both normal and low temperature-grown control cells we observed fast (~1 s) P₇₀₀⁺ rise under intense white light (WL) with no remarkable slow phase (of minute timescale) which indicates a lack of observable light-dependent activation of Calvin cycle in our conditions. The addition of SkQ1 did not influence the kinetics of but led to remarkable (up to 2-fold) increase in EPRI intensity under WL. Unfortunately, P₇₀₀⁺ and P₆₈₀⁺ EPR spectra are almost indistinguishable, and we could not exclude P₆₈₀ or additional P₇₀₀ oxidation. Our measurements performed with the other model microalga *Chlorella vulgaris* showed that P₆₈₀⁺ accumulation can be actually induced by SkQ1 due to inhibition of reducing of photooxidized P₆₈₀⁺ by the oxygen evolving complex (OEC). Such inhibition also manifests itself by occurrence of slowly decaying (in millisecond timescale) EPRII signal attributed to oxidized tyrosine Y_Z [3] which actually took place in our case. At the same time, some authors claim changes also in Y_D oxidation state at OEC damage. Still our EPR data on Y_D oxidation or reduction in control and SkQ-treated cells do not support its using as a distinct marker of the OEC activity.

SkQ addition into incubation media of the microalga in moderate concentrations (~10⁻⁵ M) did not affect substantially their tolerance to photodamage. We suggest that SkQ could take some opposite effects on the cells including “positive” (high NPQ induction) and “negative” (e.g., some membrane-targeted injury).

The authors acknowledge Russian Foundation for Basic Research (grant 19-04-00509) for financial support.

[1] Pal-Nath et al., *Algal Res.* **26**, 25 (2017).

[2] Skulachev et al., *Curr Drug Targets* **12**, 800 (2011).

[3] Styryng et al., *BBA-Bioenerg.* **1817**, 76 (2012).

Influence of the Tylopeptin B Antimicrobial Peptide on Structure of Model Biological Membranes by Spin-label EPR

Sannikova N.E.,^{1,2} Matveeva A.G.,^{1,2} Syryamina V.N.,^{1,2} De Zotti M.,³ Toniolo C.,^{4,5}
Formaggio F.,^{4,5} Dzuba S.A.^{1,2}

¹Institute of Chemical Kinetics and Combustion, Novosibirsk

²Department of Physics, Novosibirsk State University, Novosibirsk

⁴Department of Chemical Sciences, University of Padova, Padova, Italy

⁵Institute of Biomolecular Chemistry, Padova Unit, CNR, Padova, Italy

e-mail: paihuten@gmail.com

Antimicrobial peptides are recognized as a promising new class of antibiotics. There was suggested that the main mechanism of their action on the membrane is channel formation in the membrane structure. However channel formation requires high peptide concentrations in the membrane that results in cytotoxic effects and in increase of the medications costs. From the other side, change in the membrane structure takes place also at low peptide concentrations – as a consequence of modifying the membrane functioning, such as lipid formation or protein palmitoylation. Therefore there would be interesting to study peptide influence on the biological membrane properties in the broad range of the peptide/lipid ratio (P/L).

Here we describe results obtained by spin-label EPR for the medium-length peptide antimicrobial Tylopeptin B (Ac-Trp-Val-Aib-Aib-Ala-Gln-Ala-Aib-Ser-Aib-Ala-Leu-Aib-Gln-Lol). P/L value varied in the range of 1/1500 – 1/200. We used in these studies native and spin-labeled peptide analogues, spin-labeled stearic acid, and POPC (1-Palmitoyl-2-oleoyl-sn-glycero-3-phosphocholine) lipids as a main constituent of the model membrane.

The results of pulse dipolar EPR experiments showed an increase of the local concentration of spin-labeled stearic acids with the Tylopeptin B addition. This allows us to propose a peptide-induced redistribution of the fatty acids in the membrane resulting in clustering of fatty acids. This redistribution may disrupt the lipid homeostasis in the membrane and may influence lateral diffusion; which both may serve as additional mechanisms for modification of the membrane functioning.

The peptide self-assembling process was found to start at $P/L > 1/1000$. Both peptide monomers and peptide aggregates were found to have planar orientation in the membrane. There was proposed that process of fatty acids redistribution in the membrane might be associated with peptide self-association process.

This work was supported by the Russian Science Foundation, project # 15-15-00021.

Novel Spin Label Based on OX063 Trityl Applied to Study Human Serum Albumin

Anna Spitsyna^{1,2}, Olesya Krumkacheva^{3,1}, Dmitry Trukhin², Olga Rogozhnikova^{2,1}, Alexey Chubarov^{4,1}, Igor Kirilyuk², Tatyana Godovikova^{4,1}, Victor Tormyshev^{2,1} and Elena Bagryanskaya^{2,1}

¹Novosibirsk State University, Russian Federation

²N. N. Vorozhtsov Novosibirsk Institute of Organic Chemistry SB RAS, Novosibirsk, Russian Federation

³International Tomography Center SB RAS, Novosibirsk, Russian Federation

⁴Institute of Chemical Biology and Fundamental Medicine, SB RAS, Novosibirsk, Russian Federation

e-mail: a.spitsyna@alumni.nsu.ru

Human serum albumin (HSA) is the most abundant plasma protein and possess extraordinary ligand-binding properties. It transports hundreds of compounds in the blood and has various biological functions. Albumin also carries different drugs, e.g. ibuprofen, selectively accumulates in tumors and participates in amyloid formation causing neurodegenerative diseases. Albumin structural properties are of particular interest. EPR combined with site directed spin-labeling provides a powerful tool to investigate local protein mobility and measure distances on nanometric scale.

Nitroxide radicals are most common spin labels due to small size, easy synthesis and introduction inside biomolecules. However, they have short phase relaxation times at temperatures above 80 K making impossible PELDOR measurements at higher temperatures. Trityl radicals or TAMs based on Finland Trityl (FTAM) have appeared recently as an alternative source of spin labels for measuring long distances in biological systems. Their relaxation times are longer, and their narrow spectra significantly increase signal intensity in both CW EPR and PELDOR. Yet TAM synthesis is complicated, and they are rather lipophilic and susceptible to self-aggregation, to non-covalent binding with lipophilic sites of proteins.

In this work we used new hydrophilic spin label based on OX063 radical with low toxicity and little tendency for aggregation. We selectively introduced this OX063 spin label into human serum albumin and compared spectroscopic properties of spin-labelled HSA-OX063, HSA-FTAM and HSA-MTSL samples.

The new OX063 spin label demonstrates important advantages over current FTAM labels. As expected, EPR spectra of HSA-OX063 have an intense, narrow line typical of TAM radicals in solution while HSA-FTAM showed extensive aggregation. In pulse EPR measurements, the measured T_m for HSA-OX063 is 6.3 μ s at 50 K, the longest yet obtained with TAM spin labels. PELDOR and DQC experiments for HSA-OX063 at Q-band at 50 K provided the first observation of HSA dimers by dipolar EPR spectroscopy.

This study was financially supported by Russian Foundation for Basic Research (no. 18-04-00393) and by the Ministry of Science and Education of the Russian Federation (grant 14.W03.31.0034).

Structural and Dynamical Studies of the Elongation Factor P from *Staphylococcus aureus* by NMR and EPR Spectroscopy

K. Usachev^{1,2}, A. Golubev^{1,3}, I. Khusainov^{1,3,&}, Sh. Validov¹, E. Klochkova¹,
F. Murzakhanov², M. Gafurov², V. Klochkov², A. Aganov², M. Yusupov^{1,3}

¹Institute of Fundamental Medicine and Biology, Kazan Federal University, Kazan, Russian Federation

²Institute of Physics, Kazan Federal University, Kazan, Russian Federation

³Institut de Génétique et de Biologie Moléculaire et Cellulaire, CNRS UMR7104, INSERM U964, Université de Strasbourg, Illkirch, France

[&]Present address: EMBL Heidelberg, Meyerhofstraße 1, 69117 Heidelberg, Germany

e-mail: k.usachev@kpfu.ru

Protein synthesis is a key biochemical process of the cell. This process is produced by complex molecular machines - ribosomes with the additional help of protein translational factors that provide peptide bond synthesis in accordance with the mRNA nucleotide sequence. Elongation factor P (EF-P) is a three domain protein (20.5 kDa) that binds to the ribosome between P and E sites and involved in a specialized translation of stalling amino acid motifs such as polyprolines. Proteins with stalling motifs are often involved in various processes, including stress resistance and virulence. Supposed that EF-P stabilizes the P-tRNA and increases the entropy of stalled ribosome complex to compensate for rigid nature of proline residue but detailed structural mechanisms of this effect are still poorly understood.

In our research we investigated structure and dynamic of the EF-P from *Staphylococcus aureus* (SaEF-P) by NMR and EPR spectroscopy. Backbone and side chain ¹H, ¹³C and ¹⁵N chemical shift assignments from 3D NMR spectra and ¹H-¹⁵N relaxation experiments shown that EF-P structure contains 1 α -helix and 13 β -strands [1]. It was shown that to maximize the efficiency of the antistalling function, the EF-P needs the special post-translational modification in the conservative region PGKG of the loop in the domain I of the EF-P, located close to the PTC [2]. Therefore the knowledge about dynamics of the loop I could be crucial for understanding of EF-P interaction process with P-tRNA near PTC and the function of modifications. But due to high mobility and fast proton exchange of the loop between β -sheets β_2 and β_3 (residues 30-34) the amide protons of this residues have not been detected in ¹H-¹⁵N heteronuclear NMR spectra. So we decided to use a site-directed spin labeling approach in concert with EPR spectroscopy which is a powerful method for studying the nature of proteins in solution which has been especially useful for examining proteins that are large, flexible or highly dynamic [3]. To do this we cloned and expressed a mutated (K32C) SaEF-P and labeled it by MTSL spin label. In EPR spectrum we observed a line broadening due to immobilization, i.e. incomplete averaging by the motion of the g-and A component, which means that spin label was bound to the protein. Correlation time of MTSL label bound to SaEF-P was estimated as $\tau_R = 8 \cdot 10^{-10}$ s. Addition of MTSL label covalently bound to 32Cys in the highly conservative part of EF-P loop in the domain I allows us to analyze protein dynamic by EPR spectroscopy of the high mobility region which was not observed in NMR spectra.

This work was supported by the Russian Science Foundation (Grant 17-74-20009)

[1] K. Usachev, Biomolecular NMR Assignments **12**, 351-355 (2018).

[2] D. Rossi, Wiley Interdiscip Rev RNA **5**(2), 209–222 (2014).

[3] K. Usachev, SN Applied Science **1**, 442 (2019).

Unravelling the Role of Key Amino-acids in B-class Dye-decolorizing Peroxidases Using EPR Spectroscopy

S. Van Doorslaer¹, K. Nys¹, J. Roefs¹, V. Pfanzagl², C. Obinger²

¹ BIMEF lab, Department of Physics, University of Antwerp, Antwerp, Belgium,

²University of Natural Resources and Life Sciences (BOKU), Department of Chemistry, Vienna, Austria.

e-mail: sabine.vandoorslaer@uantwerpen.be

Dye-decolorizing peroxidases (DyPs) represent the most recently classified peroxide-dependent heme-peroxidase family. A conserved distal arginine and aspartate are thought to play a crucial role in the enzymatic function. DyPs are considered for technological applications in biosensors and biocatalysts due to their possibility to degrade different ligands, but a detailed characterization of the enzymatic reaction mechanism remains limited.

Here, we will focus on DyP of *Klebsiella pneumoniae* (*KpDyp*). Multi-frequency CW and pulsed EPR is used to obtain valuable information about the different paramagnetic states present during enzyme turnover, such as the ferric resting states, different inhibited forms and intermediate amino-acid radicals.

The EPR spectra of both proteins show the presence of a multitude of ferric heme centres with different EPR spectral signature. The nature of the heterogeneity and its dependence on salt and inhibitor molecules will be discussed. Furthermore, the impact of the elimination of the distal Asp and Arg residues is discussed. These distal ligands seem to influence the accessibility of larger molecules to the heme site.

Surprisingly, a remarkably stable radical is observed in the resting state of wild-type *KpDyp*. Multi-frequency EPR in combination with site-specific mutations reveal the presence of at least one tyrosyl radical. Although tyrosyl radicals are known to be formed during enzymatic turnover in different peroxidases, it has never been observed in the resting state.

Time-Resolved EPR Study of the Intersystem Crossing of Visible Light-Harvesting Electron Donor/Acceptor Dyads

Jianzhang Zhao, Zhijia Wang, Yuqi Hou, Xue Zhang and Kepeng Chen

State Key Laboratory of Fine Chemicals, School of Chemical Engineering, Dalian University of Technology, 2 Ling-Gong Road, Dalian 116024, P. R. China

e-mail: zhaojzh@dlut.edu.cn

Triplet photosensitizers are important for photocatalysts, photovoltaics, photodynamic therapy (PDT) and photon upconversion. Designing of heavy atom-free, small organic molecule as triplet photosensitizer is still a challenging task, due to the difficulty to ensure efficient ISC in these molecules. It has been known for a long time that charge recombination can induced ISC in electron donor/acceptor dyads. However, in these conventional dyads, the donor and acceptor are separated in large distance to reduce the electron spin-spin exchange interaction, to ensure the radical pair ISC mechanism. However, it is difficult to prepare these dyads because of the complicated molecular structures. Thus, it is desired to prepare small simple electron donor/acceptor dyads showing efficient ISC. Recently it was proposed that given the electron donor and acceptor's π -conjugation planes adopt perpendicular geometry, the ISC will be enhanced, due to the conservation of the angular momentum (electron spin angular momentum/molecular orbital angular momentum). This is the so-called spin-orbit charge transfer ISC (SOCT-ISC) [1].

Recently we prepared series of compact electron donor/acceptor dyads, i.e. dyads with simple short linker between the donor and acceptor [2, 3]. The orthogonal geometry ensure efficient SOCT-ISC. The charge separation and charge recombination were studied with femtosecond transient absorption spectroscopy, the triplet state was studied with nanosecond transient absorption spectroscopy. The ISC mechanisms and the triplet states were also studied with time-resolved EPR. We found that the ^3LE state and the ^3CT state can be simultaneously observed, which are rare for similar compounds.

- [1] Dance, Z.E.; Mickley, S.M.; Wilson, T.M.; Ricks, A.B.; Scott, A.M.; Ratner, M.A.; Wasielewski, M.R. *J. Phys. Chem. A* **2008**, *112*, 4194–4201.
- [2] Chen, Kepeng Yang, W.; Wang, Z.; Iagatti, A.; Bussotti, L.; Foggi, P.; Ji, W.; Zhao, J.; Di Donato, M. *J. Phys. Chem. A*, **2017**, *121*, 7550–7564.
- [3] Wang Z.; Zhao, J. *Org. Lett.*, **2017**, *19*, 4492–4495.

Development of “Knee” and “Hand” Receiving and Transmitting Systems for a Specialized MRI with a 0.4 Tesla Field

A.A. Bayazitov¹, K.M. Salikhov¹, Ya.V. Fattakhov¹, A.R. Fakhрутdinov¹, V.A. Shagalov¹, R.Sh. Khabipov¹, N.M. Reshetnikov², D.I. Abdulganieva³

¹Zavoisky Physical-Technical Institute of the FRC Kazan Scientific Center of RAS, Kazan, Russian Federation

²FRC Kazan Scientific Center of RAS, Kazan, Russian Federation

³Kazan State Medical University, Kazan, Russian Federation

e-mail: bayazitov.alfis@kfti.knc.ru

The work is devoted to the receiving-transmitting system for a small-sized specialized traumatological magnetic resonance scanner with 0.4 T magnetic field induction [1]. MRI system is developed on base of a permanent magnet, which allows us to use a less expensive thermostating system. Also, the scanner has a compact size and can be used in a mobile version. The gap of the magnet is 210 mm, which imposes some restrictions on the size of the receiving and transmitting system. The transmitting circuit and the receiving sensor are located at a small distance from each other. For this reason, the circuits are inductively coupled, which must be considered when designing and functioning of the sensor.

The paper deals with the problems of protection against external noise, noise induced from nearby gradient coils, reducing the q-factor of the sensor when the sensor is placed in a magnet, as well as shielding options.

The working area of the sensor, in which the homogeneity was estimated, is 150x120x120 mm, respectively, along the X, Y and Z axes. Based on the simulation results, prototypes were made and their characteristics were measured.

In the Fig.1 field homogeneity graphs are presented, as an example, for the sensor variant optimized with 6 loops.

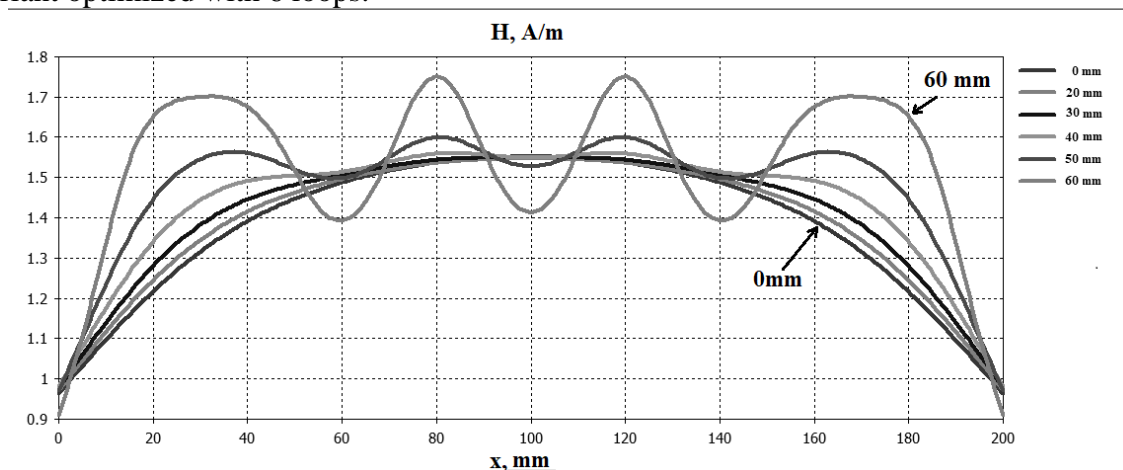


Fig.1. Mathematical calculation of the radiofrequency field distribution from the circuit with 6 loops.

[1] Bayazitov A.A., Fattakhov Ya.V., Khundiryakov V.E., Nauchnoe Priborostroenie. **29**, no.1, 98 (2019). DOI: 10.18358/np-29-1-i9298.

Hidden Magnetism in almost Multiferroic EuTiO₃

Annette Bussmann-Holder¹, Zurab Guguchia², Hugo Keller³, Krystian Roleder⁴

¹Max-Planck-Institute for Solid State Research, Heisenbergstr. 1, D-70569 Stuttgart, Germany

²Paul Scherrer Institut, Forschungsstrasse 111, CH-5232 Villigen PSI, Switzerland

³Physik-Institut der Universität Zürich, Winterthurerstr. 190, CH-8057 Zürich, Switzerland

⁴Institute of Physics, University of Silesia, Chorzów, Poland

e-mail: A.Bussmann-Holder@fkf.mpg.de

Even though perovskite oxides have been in the focus of fundamental and applied research, EuTiO₃ (ETO) has not received much attention until recently. ETO crystallizes in the cubic perovskite type structure [1] and undergoes a phase transition from paramagnetic to antiferromagnetic (AFM) at $T_N = 5.7$ K [2]. While it was long time believed that ETO remains cubic at all temperatures, it was shown in [3] that it exhibits a structural phase transition from cubic to tetragonal at $T_S = 282$ K in an analogous manner as SrTiO₃ (STO). Similar to STO, ETO has a temperature-dependent dielectric constant, which increases with decreasing temperature and exhibits a drop of 8% at T_N [4] which can be reverted by a magnetic field. The dielectric constant has been connected to the softening of a long wave length transverse optic (TO) mode – a typical signature of a displacive ferroelectric phase transition [5] which suggests that ETO might be a multiferroic. While the low temperature magnetic properties of ETO are well established, novel magnetic properties at high temperature have been observed which become apparent by shifting T_S to higher temperatures upon the application of a magnetic field [6]. Furthermore, the magnetic susceptibility traces the structural instability, and a finite and strongly temperature and magnetic field dependent muon spin relaxation (μ SR) rate is observed up to 300 K [7] with a distinct anomaly around 200 K. In addition, support for hidden magnetism at high temperature has been obtained from birefringence measurements on thin films since a magnetic field modulates substantially the onset of birefringence [8]. Moreover, several indications for various phase transitions below T_S have been obtained from these data with strong approval for their existence from μ SR [9]. Here we discuss these unusual magnetic properties of ETO and suggest their possible origins.

[1] Brous J, Frankuchen I and Banks E 1953 Acta Crystallogr. **6** 67.

[2] McGuire T R, Shafer M W, Joenk R J, Halperin H A and Pickart S 1966 J. Appl. Phys. **37** 981.

[3] Bussmann-Holder A, Köhler J, Kremer R K and Law J M 2011 Phys. Rev. B **83** 212102.

[4] Katsufuji T and Takagi H 2001 Phys. Rev. B **64** 054415.

[5] Kamba S, Nuzhnyy D, Vaněk P, Savinov M, Knížek K, Shen Z, Šantavá E, Maca K, Sadowski M and Petzelt J 2007 Europhys. Lett. **80** 27002.

[6] Caslin K, Kremer R K, Guguchia Z, Keller H, Köhler J and Bussmann-Holder A 2014 J. Phys.: Condens. Matter **26** 022202.

[7] Guguchia Z, Keller H, Kremer R K, Köhler J, Luetkens H, Goko T, Amato A and Bussmann-Holder A 2014 Phys. Rev. B **90** 064413.

[8] Bussmann-Holder A, Roleder K, Stuhlhofer B, Logvenov G, Lazar I, Soszyński J, Koperski A, Simon A and Köhler J 2017 Scientific Reports **7** 40621.

[9] Guguchia Z, Salman Z, Keller H, Roleder K, Köhler J and Bussmann-Holder A 2016, Phys. Rev. B **94** 220406(R).

Selenium-Nitrogen Free Radical ($\bullet\text{NSe}$) and its EPR Studies

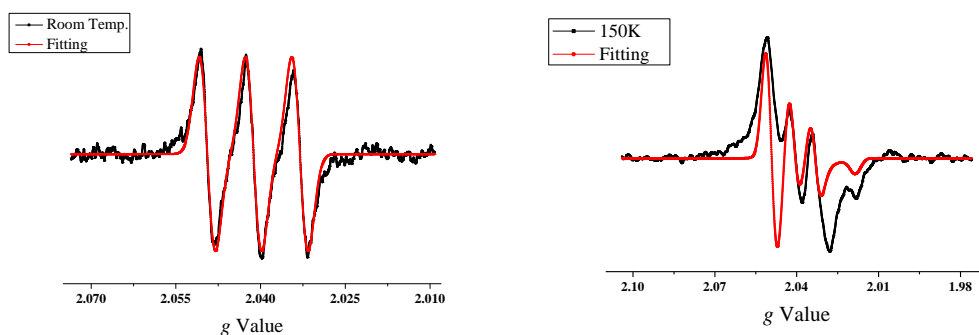
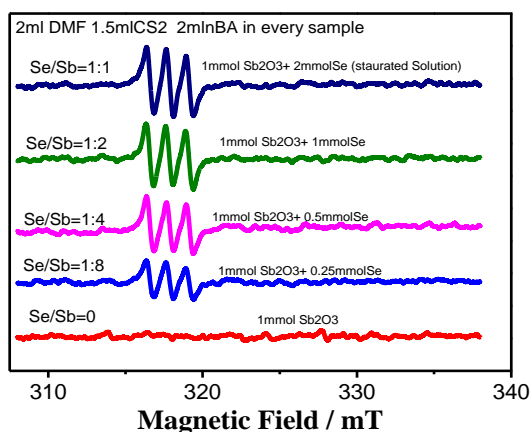
Chunyan Wu², Jiafu Chen¹

¹Hefei National Laboratory for Physical Sciences at Microscale, University of Science and Technology of China (USTC)

²School of Chemistry and Materials Science, USTC

e-mail: jfchen@ustc.edu.cn

$\text{Sb}_2\text{S}_{3-x}\text{Se}_x$ ($0 \leq x \leq 3$) is promising for practically applicable solar cell since it possesses excellent stability, suitable band gap, high extinction coefficient and abundant elemental storage. This research demonstrates a simple method of simultaneous dissolution of Se and Sb_2O_3 for direct deposition of $\text{Sb}_2\text{S}_{3-x}\text{Se}_x$ films. Related mechanism study shows that there exists free radicals in the deposition solution, further studies proved that this free radical was selenium-nitrogen radical ($\bullet\text{NSe}$), and the formation of selenium-nitrogen free radical in sulfur-containing complex is responsible for the dissolution of selenium. It's also studied the characterization of $\bullet\text{NSe}$ radical at low temperature.



[1] Ed Awere, J. Passmore et al, Can. J. Chem. 66(1988) 1776.

[2] P. Gerbaux, Yv. Van Haverbeke and R. Flammang, Inter. J. of Mass Spectro. 184 (1999) 39.

[3] C.Y. Wu, L.J. Zhang et al, Sol. Ener.Mater. and Sol. Cel. 183 (2018) 52.

The Trigonal Yb^{3+} Center in Lithium Calcium Hexafluoroaluminate

M.L. Falin¹, V.A. Latypov¹, A.M. Leushin², G.M. Safiullin¹, A.A. Shakirov²,
A.A. Shavelev²

¹Zavoisky Physical-Technical Institute, FRC Kazan Scientific Center of RAS, Kazan, Russian Federation

²Kazan (Volga Region) Federal University, Kazan, Russian Federation

e-mail: falin@kfti.knc.ru

Lithium calcium hexafluoroaluminate LiCaAlF_6 (LiCAF) is a colquirite-type fluoride with the hexagonal structure belonging to the D_{3d}^2 (P31c) space group. Six fluorine (F) atoms surround a lithium (Li), calcium (Ca), or aluminum (Al) atom [1]. The LiCAF crystals when doped with rare-earth (RE) ions (Ce^{3+} , Nd^{3+} , Er^{3+} , Tm^{3+}) are used in photonic devices because they are good hosts for optically active cations. Recent examples of applications include the use of Nd^{3+} - LiCAF in photolithography [2] and Ce^{3+} - LiCAF in ultraviolet (UV) chirped-pulse application [3]. Ce^{3+} - doped LiCAF has been reported as a leading candidate for a tunable solid-state laser in the UV region [4]. Electron paramagnetic resonance (EPR) spectra of Ce^{3+} , Dy^{3+} , Er^{3+} , Yb^{3+} ions were observed in [5,6].

This report is devoted to the detailed study of impurity RE paramagnetic centers formed by Yb^{3+} ions in the LiCAF single crystal by EPR and optical f-f spectroscopy methods.

The LiCAF crystals were grown using the Bridgman technique. EPR and optical spectroscopy of trigonal Yb^{3+} centers in LiCaAlF_6 are reported. The results of these experiments make it possible to conclude that Yb^{3+} ions replace host cation sites Ca^{2+} forming mainly one type of paramagnetic center of trigonal symmetry. Positions of lines in optical spectra were specified of the observed center. The crystal field parameters of trigonal center Yb^{3+} were determined. Structural models of the observed center are proposed (Figure). It is shown that the substitution of the Yb^{3+} ion for the Ca^{2+} ion leads to the considerable compression of the YbF_6 octahedron along the trigonal axis of the center.

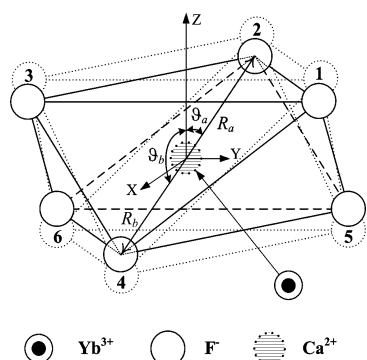


Figure. Fragment of the structure of the LiCaAlF_6 crystal and schematic model for the trigonal Yb^{3+} center.

This work was supported by the program of the Presidium of the Russian Academy of Sciences no. 5 "Electron spin resonance, spin-dependent electron effects and spin technologies" and by the subsidy of the Russian Government (agreement No.02.A03.21.0002) to support the Program of Competitive Growth of Kazan Federal University and optical spectroscopy experiments were funded by the Russian Foundation for Basic Research (project no. 18-32-00936). AML was funded by the subsidy allocated to Kazan Federal University for the state assignment in the sphere of scientific activities (project 3.672.2017/8.9).

- [1] V.W. Viebahn, Z. Anorg. Allg. Chem. **386**, 335 (1971).
- [2] E. Sarantopoulou, Z. Kollia, A.C. Cefalas, Microelectron. Eng. **53**, 105 (2000).
- [3] Z. Liu, T. Kozeki, Y. Suzuki, N. Sarukura, Opt. Lett. **26**, 301 (2001).
- [4] M.A. Dubinskii, V.V. Semashko, A.K. Naumov, R.Y. Abdulsabirov, S.L. Korableva, Laser Phys. **3**, 216 (1993).
- [5] I.N. Kurkin, L.L. Sedov, Sh.I. Yagudin, Solid State Physics **32**, 2779 (1991).
- [6] M. Yamaga, D.Lee, B. Henderson, T.P.J. Hant, H.G. Gallagher, T. Yosida, J. Phys.:Condens. Matter **10**, 3223 (1998).

Spin Properties of the Fe(III) Complexes with Tetradentate Schiff Bases and Photosensitive 4-Styrylpyridine Ligands

E.N. Frolova¹, L.V. Mingalieva¹, O.A. Turanova¹, R.G. Batulin², A.S. Semakin²,
G.G. Garifzyanova³, M.Yu. Volkov¹, L.G. Gafiyatullin¹, I.V. Ovchinnikov¹, A.N. Turanov¹

¹Zavoisky Physical-Technical Institute, FRC Kazan Scientific Center of RAS, Kazan, Russian Federation

²Institute of Physics, Kazan Federal University, Kazan, Russian Federation

³Kazan National Research Technological University, Kazan, Russian Federation

e-mail: fro-e@yandex.ru

The presence of photoisomerizable ligands in transition metal complexes makes such a compound promising for use in devices where the magnetic properties of the substance controlled by light. The presence of thermo-induced spin-crossover ($S=1/2 \leftrightarrow S=5/2$, SCO) in complexes formed by *cis*- or *trans*-isomers of the ligands is a necessary condition for observation of spin transition caused by the ligand photoisomerization. Therefore, before the study of photocontrollability of the spin state of a complex, it is reasonable to investigate the SCO properties and establish a correlation between its magnetic properties and the chemical structure (equatorial ligand, axial ligand, counterion, etc.).

This work is devoted to characterization of several complexes with the general chemical formula $[\text{Fe}(\text{SB})\text{Sp}_2]\text{BPh}_4 \cdot n\text{MeOH}$ (Sp is 4-styrylpyridine and SB is a Schiff base: salen, vanen, bzacen and acen { $\text{H}_2\text{salen} = \text{N},\text{N}'\text{-ethylenebis}(\text{salicylideneimine}), n=1$; $\text{H}_2\text{vanen} = \text{N},\text{N}'\text{-ethylenebis}(3\text{-methoxysalicylideneimine}), n=4$; $\text{H}_2\text{acen} = \text{N},\text{N}'\text{-ethylenebis}(\text{acetylacetylideneimine}), n=1$; $\text{H}_2\text{bzacen} = \text{N},\text{N}'\text{-ethylenebis}(\text{benzoylacetylacetylone}), n=1$ }), which were synthesized for the first time.

The effect of the chemical structure of the equatorial ligand on the magnetic properties of hexacoordinated Fe(III) complexes was studied by the means of the UV, NMR, EPR and magnetometry. The experiments were carried out for the complexes in powders, vitrified and liquid solutions in dichloromethane.

High spin, low spin and thermo-induced SCO for central Fe(III) were observed with the variation of the SB in the equatorial plane of the complexes.

In powders, as well as in vitrified and liquid solutions, an increase in the slope of SCO was observed in a series of the complexes with the ligands $\text{salen} \rightarrow \text{vanen} \rightarrow \text{bzacen} \rightarrow \text{acen}$. The fact that this trend persists both in polycrystalline powder samples and in solutions confirms the assumption that the SCO depends on the equatorial environment of the Fe(III) ion. For this series of complexes, it was found that the less aromatic groups in the equatorial ligand of the complex, the more abrupt SCO observed in it.

Significant changes in the shape of the EPR spectra for the powders in comparison with the vitrified solutions were registered. These facts reflect the influence of the external environment of the complex (ice of the solvent or crystal lattice) on the symmetry of the coordination node, and as a result, on the SCO parameters.

Quantum chemical calculations of the complex structure and energies of the spin states of the complexes were also carried out. The obtained values correlate well with experimental data.

EPR of Single Ions Nd^{3+} in CsCdBr_3 Monocrystals

L.K. Aminov, M.R. Gafurov, I.N. Kurkin, B.Z. Malkin, S.I. Nikitin, A.A. Rodionov

Kazan Federal University, Kazan, Russian Federation

e-mail: marat.gafurov@kpfu.ru

The admixture R^{3+} ions (Yb^{3+} , Nd^{3+}) in CsCdBr_3 monocrystals mainly form dimeric paramagnetic centers of the $\text{R}^{3+} - \text{Cd}^{2+}$ vacancy - R^{3+} type elongated along the trigonal crystal axis (see [1] and references therein). Recently EPR of single Yb^{3+} ions in this crystal have been observed [1,2], but heretofore there are no publications on EPR of single Nd^{3+} ions. The lack of EPR signal might be due to the formation of the paramagnetic centers of trigonal symmetry with $g_{\perp} = 0$ [1]. However, there are charge compensation models giving rise to the low symmetry centers, for instance, vacancy in the Cs^+ ion position close to the Nd^{3+} ion that substitutes for a Cd^{2+} ion. Therefore it seems reasonable to look further for EPR spectra of single Nd^{3+} ions in this crystal.

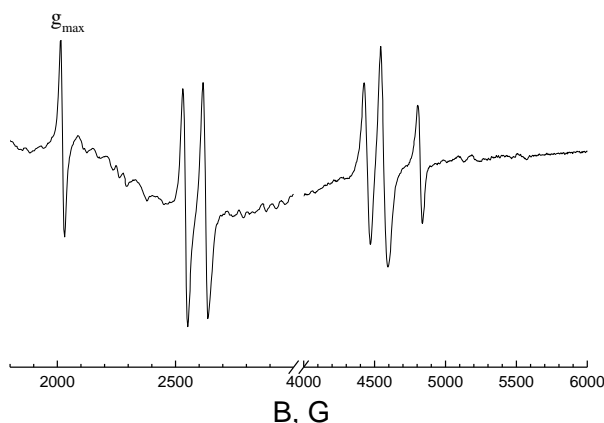


Fig.1. EPR spectrum of Nd^{3+} ions in CsCdBr_3 single crystals. $B \parallel g_{\max}$, $\nu = 9.435$ GHz, $T = 10$ K.

We have investigated EPR of CsCdBr_3 single crystals doped with Nd^{3+} grown by Bridgman method. The concentration of Nd^{3+} in starting materials varied from 0.3 to 1.0 at. %. The EPR measurements were made at X-band (the frequency is about 9.435 GHz) *cw* Bruker ESP 300 spectrometer at low temperatures $6 \div 15$ K. An intensive EPR spectrum of Nd^{3+} ions was observed at $T < 10$ K. At higher temperatures EPR lines are broadening due to the strong spin-lattice relaxation and at $T > 15$ K the spectrum is not observed. The observation of EPR only at temperatures $T < 15$ K is not typical

for Nd^{3+} ions. The similar situation took place for Nd^{3+} ions in ZnS [3].

The EPR spectrum consists of 6 magnetically nonequivalent lines due to single Nd^{3+} centers of rhombic symmetry with g -factors $g_{\max} = 3.332$, $g_{\min} = 1.174$. In fig. 1 the EPR spectrum is presented for magnetic field B parallel to the orientation of g_{\max} for one of magnetically nonequivalent centers. The observed spectrum is close to the EPR spectrum of Nd^{3+} in LaF_3 (see [4], fig.3).

The work is supported by the state assignment in the scientific sphere allocated to Kazan Federal University (project no. 3.6722.2017/8.9).

- [1] M.R. Gafurov et al., Proc. SPIE **4766**, 279 (2002).
- [2] L.K. Aminov et al., Magn. Reson. Solids **21**, 19401 (2019).
- [3] I.N. Kurkin et al., Fizika Tverdogo Tela **19**, 1211 (1977)
- [4] M.B. Schulz, C.D. Jeffries, Phys. Rev. **149**, 270 (1966).

Combining Electron Paramagnetic Resonance Methods to Investigate Materials for Organic Photovoltaics

Etienne Goovaerts

Physics Department, University of Antwerp, Universiteitsplein 1, 2610 Antwerpen, Belgium.

e-mail: Etienne.Goovaerts@uantwerp.be

Organic photovoltaic technologies are expected to make a contribution to the very important future supply of solar energy, affording low-cost devices with versatile operation. In the bulk heterojunction (BHJ) concept of the organic solar cells, the active layer consists of intermixed regions of molecules with electron donor and acceptor properties, D and A, respectively, allowing for efficient charge separation at the interface between the materials. The generated charge carriers, called positive and negative polarons, can be studied by EPR, but also other paramagnetic states are important in the operation of BHJ organic solar cells, such as polaron pairs (PPs), charge transfer (CT) excitons at the D/A interface, and triplet excitons (TEs) in each of the materials.

Various examples will be discussed, in which continuous-wave and pulsed EPR as well as electrically- and optically-detected magnetic resonance (EDMR and ODMR) are applied to detect and study the fate of these paramagnetic excitations. Pure materials and blends with fullerene [1] as well as nonfullerene [2-4] acceptors have been investigated based on the magnetic resonance signature of polarons and triplet excitons. Finally, relevant degradation mechanisms in a nonfullerene BHJ organic solar cell will be shown to involve TEs and the generation of singlet oxygen.[4]

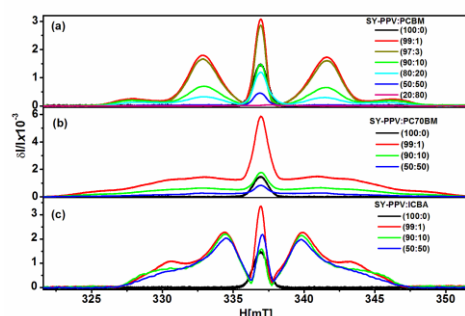


Fig. 1: EDMR of fullerene TE in blends with a donor polymer, demonstrating efficient population after photoinduced charge transfer. [1]

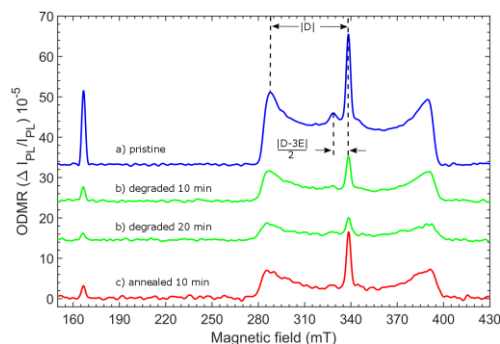


Fig. 2: ODMR of the triplet exciton in a pure films of the nonfullerene small molecule acceptor FBR, showing the effect of degradation under 447 nm light in air. [4]

- [1] B. Z. Tedlla, et al., *Adv. Energy Mater.* **5**, art. 1401109 (2015); B. Z. Tedlla, et al., *Phys. Rev. B* **91**, art. 085309 (2015).
- [2] M. Van Landeghem, et al., *J. Magn. Res.* **288**, 1, (2018); M. Van Landeghem, W. Maes, E. Goovaerts, S. Van Doorslaer, *Appl. Magn. Res.*, submitted.
- [3] M. Van Landeghem, R. Lenaerts, J. Kesters, W. Maes, E. Goovaerts, to be published.
- [4] I. Sudakov, M. Van Landeghem, R. Lenaerts, W. Maes, S. Van Doorslaer, E. Goovaerts, to be published.

The Study of Kerogen by NMR

D. Ivanov¹, A. Vahin², D. Melnikova¹, V. Skirda¹

¹Institute of Physics, Kazan Federal University, Kazan, Russian Federation

²Butlerov Institute of Chemistry, Kazan Federal University, Kazan, Russian Federation

e-mail: f.ma.dmitry@gmail.com

The kerogen deposits that make up the shale are widely developed in various oil-producing regions of the world. At high temperatures, cracking of kerogen can occur, resulting in the formation of oil components in stages, ranging from the most highly molecular and viscous – asphaltenes to light hydrocarbons and gas.

Using the capabilities of the nuclear magnetic resonance (NMR) method it was found that for a significant part of the rock kerogen molecules, the Gaussian form with the NMR relaxation time characteristic of a solid satisfactorily describes the transverse magnetization decrease. To describe the more mobile elements that make up the organic system of kerogen (formed petroleum) the Lorentz form is used. The ratio between the Gaussian and Lorentz form is 3:1.

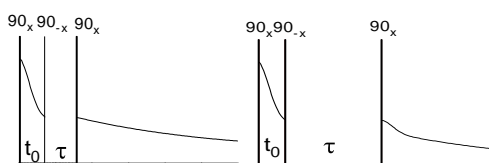


Fig.1. The effect of the Goldman-Schen pulse sequence at two different times of mixing τ .

An analysis of the relaxation attenuation obtained showed that with an increase in the mixing time τ , the fraction of the Lorentz component decreases. When the value of $t_{mix} \geq 5000 \mu s$ is reached, the ratio between the Gaussian and Lorentz components becomes constant and is approximately 3:1 (see fig.2). The obtained experimental results make it possible to unambiguously take the value of the time parameter characterizing the process of interphase redistribution by magnetization, the value $\tau = 600 \mu s$ and determine the spatial scales at which the redistribution of magnetization is carried out [2].

We hope that our results will serve as the basis for creating an express-procedure for analyzing the composition and determining the oil-generating potential of the organic matter of shale rocks.

[1] J. Leisen, *Rub.chem. and techn.* **72**, 1 (1999).

[2] G. Khutsishvili, *JETP* **15**, 5 (1962).

Since the components of the system that we found for NMR are characterized by different relaxation times, an original study of the interphase exchange was carried out. The data on the morphological features of solid-state (from NMR relaxation) structures of kerogen were obtained using the Goldman-Schen (fig.1) pulse sequence [1].

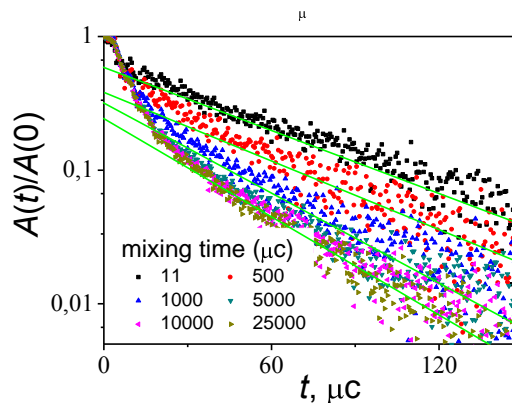


Fig.2. Relaxation attenuation normalized to the initial amplitude for the initial kerogen sample, obtained using the Goldman-Schen pulse sequence. The colors of the diffusion time are coded: black - 11 μs , red - 500 μs , blue - 1000 μs , green - 5000 μs , and rose - 10,000 μs , and brown - 25000 μs .

FMR Analysis of Magnetic Anisotropies in Co-implanted TiO₂ Rutile

Ö. Karataş^{1,2}, C. Okay³, R. I. Khaibullin⁴, S. Kazan², L. Arda¹, B. Rameev^{2,4}

¹Bahcesehir University, 34349 Besiktas, Istanbul, Turkey

²Gebze Technical University, 41400 Gebze, Kocaeli, Turkey

³Marmara University, 81040 Göztepe, Istanbul, Turkey

⁴E. Zavoisky Physical-Technical Institute, FRC Kazan Scientific Center of RAS, 420029 Kazan/Tatarstan, Russian Federation

e-mail: ozgulkaratass@gmail.com, ozgulkaratas@gtu.edu.tr

Since the observation of room temperature ferromagnetism in Co doped anatase TiO₂, a considerable attention has been paid to the Co: TiO₂ system. Recently, we have observed that Co-implanted single-crystalline rutile TiO₂ shows ferromagnetic behavior with a very high Curie-temperature [1-4].

In this work, we have been studied the magnetic anisotropies of the cobalt-ion implanted rutile TiO₂ single crystal substrates with (100), (001), (110) crystal orientations by Ferro Magnetic Resonance (FMR) technique. Single crystalline TiO₂ substrates have been implanted by Co⁺ ions with energy of 40 keV to high dose of 1.5×10^{17} ions/cm² at room temperature. FMR spectra have been recorded by using Bruker EMX X-band spectrometer (9.5 or 9.8 GHz) at various temperatures. The static magnetic field has been varied in the range of 0-22 kOe. Angular dependences of FMR spectra have been recorded with the static magnetic field rotated either in the plane of the plate-like samples (in-plane geometry) or in the perpendicular plane (out-of-plane geometry) nearly coinciding with crystallographic planes of a substrate. The field derivative of microwave power absorption (dP/dH) was recorded as a function of static magnetic field. Static magnetic properties were studied using vibrating sample magnetometry option of 9T Quantum Design Physical Property Measurement System (PPMS).

The results have revealed the room-temperature ferromagnetic behavior with extraordinary high crystal magnetic anisotropies. It has been established that the crystallographic orientation of the implanted-substrate has a strong influence on the magnetic anisotropies observed in the single-crystalline Co -TiO₂ substrates. Analysis of FMR data shows that strongly anisotropic room-temperature ferromagnetism is induced by the textured growth of magnetic cobalt nanoparticles. The growth directions of the Co nanoparticles with respect to single crystal TiO₂ rutile matrix have been discussed.

The authors ÖK, SK, LA and BR acknowledge support from the Scientific and Technical Research Council of Turkey (TUBITAK) through the Project no. 115F472.

- [1] R.I. Khaibullin, L.R. Tagirov, B.Z. Rameev, Sh.Z. Ibragimov, F. Yıldız, B. Aktaş, J. Phys.: Condens. Matter. **16**, L443–L449 (2004).
- [2] Yildiz F., B. Rameev, R. Khaibullin, L. Tagirov, M. Özdemir, and B. Aktaş, Phys. Stat. Sol. (c) **1(12)**, 3319–3323 (2004).
- [3] N. Akdogan, B.Z. Rameev, L. Dorosinsky, H. Sozeri, R.I. Khaibullin, B. Aktas, L.R. Tagirov, A. Westphalen and H. Zabel, J. Phys.: Condens. Matter. **17(34)**, L359-L366 (2005).
- [4] N. Akdogan, B.Z. Rameev, R.I. Khaibullin, A. Westphalen, L.R. Tagirov, B. Aktas, H. Zabel, J. Magn. Mater. **300**, e4–e7 (2006).

Probing Fundamental Properties of Condensed Matter Systems with Positive Muons

Hugo Keller

Physik-Institut der Universität Zürich, Winterthurerstrasse 190, CH-8057 Zürich,
Switzerland

e-mail: keller@physik.uzh.ch

The muon-spin rotation (μ SR) technique is a powerful tool for investigating fundamental magnetic and electronic properties of various condensed matter systems. In this technique the positive muon serves as a *microscopic magnetic probe* to detect local magnetic fields in the bulk of a solid. In many cases μ SR has provided important information on the microscopic magnetic properties of condensed matter systems, which are hardly obtained with other experimental techniques.

After a brief introduction to the basic principles of the μ SR technique, some typical examples of the application of μ SR for investigating local magnetic properties of various condensed matter are presented. The following topics are discussed in some detail: magnetic systems (ferro- and antiferromagnetic systems), unconventional high-temperature superconductors (cuprate and iron-based superconductors, vortex matter, coexistence of superconductivity and magnetism, phase diagrams), and multiferroic systems.

The low-energy μ SR technique developed at the Paul Scherrer Institute (PSI) is well suited for investigating multilayer structures containing superconducting and insulating (or metallic) layers. Slow positive muons of tunable energy are implanted at a very small and controllable depth below the surface of a sample on a nanometer scale. This allows all the advantages of standard μ SR to be obtained in thin samples (films), near surfaces, and as a function of depth below surfaces.

In non-metals (*e.g.* semiconductors) a positive muon μ^+ can pick up an electron e^- to form muonium (μ^+e^-) which is a hydrogen-like atom. The μ SR technique is an ideal tool to determine the hyperfine coupling constant of muonium in semiconductors, to study muonium diffusion (quantum diffusion) in non-metals, and to test chemical reaction rate theories involving muonium. Some typical examples of muonium research will be briefly discussed.

^3He in Contact with Nanostructures

Alakshin E.M.¹, Dolgorukov G.A.¹, Klochkov A.V.¹, Kondratyeva E.I.¹, Kuzmin V.V.¹,
Safiullin K.R.^{1,2}, Stanislavovas A.A.¹, Tagirov M.S.^{1,2}

¹ Kazan Federal University, 420008, Kazan, Russian Federation,

² Institute of Applied Research, 420111, TAS, Kazan, Russian Federation

e-mail: katarina.kondratyeva@gmail.com

The study of the spin kinetics of helium-3 in contact with nanostructures will be presented.

Nanoparticles. The spin kinetics data of ^3He in contact with various trifluoride nanosized powders will be presented. Results for LaF_3 nanopowder demonstrated that the nuclear magnetic relaxation of the adsorbed ^3He occurs due to the modulation of dipole-dipole interaction by the quantum motion in the adsorbed two-dimensional film. The analysis of obtained data for PrF_3 nanoparticles testifies in favor of cross-relaxation presence in the nuclear spin-lattice relaxation data, which takes place between ^3He and ^{141}Pr nuclei. The magnetic phase transition in DyF_3 is accompanied by a considerable change in the character of fluctuations of the magnetic moments of dysprosium ions, which affect the spin kinetics of ^3He in contact with the substrate. Significant changes in the relaxations rates of the longitudinal and transverse magnetizations of liquid ^3He have been discovered in the region of magnetic ordering of the solid matrix.

Nanodiamonds. In recent years nanodiamonds have become a widely investigated material for quantum engineering, biological and electronic applications. The spin-lattice (T_1) and spin-spin (T_2) relaxation times of ^3He were measured in adsorbed, gas and liquid phases in a detonation nanodiamond sample at the frequency range of 5–18 MHz and at $T = 1.6$ K temperature. The observed T_1 and T_2 are much shorter in comparison with ^3He in similar experiments for samples with restricted geometry, thus we assume a strong impact of paramagnetic centers on nuclear magnetic relaxation. Experiments with nanodiamond surface preplated with N_2 or ^4He layers will be presented. The model of ^3He relaxation in contact with detonation nanodiamonds that describes our experimental results will be proposed.

Aerogels. Earlier, we systematically studied the nuclear magnetic relaxation of ^3He in contact with silicate aerogels. The determining role of the adsorbed layer in relaxation processes of gaseous and liquid ^3He was confirmed. It is known that aerogel acts as an impurity and affects phases of superfluid ^3He . Nowadays, it is of interest to study superfluid ^3He in contact with anisotropic aerogels (group of prof. Dmitriev V.V., Moscow). An additional mechanism of the ^3He relaxation in aerogels is found and it is shown that this relaxation mechanism is not associated with the adsorbed layer. A hypothesis about the influence of intrinsic paramagnetic centers on the relaxation of gaseous ^3He is proposed.

This work was supported by the Russian Science Foundation (project no. 19-72-10061).

Dual Fluorescence-nitroxide Supermolecules as High Sensitive Redox Probes and Models for Electron Transfer: 34 Years History and Recent Developments

Likhtenshtein Gertz I.

Department of Chemistry Ben-Gurion University of the Negev, Beersheva, Israel
Institute of Problems of Chemical Physics, RAN, Chernogolovka, Russia

e-mail: gertz@bgu.ac.il

This presentation is a review on the use of tethered fluorophore- nitroxide (FN) or profluorescence nitroxide (PN) compounds as probes for redox status, antioxidant activity, oxidative stress, and free radical reaction. In addition, these supermolecules have been proved to serve as tools for study of molecular dynamics, intermolecular fluorescence quenching and electron transfer mechanism and metal analytic reagents. Keeping all properties of spin and fluorescent probes, the dual fluorophore-nitroxide compounds (FNO•) possess important new advantages. Three fundamental effects were first demonstrated in Likhtenshtein group [1]: 1) the nitroxide fragment is a strong quencher of the fluorescence, 2) the radical photoreduction can lead to the decay of the EPR signal and the drastic increase of the fluorescence intensity, and 3) the photoreduction kinetics is strongly depend on nano-second molecular dynamics of environment. These effects form basis of application of double probes for the quantitative study of redox reactions, molecular dynamics of objects of interest, and the establishment of factors affected on an electronic transfer. Next principle step was a series of excellent papers by Blough *et al.* [2] in which the potential of these tethered, optically switching molecules as potent probes of radical was realized. Works of the Likhtenshtein and Blough groups paved the way to thorough investigations of numerous radical reactions. Oxidative stress, polymer production and degradation, environment pollution are areas of the the dual fluorophore-nitroxide "reign". Another fruitful avenue of application of the NF compounds appeared to be analysis of nitric oxide, superoxide, vitamins and metal ions.. In addition, the new magnetic materials in which magnetic properties can be controlled by optical stimuli were developed by using photochromic derivatives as photofunctional units and nitroxide radical as spin sources. The organic synthetic chemistry allows to play with the chemical structure of the dual molecules of different absorption, fluorescence and ESR spectra, redox and their spin properties with variety bridges tethered to the chromophore and nitroxide segments. Thus, there is every reason to believe that the dual compounds will continue to serve as an effective tool in chemistry, biology, and material science

[1] Bystryak, I.M., G.I. Likhtenshtein, A.I. Kotelnikov, O.H. Hankovsky, K. Hideg. Russ. J. Phys. Chem. 60, 1679–1983 (1986).

[2] N.V. Blough, D.J. Simpson. J Am Chem Soc 110, 1915–1917 (1988).

Hyperfine Coupling Constants in Me-Er (Me = Cu, Ag, Au) Binary Dilute Alloys

S. Lvov and E. Kukovitsky

Zavoisky PhTI of FIC KSC RAS, 420029, Russia, Kazan, Sibirsky tract 10/7

e-mail: lvov@kfti.knc.ru

The ESR spectra of Er^{3+} in binary noble metal-erbium dilute alloys were studied. Erbium concentration was varied in the range 30–2500 ppm. Measurements were conducted in X-range at the temperature 1.7–4.2 K. The spectra corresponds to the ion in crystal field of cubic symmetry with g -factor respected to the value for Γ_7 doublet. Alloys preparation method was reported earlier [1] and allows getting ESR spectrum with fully resolved hyperfine structure of odd erbium isotopes ^{167}Er . Our results add new data to previously known for AgEr and AuEr alloys. Main feature of them is higher accuracy of HFI constant measurement (± 0.1 Oe). Another important result is data for Cu matrix. In that way, data presented allow accurate comparison of HFI constant values in the whole d^{10} row Cu-Ag-Au. On the basis of new data, the estimation of different contributions to hyperfine constant of erbium ion in noble metal matrices is provided.

Table 1. Hyperfine coupling constant values A of ^{167}Er (results of least-square fitting to experimental results).

Matrix	Er (ppm)	A_{av} (Oe)	Standard Deviation	Mean Deviation
Cu ($3d^{10}$)	30	74.14(5)	0.12(8)	0.1(0)
Ag ($4d^{10}$)	300	74.19	0.12(5)	0.10(0)
Au ($5d^{10}$)	50	74.49	0.12(5)	0.10(0)

[1] E.F. Kukovitsky, S.G. Lvov. ESR Study of CuEr Dilute Alloys. PHMM **120**, 1, 18-26 (2019).

***In situ* ESR at Elevated Temperatures and Pressures for Catalysis and Related Phenomena**

O.N. Martyanov, S.N. Trukhan, S.S. Yakushkin

Boreskov Institute of Catalysis, Novosibirsk, Russian Federation

e-mail: oleg@catalysis.ru

Nowadays, more than 90 % of chemical industries worldwide anyhow use catalysts and catalytic processes. Fast development of chemical technology during recent decades along with the appearance of new materials and the improvement of existing engineering solutions made it feasible and economically viable the implementation of the processes at elevated temperatures and pressures. A lot of realized chemical reactions *de facto* take place under sub- or supercritical (SC) conditions in so-called supercritical fluids (SCF). SCF have a unique combination of properties: the density, heat capacity and dissolving power of SCF approximate those observed in the liquids, while the diffusion and viscosity are between the corresponding values for the gaseous and liquid state that often provides unusual behavior of SCF which is beneficial for catalytic processes [1].

The number of techniques that can be effectively applied *in situ* to study the processes at elevated temperatures and pressure including SCF at the atomic and molecular scale is rather limited. ESR is unique tool to investigate the mobility of the paramagnetic particles as well as dynamics of their local environment. The analysis of ESR spectra of paramagnetic ions and spin probes providing the data on their dynamics and spin exchange can give us valuable information about clusterization process and early stages of the formation of catalytically active sites [2], including the formation of superparamagnetic nanoparticles [3], as well as about evolution of active phase during catalytic processes [4] *in situ*. The development of original approach for the precise simulation of ESR spectra of slowly rotating paramagnetic particles (clusters) while incomplete averaging of anisotropic hyperfine interaction is observed can serve as quantitative tool to study complex multicomponent hydrocarbon systems *in situ* including heavy crude oils [5]. It allows one to investigate directly the stability of dispersed oil systems as well as the aggregation/disaggregation processes of asphaltenes (heaviest oil fraction) at elevated temperatures/pressures that often determines the efficiency of the extraction and processing of heavy crudes [6].

- [1] I.V. Kozhevnikov et al., *J. Supercritical Fluids* **69**, 82 (2012); A.M. Chibiryayev et al., *Applied Catalysis A: General* **456**, 159 (2013); A.M. Chibiryayev et al., *Catalysis Today* **329** 177 (2019).
- [2] S.N. Trukhan et al., *J. Supercritical Fluids* **57**, 247 (2011).
- [3] G.A. Bukhtiyarova et al., *J. Nanoparticle Res.* **13**, 5527 (2011); S.S. Yakushkin et al., *J. Appl. Phys.* **111**, 044312 (2012); D.A. Balaev et al., *J. Appl. Phys.* **114**, 163911 (2013); V.L. Kirillov et al., *Mater. Chem. Phys.* **145**, 75 (2014); A.A. Dubrovskiy et al., *J. Appl. Phys.* **118**, 213901 (2015). V.L. Kirillov et al., *Mater. Chem. Phys.* **225**, 292 (2019).
- [4] S. S. Yakushkin et al., *Appl. Magn. Res.* **50**, 725 (2019).
- [5] S.N. Trukhan et al., *Energy & Fuels* **28**, 6315 (2014); S.N. Trukhan et al. *Energy & Fuels*, **31**, 387 (2017).
- [6] A.A. Gabrienko et al., *J. Phys. Chem. C* **119**, 2646 (2015); O.N. Martyanov et al., *Russ. Chem. Rev.*, **86**, 999 (2017); E.V. Morozov et al., *Energy & Fuels* (2019) doi: 10.1021/acs.energyfuels.9b00600.

Results Gained from Application of Dielectric and High-resolution Nuclear-Magnetic Resonance Complex for Assessment of Fluid type in a Borehole and in Core

V.M. Murzakaev¹, N.N. Belousova¹, A.V. Bragin¹, V.D. Skirda², M.S. Tagirov²,
A.S. Alexandrov², T.R. Abdullin³, M.I. Amerkhanov³

¹TNG-Group, 21 Voroshilov str., Bugulma, Russia

²Kazan Federal University, Institute of Physics, 16 Kremlevskaya str., Kazan, Russia

³NTC Tatneft, 75 Lenina str., Almetyevsk, Russia

e-mail: murza@tngf.tatneft.ru

In recent years, when well drilling is accompanied by growing quantity and importance of lateral holes, any additional information on the studied object becomes very valuable – whether it is a borehole or core samples taken from relevant intervals. Such information is required for the most effective selection of well drilling method, for clarification of effective thicknesses of reservoirs, for evaluation of fluid type, which in the end affects profitability of the Project in general.

One of direct methods used with mobile fluid is Nuclear Magnetic Logging which provides information on a potential amount of recoverable fluid. Its results may be used to clarify not only effective reserves, but also to evaluate type of fluid which saturates the pore space, using modern techniques applicable to this method.

TNG-Group has equipment developed alongside Kazan Federal University, which has resolution as good as its foreign counterparts, whereas in terms of core studies, the NML-based unit has no compatible counterparts whatsoever. Application of these tools at ultra-viscous oil fields in the Republic of Tatarstan proved high descriptiveness of this method and demonstrated various possibilities of the tools. For example, testing the 2D distribution of relaxation time method generated «2D-maps», which prove presence of high-viscosity oil in core, as well as residual oil when studying the well section. During evaluation of potential reservoirs in a borehole and selection of locations for taking representative samples by a Formation Tester (similar to MDT), special attention must be paid to studies of core samples taken from the borehole, because resolution of a 1 cm device allows a comprehensive investigation of the section with high accuracy and will not allow to skip non-permeable interlayers, which is important in the final selection of shooting points. A totally new approach in testing the new type of equipment is integration of methods and modern-day digitization techniques, as applicable to borehole investigations. Application of neuron networks in interpretation of NML and Dielectric Waveform Logging complex provides an option to evaluate oil saturation, which simplifies accomplishment of such tasks in case of an incomplete set of open-hole logging jobs. The Report provides results of such integration when studying ultra-viscous oil fields in the Republic of Tatarstan. Reliability of acquired data is verified by comparison of borehole investigations with laboratory core analysis.

Nuclear Magnetic Resonance equipment available in TNG-Group makes it possible to survey a thin-layered hole section and core due to high resolution of the tools, whereas integration of fluid typification methods increases its assessment accuracy.

EPR of Spin-Crossover Compounds $[\text{Fe}(\text{bzacen})(\text{tvp})]\cdot\text{BPh}_4\cdot n\text{CH}_3\text{OH}$

T.A. Ivanova, I.V. Ovchinnikov, O.A. Turanova

Zavoisky Physical-Technical Institute FRC KSC RAN, Kazan, Russian Federation

e-mail: igovchinnikov@gmail.com

The spin state variation of spin-crossover complexes under the temperature, pressure or photoexcitation is necessary for creation of memory system on the molecular level [1].

Our aim is EPR investigation of temperature dependence of spin crossover transition from low spin (N_{LS}) to high spin (N_{HS}) $S = 1/2 \Rightarrow S = 5/2$ in two compounds of Fe(III) A and B both have the same d^5 electron configuration and coordination core N_4O_2 . The difference in structures A and B originate at different regime of crystallization from solution only.

Temperature dependence of EPR spectra of complexes A and B and accordance integral intensities of high spin (HS, $S = 5/2$) part of spectra (low magnetic field H) normalized intensities show the following features of spin-transition:

- the existence of incomplete spin-crossover transition in temperature interval (240-320) K for A and (\sim 130-230) K for B;
- the beginning of spin-transition at 320 K for A and \sim 250 K for B;
- T_c -temperature ($N_{\text{LS}} = N_{\text{HS}}$) are 285.8 K (A) and 208.4 K (B);
- the "end" of spin-transitions is \sim 320 K (A) and 250 K (B).

To obtain the more full information on spin-transition the values of g -factors of low spin part EPR spectra were analyzed. We used the one-electron approximation for d^5 electron configuration of lower orbital triplet [2,3].

For electronic configuration d^5 in the low-spin states this method allows to solve the inverse problem of EPR spectroscopy: using the values of the g -factor components observed in EPR to determine the energy levels and wave functions of the quantum states contributing to the values of these g -factors.

The energy levels obtained as a result of the calculation fully explain the above features of spin transitions in compounds A and B.

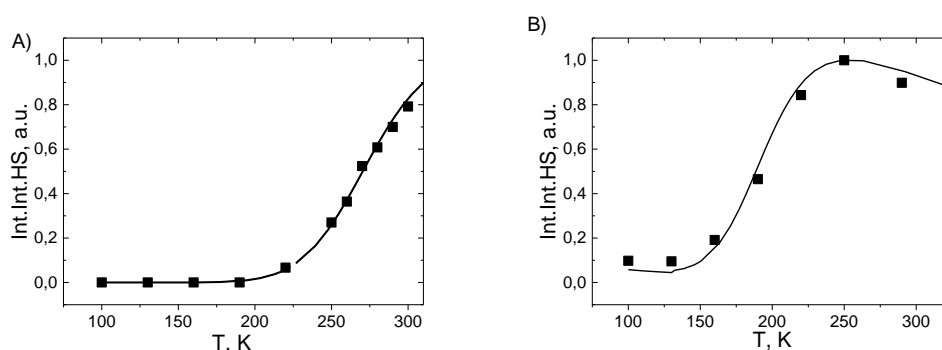


Fig. 1. Normalized integral intensity (N_{HS}) of HS part of EPR spectra for A and B.

[1] Spin Crossover in Transition Metal Compounds I-III/ Eds: Ph. Gutlich, H.A. Goodwin (2004).

[2] B. Bleaney, M.C.M. O'Brien, Proc. Phys. Soc. B **69**, 1216 (1956).

[3] T.A. Ivanova, I.V. Ovchinnikov, A.N. Turanov, Physics of the Solid State. **49**, 2132 (2007).

Direct Evidence for "Substrate-induced" Inter-Copper Electron-Transfer in Copper-Containing Nitrite Reductases (*AxNiR* and *RpNiR*-core) Probed by EPR/Cryolytic Reduction/Annealing Studies

Muralidharan Shanmugam,¹ Tobias M. Hedison,¹ Derren J. Heyes,¹
Ruth Edge,² and Nigel S. Scrutton¹

¹Manchester Institute of Biotechnology, University of Manchester, 131 Princess Street, Manchester M1 7DN, United Kingdom

²The Dalton Cumbrian Facility, The University of Manchester, Westlake Science & Technology Park, Cumbria CA24 3HA, United Kingdom

e-mail: Muralidharan.shanmugam@manchester.ac.uk

Copper-containing nitrite reductases (CuNiRs) of *Alcaligenes xylosoxidans* (*AxNiR*) and *Ralstonia pickettii* (*RpNiR*) catalyzes the one electron reduction of nitrite ion into a gaseous nitric oxide. This process involves an electron-transfer from the reduced type(I) copper(II) (T1Cu) to type(II) copper(II) center (T2Cu), where substrate binding and subsequent catalysis takes place [1]. This inter-copper electron transfer catalyzed by CuNiRs has been studied by various spectroscopic methods, but majorly suffers by selectively probing either of the redox-centers [2]. Even, serial crystallographic technique failed to address the redox-state of the type(I) Cu(II) center between the oxidized and reduced states, due to minimal/negligible changes around the first-sphere coordination environment of the type(I) copper ion [3].

Cryolytic-reduction at 77 K followed by annealing to higher temperatures have been used significantly in conjunction with EPR spectroscopy to characterize the short-living intermediates of heme monooxygenase enzymes; for example, ferrous-superoxo [5], ferric-oxo [4,6], ferric-hydroperoxo [4,6] and Compound I species [4–6]. Herein, we have employed cryolytic-reduction and cw-EPR spectroscopy to probe the inter-copper electron transfer by monitoring the spectroscopic signatures of both T1Cu and T2Cu redox centers of *AxNiR* and *RpNiR*-core with and without substrate, NO₂⁻. The analysis of the EPR data confirms the electron-transfer from the reduced type(I) Cu(II) center to type(II) Cu(II) center only in the case of nitrite-bound *AxNiR/RpNiR*-core. In this presentation, proton-coupled electron-transfer (PCET) by CuNiRs and the analysis will be discussed in details.

- [1] W.G.W. Zumft, *Microbiol. Mol. Biol. Rev.*, 1997, **61**, 533-616; T.M. Hedison, D.J. Heyes, M. Shanmugam, A.I. Iorgu and N.S. Scrutton, *Chem. Commun.*, 2019, **55**, 5863-5866.
- [2] S. Brenner, D.J. Heyes, S. Hay, M.A. Hough, R.R. Eady, S.S. Hasnain and N.S. Scrutton, *J. Biol. Chem.*, 2009, **284**, 25973-25983; L. Krzeminski, L. Ndamba, G.W. Canters, T.J. Aartsma, S.D. Evans and L.J.C. Jeuken, *J. Am. Chem. Soc.*, 2011, **133**, 15085-15093; S. Suzuki, Deligeer, K. Yamaguchi, K. Kataoka, K. Kobayashi, S. Tagawa, T. Kohzuma, S. Shidara and H. Iwasaki, *J. Biol. Inorg. Chem.*, 1997, **2**, 265-274.
- [3] S. Horrell, S.V. Antonyuk, R.R. Eady, S.S. Hasnain, M.A. Hough and R.W. Strange, *IUCrJ*, 2016, **3**, 271-281.
- [4] R. Davydov and B.M. Hoffman, *Arch. Biochem. Biophys*, 2011, **507**, 36-43.
- [5] R. Davydov, J.D. Satterlee, H. Fujii, A. Sauer-Masarwa, D.H. Busch and B.M. Hoffman, *J. Am. Chem. Soc.*, 2003, **125**, 16340-16346.
- [6] R. Davydov, A.A. Gilep, N.V. Strushkevich, S.A. Usanov and B.M. Hoffman, *J. Am. Chem. Soc.*, 2012, **134**, 17149-17156.

TR EPR Study of Photoinduced States of Metalloporphyrin. From Monomer to Oligomers

A.A. Sukhanov¹, Yu.E. Kandrashkin¹, V.K. Voronkova¹, V.S. Tyurin²

¹Zavoisky Physical-Technical Institute, FRC Kazan Scientific Center of RAS, Sibirsky Tract 10/7, Kazan 420029, Russia

²A.N. Frumkin Institute of Physical Chemistry and Electrochemistry, Russian Academy of Sciences, Leninsky Prospect 31, Moscow 119071, Russian Federation

e-mail: ansukhanov@mail.ru

Natural metalloporphyrins are very important types of compounds being key fragments of enzymes, hemoglobins, photosynthetic centers, etc [1]. Synthetic derivatives of natural metalloporphyrins found wide applications in many fields of science and technology, and, especially, in medicine. The synthesis of multiporphyrin systems having new properties compared with their monomeric fragments. It is expected that the porphyrin oligomers can be applied as photoconverter devices [2,3]. Photo-induced states of metalloporphyrin monomers is studied actively [4,5]. New photo-induced states are expected for multiporphyrin systems with paramagnetic ions compared with their monomeric fragments, since in such systems, additional interactions are implemented. The methods of the transient electron paramagnetic resonance (TREPR) are one of the best techniques available to study photo-induced paramagnetic states.

We study copper complexes of coproporphyrin I (CuCPP) by continuous wave EPR (CW EPR) and TR EPR. CW EPR spectra of the CuCPP complex in *o*-terphenyl indicate the presence of only monomer fragments, while in the solution of the chloroform and isopropanol mixture, the complexes dimerize and the amount of dimers. TREPR spectra of CuCPP complexes in *o*-terphenyl and in the chloroform and isopropanol mixture after the laser photo-excitation are mainly due to spin-polarized ground states of monomer and dimer complexes, respectively [6]. The TREPR study of zinc complexes of coproporphyrin I tetraethyl ester (ZnCPP) showed that in the frozen solution of *o*-terphenyl, only one type of the triplet state is observed, which corresponds to ZnCPP monomer fragments. In addition to this spectrum, we observed new TREPR spectrum appears in chloroform/isopropanol. Based on the results of the data on CuCPP, there is a reason to believe that the dimerization effect is observed in the solvent mixture and this spectrum corresponds to the spectrum of the photoexcited triplet of the ZnCPP dimers [7].

- [1] K.M. Kadish, K.M. Smith, and R. Guilard, *The Porphyrin Handbook* (Academic Press, 2000).
- [2] C.M. Drain, A. Varotto, and I. Radivojevic, *Chem. Rev.* (2009).
- [3] I. Beletskaya, V.S. Tyurin, A.Y. Tsivadze, R. Guilard, and C. Stern, *Chem. Rev.* (2009).
- [4] V. Rozenshtein, A. Berg, H. Levanon, U. Krueger, D. Stehlik, Y. Kandrashkin, and A. Van Der Est, *Isr. J. Chem.* **43**, 373 (2003).
- [5] M. Gouterman, R.A. Mathies, B.B. Smith, and W.S. Caughey, *J. Chem. Phys.* (1970).
- [6] A.A. Sukhanov, Y.E. Kandrashkin, V.K. Voronkova, and V.S. Tyurin, *Appl. Magn. Reson.* **49**, 239 (2018).
- [7] A.A. Sukhanov, V.S. Tyurin, I.K. Budnikova, and V.K. Voronkova, *Appl. Magn. Reson.* **50**, 455 (2019).

EPR Study of Monoisotopic ^{53}Cr Impurity Ions in Forsterite Single Crystal

A.A. Sukhanov¹, V.F. Tarasov¹, A.S. Apreleva², K.A. Subbotin^{3,4}, E.V. Zharikov³

¹Zavoisky Physical-Technical Institute, Kazan, Russian Federation

²Institute of Physics, Kazan Federal University, Kazan, Russian Federation

³Prokhorov General Physics Institute, Moscow, Russian Federation

⁴Mendeleev University of Chemical Technology, Moscow, Russian Federation.

e-mail: tarasov@kfti.knc.ru

Currently, the search and study of materials for practical implementation of high-effective devices for quantum informatics, including quantum computing and long distance quantum communications is an important scientific task with fundamental and applied aspects. Dielectric crystals activated with rare-earth ions are intensively studied as one of the most promising materials for quantum memory in optic band due to the long time of storage of the coherent state of nuclear spins in crystals and possibility to transfer of coherence between photons and electron-nuclear spin states of impurity rare-earth ions in crystals [1, 2]. In the field of quantum computing the great progress is made in the practical implementation of quantum computers based on superconducting qubits, the characteristic operating frequencies of which lie in the microwave range. Therefore there is an interest in the quantum memory of the microwave range. We suppose that effective quantum memory in the microwave region can be based on electron-nuclear spin systems of impurity transition metal ions in crystals.

With this in mind we grown forsterite (Mg_2SiO_4) single crystal doped with monoisotopic ^{53}Cr ions with nuclear spin $I=3/2$ and studied continuous wave EPR spectra and relaxation times of paramagnetic centers formed by chromium ions in this crystal. The crystal was grown from the melt with 0.14 wt. % of chromium by the Czochralski technique in slightly oxidizing atmosphere (argon + 2 vol. % of oxygen). EPR measurements were carried out in X-band on Bruker ELEXSYS E680 spectrometer with a dielectric resonator ER4118X-MD5-W1.

It is confirmed that chromium forms two-, three- and four-valent ions in forsterite crystal lattice. The Cr^{2+} and Cr^{4+} ions substitute Mg^{2+} and Si^{4+} ions, respectively. In this case, no special charge compensations are necessary. The Cr^{3+} ions substitute Mg^{2+} as a single ion with nonlocal charge compensation and as a dimer associate formed by two closely spaced Cr^{3+} ions and nearby Mg^{2+} vacancy. It is found that the integral intensity of resonance transitions belonging to the chromium dimer associates is much higher than that to be expected for the statistical distribution of the impurity Cr^{3+} ions in the forsterite host. Therefore, there is a mechanism favoring the self-organization of the Cr^{3+} ions in dimer associates during the crystal growth.

[1] A. Louchet, et al. Phys. Rev. B, **77**, 195110 (2008).

[2] Ph. Goldner, et al. Phys. Rev. A, **79**, 033809 (2009).

Multi-Frequency EPR/ENDOR, DNP and AWG Pulse MW Spectroscopy of *g*-Engineered Trityl-Aryl-Nitroxide biradicals

K. Sato,¹ R. Hirao,¹ I. Timofeev,^{2,3,4} O. Krumkacheva,^{2,3,4} E. Zaytseva,^{2,4} O. Rogozhnikova,^{2,4} V. Tormyshev,^{2,4} D. Trukhin,^{2,4} E. Bagryanskaya,^{2,4,*} T. Gutmann,⁵ V. Klimavicius,⁵ G. Buntkowsky,⁵ K. Sugisaki,¹ S. Nakazawa,¹ H. Matsuoka,¹ K. Toyota,¹ D. Shiomi,¹ T. Takui¹

¹Department of Chemistry and Molecular Materials Science, Graduate School of Science, Osaka City University, Osaka, Japan

²N. N. Vorozhtsov Novosibirsk Institute of Organic Chemistry SB RAS, Novosibirsk, Russia

³International Tomography Center SB RAS, Novosibirsk, Russia

⁴Novosibirsk State University, Novosibirsk, Russia

⁵Technische Universität Darmstadt, Darmstadt, Germany

e-mail: timofeev.itc@gmail.com

In this work, trityl and nitroxide radicals connected by π -topologically controlled aryl linkers generate genuinely *g*-engineered biradicals (Figure). They serve as a typical model for biradicals in which the exchange (J) and hyperfine interactions compete with the *g*-difference electronic Zeeman interactions. The magnetic properties, including J 's, underlying the biradical spin Hamiltonian for solution are determined by multi-frequency CW EPR and ¹H-ENDOR spectroscopy and compared with those obtained by quantum chemical calculations. The experimental J -values agree with the quantum chemical calculations. The *g*-engineered biradicals are tested as a prototype for AWG (Arbitrary Wave Generator) based spin manipulation techniques for GRAPE (GRADient Pulse Engineering) microwave control of spins in molecular magnetic resonance spectroscopy and the implementation of molecular spin quantum computers, demonstrating efficient signal enhancement of selective and weakened hyperfine signals. DNP effects of the biradicals for 400 MHz NMR signal enhancement are examined, giving the efficiency factor of 30 for ¹H and 27.8 for ¹³C nuclei. The marked DNP results show the feasibility of these biradicals to produce DNP hyperpolarization.

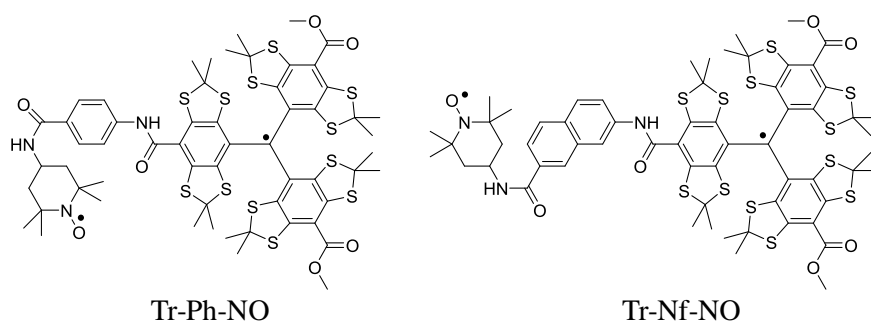


Figure. Molecular structures of trityl-aryl-nitroxide biradicals.

EPR of the $\text{Pb}_{1-x}\text{Gd}_x\text{S}$ Narrow Gap Semiconductor Crystals: Observation of Strong Dependence of the EPR Line Profiles on Gadolinium Concentration

V.A. Ulanov^{1,2}, I.V. Yatsyk², R.R. Zainullin¹

¹ Kazan State Power Engineering University, Kazan, Russian Federation

² Zavoisky Physical-Technical Institute, Kazan, Russian Federation

e-mail: ulvlad@inbox.ru

The PbS compound belongs to the group of lead chalcogenides (PbS, PbSe, and PbTe) which are direct narrow-gap semiconductors with a NaCl-type lattices. These compounds are used for producing the electronic and optoelectronic devices that operate in the mid-infrared range. At present the behavior of foreign magnetic impurities in lead chalcogenides is a subject of considerable interest because their highly tunable magnetic properties are suited for adding spintronic functionalities to semiconductor technologies.

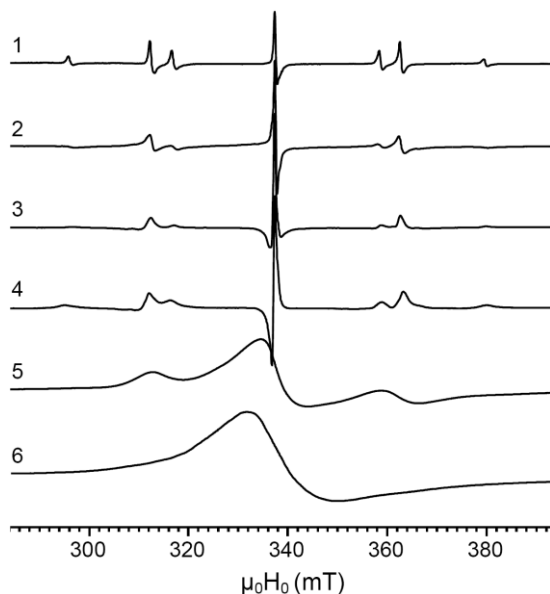


Fig.1. EPR spectra of the crystalline $\text{Pb}_{1-x}\text{Gd}_x\text{S}$ samples ($T = 5,2$ K; $f_{\text{EPR}} = 9.33$ GHz; $H_0 \parallel \langle 001 \rangle$; 1 $\rightarrow x = 3.2 \cdot 10^{-4}$; 2 $\rightarrow x = 1.1 \cdot 10^{-3}$; 3 $\rightarrow x = 4.3 \cdot 10^{-3}$; 4 $\rightarrow x = 5.5 \cdot 10^{-3}$; 5 $\rightarrow x = 8.7 \cdot 10^{-3}$; 6 $\rightarrow x = 1.4 \cdot 10^{-2}$).

very strong dependence of the EPR line profiles on gadolinium concentration (x) was revealed (see Fig.1). In the samples with $x = 4.3 \cdot 10^{-3}$ and $5.5 \cdot 10^{-3}$ the “reversed” Dysonian profiles were observed, while the samples with low Gd concentrations demonstrated the typical Dysonian line profiles. Such “reversed” Dysonian line profile was found in a dilute Au:Er alloy by [4] and was subscribed to a near-surface layer formed by metallurgical treatment of the samples under investigation. Further increasing of Gd concentration gave the spectra with “normal” Dysonian line shapes again, but lines were much broadened. The nature of the experimental facts got in this work is discussed.

It was found (see, for instance, [1-2]), the presence of magnetic ions in the lead chalcogenide compounds and exchange interactions between magnetic impurities and carriers results in a number of new effects. Because the mechanisms of carrier-impurity spin transfer in these compounds are very difficult to study and have not been fully understood up to the present, new experimental investigations of the crystalline lead chalcogenides activated by magnetic impurities can fill this gap. In the present work it was established by EPR method that in the $\text{Pb}_{1-x}\text{Gd}_x\text{S}$ crystals gadolinium replaced lead atom and found itself in $\text{Gd}^{3+}(4f^7, {}^8S_{7/2})$ state. As these crystals had rather high conductivity, one would observe in them the EPR spectral lines with Dysonian profiles. But in our study a

[1] Cygorek M., Axt V.M., Semicond. Sci. Technol. **30**, 085011 (2015).

[2] Kapetanakis M.D., Wang J., Perakis I.E.: J. Opt. Soc. Am. B. 29, A95 (2012).

[3] Raizman A., Suss J.T., Seidman D.N., Shaltiel D., Zevin V., Phys. Rev. Lett. 46, 141 (1981).

EPR of the $\text{BaF}_{2+x}:\text{Ni}$ crystals: Peculiarities of an Analysis of SHFS of the EPR Spectra of Ni^{3+} Centers when $H_{\text{ZFS}} \gg H_{\text{eZ}} \gg H_{\text{SHFI}}$

V.A. Ulanov^{1,2}, I.V. Yatsyk², R.B. Zaripov², G.S. Shakurov², R.R. Zainullin¹

¹ Kazan State Power Engineering University, Kazan, Russian Federation

² Zavoisky Physical-Technical Institute, Kazan, Russian Federation

e-mail: ulvlad@inbox.ru

The BaF crystal belongs to fluorite compounds (such as CdF_2 , CaF_2 , SrF_2 , BaF_2) and has a cubic crystal structure in which each cation is located in the center of a coordination cube formed by eight anions. In turn, each anion is located in the center of coordination tetrahedron formed by four cations. Taking into account that these crystals are transparent in a wide range of optical frequencies and are chemically stable, they can be used as a basis for active (with respect to electromagnetic radiation) media.

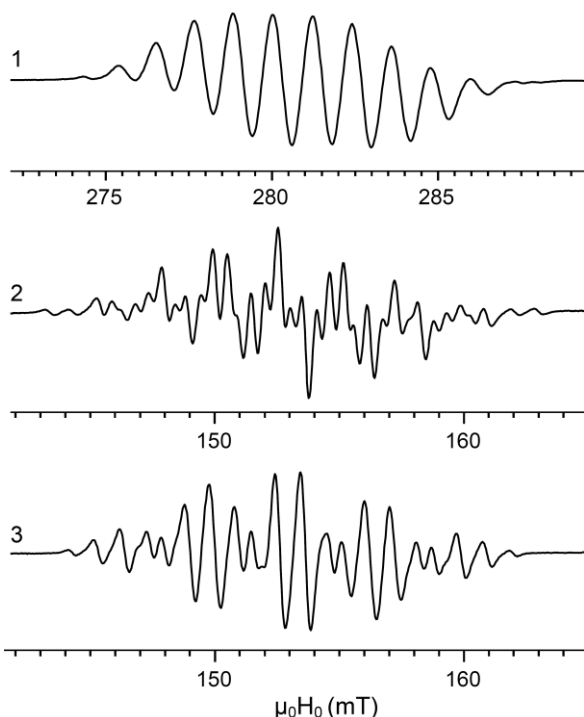


Fig.1. EPR spectra of the $[\text{NiF}_4\text{F}_4\text{F}_{\text{int}}]^{6-}(\text{C}_{4v})$ synthesized in a $\text{BaF}_{2+x}:\text{Ni}$ crystals ($f_{\text{EPR}} = 9.4$ GHz; $T = 20\text{K}$; 1 – $H_0 \parallel \langle 001 \rangle \parallel C_{4v}$; $H_0 \parallel \langle 010 \rangle \perp C_{4v}$; $H_0 \parallel \langle 110 \rangle \perp C_{4v}$)

form a stable structure with $S = 3/2$. Due to crystal field of tetragonal symmetry, energy interval between spin doublets ($|\pm 3/2\rangle$ and $|\pm 1/2\rangle$) is equal to 255 GHz. Temperature dependence of integral intensity of the EPR spectrum shows that the $|\pm 3/2\rangle$ spin doublet is lowest. Electron Zeeman interaction can be characterized by $g_{\parallel} = 2.385 \pm 0.002$ and $g_{\perp} = 2.185 \pm 0.002$.

Superhyperfine structures (SHFS) of the EPR spectra of the $[\text{NiF}_4\text{F}_4\text{F}_{\text{int}}]^{6-}(\text{C}_{4v})$ centers are shown in Fig.1. One can see that all nine fluorine ions are represented in these spectra. The complex SHFS was analyzed using perturbation theory. The analytical expressions were got taking into account the obvious relations ($H_{\text{ZFS}} \gg H_{\text{eZ}} \gg H_{\text{SHFI}}$).

Even though the properties of most active impurity centers have been the subject of a wide range of studies, they are still interesting because of the special features of fluorite crystal structure. One of the most important features of fluorites is that their crystal lattice contains quite volumetric interstices (so-called octahedral voids), which make intense anion diffusion possible in the crystal bulk at elevated temperatures. Due to the special features of the fluorite structure, superionic conductivity via correlated diffusion of charged defects can occur in an external electric field.

Our experiments with $\text{BaF}_{2+x}:\text{Ni}$ show that controlled synthesis of impurity defects associated with interstitial fluorine ions is possible in fluorite crystals. It was shown by EPR method that at some conditions one can get the crystals containing only $[\text{NiF}_4\text{F}_4\text{F}_{\text{int}}]^{6-}(\text{C}_{4v})$ paramagnetic centers where Ni^{3+} impurity ion and nearest interstitial F^- fluorine ion

EPR Parameters Temperature Dependences of Carbon-containing Composites

A.M. Zyuzin, N.V. Yantsen, A.A. Karpeev

National Research Mordovia State University, Saransk, Russian Federation

e-mail: nkyancen@yandex.ru

The influence of temperature on the main EPR parameters of composites based on ethylene vinyl acetate with various content of carbon black (BC) was investigated. The spectra were recorded on a radio spectrometer PS100.X at a microwave frequency of 9.3 GHz. For comparison, the temperature dependences of the EPR parameters of pure carbon black C40 were also investigated.

In the investigated temperature range the g-factor value in all samples remained equal to 2.0. From Fig.1.a it follows that the EPR absorption line width ΔH_{pp} of both composites and pure BC suffers small changes with increasing temperature. It is seen (Fig. 1.b) that the EPR line intensity of pure BC decreases with increasing temperature T . The observed decrease can be explained by the effect of the temperature factor on the population difference of the lower and upper energy levels and on the EPR signal magnitude:

$$A \sim \Delta N = \frac{N}{2} \left(e^{\frac{g\mu_B H}{2kT}} - e^{-\frac{g\mu_B H}{2kT}} \right) = N \sinh \frac{g\mu_B H}{2kT} \approx N \frac{g\mu_B H}{2kT} \quad (1)$$

It is shown that there is a good agreement between the experimental dependence $A(T)$

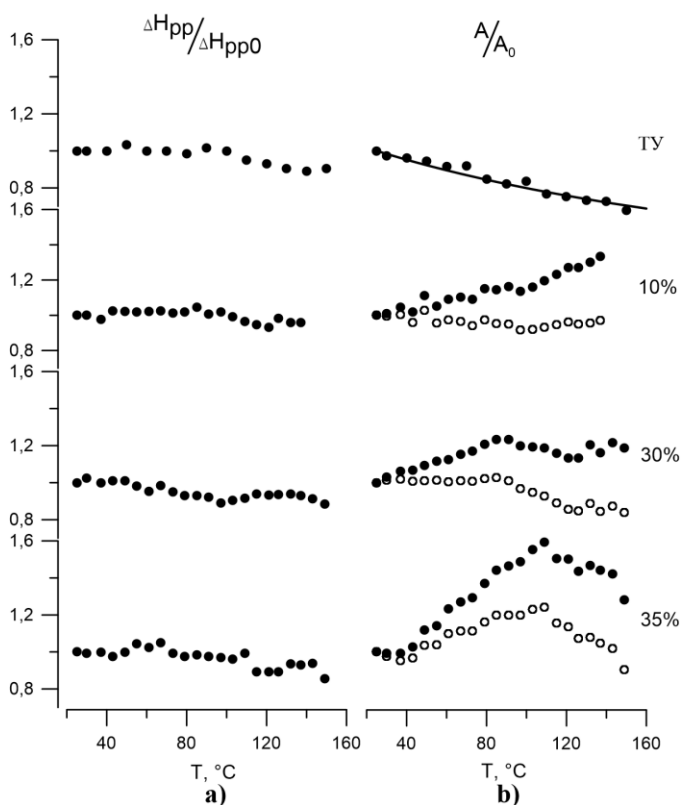


Fig.1. Temperature dependences of the normalized values of the line width ΔH_{pp} and the area under the absorption curve A . The solid line is the calculation.

and the calculated $\Delta N(T)$. From this, we can conclude that the concentration of unpaired electrons in a pure BC does not change in this temperature range. The same figure shows the dependences of $A(T)$ for composites with BC content of 10, 30 and 35%. Dependences $A(T)$ are plotted taking into account the adjustment for the temperature factor effect (dark circles, Fig. 1.b). For this purpose, the experimental value of $A(T)/A_0$ (light circles) was divided by the value $\sinh \frac{g\mu_B H}{2kT} / \sinh \frac{g\mu_B H}{2kT_0} \approx \frac{T_0}{T}$.

An increase in A with an increase in temperature indicates an increase in N , which is apparently due to the interacting electrons pairs rupture with opposite spins belonging to different BC particles in the composite material matrix, due to different values of the temperature coefficient of linear expansion of carbon black and polymer matrices.

The reported research was funded by Russian Foundation for Basic Research and the government of Mordovia Republic of the Russian Federation, grant № 18-48-130015 r_a.

Application of multiple-quantum (MQ) NMR to study the structure and dynamics of dipolar coupled $\frac{1}{2}$ spin networks in amorphous and crystalline solids

S.G. Vasil'ev

¹ Institute of Problems of Chemical Physics of Russian Academy of Sciences, Chernogolovka, Russia

e-mail: viesssw@mail.ru

NMR methods based on the excitation of multiple-quantum (MQ) NMR coherences among dipolar coupled spins nowadays occupy an important place in the investigation of structure of solids. In contrast to traditional NMR spectroscopy, where the transitions of individual spins are observed, in MQ NMR experiments the transitions among groups of interacting spins are observed. These transitions are not necessarily the transitions in the traditional sense in which the energy changes as a result of emission or absorption of electromagnetic radiation whose energy equals to the gap between the two levels. Instead the excitation may result in the appearance of the phase coherence among group of spins in the superposed state. For spins $\frac{1}{2}$ in the strong external magnetic field coupled by the dipole-dipole interaction in solids the observation of such transitions is feasible in two-dimensional multi-pulse experiments.

Pines and coworkers [1] introduced the MQ NMR experiment for large spin systems in which individual spins become correlated with one another by a virtue of their dipolar couplings. MQ NMR coherences are created on the preparation period of the experiment by a proper pulse sequence which transforms the Hamiltonian of the magnetic dipole-dipole interactions into the two-spin/double-quantum average Hamiltonian. The most illustrative application of the technique is the "spin counting", which allows determination of the number of nuclei in a bounded cluster. The underlying principle is that the maximum number of absorbed quanta equals the total number of the dipole-coupled nuclei. The growth rate of MQ coherences gives information about the magnitude and the number of dipolar couplings within the investigated systems. To establish these multiple-spin correlations, the spins need time to communicate on the order of the inverse of the size of their mutual coupling. Thus the method allows distinguishing extended spin networks from a cluster and estimating the size of the latter. This method is typically applied to the investigations of the disordered solids [2]. The benefit of the investigation of crystals is a known arrangement of spins and thus the dipolar couplings among them. Another feature is that the MQ NMR dynamics can be altered by the adjustment of the orientation of the crystal with respect to the external magnetic field.

Nuclear spins provide an insightful model of qubits owing to good isolation from the environment and wide opportunities to manipulate spin system by radiofrequency electromagnetic fields. In particular, spin-1/2 nuclei exhibit a simple two-state structure of qubits Therefore MQ NMR is attractive as the model for studying of different problems of quantum information. The interactions of the system of qubits with the environment degrade quantum correlations. This process, known as decoherence, is usually considered the main obstacle in the implementation of quantum devices. MQ NMR allow experimentally investigate the decoherence process in the systems of correlated spins [3].

This work was performed as part of the state task, state registration No. 0089-2019-0002. The work was supported by Russian Foundation for Basic Research, project no. 18-33-20166.

[1] J. Baum, M. Munowitz, A. N. Garroway, A. Pines J. Chem. Phys. 83(5), (1985), 2015

[2] S.G. Vasil'ev et al. J. Non-Cryst. Solids 489, (2018), 6–15

[3] G.A. Bochkin et al. J. Magn. Reson. 301, (2019), 10–18

The self-diffusion of polymethylsilsequioxane dendrimers in dilute solutions and melts

S.G. Vasil'ev¹, K.L. Boldyrev², E. V. Selezneva², E.A. Tatarinova², A.M. Muzafarov²

¹ Institute of Problems of Chemical Physics of Russian Academy of Sciences, Chernogolovka, Russia

² Institute of Synthetic Polymeric Materials of Russian Academy of Sciences, Moscow, Russia

e-mail: viesssw@mail.ru

Dendrimers are unique class of macromolecules in which the three dimensional structure is formed by the regular branching from a single focal point. These unique features provide great opportunities for encapsulation of small molecules and nanoparticles, adding useful functionality to the terminal groups as well as to the interior groups. In the present work we investigate the self-diffusion of polymethylsilsequioxanes (PMSSO) dendrimers. The peculiarity of the PMSSO dendrimers is that the backbone of the molecule is formed by the inorganic Si-O-Si bonds while the organic methyl groups are attached as side groups. Though the PMSSO dendrimers are among the first dendritic structures discovered the detailed studies were constrained by the absence of the non-functional derivatives until recent times.

The objects investigated in the present study are trimethylsilyl terminated PMSSO dendrimers of 1-4 generations. The self-diffusion coefficients (SDCs) were measured using spin-echo PFG NMR on a Bruker Avance III spectrometer on ¹H nuclei at 400 MHz (9.4 T). Maximum magnetic field gradient amplitude was $g=30$ T/m. The samples were diluted in toluene and also were studied in bulk. The temperature of measurements was varied between -50 and 80 °C. In the ¹H spectra of the solutions there were three resolved regions corresponding to aromatics and methyl groups of toluene and methyl groups of dendrimers. The SDCs were determined separately for these lines. The decay of the spin-echoes was linear in the coordinates of $\ln A$ vs g^2 . The SDCs of toluene in dendrimer solutions coincided among different generations and corresponded to the SDC of bulk toluene. The hydrodynamic radii of dendrimers were determined using Stock-Einstein equation. The activation energies determined from the temperature dependence using the Arrhenius equation for different generations of dendrimers in diluted solutions were almost identical (11.5 ± 0.3 kJ/mol). This value is also close to the activation energies of the self-diffusion (~ 11.0 kJ/mol) and the viscosity (~ 9.3 kJ/mol) of the neat toluene.

The changes of the SDCs with temperature in neat PMSSO dendrimers are noticeably different. Besides the increase of the activation energy compared to diluted solutions there is a significant dependence on the generation number. The dependence of the activation energy on the generation number appears to have a maximum at the third generation. Such behavior can be attributed to the densification of the structure for higher generations predicted by simulations for PMSSO dendrimers. In addition there is a deviation from a simple Arrhenius dependence for the 3-rd generation. This dependence can be more precisely described by the two different regions in the Arrhenius plot. The activation energies for the high-temperature region of the 3-d generation and other dendrimers have a good correlation with the activation energy determined from the viscosity measurements. Though the molecular mass dependence of SDCs resembles to that of the objects with dense mass distribution (determined for diluted solutions), the changes of the activation energy for the 3-rd generation may indicate some interpenetration of the dendrimer molecules.

The work was supported by Russian Foundation for Basic Research, project no. 18-33-20166

Investigation of the free induction decay in fluorine spin chains in fluorapatite in multi-pulse NMR experiment

G.A. Bochkin¹, A.V.Fedorova¹, E.B.Fel'dman¹, S.G.Vasil'ev¹

¹Institute of Problems of Chemical Physics of RAS, Chernogolovka, Moscow region, 142432, Russia

e-mail: bochkin.g@yandex.ru

In multiple quantum (MQ) NMR experiments, pulse sequences are used to cause the system to evolve under the action of a Hamiltonian different from the usual dipolar one. Here, we consider the free induction decay (FID) in spin-1/2 quasi-one-dimensional chains being irradiated by a periodic sequence of resonance 90-degree pulses used in MQ NMR experiments. The evolution of such a system is described by a two-spin/two-quantum average Hamiltonian (in the approximation of nearest neighbor interactions)

$$H_{MQ} = -\frac{D}{2} \sum_i^{N-1} (I_i^+ I_{i+1}^+ + I_i^- I_{i+1}^-),$$

where D is the dipolar coupling constant between adjacent spins, I_i^+ and I_i^- are, respectively, the raising and lowering spin angular momentum operators acting on spin i , and N is the number of spins in the chain.

The system is assumed to be in the thermodynamic equilibrium state initially. The FID $G(t)$ can be calculated using the exact solution of the Liouville equation from [1], namely, it is [2]:

$$G(t) = (2N + 1)2^{N-3} J_0(2Dt) - 2^{N-3} \cos 2Dt,$$

or, in infinite chains ($N \rightarrow \infty$) and after normalization so that $G(0)=1$,

$$G(t) = J_0(2Dt),$$

where t is the time after the start of the irradiation, and J_0 is the order-0 Bessel function of the first kind. The analytical solution is compared with the experimentally observed FID in fluorapatite, and a satisfactory agreement was found.

The FID was also calculated analytically for the low temperature case, but found to be identical to the high-temperature case up to normalization [2].

This work is supported by RFBR (project № 19-32-80004) and Presidium of RAS program № 5 “Photonic technologies in probing inhomogeneous media and biological objects”.

[1] S. I. Doronin, I. I. Maksimov, and E. B. Fel'dman. Multiple-quantum dynamics of one-dimensional nuclear spin systems in solids. J. Exp. Theor. Phys., **91**(3):597-609, 2000.

[2] G.A.Bochkin, E.B.Fel'dman, S.G.Vasil'ev The exact solution for the free induction decay in a quasi-one-dimensional system in a multi-pulse NMR experiment. Physics Letters A **383** (24), 2993-2996, **2019**

¹⁴N NMR and magnetic susceptibility of UN in the paramagnetic state

A.Yu. Germov¹, V.V. Oglobichev¹, A.M. Potapov², S.V. Verkhovskii¹

¹ M.N. Miheev Institute of Metal Physics of the Ural Branch of the Russian Academy of Sciences, Yekaterinburg, Russia

² Institute of High-Temperature electrochemistry of the Ural Branch of the Russian Academy of Sciences, Yekaterinburg, Russia

e-mail: germov@imp.uran.ru

Uranium nitride is promising compound for various branches of energy industry, because it is relatively simple magnetic system with low resistivity and high thermal conductivity. The fundamental question is the applicability of localized or itinerant electron models to describe magnetism in UN [1,2]. Properties of actinide compounds significantly depend on the degree of localization of 5*f*-electrons, which is usually characterized by the Hill's criterion [3] proposed in 1970. The criterion is determined by the ratio of the average radius of the 5*f*-shell of atom to half the distance between the actinide atoms.

The NMR method has not yet been used to the full extent in order to study the properties of uranium mononitride. Early application of NMR was limited to the recording of the resonance spectra on the isotopes ¹⁴N [4] and ¹⁵N [5], while there hasn't been a systematic measurement of the relaxation characteristics of the nuclear moments.

At this study the ¹⁴N NMR spectra, nuclear spin-lattice relaxation and magnetic susceptibility have been measured in uranium mononitride at the temperature region from 84 K to 375 K. As a result, it is shown that the temperature-dependent contribution to the NMR line shift of nitrogen is due to the magnetism of 5*f*-electrons of uranium at the paramagnetic phase of UN. The linear approximation of the $K(\chi)$ diagram gives an estimate of the constant value of the hyperfine field $H_{\text{hf}} = 2.6 \pm 0.2$ kOe/ μ_B created on the nitrogen nucleus by the 5*f*-electrons of the shell of one of the six neighboring uranium atoms. The spin-lattice relaxation data indicate that the localization of 5*f*-shell electrons of uranium takes place. The spin fluctuation energies, $\Gamma_{\text{nmr}}(T) \propto T^{0.54 \pm 0.02}$, are close to the dependence $\Gamma(T) \propto T^{0.5}$ of concentrated Kondo systems above the temperature of formation of the coherent state [6,7]. However, NMR studies over a wider temperature range are needed to obtain the degree of localization of *f*-electrons in UN.

This work was supported by the Russian Science Foundation (project № 18-72-10022).

- [1] R. Troć, Pnictides and chalcogenides III (Actinide mononictides), ed. by H. P. J. Wijn, Landolt-Börnstein, New Series, Group III, Vol. 27 Springer-Verlag, Berlin (2006).
- [2] A.Z. Solontsov, V.P. Silin, *The Physics of Metals and Metallography*, **97**, 35 (2004).
- [3] H. H. Hill, in Plutonium and Other Actinides, ed. by W. N. Miner, AIME, New York, p. 2 (1970)
- [4] M. Kuznietz, *Phys. Rev.* **180**, 476 (1969).
- [5] M. Kuznietz and D.O. van Ostenburg, *Physical Review B*, **2**, 3453 (1970).
- [6] D. L. Cox, N.E. Bickers, and J.W. Wilkins, *J. Appl. Phys.* **57**, 3166 (1985).
- [7] V.V. Oglobichev et al., *JETP Letters* **108**, 650 (2018).

Investigation of the interconversion process of pillar[5]arene using NMR spectroscopy and DFT method

A.V. Ivanova^{1,2}, E.A. Ermakova¹, D.N. Shurpik², I.I. Stoykov², B.I. Khayrutdinov^{1,2},
Y.F. Zuev¹

¹ Kazan Institute of Biochemistry and Biophysics, FRC Kazan Scientific Center of RAS,
420111, Kazan, Russia

² Institute of Physics, Kazan Federal University, 420008, Kazan, Russia

e-mail: aivanova6405@gmail.com

Development of principles for the construction of new multifunctional receptors capable of molecular recognition of biologically significant substrates is one of the rapidly developing areas of modern supramolecular chemistry. Understanding the intramolecular mobility of the host molecule is important for controlling the complexation process. The object of the study was a new class of macrocyclic compounds - pillar[5]arenes, capable of forming "host-guest" complexes [1], [2]. The aim of the work is to study the intramolecular mobility of an aqueous solution of decaammonium salt 4,8,14,18,23,26,28,31,32,35-deca (carboxymethoxy) - pillar[5]arene (hereinafter pillar [5] arene **1**).

The NMR spectroscopy was used to study the process of *pS*- and *pR*-enantiomers interconversion of pillar[5]arene **1**. The CPMG pulse sequence (Carr-Purcell-Meiboom-Gill) that allows measuring the chemical exchange rate constant of conformational process in a time range from 0.5 to 5 ms was applied. Using temperature dependence of chemical exchange rate constant the thermodynamic parameters of *pS*- and *pR*-enantiomers interconversion process were determined from the Eyring equation. Theoretical spatial models of both types of enantiomers of the studied pillar[5]arene **1** were constructed. Calculations were made to search for the transition state of aromatic rings rotation upon transition from *pS* to *pR* enantiomer. The energies of intermediates and transition states of pillar[5]arene **1** were calculated.

This work was supported by the Russian Foundation for Basic Research grant 17-03-00858a.

[1] T. Ogoshi, J. Am. Chem. Soc. 130, 5022-5023 (2008)

[2] D. Cao. As. J. Org. Chem. 3, 244-262 (2014).

Features of photoelectric of GaS monocrystal with doped rare earth elements (Yb, Sm)

A.Sh. Khaliqzadeh¹

¹Institute of Radiation Problems of ANAS, 9 B.Vahabzade str., Baku, Azerbaijan

e-mail: aydanxaliqzade@gmail.com

In recent years, intensive development of nuclear physics, photoelectronics and space research aims the opportunities of new physical properties and the preparation of new functional devices based on them in front of semiconductors. Therefore, it has a great scientific importance of studying of the physical properties of $A^{III}B^{VI}$ coupling semiconductors can be controlled by additive atoms [1]. GaS monocrystal belonging to the $A^{III}B^{VI}$ type of compounds is layered semiconductor and has a broadly prohibited zone ($E_g = 2.5\text{eV}$). GaS single crystals has heksogonal structure, lattice parameters $a = 0,359\text{ nm}$, $1,549\text{ nm}$ and $c = [1,2]$, has sequence of atoms the S-Ga-Ga-S. Each Ga atom is tetrahedrally bonded to a Ga and three S atoms [2,3].

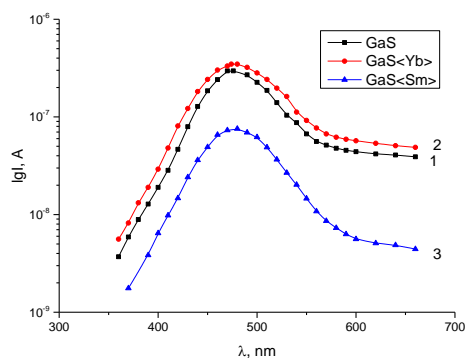


Figure 1. The spectral distribution of photocurrent of pure and doped with rare earth elements (Yb, Sm) GaS monocrystal

Figure 1 shows the spectral distribution of photocurrent of pure and doped (Yb, Sm) GaS monocrystal. The maximum at $\lambda=495\text{ nm}$ wavelength is observed in all three crystals. When the GaS monocrystalline is doped with Yb, the value of photocurrent is increasing than the pure GaS monocrystalline at the spectrum region of ($\lambda = 360\text{-}700\text{nm}$). After doping with Sm, we can observe that, the value of the photocurrent is reducing than compared pure crystals. This can be explained by the reduction of crystal photocurrent as a result of the increased effectiveness of recombination centers treating GaS monocrystal with Sm.

- [1] R. S. Madatov, A. I. Najafov, T. B. Tagiev, and A. R. Mobili. Effect of gamma irradiation on the electrical conductivity of the layered compound GaS. *Neorganicheskiye Materialy*, (2008), p.140-143, 10.1134/S0020168508020039 .
- [2] R.Zallen and F.Blossey. The optical properties, electronic structure and photoconductivity of arsenic chalcogenide layer crystals, 1976, 231-272.
- [3] M. Caraman , V. Chiricenco , L. Leontie , I.I. Rusu. Photoelectrical properties of layered GaS single crystals and related structures. *Materials Research Bulletin* 43 (2008) 3195–3201

EPR investigation of the irradiation crosslinking process of nitrile-butadiene rubber with added various types of nano-metal oxides

R.F. Khankishiyeva¹, Sh.M. Mammadov¹, H.N. Akhundzada¹, P.I. Isamyilova¹

¹Institute of Radiation Problems of ANAS, 9 B.Vahabzade str., Baku, Azerbaijan

e-mail: renanamazova0@gmail.com

The current work has been conducted the influence of various of nano-metal oxides (ZnO, Al₂O₃, ZrO₂) and aromatic disulphochloride benzene compounds (DSChB) on the properties of butadiene nitrile rubber (NBR) crosslinking by gamma rays processing. Via Electron Paramagnetic Resonance (EPR) provide a detailed characterization of the synthesized nanocomposites the active radical species.

The exposure to radiochemical processing was performed in air at room temperature inside of the source Co60 γ -radiation was used for irradiation giving a dose rate of about 4.9 kGy/h. The EPR measurements were carried out on a Bruker EMX micro X spectrometer operating in the X-frequency range, with a modulation frequency of $9.8 \cdot 10^9$ Hz ($\lambda = 3$ cm).

The concentration of paramagnetic centers and g factors were determined by the known method [1].

The method of EPR is for quantitative and qualitative estimation of free radicals in irradiated polymers. Radicals are responsible for the splitting and crosslinking of the chain. Since the free radicals are formed after irradiation, they are reacting to monomers with the helping of molecular molecules of the greatest radicals. At last, in turn, react with the monomers, and thus the chain process develops [2]. The peaks which are shown with nanocomposites in Fig. 1 are "clearly defined", whereas the spectrum of pure NBR peak is wider and it has a lower intensity. Reliable

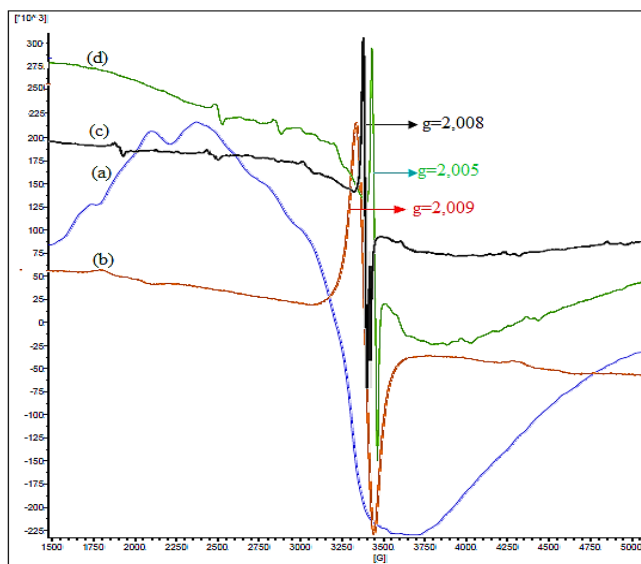


Figure 1. EPR spectrum of pure NBR (a) and irradiated nanocomposites with ZnO (b), Al₂O₃ (c),

research has shown that all three-way radiation nanocomposites have similar EPR signals. The value of g-factor for composites with ZnO, Al₂O₃ and ZrO₂ equals 2.005, 2.008 and 2.009 respectively.

The data obtained shows the behavior of the concentration of free radicals depending on the type of metal oxide, and also gives an idea of the rates of generation and recombination of free radicals after irradiation with the participation of the DSChB [3].

According to the EPR analyzes, it is revealed that the oxides of the metals on which the molecular chains of the elastomer are adsorbing and oriented and the spatial network of the polymer is formed by activation with the influence of radiation.

[1] G. Jeschke, G. Panek, S. Schleidt, J. Ulrich, *Polym.Eng.Sci.* **44**, 1112 (2004)

[2] M. Przybyszewska, M. Zaborski, *eXPRESS Polym. Lett.* **3**, 542 (2009)

[3] M. Sen, C. Uzun, Ö. Kantoğlu, *Nucl. Instrum. Methods Phys. Res. B.* **208**, 480 (2003)

Studying cyclosporin D – micelle complex by high-resolution NMR: Obtaining information on the spatial structure

P.P. Kobchikova¹, S.V. Efimov¹, V.V. Klochkov¹

¹Institute of Physics, Kazan Federal University, Kazan, 420008 Russian Federation

e-mail: pollymoon@ya.ru

There has been a great deal of interest in cyclic peptides as scaffolds in the development of drugs against difficult targets such as protein–protein interactions, based on the premise that large macrocycles are better suited to the inhibition of large binding surfaces. Solving conformations of cyclic peptides can provide insight into structure–activity and structure–property relationships, which can help in the design of compounds with improved bioactivity and/or ADME characteristics [1].

Considerable progress in transplantation of the last few decades is due to the development and introduction of immunosuppressive drugs to clinical practice, that increase the survival rates of both patients and transplants [2].

For an in-depth understanding of the mechanism of cyclosporin's activity, it should be considered in combination with micelles. Since micelles can be used to model biological membranes (on a basic level), such an experiment will allow us to draw certain conclusions regarding the conformation of cyclosporin when interacting with a cell [3].

Cyclosporin D is a congener of cyclosporin A, an immunosuppressive drug that binds to cyclophilin, inhibiting the phosphatase activity of calcineurin in T cells. The molecule of CsD consists of 11 amino acids.

Different tendencies of cyclosporin variants A, D etc. to formation of complexes with proteins (especially, cyclophilins) lead to observed differences in their biological activity. CsD interests us because the question of significance of conformation as the main factor, affecting substance's properties, is raised. The only difference between CsD's and CsA's compositions is the second amino acid residue.

Measurements were carried out on a Bruker Avance III HD 700 spectrometer. Signal assignment was made using a combination of 2D spectra: DQF-COSY, TOCSY, HSQC and HMBC, recorded at 25°C. Also ROESY technique was used for obtaining structural parameters (distances between nuclei).

Substitution of the second residue with different amino acids influences mainly the backbone chemical shifts in positions 2, its neighbors 1 and 3, and in more distant positions 5 (valine) and 8 (D-alanine). Residues 5 and 8 were the most sensitive to the amino acid substitution at the position 2.

In experiments with DPC micelles a severe overlap of signals in the high-field region (side chains) is observed; nevertheless, we can still assign the signals of the main chain. The assignment of the backbone signals should be performed anew, since the new spectrum is different from what we observed in chloroform. Since the spectra were recorded in heavy water, the signals of all α -CH groups appear quite well. Changes in their resonance frequencies allow concluding that the backbone conformation has become different after binding of the peptide molecules to the micelles, like it was reported in [4] for CsA.

[1] V.K. Gombar, *Curr. Top. Med. Chem.* **3(11)**, 1205–25 (2003)

[2] D.J. Craik, *Science* **311**, 1536-1564 (2006)

[3] D.H. Gillian, *Meth. Enzymol.* **239**, 515-535 (1994)

[4] F. Bernardi, N. D'Amelio, *J. Phys. Chem. B*, **112**, 828-835 (2008)

Glycyrrhizin-induced changes in the dynamics of single-component and multi-component phospholipid bilayers

P.A. Kononova^{1,2}, O.Yu. Selyutina¹, E.A. Shelepova^{1,2}, M.V. Zelikman^{1,2}, N.E. Polyakov^{1,3}

¹Voevodsky Institute of Chemical Kinetics and Combustion, Novosibirsk, Russian Federation

²Novosibirsk State University, Novosibirsk, Russian Federation

³Institute of Solid State Chemistry and Mechanochemistry, Novosibirsk, Russian Federation

e-mail: kononova_polina@bk.ru

Many drugs have low bioavailability. In this work, glycyrrhizic acid (GA) was studied. GA can increase bioavailability by increasing membrane permeability. GA is the main component of licorice root, which is widely used in medicine. The purpose of this work was to study the effect of GA on the molecular mobility of lipids in the phospholipid liposome under various conditions. Three types of phospholipids were used: dioleoyl-phosphatidylcholine (DOPC), palmitoyl-oleoyl-phosphatidylcholine (POPC), dipalmitoyl-phosphatidylcholine (DPPC).

Using NMR allows us to make assumptions about the localization of GA in the membrane. The NMR spectrum of protons allows you to observe various functional groups of the phospholipid. GA influence on the mobility of lipid molecules was studied by NMR relaxation technique with shift-reagents addition. Shift-reagent allows separating the inner and the outer part of the lipid bilayer. Spin-lattice relaxation times depend on molecular phospholipid rotations. Spin-spin relaxation times depend on lateral diffusion of phospholipids. Also, NMR spectroscopy allows determining the phase transition temperature in the membranes. Molecular dynamics simulation of GA interaction with lipid bilayer was also carried out.

We conducted experiments to determine the concentration dependence. A strong dependence of lipid mobility on GA concentration was detected. There are decrease spin-lattice relaxation times with increasing GA concentration for all types of liposomes. It could mean GA incorporates into lipid bilayer. This is in good agreement with the results of molecular dynamics. GA can form stable associations in some membranes. The probability of associate formation is higher for more ordered membranes. The most ordered membranes are DPPC membranes. There is a dependence of the spin-spin relaxation times on the concentration for DPPC and for mixture of DPPC and DOPC. And there is no dependence for DOPC. GA tends to form associates in more ordered membranes.

Many drugs are taken orally. The drugs go through environments with different pH. It is known that the process of self-association of GA depends on the acidity of the medium. GA forms micelles in an acidic environment. The NMR spectra of phospholipid POPC with GA in non-micellar form and micellar form shows a drop in intensity and an increase in signal width, when pH gradually increases. The spin-spin relaxation time decreases with increasing pH for DOPC with GA in non-micellar form. GA in the deprotonated form accumulates on the membrane surface; in the protonated form is located inside the lipid bilayer. Experiments with more ordered POPC did not show pH dependencies. GA probably forms fairly stable associates in the lipid bilayer and does not reach the membrane surface.

Experiments at studying phase transitions were performed with liposomes from DPPC and from a mixture of DPPC and DOPC. GA increases the collectivity of the phase transition and increases its temperature.

This study was supported by the Russian Foundation for Basic Research (grants No 18-33-00662 and 18-416-540007).

Cucurbit[7]uril behavior in PBS buffer solution and RPMI-1640 cell growth mediumE.A. Kovalenko¹, I. V. Mirzaeva¹, I. V. Andrienko¹, E. A. Pashkina²¹Nikolaev Institute of Inorganic Chemistry SB RAS, Novosibirsk, Russia²Research Institute of Fundamental and Clinical Immunology, Novosibirsk, Russia

e-mail: e.a.kovalenko@niic.nsc.ru

We checked the organic macrocyclic cavitand cucurbit[7]uril (CB[7]) behavior in PBS buffer solution and RPMI-1640 cell growth medium. While PBS is a rather simple system, it contains NaCl, KCl, Na₂HPO₄, KH₂PO₄; RPMI-1640 is a very complex medium, it contains a variety of salts (NaCl, NaHCO₃, Na₂HPO₄, KCl, MgSO₄, Ca(NO₃)₂), all essential amino acids, vitamins (i-inositol, choline chloride, para-aminobenzoic acid, folic acid, nicotinamide, pyridoxine hydrochloride, and thiamine hydrochloride, calcium pantothenate, biotin, riboflavin, cyanocobalamin), glucose and a pH indicator (phenol red). Therefore, the ¹H NMR spectrum of PBS contains only one significant signal at 3.62 ppm, except for the main H₂O signal; and RPMI-1640. The spectrum of CB[7] in D₂O (Fig.1) shows three main signals (doublets at 5.78 ppm and 4.22 ppm and a singlet at 5.51 ppm). However, there are very small additional signals at the feet of main signals which, supposedly, correspond to protonated forms of CB[7]. Upon addition of CB[7] to PBS solution, there appear some additional small signals at the foot of the 3.62 ppm signal, which indicate that there is some interaction between CB[7] and PBS medium. Also, small signals that may refer to protonated forms of CB[7] become more intense. CB[7] is known for binding positively charged cations with portal oxygen atoms. More significant changes upon the addition of CB[7] to the RPMI-1640 medium, especially with the group of signals around 0.9 ppm (Fig. 1). The triplet at 0.89 ppm

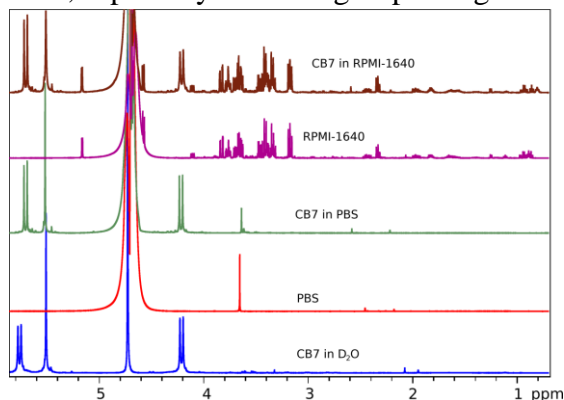


Figure 1. ¹H NMR spectra of CB[7] in D₂O, PBS, and RPMI-1640.

moves to 0.81 ppm. Other signals of the group also slightly move (about ~0.01 ppm). Such a change may indicate the formation of some stable complex with CB[7] as a result from additional shielding from the ring currents at CB[7] walls. Similar upfield shifts of the signals were registered in the systems of cucurbit[n]urils with various aminoacids [1, 2] and with Zn(II) and Cu(II) complexes [3].

The work was supported by the RFBR grant 18-315-00158 mol_a

- [1] M.E. Bush, J. Am. Chem. Soc. **127**, 14511 (2005).
 [2] E.A. Kovalenko, Appl. Magn. Reson. **46**, 281 (2015).
 [3] E.A. Kovalenko, Russ. Chem. Bull. **60**, 841 (2011).

Protein-protein interactions according to protein translational diffusion

A.M. Kusova¹, A.E. Sitnitsky¹, Yu.F. Zuev¹

¹Kazan Institute of Biochemistry and Biophysics, FRC Kazan Scientific Center, Russian Academy of Sciences, Lobachevsky Str., 2/31 Kazan, 420111, Russian Federation.

e-mail: alexakusova@mail.ru

Translational mobility of proteins is of great importance for the functioning of biological systems. Transport, thermodynamic stability, and functional activity of proteins are associated with it. Understanding the nature of the protein diffusion mobility in concentrated solutions is critically important for predicting their interactions and functional behavior. Information on intermolecular interactions can be obtained by combining experimental diffusion data with theoretical approaches.

We have proposed a complex approach to study mobility and interactions of protein molecules using the example of unstructured α_S -casein, hard globular α -chymotrypsin and rod-shaped fibrinogen. Self-diffusion and mutual diffusion of proteins were studied using nuclear magnetic resonance (NMR) and dynamic light scattering (DLS) techniques. The theoretical description of experimental data was based on the friction formalism of nonequilibrium thermodynamics [1] and the model, based on protein – protein potential of mean force, which contains the description of charge – charge, charge – dipole, dipole – dipole, dispersion Hamaker and the mean force osmotic-attraction potentials [2].

Combining the above methods, we obtained the characteristics of intermolecular interactions as friction and virial coefficients. For all proteins it yields essentially higher friction coefficients between proteins themselves than those between protein and solvent. The fibrinogen protein-protein friction coefficient is much larger than for the other studied proteins. Firstly, fibrinogen has a higher molecular weight compared to other proteins. Secondly, the fibrinogen molecules have an elongated shape, and there are moving parts at the ends of the molecule that increase the mechanical friction between them. Also from virial coefficients, it was found that the dominant contribution to the intermolecular fibrinogen interaction is given by dispersion Hamaker potential, to the α_S -casein interaction the dominant contribution is given by repulsive charge – charge potential, whereas for the case of α -chymotrypsin the contributions to the second virial coefficient from other interactions are of importance. It was determined that the proposed approach based on translational diffusivity is well suited to describe the interactions of globular, rod-shaped and intrinsically disordered proteins.

[1] H. Vink, J. Chem. Soc. Faraday Trans. 1, 1985, 81, 1725-1730.

[2] C. J. Coen, H. W. Blanch, J. M. Prausnitz, AIChE Journal, 1995, 41, 996–1004.

Confirmation preferences of carbamazepine molecules in chloroform and supercritical CO₂ by NMR spectroscopy

M.S. Kuzmikov¹, K.V. Belov², M.A. Krestyaninov², A.A. Dyshin², I.A. Khodov^{2,3}

¹Ivanovo State University of Chemistry and Technology, Ivanovo, Russian Federation

²G.A. Krestov Institute of Solution Chemistry of the Russian Academy of Sciences, Ivanovo, Russian Federation

³Institute of Physics, Kazan Federal University, Kazan, Russian Federation

e-mail: iakh@isc-ras.ru

Information on the conformational preferences of molecules of biologically active compounds is important for finding effective ways to create new drugs, as well as for improving existing ones. In the process of this work, a conformational analysis of carbamazepine in deuterated chloroform was carried out using modern two-dimensional NMR spectroscopy technique. Usually, conformational NMR-analysis is based on the internuclear distances, obtained from the experiments (¹H-¹H 2D NOESY) and quantum chemical calculations. However, due to the symmetry of the carbamazepine molecule, it is not possible to determine the conformation-dependent distance using this approach. This is due to the fact that the conformational mobility of the carbamazepine molecule is determined by the amino group. For identification of the conformations, the approach using heteronuclear two-dimensional spectroscopy ¹H-¹⁵N 2D HMBC was used. This analysis revealed minor conformations of carbamazepine molecules, that are in equilibrium with the dominant conformer fraction in solution at room temperature.

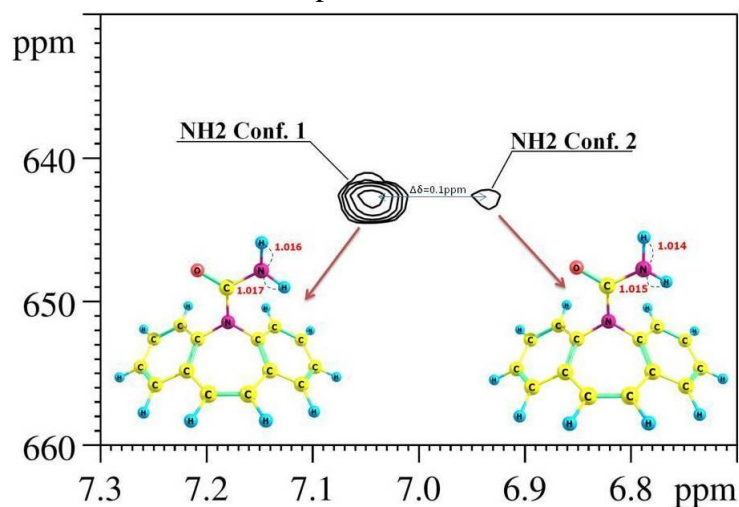


Figure 1. ¹H-¹⁵N HMBC spectrum of carbamazepine in chloroform at room temperature.

In the presented figure 1, two cross-peaks are observed, indicating the presence of two conformers with different N-H bond lengths. This approach was used for carbamazepine in supercritical carbon dioxide (CO₂) and allowed to determine the distribution of conformers at high pressure and high temperature.

Acknowledgements. The study was carried out at the USE “Molecular Fluid Spectroscopy Complex” at the expense of the Russian Federal Program grant no. RFMEFI61618×0097 (Project Number: 14.616.21.0097).

[1] I.A. Khodov, S.V. Efimov, M.Y. Nikiforov, V.V. Klochkov, and N. Georgi, *J. Pharm. Sci.*, 103 (2014).

[2] I.A. Khodov, S.V. Efimov, M.G. Kiselev, L.A.E. Batista De Carvalho, and V.V. Klochkov, *J. Mol. Struct.*, 1113 (2016).

Adiabatic excitation for NMR spectroscopy in magnetic materials

I.G. Mershie¹, G.S. Kupriyanova¹, S. Wurmehl²

¹Immanuel Kant Baltic Federal University, Kaliningrad, Russian Federation

²Leibniz Institute for Solid State and Materials Research, Dresden, Germany

e-mail: IMershie¹@kantiana.ru

Nuclear magnetic resonance spectroscopy is a well-established method for surveying the structural properties of matter. One of the applications of NMR is spectroscopy in internal magnetic field of magnetic materials. It has a few differences in comparison to conventional NMR methods: the measurements are usually performed in a gradient of hyperfine field of several Tesla, and broad spectra are acquired by spin-echo frequency sweeping. NMR is widely used for the research of nanostructures and spin-polarized materials as a tool that allows probing a local environment of the nuclei [1].

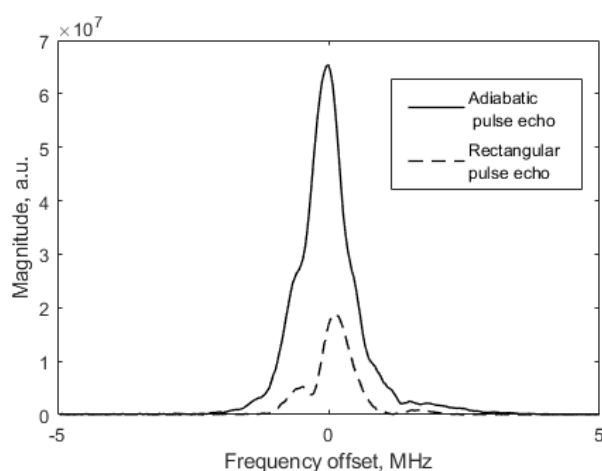


Figure 1. Fourier transforms of ^{61}Co spin echo signals of Co_2FeGa sample at 180 MHz, 295K, obtained with adiabatic hyperbolic secant pulses and conventional pulses.

walls result in a gradient of excitation field across the spin magnetization. Broadband radiofrequency pulse with compensation of B_1 field inhomogeneity is able to provide an equal excitation condition for all the spins in the domain walls. The use of adiabatic excitation pulses [3] allows both limited excitation bandwidth for spin-echo experiments with frequency sweeping and the increase in power for the spin-echo signal. In experiments with polycrystalline sample of Co_2FeGa alloy, a significant increase in signal power was obtained in comparison with conventional method. The results are applicable to the internal field NMR spectroscopy of nanostructures and samples with low natural abundance nuclei (^{53}Cr , ^{57}Fe , ^{61}Ni , etc).

This work is supported by Russian Ministry of Science and Education, project 3.12718.2018/12.2

[1] S. Wurmehl, *J. Phys. D. Appl. Phys.*, vol. 41, no. 17, p. 173002, 2008.

[2] M. B. Stearns, *Phys. Rev.*, vol. 162, no. 2, pp. 496–509, 1967.

[3] J. Baum, *Phys. Rev. A*, vol. 32, no. 6, pp. 3435–3447, Dec. 1985.

The study of ^{169}Tm in a single crystal $\text{LiYF}_4:\text{Tm}^{3+}$ (2%) by pulsed NMR method

A.S. Parfishina¹, A.V. Egorov¹, A.G. Kiyamov¹, S.L. Korableva¹, I.V. Romanova¹,
K.R. Safiullin¹, M.S. Tagirov¹

¹Institute of Physics, Kazan Federal University, Kazan, Russian Federation

e-mail: arina.parfishina@gmail.com

In this work we report the NMR studies of ^{169}Tm nucleus in a single crystal LiYF_4 with 2% impurity of Tm^{3+} ions, replacing of Y ions. These compounds are Van Vleck paramagnets. The crystalline electric field splits the energy states ground multiplet to the singlet and the nearest doublet [1]. Interesting features on the NMR spectra and relaxation characteristics in the concentrated Van Vleck paramagnets were observed [1]. The hyperfine interactions between nucleus and unfilled 4f-electron shell of rare-earth ions induce strong magnetic field at the nucleus. This is so-called “enhanced” NMR [1].

The single crystal $\text{LiYF}_4:\text{Tm}^{3+}$ has a tetragonal structure of scheelite (CaWO_4) with the space group C_{4h}^6 [2] and was grown up by the Bridgman – Stockbarger method. Crystallographic axes were found by automatic X-ray diffractometer Bruker D8 Advance and quality control of monocrystallinity of the sample was carried out. LiYF_4 crystals activated by Ho^{3+} , Er^{3+} , Tm^{3+} , Dy^{3+} ions are frequently used in lasers as a converters of the frequency of radiation into the infrared and visible spectral regions [3]. NMR-studying of the sample was carried out with using of pulse home-built spectrometer. The working range of magnetic field is 0–0.8 T, the frequency range is 3–50 MHz and the temperature range is 1.6–300 K.

In this work an angular dependencies of spin-lattice relaxation time (T_1) and spin-spin relaxation time (T_2) relatively crystallographic axes were measured. We also measured an angular dependence of the linewidth in a resonance magnetic field and a temperature dependence of spin-lattice relaxation time and spin-spin relaxation time. The difference in the distance from the ground multiplet to the nearest excited doublet for the $\text{LiYF}_4:\text{Tm}^{3+}$ were found (27 cm^{-1}). The value that was obtained earlier for the concentrated LiTmF_4 is 31 cm^{-1} [4]. We have also seen a strong anisotropic of the spin-lattice relaxation time. The angular dependence of effective gyromagnetic ratio for the diluted single crystal $\text{LiYF}_4:\text{Tm}^{3+}$ (2%) is completely matched with the angular dependence of effective gyromagnetic ratio for the concentrated paramagnet LiTmF_4 [1]. Our further plans are to continue studying of a diluted Van Vleck paramagnet and to conduct a detailed analysis in a comparison with the concentrated compounds.

The work was supported by Russian Foundation for Basic Research (grant №18-42-160012 p_a).

- [1] Aminov L K, Teplov M A “Nuclear magnetic resonance of rare-earth Van Vleck paramagnets” *Sov. Phys. Usp.* **28** 762-783 (1985)
- [2] Garcia E., Ryan R.R. *Acta Cryst.C.* **49** 2053-2054 (1993)
- [3] Walsh. B.M. “Review of Tm and Ho Materials; Spectroscopy and Lasers” *Laser Physics.* **19** 855-866 (2009)
- [4] S. Salaun, M.T. Fornoni, A. Bulou, M. Rousseau, P. Simon, J. Y. Gesland “Lattice dynamics of fluoride scheelites: I. Raman and infrared study of LiYF_4 and LiLnF_4 (Ln=Ho, Er, Tm and Yb)” *Phys.:Condens. Matter J.* **9** 6941-6957 (1997)

NMR study of carbon encapsulated Ni@C nanoparticles

D.A. Prokopyev¹, A.Yu. Germov¹, K.N. Mikhalev¹, M.A. Uimin¹, A.E. Yermakov¹,
S.I. Novikov¹, A.S. Konev¹, V. S. Gaviko¹

¹M.N. Miheev Institute of Metal Physics of Ural Branch of Russian Academy of Sciences,
Yekaterinburg, Russia

e-mail: prokopev.dima@mail.ru

Interest in the study of magnetic nanomaterials is due to their use in chemistry, biology and medicine. Magnetic nanoparticles can be used as catalysts for chemical reactions [1], as a contrast agent for magnetic resonance imaging [2] and for targeted drug delivery [3]. Special interest is caused by changing in the magnetic and chemical properties of nanoparticles depending on their size and shape [4]. Conventional methods for studying the phase composition and crystal structure of nanoparticles such as X-ray and neutron diffraction are not always applicable. NMR is convenient, universal and effective method in this case [5]. It allows to obtain the information about different phases using analysis of the nearest environment of nickel.

In this study, nanoparticles Ni@C were synthesized by gas-phase method in an inert gas stream (argon) containing hydrocarbons. The average size is 5 nm. The heated metal droplets are transferred by the argon flow to the colder part of the reactor where the nanoparticles are condensed. Then, the nanopowder was collected on a special filter.

The shell consists of several layers of carbon and can be varied depending on the hydrocarbons content in argon. The average particle size could be controlled by metal drop temperature, argon pressure in the system and the flow rate near the melting drop.

Together with the data of X-ray diffraction and magnetization, the NMR spectra ⁶¹Ni, ¹³C are presented, which allow to determine the structure and phase composition of nanoparticles.

The NMR spectra have been obtained using a Bruker AVANCE 500 pulsed NMR spectrometer in an external magnetic field, $H_0 = 11.747$ T at a room temperature (295K). The spin echo signals of ⁶¹Ni NMR have been obtained in a zero external magnetic field at a temperature of 4.2 K.

According to the analysis of NMR spectra ⁶¹Ni, the nuclei of Ni@C nanoparticles consist of metallic Ni (56 %), solid solution Ni-C (37 %) and Ni₃C carbide (7 %).

The study was performed within the state assignments of the Miheev Institute of Metal Physics of the Ural Branch of the Russian Academy of Science (state program «Function» No AAAA-A19-119012990095-0; state program «Magnit» No AAAA-A18-118020290129-5, state program «Alloys») and supported by the project of UB RAS № 18-10-2-37.

[1] Erokhin et al. Russ. J. Phys. Chem. 88, 12 (2014)

[2] D. González-Mancebo et al., Particle and Particle Systems Characterization 34, 10 (2017)

[3] A.M. Demin et al., Langmuir, 34(11), 3449 (2018)

[4] Y. Zhang et al., RSC Adv.6, 81989 (2016)

[5] K.N. Mikhalev et al., Physics of the Solid State 59, 3, 514–519 (2017)

High frequency EPR of rare-earth metal ions in LiYF₄

E.A. Razina¹, E.I. Baibekov¹, I.N. Kurkin¹, G.V. Mamin¹, M.R. Gafurov¹, S.B. Orlinski¹

¹Kazan Federal University, 420008, Kremlevskaya str.18, Kazan, Russian Federation.

e-mail: helenrazi@yandex.ru

Even though LiYF₄ microcrystals activated by rare-earth ions have been studied for decades and are well-known model systems in theoretical spectroscopy, they have recently gained attention once again due to the possibility of their application as optical elements of quantum memory. Therefore, their investigation by various methods keeps being an actual task.

The EPR spectra of one LiYF₄ doped by U³⁺ microcrystal in perpendicular orientations is shown in figure 1. The EPR spectra were measured by W-band Bruker Eleksys – 680 spectrometer at a temperature of 10K.

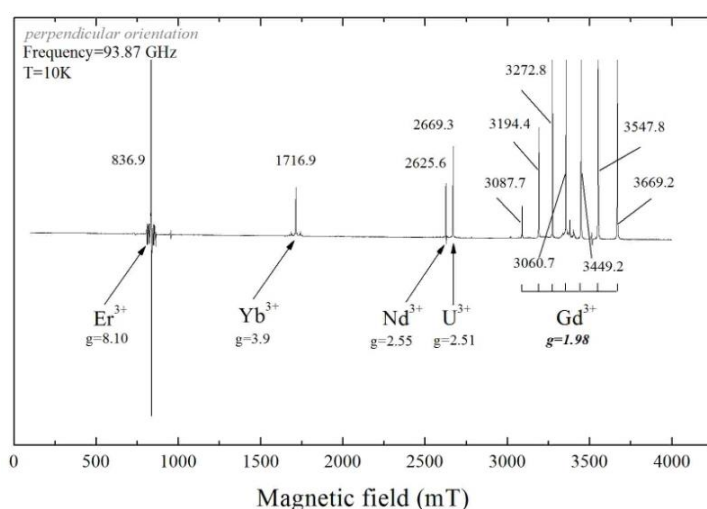


Figure 1. EPR spectra of LiYF₄ doped by rare-earth metal ions in perpendicular orientation

Rare-earth paramagnetic dopants were detected in the sample. The dopants were identified by comparing their spectroscopic parameters with the ones defined in the article [1] for the X-band.

Of particular interest are Gd³⁺ dopants, since they have $S=7/2$ and demonstrate a strong EPR signal already at room temperature.

LiYF₄ microcrystals have a tetragonal symmetry, that is, a space group I41/a. The ligands replace Y³⁺ in the nodes with a local symmetry of S₄. Therefore, the Hamiltonian can be written as:

$$H = \beta g_{\parallel} \beta H_z S_z + g_{\perp} (H_x S_x + H_y S_y) + \frac{1}{3} b_2^0 O_2^0 + \frac{1}{60} (b_4^0 O_4^0 + b_4^4 O_4^4) + \frac{1}{1260} b_6^0 O_6^0$$

Further calculations of the spin Hamiltonian parameters were performed by using Easyspin. As the initial parameters B₂, B₄, B₆ the ones given in the article [1] were used. Then the parameters were varied so that the square of the total deviation of all calculated lines from the position of practically registered lines was minimal.

Table 1. Parameters B₂⁰, B₄⁰, B₄⁴, B₆⁰

	B ₂ ⁰	B ₄ ⁰	B ₄ ⁴	B ₆ ⁰
Calculated	861.7438	97.7906	18.9978	-0.1191
Obtained in [1]	827	101	19	-0.002

Finally, as the result of the work, the quantum mechanical parameters for Gd³⁺ ions in LiYF₄ in any intermediate orientation can be calculated.

[1] Y. Valls, Solid State Communications V 45, 1093 (1983).

Emergent Ferromagnetism and Flux Trapping in Dispersed Pyrolytic Graphite Flakes by Mild Vacuum Annealing

M. Saad¹, S.I. Nikitin¹, D.A. Tayurskii¹, R.V. Yusupov¹

¹Institute of Physics, Kazan Federal University, Kazan, Russian Federation

e-mail: msaad797@gmail.com

Research on slightly twisted nanoflakes of highly ordered pyrolytic graphite (HOPG) and twisted bilayer graphene (TBG) have seen recently a new surge of interest in the search for exotic quantum phenomena, especially manifestations of high-temperature superconductivity [1–4]. Most recently, few published papers predicted the onset of superconductivity in the structure of two slightly twisted graphene bilayers, characterized by the presence of flat energy bands [2]. It is shown that the flat band of low energy is not inherited to graphene or crystalline graphite but are formed at the interfaces when the graphene/graphite sheets are twisted one with respect to another [3] by certain theoretically predicted angle (so called “magic angle”) [2]. In addition to the appearance of superconductivity, some researchers have found recently that in graphene bilayers with a small twisting angle the electrons organize themselves into a new kind of ferromagnetic state due to the orbital polarization [4]. These recent developments in twisted bilayer graphene creates a new platform for the search for exotic quantum phenomena such as superconductivity and ferromagnetism in two-dimensional carbon systems.

Following recent concepts, we experimentally prepared thin graphite flakes by an extended dispersion process and then annealed at 400°C for 48 hours either in the air [1] or in high vacuum. Using the electron microscopy, we observed large number of twisted and twinned graphite planes that were formed during the dispersion and subsequent annealing processes. In our opinion, superconducting phase inclusions in the samples appear after their annealing and reveal themselves in the observation of a stable magnetic flux trapping, that in turn is manifested in the displacement of the magnetic hysteresis loop along the magnetic moment axis after its cooling down to 10 K in magnetic field ($B = \pm 1$ T). Temperature dependences of the annealed samples remnant magnetization indicates the persistence of the flux trapping up to at least $T = 350$ K, above the room temperature. In addition, annealing of the sample in high vacuum leads to a prominent increase in the ferromagnetic component while annealing in the air suppresses it, which is most probably related to the formation of magnetically ordered states at the flake edges. Moreover, temperature dependences of the coercivity H_c (T) and saturation magnetization $M_s(T)$ analysis at $T < 100$ K present an anomalous magnetic behaviour along with the mutual influence (proximity effect) of the local ferromagnetic and superconducting constituents of the annealed in vacuum sample.

In our opinion, the observed trapped magnetic flux may be due to the appearance of superconducting regions presumably at the interfaces between graphite sheets twisted relative to each other at “magic angles” where induced persistent currents provide trapping of the magnetic flux upon cooling the sample in a magnetic field.

- [1] Saad, M. et al., JETP Letters **107**, 37 – 41 (2018).
- [2] Cao, Y. et al., Nature **556**, 7699 (2018).
- [3] Volovik, G. E. JETP Letters **107**, 516 – 517 (2018).
- [4] Sharpe et al., Science **365**, 605 – 608 (2019).

Amplification of nuclear magnetostatic oscillations in ferromagnets

S.P. Savchenko¹, M.A. Borich¹

¹M.N. Miheev Institute of Metal Physics of Ural Branch of Russian Academy of Sciences,
620108, Sofia Kovalevskaya st. 18, Ekaterinburg, Russia

e-mail: sergeysavch@imp.uran.ru

The present report is devoted to a detailed analytical investigation of the problem of coupled electron-nuclear magnetostatic oscillations in magnetic materials. The problem of magnetostatic waves propagation in a finite sample was set long time ago. It was firstly described by L.R.Walker by taking into account both magnetic moment dynamics and corresponding boundary conditions for a sample of spheroidal shape [1]. The problem of coupled electron-nuclear waves in magnetic materials also has been the object of investigation since the 70th of the XXth century [2]. It was shown that some peculiarities of spin wave dynamics occur in the vicinity of nuclear magnetic resonance (NMR) frequencies. Firstly, NMR frequency in magnetic solids is defined mainly by local magnetization, the value of which can differ significantly from external magnetic field. Secondly, resonance transitions of nuclear spins are induced mainly by variable part of electronic magnetization. Small perturbing field produces quite a big oscillations of hyperfine field, which is proportional to the dynamic part of electronic susceptibility at the NMR frequency. This phenomenon is described as the effect of amplification of external magnetic field (the effective field can be presented as $H_{\text{eff}} = \eta H_{\text{ext}}$; the order of amplification coefficient η usually is about $10 - 10^3$). Thirdly, at low temperatures, the indirect Suhl-Nakamura interaction (SNI) between nuclear spins plays an important role in magnetic dynamics [3]. It effects in substantial broadening of NMR line and in dynamic frequency shift, the value of which depends on the temperature and on the amplitude of nuclear magnetization. The broadening of NMR line and frequency pulling produce specific features in the system dynamics. For example, as it was shown in [4,5], the relaxation in nuclear subsystem can be produced through relaxation in electronic subsystem. In this case the absolute value of nuclear magnetization remains constant and hence, the relaxation differs from the Bloch type.

In this report, the homogeneous oscillations of spins in a ferromagnetic sample of spheroidal shape are investigated. Nuclear and electronic spin subsystems couple via hyperfine interaction. The sample's shape is taken into account through magnetostatic boundary conditions and corresponding boundary problem formulation. The amplification factor of nuclear spin waves is considered as a function of sample's shape and demagnetization factors. The effects of Hilbert-type dissipation in electronic subsystem and Bloch-type dissipation in nuclear subsystem on the resonance frequencies are studied as well. Based on the above provisions, we describe some previously unexplored analytical peculiarities of the problem. One of these peculiarities is that the exact mathematical expressions for amplification factor η and the effective demagnetization tensor dependent on the kind of oscillations can be analytically obtained for oscillations with $m=n$ and $m=n-1$ indexes; another peculiarity is that the consideration of dissipation terms in electron and nuclear subsystems insignificantly change the real parts of analytically-described eigenfrequencies – these real parts decrease by 0-1%.

The research was supported by UB RAS project No.18-10-2-37.

[1] L.R.Walker, Phys.Rev. **105**, 390 (1957).

[2] Turov E., Petrov M., Nuclear Magnetic Resonance in Ferro- and Antiferromagnets (Halstead Press, New York, 1972) [in Russian: Nauka, Moscow (1969)].

[3] de Gennes P., Pinkus P., Hartman-Boutron F., Winter J., Phys. Rev. **5**, 1105 (1963).

[4] Borich M., Bunkov Y., Kurkin M., Tankeyev A., JETP Letters **105**, 21 (2017).

[5] Abdurakhimov L., Borich M., Bunkov Y., Gazizulin R., Konstantinov D., Kurkin M., Tankeyev A., Phys. Rev. B **97**, 024425 (2018).

The influence of chelators on lipid oxidation

O. Selyutina¹, V. Timoshnikov^{1,2}, N. Polyakov¹

¹Voevodsky Institute of Chemical Kinetics and Combustion SB RAS, Institutskaya 3,
Novosibirsk, 630090, Russia

²Novosibirsk State University, Pirogova 2, Novosibirsk. 630090, Russia

e-mail: olga.gluschenko@gmail.com

Oxidative stress plays a huge role in the functioning of living systems and an important aspect of this problem is the oxidation of lipids, which form the basis of the cell membrane. Changes in lipids are of great importance for understanding the effect of oxidative stress on membrane interactions and processes. It is known that the oxidation of lipids leads to a change in the packing and ordering of the lipid bilayer. Here, in turn, these changes can affect a number of functional characteristics of the membrane that are important for the functioning of the membrane. In addition, oxidative stress is one of the factors that induce apoptosis. It is known that metal ions, in particular iron, play an important role in the functioning of living systems. Both their deficiency and excess can be damaging to the cells. In particular, iron ions induce lipid peroxidation in the membranes of living cells, which can lead to their destruction and death. The balance of metal ions can be controlled by means of chelator compounds. It is known that different chelators can both inhibit and enhance the negative effect of iron ions on living cells, which can be used in particular in cancer therapy.

This work is devoted to study of influence of different chelators (deferipron, mitoxantron, emadin) on dark and photo-induced oxidation of lipids by means of NMR and CIDNP techniques. In particular, it was found that deferipron completely inhibits Fenton reaction with linoleic acid and ions of Cu(II) and Fe(II). Emodin and mitoxantron also demonstrate the influence of Fenton reaction. Besides that, the influence of these chelators on Fenton reaction with Cu(II) and Fe(II) in liposomes consisting of phospholipids and linoleic acid was studied. We also investigated photo-induced oxidation of linoleic acid by different chelators in water and organic solvents.

We hope that the obtained results will help to better understand the additional aspects of the action of chelators in the body and their role in regulating oxidative stress.

The reported research was funded by Russian Foundation for Basic Research, grant №18-34-00343

Lovastatin and Their Interaction with Model Membranes by NMR Data

G.S. Shurshalova¹, D.A. Sharapova¹, A.V. Aganov¹, V.V. Klochkov¹

¹Institute of Physics, Kazan Federal University, Kazan, Russian Federation

e-mail: guzel.musabirova@bk.ru

Lovastatin is an inhibitor of 3-hydroxy-3-methylglutaryl coenzyme A (HMG-CoA) reductase which regulates low-density lipoprotein cholesterol level or otherwise bad cholesterol. This molecule is hydrophobic and is administered as inactive lactone forms, which have to be enzymatically hydrolyzed to generate active forms. In spite of this, statin molecules are very similar to each other, but their pharmacological properties vary significantly. There is a hypothesis that pharmacological features of statins depend on their location in the cell membrane, but to the present day there is a lack of information in literature on interactions of lovastatin with the surface of the cell membrane in liquid media.

In this work, as a membrane model, dodecylphosphocholine (DPC) and sodium dodecylsulfate (SDS) micelles were used. They are effectively used as surfactants in membrane modeling in NMR field due to their small size and relatively easy sample preparation.

As an experiment technique, nuclear Overhauser effect NMR spectroscopy was used. It can provide us information about the structure of the molecular complex and the exact fragment of the molecule which is responsible for the binding. Also, 2D DOSY NMR experiment was conducted for lovastatin in liquid media in the presence of micelles and without them.

The results of 2D DOSY NMR experiment showed that the self-diffusion coefficient of lovastatin is about one order lower in the presence of micelle than without it. This means a molecular complex of lovastatin + micelle is formed. According to the results of 2D NOESY NMR experiments, we can establish the location of lovastatin in DPC and SDS micelle. Despite the fact that lovastatin differs from simvastatin by one methyl group, their behavior considerably differs in DPC micelle, while there is almost no difference in localization with SDS micelle. Perhaps, this is due to the different charge of the used micelles. Lovastatin basically permeates into the hydrocarbon tails of the micelle.

Thanks to previous work, where we investigated the complex of atorvastatin, fluvastatin, simvastatin, cerivastatin and pravastatin with DPC micelle, we can estimate the dependence between the location of statin and their pharmacological features.

Acknowledgments

This work was supported by the research grant of Kazan Federal University.

Nuclear magnetic resonance study of a carbon-substituted *closo*-hydroborate NaCB₁₁H₁₂ in nanoporous silica SBA-15

R.V. Skoryunov¹, O.A. Babanova¹, A.V. Soloninin¹, A.V. Skripov¹, V. Stavila²,
M. Dimitrievska^{3,4}, M. Psurek⁵, T.J. Udovic³

¹M.N. Miheev Institute of Metal Physics, Ekaterinburg, Russian Federation

²Sandia National Laboratories, Livermore, California, USA

³NIST Center for Neutron Research, Gaithersburg, Maryland, USA

⁴National Renewable Energy Laboratory, Golden, Colorado, USA

⁵University of Maryland, College Park, Maryland, USA

e-mail: skoryunov@imp.uran.ru

Complex hydrides are known to be ionic crystals, consisting of metal cations and complex anions, such as [BH₄]⁻, [NH₂]⁻, [SiH₃]⁻, [B₁₀H₁₀]²⁻, or [B₁₂H₁₂]²⁻. Some of these systems can be potentially used as solid electrolytes in batteries [1]. To investigate the mechanisms of cation diffusion in a prospective solid electrolyte, we present the results of NMR study of atomic motion in a carbon-substituted *closo*-hydroborate NaCB₁₁H₁₂ in nanoporous SiO₂ material SBA-15 with the average pore diameter of 8 nm. The proton spin-lattice relaxation rates R_1^H measured at the resonance frequencies $\omega/2\pi = 14$ and 28 MHz as functions of the inverse temperature are shown in fig.1. The behavior of R_1^H in NaCB₁₁H₁₂/SBA-15 is governed by reorientations of complex anions via the mechanism of motionally-modulated dipole-dipole interactions between nuclear spins and it strongly differs from the behavior observed for the bulk NaCB₁₁H₁₂ [2].

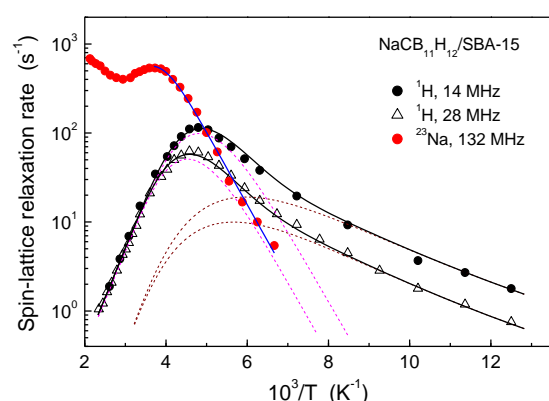


Figure 1. ¹H and ²³Na spin-lattice relaxation rates for NaCB₁₁H₁₂/SBA-15 as functions of the inverse temperature.

The observed R_1^{Na} is dominated by the quadrupole mechanism related to electric-field-gradient fluctuations due to Na⁺ diffusive jumps. According to the temperature dependence of the ²³Na NMR line widths, we can conclude that high ionic conductivity in the NaCB₁₁H₁₂/SBA-15 appears at a significantly lower temperature (~ 200 K), than in the bulk NaCB₁₁H₁₂ (~ 370 K) [2]. It makes NaCB₁₁H₁₂/SBA-15 more prospective for using as solid electrolyte in batteries.

This work was performed within the assignment of the state program No. AAAA-A19-119012990095-0, supported in part by the RFBR (Grant No. 19-03-00133).

[1] A. Unemoto et al., Appl. Phys. Lett., **105**, 083901 (2014).

[2] A.V. Skripov et al., J. Phys. Chem. C, **119**, 26912-26918 (2015).

NMR in the study of pillar[5]arene-DNA complexes

P. Skvortsova¹, D. Shurpik², I. Stoikov², B. Khairutdinov^{1,2}

¹Kazan Institute of Biochemistry and Biophysics, FRC Kazan Scientific Center of RAS,
Kazan, 420111, Russian Federation

²Kazan Federal University, Kazan, 420008, Russian Federation

e-mail: skvpolina@gmail.com

In the field of modern medicine, much attention is paid to the development of systems for targeted drug delivery, including for transfection of nucleic acids. The need to use systems for the delivery of genetic material is due to the weak transfection activity of non-viral vectors, such as plasmid DNA. In addition, the use of targeted delivery systems will allow for selective action on individual cell types. Therefore, the study of complexes of biomolecules with various synthetic compounds is of interest.

Nuclear magnetic resonance (NMR) spectroscopy is a powerful method for studying of intermolecular interactions. Different NMR techniques provide direct and indirect information about molecular complexes. Relaxation property, which changes in complexation process, and chemical shifts, which changes together with the local magnetic field, can be called indirect data. The cross peaks in the NOESY spectra provide direct information about the distances between the atoms of the molecules in the complex.

In this work the 4,8,14,18,23,26,28,31,32,35-decakis-[(N-(2', 2', 2'-triethylaminoethyl) - carbamoylmethoxy]-pillar[5]arene deca-iodide and deca-chloride in complexes with the palindromic DNA decamer were investigated by high resolution NMR spectroscopy. The NMR spectra of pillar[5]arenes were assigned using homo- and heteronuclear correlation experiments: ¹H-¹H COSY, ¹H-¹H NOESY, ¹H-¹³C HSQC, ¹H-¹³C HMBC. The formation of the pillar[5]arene complex with the DNA was shown by two-dimensional NOESY spectroscopy. The diffusion coefficients of pillar[5]arene and DNA molecules in free state and in the complex was determined by DOSY method.

This work was supported by the Russian Foundation for Basic Research No. 17-03-00858a.

Investigation of Deferiprone Influence on Generation Oxygen Species in Redox Reactions with Iron and Copper Ions using EPR Spectroscopy with Spin Traps

V.A. Timoshnikov^{1,2}, T.V. Kobzeva², O.Yu. Selyutina², N.E. Polyakov²,
G.J. Kontoghiorghes³

¹Novosibirsk State University, Novosibirsk, Russian Federation

²Institute of Chemical Kinetics and Combustion, Novosibirsk, Russian Federation

³Postgraduate Research Institute of Science, Technology, Environment and Medicine, Limassol, Cyprus

e-mail: timoshnikov@kinetics.nsc.ru

There are many iron and copper overload diseases, such as thalassemia, hemosiderosis, hemochromatosis, Wilson's disease etc. The main negative effect of these diseases is the ability of generation of reactive oxygen species (ROS) in various redox reactions with free iron and copper ions. Chelators – molecules, using for treatment metal overload diseases. Deferiprone (L1) is the drug-chelator, which is used to treat iron overload diseases, for example thalassemia. The antioxidant activity of L1 was described in the literature but detail mechanism is unknown. Moreover, it has the interest of the influence of L1 on ascorbic acid oxidation with iron and copper ions. Thus, the following tasks were set: firstly, investigation of antioxidant activity of L1 in Fenton reaction with iron and copper ions; secondly, investigation the L1 influence on oxidation of ascorbic acid with iron and copper ions. All investigations were made using optical spectrometry and EPR spectroscopy with spin traps TMIO and PBN.

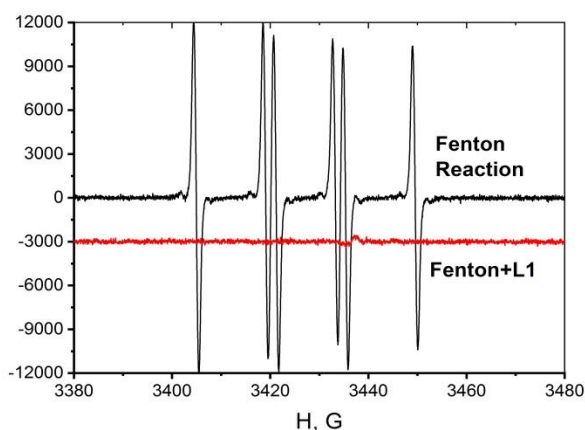


Figure 1. EPR spectra of TMIO–OH spin adducts with and without of 10 mM L1 in phosphate buffer (7.4 pH). 1 mM FeSO₄, H₂O₂ 1 mM, TMIO 10mM.

It was shown, that under addition of L1 in solution OH adduct signal was disappearing [1,2] (Fig. 1). Also, L1 decrease ascorbic acid oxidation rate in the presence of iron and copper ions. The maximum effect was observed under L1 concentration higher than 3 times concentration of Fe ions and 2 times for Cu ions.

As a result, it was shown, that L1 has antioxidant activity in Fenton and ascorbic acid oxidation reactions with iron and copper ions. The mechanism of L1 antioxidant activity based on full complexation of metal ions.

The reported research was funded by Russian Foundation for Basic Research, grant №18-34-00343

[1] V.A. Timoshnikov, Free Rad. Biol. Med. **78**, 118 (2015).

[2] V.A. Timoshnikov, J. Biol. Inor. Chem. **24**, 331 (2019).

Ferromagnetic Resonance in Exchange Coupled Ultrathin Epitaxial CoO_x/Co/Ag/Fe/MgO Heterostructures

I.V. Yanilkin¹, R.V. Yusupov¹, A.A. Rodionov¹, B.F. Gabbasov¹, M.N. Aliyev²,
L.R. Tagirov^{1,3}

¹Institute of Physics, Kazan Federal University, Kazan, Russia

²Baku State University, Baku, Azerbaijan

³Zavoisky Physical-Technical Institute, FRC Kazan Scientific Center of RAS, Kazan, Russia

e-mail: yanilkin-igor@yandex.ru

One of the physical phenomena put into a base of modern spintronics is interlayer exchange coupling in magnetic heterostructures and multilayers [1]. It is achieved utilizing ultrathin layers of ferromagnetic metals separated by non-magnetic spacer layers.

Three samples of CoO_x(8nm)/Co(4nm)/Ag(4nm)/Fe(*x*)/MgO(001) heterostructures were synthesized using combination of UHV molecular beam epitaxy (MBE) and magnetron sputtering methods. The first iron layer of the thickness *x* = 1.5, 3.3 and 5 nm and the silver layer were grown with the substrate temperature of 100°C and deposition rate of 0.1 nm/min. *In situ* LEED (low energy electron diffraction by SPECS) has shown perfect crystallinity of both layers. Next, the substrate was moved to the magnetron chamber. The metallic cobalt layer was deposited at room temperature with a rate of 1.2 nm/min, and finally, the cobalt oxide layer was deposited by reactive sputtering at a rate of 2.7 nm/min.

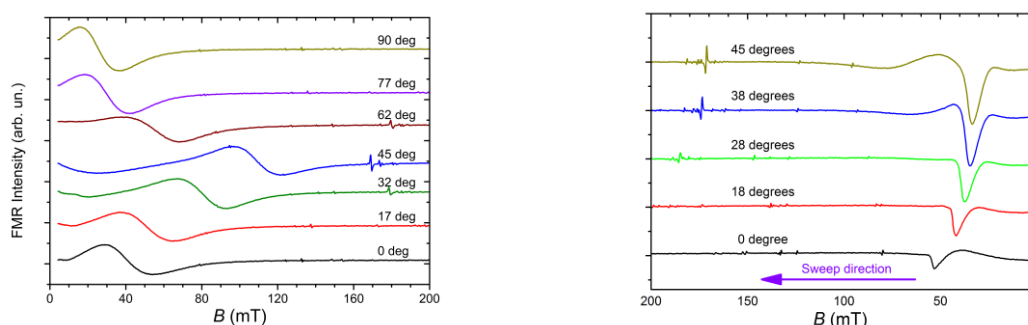


Figure 1. In-plane angular variation of the FMR spectrum of the Fe/Ag/Co/CoO heterostructure on MgO (001): left – at $T = 355$ K; right – recorded for different angles with respect to the direction [1-10] of the freezing field (4000 Oe at 180 K), when the field is cycled along the magnetic hysteresis.

Fig. 1 shows angular variation of the FMR spectrum recorded at two temperatures: left – at the temperature well above the Néel temperature of CoO ($T_N = 291$ K); right – a fragment of the FMR spectra recorded upon cycling the magnetic field along the exchange biased magnetic hysteresis loop [2] after field-cooling the sample at 0.4 T to $T = 180$ K. The single line is observed in the left panel at all angles representing a synphase ("acoustic") mode of the coupled precession of the two, iron and cobalt, layers, which occur only if the layers are interacting. In the presence of the exchange bias (right panel) two resonances are present, *e.g.* at the angle of 45°, due to a strong internal field imposed by the exchange bias: the resonances originate from the coupled oscillations of two ferromagnetic layers.

This work was supported by the RSF project No. 18-12-00459.

[1] Y. Xu, D.D. Awschalom, J. Nitta (eds.), Handbook of Spintronics, Springer Science and Business Media Dordrecht (2016), 1602 p.

[2] I.V. Yanilkin *et al.*, Magn. Res. Sol. EJ **20**, 18204 (2018).

Author index

Abdulganieva D.I.	154	Biondi B.	127
Abdullin T.R.	168	Blank A.	57, 58
Aganov A.V.	151, 196	Bochkin G.A.	179
Akhmetov M. M.	32	Bode B.	52
Akhundzada H.N.	183	Bogach A.	89
Alakshin E.M.	164	Böhme M.	39
Alexandrov A.S.	168	Boldyrev K.L.	178
Aliyev M.N.	81, 200	Bolton D.R.	52
Allision M.	86	Bordács S.	93
Al-Muntaser A.A.	33, 54	Borich M.A.	194
Amerkhanov M.I.	168	Borisenko N.I.	107
Aminov L.K.	159	Borisenko S.N.	107
Analytis J.G.	87	Borodkin G.S.	107
Andersen M.	133	Boukhvalov D.	99
Andrienko I.V.	186	Bowman M.K.	22
Andronenko S.I.	105	Bragin A.V.	168
Anisimov M.	89	Buchanan L.	37
Anisimov N.V.	134, 135	Buechner B.	70, 71, 72, 78, 131, 132
Annino G.	39	Bunkov Yu.M.	34
Antonschmidt L.	142	Buntkowsky G.	35, 173
Apreleva A.S.	172	Bussmann-Holder A.	155
Arda L.	162	Butykai Á.	93
Artzi Y.	57	Caneschi A.	39
Atsarkin V.A.	64	Carmieli R.	65
Augustyniak-Jabłokow M.A.	65	Chachkov D.	76
Avdoshenko S.	132	Chen Jiafu	156
B chner B.	60	Chen Kepeng	153
Babanova O.A.	197	Chernov N.M.	125
Badelin A.G.	98	Chervonova U.	95
Bagryanskya E.G.	136, 146, 147, 150, 173	Chinak O.A.	147
Bahrenberg T.	141	Chubarov A.S.	136, 146, 150
Baibekov E.I.	66, 192	Cini A.	39
Baines C.	86	Cox M.	62
Bakirov M.M.	21, 111, 112	Cruickshank P.A.S.	52
Bales B.L.	21	Curro N.J.	87
Barbon A.	113	De Zotti M.	149
Batista de Carvalho L.A.E.	106	Degtyarev Ye.N.	116
Batth A.	142	Deminov R.G.	73
Batulin R.G.	158	Demishev S.V.	67, 74, 89
Bayazitov A.A.	154	Dengre S.	86
Becker D.	142	Dikanov S.A.	137
Becker S.	142	Dimitrievska M.	197
Belousova N.N.	168	Dolgorukov G.A.	164
Belov K.V.	106, 128, 188	Drescher M.	138
Bibi E.	141	Dudysheva N.	108
		Dvinskikh S.V.	36
		Dyrkheeva N.	136

Dyshin A.A.	188	Gafurov M.R.	66, 126, 151, 159, 192
Dzheparov F.S.	23, 61	Gafurov Z.N.	131
Dzuba S.A.	108, 127, 139, 149	Gaifullin R.R.	73
Eaton G.R.	37, 109	Galeev R.T.	96
Eaton S.S.	37, 109	Gardner J.	86
Edge R.	170	Gareth Williams J.A.	62
Efimov S.V.	106, 110, 114, 128, 184	Garif'yanov N. N.	60
Egorov A.V.	190	Garifullin I. A.	60
Egorova A.S.	122	Garifzyanova G.G.	158
Ehlers D.	84, 93	Gaviko V.S.	191
Eichele G.	142	Geirhos K.	93
Eichhoff U.	38	Germov A.Yu.	180, 191
El Mkami H.	52	Geru I.I.	25, 40
Engelke M.	142	Gescheidt G.	113
Eremeev I.E.	128	Giambastiani G.	131
Eremin M.V.	68	Giese A.	142
Eremina R.M.	69, 98	Gilmanov M.I.	74, 89
Ermakova E.A.	181	Gizatullin B.	41
Ermolaeva O.	90	Godovikova T.	136, 150
Esmacili A.M.	81	Goldfarb D.	141
Fakhrutdinov A.R.	154	Goldner P.	59
Falin M.L.	157	Golubev A.	151
Farhutdinov A.R.	34	Golubov A.A.	73
Fatkullin N.F.	121	Golyshev V.M.	147
Fattakhov Ya.V.	154	Golysheva E.	108
Fedaruk R.	65	Goovaerts E.	62, 160
Fedin M.V.	136, 146	Gorelysheva V.E.	122
Fedorova A.V.	179	Gorev R.	90
Fedotov A.	126	Goryunov Yu.V.	75
Fel'dman E.B.	24, 179	Grafe H-J.	70, 72
Fielding A.	140	Graham B.	141
Filatov A.S.	124	Griesinger C.	142
Filipov V.B.	74, 89	Gruzdev M.	95
Fischer A.	142	Gu Genda	100
Fittipaldi M.	39	Gubaidullin A.T.	78
Flitsch S.L.	140	Gubkin A.	99
Fomin A.S.	147	Guguchia Z.	155
Fomina D.V.	134	Gumarov A.I.	26, 81, 101, 103
Fominov Ya. V.	60	Gumarov G.G.	111, 112
Formaggio F.	127, 149	Gusev N.	90
Frolova E.N.	158	Gutmann T.	173
Fuentes J.C.	142	Hagiwara M.	91
Gabbasov B.F.	103, 200	Hälg M.	92
Gabidullina A.A.	98	Han Songi	53
Gafarova A.R.	111, 112	Hara S.	83
Gafiyatullin L.G.	32, 158	Hedison T.M.	170
Gafurov D.	70, 71, 72	Hernandez A.Martinez	142
		Herrmannsdörfer T.	86

Heyes D.J.	170	Kintzel B.	39
Hirao R.	173	Kirillov V.L.	97
Hirata H.	143	Kirilyuk I.	150
Hiroi Z.	83	Kiselev M.G.	114
Höfer P.	38	Klauss H.-H.	86, 87
Hollas M.A.	140	Klimavicius V.	173
Hou Yuqi	153	Klochkov A.V.	164
Huber M.	42	Klochkov V.V.	110, 128, 151, 184, 196
Huber T.	141	Klochkova E.	151
Hunter R.I.	52	Kobchikova P.P.	184
Iakovleva M.	70, 71	Kobzeva T.V.	199
Isaev N.P.	148	Kochelaev B.I.	79
Isamyilova P.I.	183	Kokorin A.I.	115, 116
Ivanov D.	161	Komlev V.	126
Ivanova A.V.	181	Kondratyeva E.I.	164
Ivanova T.A.	76, 169	Konev A.S.	99, 191
Jeziarska J.	130	Kononova P.A.	185
Kabanov V.V.	77	Konov K.	117
Kamashev A. A.	60	Konstantinova E.A.	44, 45, 46, 115, 116
Kandrashkin Yu.E.	27, 171	Kontoghiorghes G.J.	199
Kaptein R.	144	Koopmans B.	62
Karataeva F.Kh.	110	Korableva S.L.	190
Karataş Ö.	162	Korolev A.	99
Karpasuk V.K.	98	Kororin A.I.	44
Karpeev A.A.	31, 176	Kovalenko E.	186
Karschin N.	142	Kremer R.K.	80
Karube K.	84	Krestyaninov M.A.	188
Kataev V.	60, 70, 72, 78, 131, 132	Krug von Nidda H.-A.	69, 84, 93
Kazan S.	162	Krumkacheva O.	136, 146, 150, 173
Keeble D.	52	Kühn J.	142
Keller H.	155, 163	Kukovitsky E.	166
Kézsmárki I.	84, 93	Kulbachinskii V.A.	46
Khabipov R.Sh.	154	Kuligina E.V.	147
Khaibullin R.I.	103, 162	Kulik L.V.	148
Khairutdinov B.	198	Kupriyanov M.Yu.	73
Khairuzhdinov I.T.	21, 28, 132	Kupriyanova G.S.	189
Khaliqzadeh A.Sh.	182	Kurkin I.N.	66, 159, 192
Khankishiyeva R.F.	183	Kushnir V.N.	73
Khasanova N.M.	33, 43, 54	Kusova A.M.	187
Khayrutdinov B.I.	181	Kuzhelev A.A.	136
Khizrieva S.S.	107	Kuzmikov M.S.	188
Khodov I.A.	106, 114, 128, 188	Kuzmin V.V.	164
Khramtsov V.V.	145	Lapina O.B.	118
Khusainov I.	151	Latypov V.A.	157
Khusnuriyalova A.F.	78, 131	Lavrik O.	136
Kida T.	91	Leonov A.	142
Kiiamov A.G.	26, 101, 103, 190	Leushin A.M.	157

Likhtenshtein G.I.	165	Nosov I.Yu.	82
Ling C. D.	86	Novikov S.I.	191
Lomzov A.	136	Nurgaliev D.K.	43, 54
Lorenz W.E.A.	92	Nuzhdin V.I.	103
Lovett J.E.	52	Nys K.	152
Lukoni L.	131	Obinger C.	152
Lundin A.A.	30	Ogloblichev V.V.	180
Lunkenheimer P.	93	Ohmichi E.	83
Lvov S.	166	Ohta H.	48, 83
Maier J.	142	Okamoto T.	83
Majchrzycki Ł.	65	Okay C.	162
Maksimenko E.V.	107	Okubo S.	83
Malkin B.Z.	66, 85, 159	Okuma R.	83
Mamin G.V.	66, 126, 192	Opherden L.	86
Mammadov Sh.M.	183	Orekhov N.D.	120
Martyanov O.N.	97, 167	Orian J.-C.	86
Martyshov M.N.	45	Orlinskii S.B.	66, 126, 192
Matsuoka H.	173	Ostroumova G.M.	120
Mattea C.	41	Ostrovskaya I.K.	121
Matveeva A.G.	127, 149	Ovcherenko S.S.	147
Matysik J.	47	Ovchinnikov I.V.	76, 158, 169
Mchaourab H.S.	141	Ozarowski A.	130
McPeak J.	37	Papulovskiy E.	118
Mei Z.	87	Parfishina A.S.	190
Melnikova D.	161	Pashkina E.A.	186
Mershiev I.G.	189	Pavlikov A.V.	45
Mikhalev K.N.	191	Pavlova O.S.	134, 135
Miksch B.	93	Peng Y.	96
Mingalieva L.V.	96, 158	Petr A.	78, 131
Minin A.	99	Petrenko O.	91
Mironov V.	90	Petrov A.V.	101
Mirzaeva I.V.	186	Petukhov V.Yu.	111, 112
Mishra S.	141	Pfanzagl V.	152
Misra S.K.	105	Pichkovskiy I.S.	63
Möbius K.	119	Pirkuliyeva S.	142
Mohammed W.M.	81	Pirogov Yu.A.	134
Molochnikov L.	99	Plass W.	39
Morozov O.	85	Pliotas C.	52
Morozov V.	131	Poggio M.	93
Morozov V.I.	78	Pokrovskii V.Ya.	88
Morozov V.P.	43	Polienko Yu.F.	136, 146
Mukhamedshin I.R.	88	Politanskaya L.V.	146
Murzakaev V.M.	168	Polyakov N.E.	185, 195, 199
Murzakhanov F.	151	Popov A.	132
Muzafarov A.M.	178	Potapov A.M.	180
Nakazawa S.	173	Povarov K.Yu.	92
Nateprov A.N.	75	Powell A.K.	96
Nath N.	142	Prando G.	72
Nikitin S.I.	101, 159, 193	Preißinger M.	84
Norman D.	52	Prisner T.F.	49

Prokopyev D.A.	191	Seidov Z.I.	98
Psurek M.	197	Selezneva E.V.	178
Ptushenko V.V.	148	Selivanov S.I.	124, 125
Pyshnaya I.A.	147	Selyutina O.Yu.	185, 195, 199
Pyshnyi D.	136	Semakin A.S.	88, 158
Quine R.W.	37	Semeno A.	89
Rameev B.	162	Sergeicheva E.	85
Ranjan V.	50	Sessoli R.	39
Razina E.A.	192	Shagalov V.A.	154
Reggelin M.	142	Shakirov A.A.	157
Reshetnikov N.M.	154	Shakurov G.S.	175
Richter V.A.	147	Shanmugam M.	170
Rinard G.A.	37	Sharapova D.A.	196
Robertson D.A.	52	Shavelev A.A.	157
Rodionov A.A.	26, 66, 159, 200	Shelepova E.A.	185
Roefs J.	152	Sherman A.	58
Rogov A.M.	26	Shernyukov A.V.	147
Rogozhnikova O.	146, 150, 173	Shevelev G.	136
Roleder K.	155	Shi Y.	37
Romanova I.V.	85, 190	Shimoshiro S.	83
Rosenfeld E.	99	Shinkarev A.A.	122
Rüffer T.	132	Shiomi D.	173
Ruiz A.	87	Shitsevalova N.Yu.	74, 89
Ryzanov S.	142	Shtirberg L.	57
Saad M.	193	Shubin A.A.	118
Sadykhov E.G.	134	Shurpik D.	181, 198
Safin T.R.	34	Shurshalova G.S.	196
Safiullin G.M.	157	Shurtakova D.V.	126
Safiullin K.R.	164, 190	Sieme D.	142
Saito Y.	83	Sinyashin O.G.	78, 131
Sakharov B.V.	33, 43, 54	Sitnitsky A.E.	187
Sakurai T.	83	Sivak M.V.	116
Salikhov K.M.	21, 29, 132, 154	Skirda V.D.	161, 168
Samarin A.N.	74	Skorokhodov E.	90
Samoson A.	51	Skoryunov R.V.	197
Sannikova N.E.	149	Skripov A.V.	197
Sapozhnikov M.	90	Skvortsova P.	198
Sarkar R.	86, 87	Slageren J. van	123
Sato K.	173	Sluchanko N.E.	74
Savchenko S.P.	194	Smirnov A.I.	91, 92
Savinkov A.V.	122	Smirnov I.	126
Schäfter D.	123	Smith G.M.	52
Scheffler M.	93	Smorygina A.S.	127
Schmallegger M.	113	Sobornova V.V.	128
Schumann J.	60	Söhnel T.	86
Schwartz R.N.	21	Soldatov T.A.	91, 92
Scrutton N.S.	170	Soloninin A.V.	197
Scurschii I.	70	Solovchenko A.E.	148
		Sosin S.	85
		Spitsyna A.	150

Stanislavovas A.A.	164	Tuck K.L.	141
Stankevich K.L.	23, 61	Turanov A.N.	32, 158
Stapf S.	41	Turanova O.A.	32, 76, 158, 169
Stavila V.	197	Tyurin V.S.	171
Stegailov V.V.	120	Udovic T.J.	197
Stein R.A.	141	Uhlarz M.	86
Stepakov A.V.	124	Uimin M.A.	99, 191
Stoikov I.	198	Ulanov V.A.	174, 175
Stoykov I.I.	181	Usachev K.	151
Strzelczyk R.	65	Vagizov F.G.	82, 98, 103
Sturza M.-I.	70, 71	Vahin A.	161
Subbotin K.A.	172	Vakhitov I.R.	81
Sudakov I.V.	62	Valeev V.F.	103
Sugisaki K.	173	Validov A.A.	60
Sukhanov A.A.	96, 171, 172	Validov Sh.	151
Sukhov A.V.	78	Van Doorslaer S.	62, 152
Sun H.	142	Varfolomeev M.A.	33, 43, 54
Suwaid M.A.	33	Vasil'ev S.G.	177, 178, 179
Sviridov D.V.	116	Vavilova E.	70, 71, 72
Sviridov E.A.	147	Vemulapalli P.	142
Sviridova T.V.	116	Verkhovskii S.V.	180
Sryamina V.N.	127, 149	Vetoshko P.M.	34
Szigeti B.G.	84, 93	Vindigni A.	39
Tadyszak K.	65	Volegov A.	99
Tagirov L.R.	26, 73, 81, 94, 101, 200	Volkov M.Yu.	32, 158
Tagirov M.S.	34, 85, 164, 168, 190	Volkov V.I.	129
Taguchi Y.	84	Volkov V.Y.	33, 43, 54
Takahshi H.	83	Vorobeva V.	95
Takata A.	91	Voronkova V.K.	96, 132, 171
Takui T.	173	Wang S.	124
Tarasov V.F.	172	Wang Zhijia	153
Tarasova A.A.	134	Webb S.J.	140
Tatarinova E.A.	178	Weheabby S.	132
Tayurskii D.A.	193	Weiner L.	113
Tedlla B.Z.	62	Welinski S.	59
Timofeev I.	146, 173	White J.S.	93
Timoshnikov V.A.	195, 199	Whittle V.L.	62
Toniolo C.	149	Wienands J.	142
Tormyshev V.	136, 146, 150, 173	Witwicki M.	130
Toyota K.	173	Wong L.	142
Tretyakov E.V.	146	Woodcock L.	37
Trubitsin B.V.	148	Wu Chunyan	156
Trukhan S.N.	167	Wurmehl S.	189
Trukhin D.	146, 150, 173	Wylde R.	52
Trusov G.V.	46	Yakhvarov D.G.	78, 131
Tsai Ping-Chun	100	Yakovlev I.P.	125
Tsurkan V.	84, 93	Yakushkin S.S.	97, 167
		Yanilkin I.V.	26, 81, 101, 200

Yantsen N.V.	31, 176
Yardeni E.H.	141
Yarnykh V.L.	135
Yatsyk I.V.	98, 174
Yatsyk I.V.	175
Yermakov A.E.	99, 191
Young Ben-Li	100
Yusupov M.	151
Yusupov R.V.	26, 81, 101, 103, 193, 200
Zainullin R.R.	17, 175
Zaitzev V.B.	44
Zapasskii V.S.	55
Zapevalov V.E.	56
Zaripov R.B.	28, 132, 175
Zaytseva E.	173
Zelikman M.V.	185
Zgadzai O.	57
Zhang Xue	153
Zhao Jianzhang	153
Zharikov E.V.	172
Zheludev A.	92
Zhitomirsky M. E.	91
Zhu F.	62
Ziatdinov A.M.	102
Zinnatullin A.L.	82, 98, 103
Zobov V.E.	30, 63
Zomot E.	141
Zuev Yu.F.	181, 187
Zvyagin S.	104
Zybtsev S.G.	88
Zyuzin A.M.	31, 176

CONTENTS

Theory of Magnetic Resonance

<i>M.M. Bakirov, B.L. Bales, I.T. Khairuzhdinov, K.M. Salikhov, R.N. Schwartz</i> Spin-Lattice Relaxation Times of a Nitroxide Radicals in Solution Under the Influence of Spin-Exchange and Dipole-Dipole Interactions.....	21
<i>M.K. Bowman</i> Electron Spin Relaxation and Motion in Solids: Spin, Spatial, Spectral.....	22
<i>F.S. Dzheparov, K.L. Stankevich</i> Theory of Spin Pumping in Fe/NM.....	23
<i>E. Feldman</i> Multiple quantum NMR dynamics and relaxation in one-dimensional systems..	24
<i>I.I. Geru</i> The Time Reversal Symmetry and a Virtual Time Reversal Method in EPR Spectroscopy.....	25
<i>A.I. Gumarov, I.V. Yanilkin, A.A. Rodionov, A.G. Kiiamov, A.M. Rogov, R.V. Yusupov, L.R. Tagirov</i> FMR Studies of Thin Epitaxial Pd _{0.92} Fe _{0.08} /Pd _{0.96} Fe _{0.04} and Pd _{0.92} Fe _{0.08} /Ag/Pd _{0.96} Fe _{0.04} Heterostructures.....	26
<i>Yu.E. Kandrashkin</i> Hyperfine Interaction Promoted Intersystem Crossing.....	27
<i>I. Khairuzhdinov, R. Zaripov</i> Determination T ₁ and T ₂ Relaxation Times from CPMG Phase Cycle Pulse Sequences.	28
<i>K.M. Salikhov</i> Spin Exchange in Solutions of Paramagnetic Particles. <i>Paradigm Shift</i>	29
<i>A.A. Lundin, V.E. Zobov</i> Multiple-Quantum NMR Spectroscopy and Quantum Information Delocalization in Solids in the Presence of Magnetic Fields Inhomogeneities.....	30
<i>A.M. Zyuzin, A.A. Karpeev, N.V. Yantsen</i> Intensity of EPR Absorption Lines in Semiconducting Substances.....	31

New Methods and Techniques

<i>M. Volkov, O. Turanova, A. Turanov, L. Gafiyatullin, M. M. Akhmetov</i> Determination of Insulating Oil Moisture Content by NMR Spectroscopy.....	32
<i>A.A. Al-Muntaser, M.A. Varfolomeev, V.Y. Volkov, N.M. Khasanova, B.V. Sakharov, M.A. Suwaid</i> SARA Analysis and NMR Relaxation as Prediction Techniques to Estimate the SARA Composition of Heavy and Light Oils – Correlations and Deviations.....	33
<i>Yu.M. Bunkov, A.R. Farhutdinov, T.R. Safin, M.S. Tagirov, P.M. Vetoshko</i> Spin Superfluidity at Room Temperature.....	34

<i>G. Buntkowsky</i> Hyperpolarisation Techniques for the Investigation of Enzyme-Inhibitors and Functional Nanomaterials.....	35
<i>S.V. Dvinskikh</i> Multinuclear Dipolar NMR Spectroscopy in Liquid Crystals.....	36
<i>S.S. Eaton, L. Buchanan, L. Woodcock, J. McPeak, G.A. Rinard, R.W. Quine, Y. Shi, G.R. Eaton</i> Multi-frequency Rapid-scan EPR.....	37
<i>P. Höfer, U. Eichhoff</i> Milestones in the 62 years Bruker EPR History.....	38
<i>M. Fittipaldi, A. Cini, G. Annino, A. Vindigni, A. Caneschi, B. Kintzel, M. Böhme, W. Plass, R. Sessoli</i> Spin-Electric Coupling Revealed by Electric Field Modulated EPR.....	39
<i>I.I. Geru</i> Deceleration of Proton Spin-Lattice Relaxation in Water under Ultrasonic Radiation....	40
<i>B. Gizatullin, C. Mattea, S. Stapf</i> Fast Field Cycling NMR Relaxometry enhanced by DNP for Study Complex Systems..	41
<i>M. Huber</i> EPR Approaches to Amyloid Protein Aggregation.....	42
<i>N.M. Khasanova, B.V. Sakharov, V.P. Morozov, V.Y. Volkov, M.A. Varfolomeev, D.K. Nurgaliev</i> Quantitative Characterization of the Kerogen Domanic by Low-Field NMR and EPR methods.....	43
<i>E.A. Konstantinova, A.I. Kororin, V.B. Zaitzev</i> EPR Spectroscopy of Semiconductor Nanomaterials: New Approaches.....	44
<i>E.A. Konstantinova, A.V. Pavlikov, M.N. Martyshov</i> Defect Properties of Titania Obtained by Laser Sintering.....	45
<i>E.A. Konstantinova, G.V. Trusov, V.A. Kulbachinskii</i> EPR Study of Titania Microspheres with Different Chemical Composition.....	46
<i>J. Matysik</i> Photo-CIDNP in solids.....	47
<i>H. Ohta</i> Multi-Extreme THz ESR -Recent Applications and the Future-.....	48
<i>T.F. Prisner</i> Shaping up EPR: Phase/Amplitude Modulated Pulses for Dipolar Spectroscopy.....	49
<i>V. Ranjan</i> High Sensitivity Quantum-limited Electron Spin Resonance.....	50
<i>A. Samoson</i> H-MAS.....	51
<i>R.I. Hunter, H. El Mkami, D.R. Bolton, J.E. Lovett, B. Bode, C. Pliotas, D. Norman, D. Keeble, R. Wylde, D.A. Robertson, P.A.S. Cruickshank, G.M. Smith</i> High Concentration Sensitivity, High Bandwidth and Low Deadtime Pulsed EPR.....	52

<i>Songi Han</i> Dynamic Manipulation of Electron Spin Dynamics to boost Dynamic Nuclear Polarization.....	53
<i>V.Y. Volkov, B.V. Sakharov, N.M. Khasanova, A.A. Al-Muntaser, M.A. Varfolomeev, D.K. Nurgaliev</i> Low-Field NMR Full FID Method for the Study of Heterogeneous Objects.....	54
<i>V.S. Zapasskii</i> Spin Noise Spectroscopy as an Alternative to Zavoisky’s Technique.....	55
<i>V.E. Zapevalov</i> Modern Gyrotrons and Their Applications.....	56
<i>O. Zgadzai, L. Shtirberg, Y. Artzi, A. Blank</i> Selective Addressing and Readout of Optically Detected Electron Spins.....	57
Spin Technologies and Devices	
<i>A. Blank, A. Sherman</i> Diamond-Based Quantum Amplifier.....	58
<i>S. Welinski, P. Goldner</i> Optically Detected Spin Resonance in Rare Earth Doped Crystals for Quantum Technologies.....	59
<i>A. A. Kamashev, N. N. Garif’yanov, A. A. Validov, J. Schumann, V. Kataev, B. Büchner, Ya. V. Fominov, I. A. Garifullin</i> Superconducting Spin-Valve Effect in a Heterostructures Containing the Heusler Alloy as Ferromagnetic Layers.....	60
<i>F.S. Dzheparov, K.L. Stankevich</i> Spin Pumping Theory of Ferromagnetic – Normal Metal Structures (in the case of $\text{La}_{2/3}\text{Sr}_{1/3}\text{MnO}_3/\text{NM}$ Bilayers).....	61
<i>I.V. Sudakov, B.Z. Tedlla, F. Zhu, M. Cox, B. Koopmans, V.L. Whittle, J.A. Gareth Williams, S. Van Doorslaer, E. Goovaerts</i> Photon Upconversion via Triplet Exciton Fusion in the Super-yellow PPV:PtTPBP Host–sensitizer System.....	62
<i>V.E. Zobov, I.S. Pichkovskiy</i> Associative Memory on Qutrits by means of Quantum Annealing.....	63
Low-dimensional, Nanosized, Strongly Correlated Electronic Systems	
<i>V.A. Atsarkin</i> Spin Current Induced by Magnetic Resonance in Ferromagnet-normal Metal Bilayers...	64
<i>M.A. Augustyniak-Jablokow, K. Tadyszak, R. Strzelczyk, R. Fedaruk, R. Carmieli, Ł. Majchrzycki</i> Slow Paramagnetic Relaxation in Graphene Oxide and Partially Reduced Graphene Oxide.....	65

<i>E.I. Balbekov, G.V. Mamin, M.R. Gafurov, S.B. Orlinskii, B.Z. Malkin, A.A. Rodionov, I.N. Kurkin</i> Experimental Realization of Qubit and Qutrit Quantum Manipulations using EPR of Rare Earth Ions in Single Crystals.....	66
<i>S.V. Demishev</i> Three and a Half Puzzles in EPR Physics of Strongly Correlated Materials.....	67
<i>M.V. Eremin</i> Toward the Theory of the Spins and Orbital Moments Coupling with Electric Field.....	68
<i>R. Eremina, H.-A. Krug von Nidda</i> Anisotropic Exchange Interaction in Low Dimensional Systems.....	69
<i>D. Gafurov, M. Iakovleva, I. Scurschii, M.-I. Sturza, H-J. Grafe, V. Kataev, B. Buechner, E. Vavilova</i> Study of Nonmagnetic Impurities in the Frustrated S=1/2 Spin Chains: NMR and Magnetization Study.....	70
<i>D. Gafurov, M. Iakovleva, M.-I. Sturza, B. Buechner, E. Vavilova</i> Effect of Lithium Deficiency on the Ion Mobility in Frustrated $\text{Li}_{1-x}\text{CuSbO}_4$ Compound Studied by NMR.....	71
<i>D. Gafurov, E. Vavilova, G. Prando, H-J. Grafe, V. Kataev, B. Buechner</i> Temperature Evolution of Magnetic Properties of Sodium Iridates $\text{Na}(3/2)\text{M}(1/2)\text{IrO}_3$ (M = Ni, Cu, Zn) probed by NMR and μSR	72
<i>R.R. Gaifullin, V.N. Kushnir, R.G. Deminov, L.R. Tagirov, M.Yu. Kupriyanov, A.A. Golubov</i> Comparative Study of S/F/S/F and S/F/N/F superconducting Spin-Valves.....	73
<i>M.I. Gilmanov S.V. Demishev, A.N. Samarina, N.Yu. Shitsevalova, V.B. Filipov, N.E. Sluchanko</i> Electron Paramagnetic Resonance Study of $\text{Ho}_x\text{Lu}_{1-x}\text{B}_{12}$ Solid Solutions.....	74
<i>Yu.V. Goryunov, A.N. Nateprov</i> Effect of Landau Levels on the SHFS of the EPR Spectra of Fe^{3+} Precipitates in the 3D Dirac Semimetal Cd_3As_2	75
<i>T. Ivanova, D. Chachkov, O. Turanova, I. Ovchinnikov</i> Weak Ferromagnetism in Antiferromagnetic Chains $[\text{Fe}(\text{salen})(2\text{-Me-Him})]_n$	76
<i>V.V. Kabanov</i> Symmetry Enforced Dirac Points in Antiferromagnetic Semiconductors.....	77
<i>A.F. Khusnuriyalova, A. Petr, A.T. Gubaidullin, A.V. Sukhov, V.I. Morozov, B. Büchner, V. Kataev, O.G. Sinyashin, D.G. Yakhvarov</i> The Observation by Magnetic Resonance of the Electrochemically Generated Superparamagnetic Cobalt Nanoparticles.....	78
<i>B.I. Kochelaev</i> EPR in Superconductors and Kondo-Lattices with heavy Fermions.....	79
<i>R.K. Kremer</i> Search for the Spin-Nematic Phase in the $J_1 - J_2$ Frustrated Quantum Antiferromagnet LiCuVO_4	80

<i>W.M. Mohammed, R.V. Yusupov, I.V. Yanilkin, I.R. Vakhitov, A.I. Gumarov, A.M. Esmaili M.N. Aliyev, L.R. Tagirov</i> Synthesis and Ferromagnetic Resonance Studies of Epitaxial VN/Pd _{0.96} Fe _{0.04} Heterostructure Grown on Single-Crystalline MgO Substrate.....	81
<i>I.Yu. Nosov, A.L. Zinnatullin, F.G. Vagizov</i> Mössbauer Effect Studies of Eu doped BiFeO ₃	82
<i>S. Okubo, S. Shimoshiro, Y. Saito, S. Hara, T. Sakurai, T. Okamoto, H. Takahshi, E. Ohmichi, H. Ohta, R. Okuma, Z. Hiroi</i> High-field and High-frequency ESR studies of Comprising Tetrahedral Clusters Arranged in the Cubic Lattice.....	83
<i>M. Preißinger, D. Ehlers, K. Karube, H.-A. Krug von Nidda, B. Szigeti, Y. Taguchi, V. Tsurkan, I. Kézsmárki</i> Effects of Magnetocrystalline Anisotropy on the Triangular to Square Lattice Transformation of Skyrmions.....	84
<i>I. Romanova, B.Z. Malkin, O. Morozov, M.S. Tagirov, E. Sergeicheva, S. Sosin</i> Magnetic Resonance in a Dipolar Ferromagnet LiHoF ₄	85
<i>S. Dengre, R. Sarkar, J.-C. Orian, C. Baines, L. Opherden, M. Uhlarz, T. Herrmannsdörfer, T. Söhnle, C. D. Ling, M. Allision, J. Gardner, H.-H. Klauss</i> Local Anisotropy and Spin Dynamics in a New Kagome Compound Fe ₄ Si ₂ Sn ₇ O ₁₆	86
<i>R. Sarkar, Z. Mei, A. Ruiz, H.-H. Klauss, J.G. Analytis, N.J. Curro</i> NMR Studies on the Single Crystalline Na ₂ IrO ₃ : A Model System to Realize Kitaev Interaction.....	87
<i>A.S. Semakin, I.R. Mukhamedshin, S.G. Zybtssev, V.Ya. Pokrovskii</i> NMR Study of Charge Density Waves in NbS ₃ Compound.....	88
<i>A. Semeno, M. Anisimov, A. Bogach, M. Gilmanov, V.B. Filipov, N.Yu. Shitsevalova, S.V. Demishev</i> ESR Evidence of Spin Glass Behavior in the Absence of the Intrinsic Randomness in GdB ₆	89
<i>E. Skorokhodov, R. Gorev, M. Sapozhnikov, N. Gusev, O. Ermolaeva, V. Mironov</i> Magnetic Resonance Force Spectroscopy of Co/Pt Multilayer Films with Perpendicular Anisotropy.....	90
<i>A.I. Smirnov, T.A. Soldatov T. Kida A. Takata M. Hagiwara O. Petrenko, M. E. Zhitomirsky</i> Order by Dynamic or Static Disorder in a Triangular Antiferromagnet RbFe(MoO ₄) ₂ ...	91
<i>T.A. Soldatov, A.I. Smirnov, K.Yu. Povarov, M. Hälg, W.E.A. Lorenz, A. Zheludev</i> Spinon resonance in spin-chain antiferromagnets with uniform Dzyaloshinsky-Moriya interaction.....	92
<i>B.G. Szigeti, S. Bordács, Á. Butykai, K. Geirhos, D. Ehlers, B. Miksch, J.S. White, H.-A. Krug von Nidda, P. Lunkenheimer, V. Tsurkan, M. Scheffler, M. Poggio, I. Kézsmárki</i> New Findings in the Magnetic Phase Diagram of GaV ₄ Se ₈	93
<i>L.R. Tagirov</i> Ferromagnetic Resonance – a Powerful Tool to Characterize Magnetic Heterostructures.....	94

<i>V. Vorobeva, M. Gruzdev, U. Chervonova</i> EPR Study of Azomethine Iron(III) Complexes.....	95
<i>V.K. Voronkova, R.T. Galeev, L.V. Mingalieva, A.A. Sukhanov, Y. Peng, A.K. Powell</i> Heteronuclear Clusters Containing Dysprosium Ions: SMM Properties and EPR Possibility.....	96
<i>S.S. Yakushkin, V.L. Kirillov, O.N. Martyanov</i> Fe ₃ O ₄ /DMSO Ferrofluid Synthesis, ESR <i>in situ</i> Study.....	97
<i>R.M. Eremina, I.V. Yatsyk, A.A. Gabidullina, A.L. Zinnatullin, F.G. Vagizov,</i> <i>A.G. Badelin, V.K. Karpasuk, Z.I. Seidov</i> Magnetic Properties of Lanthanum Strontium Ferromanganites Doped with Zinc.....	98
<i>A. Yermakov, A. Gubkin, M. Uimin, A. Korolev, L. Molochnikov, E. Rosenfeld,</i> <i>A. Minin, A. Volegov, D. Boukhvalov, S. Konev</i> Formation of Antiferromagnetic Fe–Fe Dimers in Fe Doped TiO ₂ Nanoparticles investigated by EPR and Magnetic Methods.....	99
<i>Ben-Li Young, Ping-Chun Tsai, Genda Gu</i> Electronic Structures in In-doped Topological Insulator (Pb _{0.5} Sn _{0.5}) _{1-x} In _x Te Probed by NMR Spectroscopy.....	100
<i>R.V. Yusupov, A.V. Petrov, S.I. Nikitin, I.V. Yanilkin, A.I. Gumarov, A.G. Kiiamov,</i> <i>L.R. Tagirov</i> Probing Magnetic Inhomogeneity of Pd _{1-x} Fe _x Thin Films with Ultrafast Optical and Magneto-optical Spectroscopy.....	101
<i>A.M. Ziatdinov</i> Electronic Structure near the Fermi Level in Nanostructured Phase of Thermally Reduced Graphene Oxide: ESR, CESR and Magnetic Susceptibility Studies.....	102
<i>A.L. Zinnatullin, A.I. Gumarov, A.G. Kiiamov, B.F. Gabbasov, R.V. Yusupov,</i> <i>F.G. Vagizov, V.I. Nuzhdin, V.F. Valeev, R.I. Khaibullin</i> Mössbauer Effect and Magnetic Studies of Fe Implanted ZnO Film.....	103
<i>S. Zvyagin</i> Pressure-Tuning the Quantum Spin Hamiltonian of the Triangular Lattice Antiferromagnet Cs ₂ CuCl ₄ : High-Field ESR Studies.....	104
Structure and Dynamics of Chemical Systems	
<i>S.K. Misra, S.I. Andronenko</i> An EPR Study of the V ⁴⁺ and Cu ²⁺ Ions in Single Crystals of β-Mg ₂ V ₂ O ₇ and α- Zn ₂ V ₂ O ₇ : non-coincident ² and ² Tensors.....	105
<i>I.A. Khodov, S.V. Efimov, K.V. Belov, L.A.E. Batista de Carvalho</i> An Investigation of the Conformational Properties of Mefenamic Acid in DMSO by Two-dimensional NMR.....	106
<i>S.N. Borisenko, E.V. Maksimenko, S.S. Khizrieva, G.S. Borodkin, N.I. Borisenko</i> NMR Study of Synthesis of the Phenanthridone Alkaloids from Herbal's Aporphine Alkaloids by Subcritical Water.....	107
<i>N. Dudysheva, E. Golysheva, S. Dzuba</i> Spin Probe Nanostructure Formation in Glassy Media Studied by EPR.....	108

<i>S.S. Eaton, G.R. Eaton</i> Intramolecular Effects on Electron Spin Relaxation.....	109
<i>S.V. Efimov, F.Kh. Karataeva, V.V. Klochkov</i> Phosphorylotropic Rearrangement in Crown Ester Observed by ^1H , ^{13}C , and ^{31}P NMR..	110
<i>A.R. Gafarova, G.G. Gumarov, M.M. Bakirov, V.Yu. Petukhov</i> EPR Study of γ -Irradiated Magnesium and Zinc Gluconates.....	111
<i>A.R. Gafarova, G.G. Gumarov, M.M. Bakirov, V.Yu. Petukhov</i> Study of Radiation Induced Radicals in Sodium Gluconate.....	112
<i>G. Gescheidt, L. Weiner, A. Barbon, M. Schmallegger</i> Applications of EPR and Light-Induced Reactions in Biomimetic Systems and Catalysis.....	113
<i>I.A. Khodov, S.V. Efimov, M.G. Kiselev</i> High-pressure NMR Characterization of Conformation Preferences of Small-Molecules Dissolved in Supercritical Carbon Dioxide.....	114
<i>A.I. Kokorin, E.A. Konstantinova</i> EPR Spectroscopy of Metal-Oxide Photocatalysts.....	115
<i>A.I. Kokorin, E.A. Konstantinova, Ye.N. Degtyarev, M.V. Sivak, T.V. Sviridova, D.V. Sviridov</i> EPR Study of Structural Peculiarities of Metal Oxides Intercalated by Benzoazoles.....	116
<i>K. Konov</i> CW EPR and ESEEM Study of the Verdazyl Radicals.....	117
<i>O.B. Lapina, A.A. Shubin, E. Papulovskiy</i> Catalysts Structure Identification Using DFT-Confirmed NMR Signatures.....	118
<i>K. Möbius</i> Mechanisms for Life without Water - High-field EPR studies of protein/matrix interactions.....	119
<i>G.M. Ostroumova, N.D. Orekhov, V.V. Stegailov</i> Reactive Molecular-Dynamics Study of Onion-like Carbon Nanoparticle Formation....	120
<i>I.K. Ostrovskaya, N.F. Fatkullin</i> On the Theory of Dynamic Heterogeneity of Segments of Linear Macromolecules Generated by the End Segments: the Frequency Nature of This Effect and Possibility of Its Experimental Detection Using the Free Induction Decay of Deuterium Nuclei.....	121
<i>A.V. Savinkov, A.A. Shinkarev, V.E. Gorelysheva, A.S. Egorova</i> Molecular Mobility and State of n-Hexane Adsorbed in Pillared Montmorillonite Studied by 2D ^1H NMR Relaxometry.....	122
<i>D. Schäfter, J. van, Slageren</i> Novel potential Multi-Qubit Systems with Very Rigid Bridging Ligands.....	123
<i>S.I. Selivanov, S. Wang, A.S. Filatov, A.V. Stepakov</i> Scalar Relaxation Effects of the First and Second Kinds in NOESY Spectra of Small Organic Molecules in Liquid.....	124
<i>S.I. Selivanov, N.M. Chernov, I.P. Yakovlev</i> Conformational Analysis of Flexible Molecules in Liquid at Fast Exchange Condition and Population Ratio Determination on Base eNOE Data.....	125

<i>D.V. Shurtakova, G.V. Mamin, M.R. Gafurov, S.B. Orlinskii, I. Smirnov, A. Fedotov, V. Komlev</i> Investigation of Octacalcium Phosphate by EPR Methods.....	126
<i>A.S. Smorygina, A.G. Matveeva, V.N. Syryamina, B. Biondi, F. Formaggio, S.A. Dzuba</i> Antimicrobial Peptide Chalciporin A in the Model Membrane.....	127
<i>V.V. Sobornova, K.V. Belov, S.V. Efimov, V.V. Klochkov, I.E. Ereemeev, I.A. Khodov</i> Experimental Observation of Hidden Conformations of Strychnine by NMR Spectroscopy.....	128
<i>V.I. Volkov</i> Ionic and Molecular Transport in Synthetic and Biological Membranes Studied by NMR.....	129
<i>M. Witwicki, J. Jezierska, A. Ozarowski</i> Application of Experimental and Computational EPR Spectroscopy to Radical Systems	130
<i>D.G. Yakhvarov, A.F. Khusnuriyalova, A. Petr B. Büchner, V.I. Kataev, V. Morozov, Z.N. Gafurov, G. Giambastiani, L. Lukoni, O.G. Sinyashin</i> Application of <i>in situ</i> EPR Spectroelectrochemistry for Generation, Observation and Activation of High Reactive Mono-, Bi- and Polynuclear Complexes.....	131
<i>R.B. Zaripov, S. Avdoshenko, I.T. Khairuzhdinov, K.M. Salikhov, V.K. Voronkova, S. Weheabby, T. Rüffer, A. Popov, B. Büchner, V. Kataev</i> ENDOR and DFT Studies of the Cu(II)-bis(oxamato) Complex.....	132
Spectroscopy and Imaging of Biological Systems	
<i>M. Andersen</i> EPR and Beer - a Good Combination!	133
<i>N.V. Anisimov, E.G. Sadykhov, O.S. Pavlova, D.V. Fomina, A.A. Tarasova, Yu.A. Pirogov</i> Whole Body Sodium MRI at 0.5 Tesla.....	134
<i>N.V. Anisimov, O.S. Pavlova, V.L. Yarnykh</i> Fast Macromolecular Proton Fraction Mapping at 0.5 Tesla.....	135
<i>E.G. Bagryanskaya, O.A. Krumkacheva, G. Shevelev, A. Lomzov, N. Dyrkheeva, A.A. Kuzhelev, V.M. Tormyshev, Yu. Polienko, M. Fedin, D. Pyshnyi, O. Lavrik, A. Chubarov, T. Godovikova</i> DNA and RNA Complexes with Human Proteins : Structural Insights revealed by Pulsed Dipolar EPR with Orthogonal Spin Labeling.....	136
<i>S.A. Dikanov</i> Influence of Hyperfine Coupling Strain on Two-Dimensional ESEEM Spectra from I=1/2 Nuclei.....	137
<i>M. Drescher</i> In-cell EPR Spectroscopy.....	138
<i>S. Dzuba</i> Lipid-Mediated Clustering in Biological Membranes by Spin-Label EPR.....	139
<i>A. Fielding, M.A. Hollas, S.J. Webb, S.L. Flitsch</i> A Bifunctional Spin Label for Ligand Recognition on Surfaces.....	140

<i>E.H. Yardeni, T. Bahrenberg, R.A. Stein, S. Mishra, E. Zomot, B. Graham, K.L. Tuck, T. Huber, E. Bibi, H.S. Mchaourab, D. Goldfarb</i> Probing the Solution Structure of the E.coli Multidrug Transporter MdfA using DEER Distance Measurements with Nitroxide and Gd(III) Spin Labels.....	141
<i>L. Wong, J. Maier, D. Sieme, J.C. Fuentes, N. Nath, P. Vemulapalli, N. Karschin, H. Sun, J. Kühn, S. Pirkuliyeva, A. Batth, M. Engelke, S. Ryzanov, L. Antonschmidt, A. Martinez, Hernandez, A. Fischer, G. Eichele, D. Becker, S. Becker, A. Leonov, M. Reggelin, J. Wienands, A. Giese, C. Griesinger</i> NMR Spectroscopy in Chemistry and Biology with Applications in Immunology and Neuroprotection.....	142
<i>H. Hirata</i> Recent Progress in 3D Extracellular pH Mapping of Tumors Using EPR.....	143
<i>R. Kaptein</i> NMR studies of Protein-DNA interaction: target location and allosteric mechanism of induction.....	144
<i>V.V. Khrantsov</i> In Vivo Molecular EPR-Based Spectroscopy and Imaging of Cancer.....	145
<i>O.A. Krumkacheva, I.O. Timofeev, L.V. Politanskaya, Yu.F. Polienko, E.V. Tretyakov, O.Yu. Rogozhnikova, D.V. Trukhin, V.M. Tormyshev, A.S. Chubarov, E.G. Bagryanskaya, M.V. Fedin</i> Triplet Fullerenes as Prospective Spin Labels for Nanoscale Distance Measurements by Pulsed Dipolar EPR.....	146
<i>S.S. Ovcherenko, A.V. Shernyukov, O.A. Chinak, E.A. Sviridov, V.M. Golyshev, A.S. Fomin, I.A. Pyshnaya, E.V. Kuligina, V.A. Richter, E.G. Bagryanskaya</i> Structural and Aggregational Features of Intrinsically Disordered Peptide RL2 – Human Milk κ -Casein Fragment with Antitumor and Cell Penetrating Properties.....	147
<i>V.V. Ptushenko, N.P. Isaev, L.V. Kulik, A.E. Solovchenko, B.V. Trubitsin</i> Photosynthetic Electron Transfer Reactions in Microalga <i>Lobosphaera incisa</i>	148
<i>N.E. Sannikova, A.G. Matveeva, V.N. Syryamina, M. De Zotti, C. Toniolo, F. Formaggio, S.A. Dzuba</i> Influence of the Tylopeptin B Antimicrobial Peptide on Structure of Model Biological Membranes by Spin-label EPR.....	149
<i>A. Spitsyna, O. Krumkacheva, D. Trukhin, O. Rogozhnikova, A. Chubarov, I. Kirilyuk, T. Godovikova, V. Tormyshev, E. Bagryanskaya</i> Novel Spin Label Based on OX063 Trityl Applied to Study Human Serum Albumin....	150
<i>K. Usachev, A. Golubev, I. Khusainov, Sh. Validov, E. Klochkova, F. Murzakhanov, M. Gafurov, V. Klochkov, A. Aganov, M. Yusupov</i> Structural and Dynamical Studies of the Elongation Factor P from <i>Staphylococcus aureus</i> by NMR and EPR Spectroscopy.....	151
<i>S. Van Doorslaer, K. Nys, J. Roefs, V. Pfanzagl, C. Obinger</i> Unravelling the Role of Key Amino-acids in B-class Dye-decolorizing Peroxidases Using EPR Spectroscopy.....	152
<i>Jianzhang Zhao, Zhijia Wang, Yuqi Hou, Xue Zhang, Kepeng Chen</i> Time-Resolved EPR Study of the Intersystem Crossing of Visible Light-Harvesting Electron Donor/Acceptor Dyads.....	153

Other Applications of Magnetic Resonance and Related Phenomena

<i>A.A. Bayazitov, K.M. Salikhov, Ya.V. Fattakhov, A.R. Fakhrutdinov, V.A. Shagalov, R.Sh. Khabipov, N.M. Reshetnikov, D.I. Abdulganieva</i> Development of “Knee” and “Hand” Receiving and Transmitting Systems for a Specialized MRI with a 0.4 Tesla Field.....	154
<i>A. Bussmann-Holder, Z. Guguchia, H. Keller, K. Roleder</i> Hidden Magnetism in Almost Multiferroic EuTiO ₃	155
<i>Chunyan Wu, Jiafu Chen</i> Selenium-Nitrogen Free Radical (\bullet NSe) and its EPR Studies.....	156
<i>M.L. Falin, V.A. Latypov, A.M. Leushin, G.M. Safiullin, A.A. Shakirov, A.A. Shavelev</i> The Trigonal Yb ³⁺ Center in Lithium Calcium Hexafluoroaluminate.....	157
<i>E.N. Frolova, L.V. Mingalieva, O.A. Turanova, R.G. Batulin, A.S. Semakin, G.G. Garifzyanova, M.Yu. Volkov, L.G. Gafiyatullin, I.V. Ovchinnikov, A.N. Turanov</i> Spin Properties of the Fe(III) Complexes with Tetradentate Schiff Bases and Photosensitive 4-Styrylpyridine Ligands.....	158
<i>L.K. Aminov, M.R. Gafurov, I.N. Kurkin, B.Z. Malkin, S.I. Nikitin, A.A. Rodionov</i> EPR of Single Ions Nd ³⁺ in CsCdBr ₃ Monocrystals.....	159
<i>E. Goovaerts</i> Combining electron paramagnetic resonance methods to investigate materials for organic photovoltaics.....	160
<i>D. Ivanov, A. Vahin, D. Melnikova, V. Skirda</i> The Study of Kerogen by NMR.....	161
<i>Ö. Karataş, C. Okay, R.I. Khaibullin, S. Kazan, L. Arda, B. Rameev</i> FMR Analysis of Magnetic Anisotropies in Co-implanted TiO ₂ Rutile.....	162
<i>H. Keller</i> Probing Fundamental Properties of Condensed Matter Systems with Positive Muons....	163
<i>E.M. Alakshin, G.A. Dolgorukov, A.V. Klochkov, E.I. Kondratyeva, V.V. Kuzmin, K.R. Safiullin, A.A. Stanislavovas, M.S. Tagirov</i> ³ He in Contact with Nanostructures.....	164
<i>G.I. Likhtenshtein</i> Dual Fluorescence-nitroxide Supermolecules as High Sensitive Redox Probes and Models for Electron Transfer: 34 Years History and Recent Developments.....	165
<i>S. Lvov, E. Kukovitsky</i> Hyperfine Coupling Constants in Me-Er (Me = Cu, Ag, Au) Binary Dilute Alloys.....	166
<i>O.N. Martyanov, S.N. Trukhan, S.S. Yakushkin</i> <i>In situ</i> ESR at Elevated Temperatures and Pressures for Catalysis and Related Phenomena.....	167
<i>V.M. Murzakaev, N.N. Belousova, A.V. Bragin, V.D. Skirda, M.S. Tagirov, A.S. Alexandrov, T.R. Abdullin, M.I. Amerkhanov</i> Results Gained from Application of Dielectric and High-resolution Nuclear-Magnetic Resonance Complex for Assessment of Fluid Type in a Borehole and in Core.....	168

<i>T.A. Ivanova, I.V. Ovchinnikov, O.A. Turanova</i> EPR of Spin-Crossover Compounds [Fe(bzacen)(tvp)]·BPh ₄ ·nCH ₃ OH.....	169
<i>M. Shanmugam, T.M. Hedison, D.J. Heyes, R. Edge, N.S. Scrutton</i> Direct Evidence for "Substrate-induced" Inter-Copper Electron-Transfer in Copper-Containing Nitrite Reductases (A _x NiR and R _p NiR-core); Probed by EPR/Cryolytic Reduction/Annealing Studies.....	170
<i>A.A. Sukhanov, Yu.E. Kandrashkin, V.K. Voronkova, V.S. Tyurin</i> TR EPR Study of Photoinduced States of Metalloporphyrin. From Monomer to Oligomers.....	171
<i>A.A. Sukhanov, V.F. Tarasov, A.S. Apreleva, K.A. Subbotin, E.V. Zharikov</i> EPR Study of Monoisotopic ⁵³ Cr Impurity Ions in Forsterite Single Crystal.....	172
<i>K. Sato, R. Hirao, I. Timofeev, O. Krumkacheva, E. Zaytseva, O. Rogozhnikova, V. Tormyshev, D. Trukhin, E. Bagryanskaya, T. Gutmann, V. Klimavicius, G. Buntkowsky, K. Sugisaki, S. Nakazawa, H. Matsuoka, K. Toyota, D. Shiomi, T. Takui</i> Multi-Frequency EPR/ENDOR, DNP and AWG Pulse MW Spectroscopy of g-Engineered Trityl-Aryl-Nitroxide biradicals.....	173
<i>V.A. Ulanov, I.V. Yatsyk, R.R. Zainullin</i> EPR of the Pb _{1-x} Gd _x S Narrow Gap Semiconductor Crystals: Observation of Strong Dependence of the EPR Line Profiles on Gadolinium Concentration.....	174
<i>V.A. Ulanov, I.V. Yatsyk, R.B. Zaripov, G.S. Shakurov, R.R. Zainullin</i> EPR of the BaF _{2+x} ·Ni crystals: Peculiarities of an Analysis of SHFS of the EPR Spectra of Ni ³⁺ Centers when $H_{ZFS} \gg H_{eZ} \gg H_{SHFI}$	175
<i>A.M. Zyuzin, A.A. Karpeev, N.V. Yantsen</i> EPR Parameters Temperature Dependences of Carbon-containing Composites.....	176
XXI International Youth Scientific School "Actual problems of magnetic resonance and its application"	
<i>S.G. Vasil'ev</i> Application of multiple-quantum (MQ) NMR to study the structure and dynamics of dipolar coupled 1/2 spin networks in amorphous and crystalline solids.....	177
<i>S.G. Vasil'ev, K.L. Boldyrev, E.V. Selezneva, E.A. Tatarinova, A.M. Muzafarov</i> The self-diffusion of polymethylsilsequioxane dendrimers in dilute solutions and melts	178
<i>G.A. Bochkin, A.V. Fedorova, E.B. Fel'dman, S.G. Vasil'ev</i> Investigation of the free induction decay in fluorine spin chains in fluorapatite in multi-pulse NMR experiment	179
<i>A.Yu. Germov, V.V. Ogloblichev, A.M. Potapov, S.V. Verkhovskii</i> ¹⁴ N NMR and magnetic susceptibility of UN in the paramagnetic state.....	180
<i>A.V. Ivanova, E.A. Ermakova, D.N. Shurpik, I.I. Stoykov, B.I. Khayrutdinov, Y.F. Zuev</i> Investigation of the interconversion process of pillar[5]arene using NMR spectroscopy and DFT method.....	181
<i>A.Sh. Khaliqzadeh</i> Features of photoelectric of GaS monocrystal with doped rare earth elements (Yb, Sm)	182

<i>R.F. Khankishiyeva, Sh.M. Mammadov, H.N. Akhundzada, P.I. Isamyilova</i> EPR investigation of the irradiation crosslinking process of nitrile-butadiene rubber with added various types of nano-metal oxides.....	183
<i>P.P. Kobchikova, S.V. Efimov, V.V. Klochkov</i> Studying cyclosporin D – micelle complex by high-resolution NMR: Obtaining information on the spatial structure.....	184
<i>P.A. Kononova, O.Yu. Selyutina, E.A. Shelepova, M.V. Zelikman, N.E. Polyakov</i> Glycyrrhizin-induced changes in the dynamics of single-component and multi-component phospholipid bilayers.....	185
<i>E. Kovalenko, I.V. Mirzaeva, I.V. Andrienko, E.A. Pashkina</i> Cucurbit[7]uril behavior in PBS buffer solution and RPMI-1640 cell growth medium...	186
<i>A.M. Kusova, A.E. Sitnitsky, Yu.F. Zuev</i> Protein-protein interactions according to protein translational diffusion.....	187
<i>M.S. Kuzmikov, K.V. Belov, M.A. Krestyaninov, A.A. Dyshin, I.A. Khodov</i> Confirmation preferences of carbamazepine molecules in chloroform and supercritical CO ₂ by NMR spectroscopy.....	188
<i>I.G. Mershev, G.S. Kupriyanova, S. Wurmehl</i> Adiabatic excitation for NMR spectroscopy in magnetic materials.....	189
<i>A.S. Parfishina, A.V. Egorov, A.G. Kiyamov, S.L. Korableva, I.V. Romanova, K.R. Safiullin, M.S. Tagirov</i> The study of ¹⁶⁹ Tm in a single crystal LiYF ₄ :Tm ³⁺ (2%) by pulsed NMR method.....	190
<i>D.A. Prokopyev, A.Yu. Germov, K.N. Mikhalev, M.A. Uimin, A.E. Yermakov, S.I. Novikov, A.S. Konev, V.S. Gaviko</i> NMR study of carbon encapsulated Ni@C nanoparticles.....	191
<i>E.A. Razina, E.I. Baibekov, I.N. Kurkin, G.V. Mamin, M.R. Gafurov, S.B. Orlinskii</i> High frequency EPR of rare-earth metal ions in LiYF ₄	192
<i>M. Saad, S.I. Nikitin, D.A. Tayurskii, R.V. Yusupov</i> Emergent Ferromagnetism and Flux Trapping in Dispersed Pyrolytic Graphite Flakes by Mild Vacuum Annealing.....	193
<i>S.P. Savchenko, M.A. Borich</i> Amplification of nuclear magnetostatic oscillations in ferromagnets.....	194
<i>O. Selyutina, V. Timoshnikov, N. Polyakov</i> The influence of chelators on lipid oxidation.....	195
<i>G.S. Shurshalova, D.A. Sharapova, A.V. Aganov, V.V. Klochkov</i> Lovastatin and Their Interaction with Model Membranes by NMR Data	196
<i>R.V. Skoryunov, O.A. Babanova, A.V. Soloninin, A.V. Skripov, V. Stavila, M. Dimitrievska, M. Psurek, T.J. Udovic</i> Nuclear magnetic resonance study of a carbon-substituted closo-hydroborate NaCB ₁₁ H ₁₂ in nanoporous silica SBA-15.....	197
<i>P. Skvortsova, D. Shurpik, I. Stoikov, B. Khairutdinov</i> NMR in the study of pillar[5]aren-DNA complexes.....	198

<i>V.A. Timoshnikov, T.V. Kobzeva, O.Yu. Selyutina, N.E. Polyakov, G.J. Kontoghiorghes</i> Investigation of Deferiprone Influence on Generation Oxygen Species in Redox Reactions with Iron and Copper Ions using EPR Spectroscopy with Spin Traps.....	199
<i>I.V. Yanilkin, R.V. Yusupov, A.A. Rodionov, B.F. Gabbasov, M.N. Aliyev, L.R. Tagirov</i> Ferromagnetic Resonance in Exchange Coupled Ultrathin Epitaxial CoO _x /Co/Ag/Fe/MgO Heterostructures.....	200
Author index	201